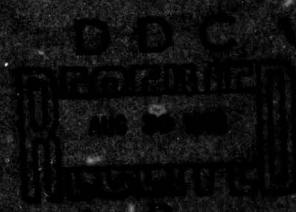


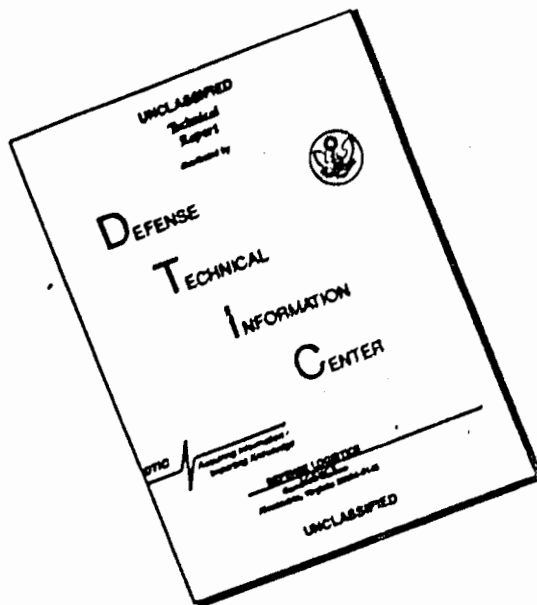
AD NO.
DDC FILE COPY

ADA058270

1987
NIST Research Laboratory
100 Bureau Blvd., Gaithersburg, MD
20899



DISCLAIMER NOTICE



THIS DOCUMENT IS BEST QUALITY AVAILABLE. THE COPY FURNISHED TO DTIC CONTAINED A SIGNIFICANT NUMBER OF PAGES WHICH DO NOT REPRODUCE LEGIBLY.



FINAL REPORT

6 MICROWAVE GALLIUM ARSENIDE FET AMPLIFIERS

BY

10 H. F. COOKE
S. HENNIES

16 F54581,
F54545

17 XF54581004,
XF54545602

PREPARED FOR: NAVAL RESEARCH LABORATORY
WASHINGTON, D.C. 20375

9 Final rept.
FOR PERIOD JUNE 1975 - NOVEMBER 1977

CONTRACT NO. N00014-75-C-1163

15 JUNE 1978

11 12 208 p.

DDC
RECEIVED
AUG 30 1978
B

AVANTEK, INC.
3175 BOWERS AVENUE
SANTA CLARA, CA. 95051

78 08 24 091

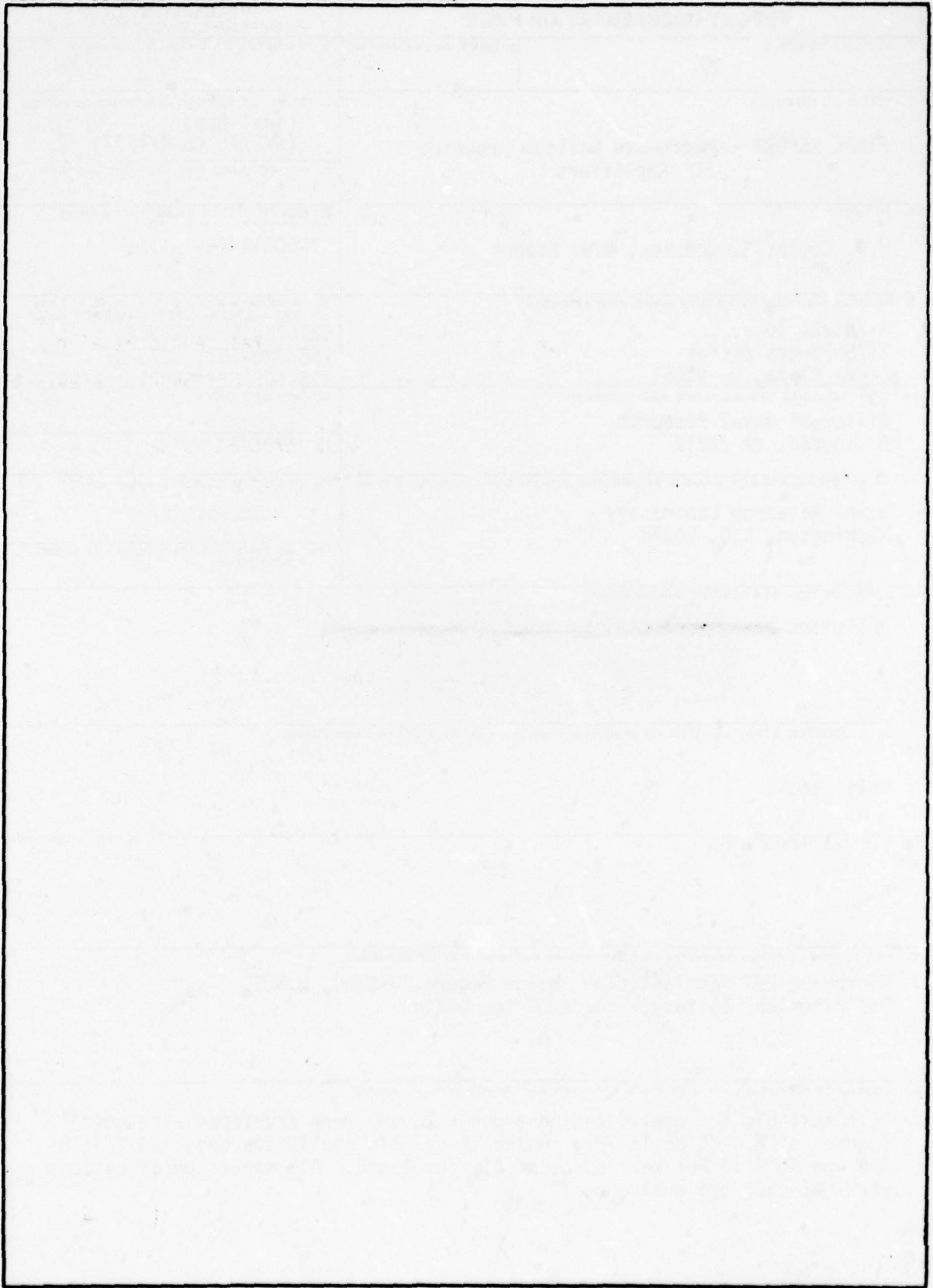
DISTRIBUTION STATEMENT A
Approved for public release;
Distribution Unlimited

389421

Handwritten signature

REPORT DOCUMENTATION PAGE		READ INSTRUCTIONS BEFORE COMPLETING FORM
1. REPORT NUMBER	2. GOVT ACCESSION NO.	3. RECIPIENT'S CATALOG NUMBER
4. TITLE (and Subtitle) FINAL REPORT - Microwave Gallium Arsenide FET Amplifiers		5. TYPE OF REPORT & PERIOD COVERED Final Report JUNE 1975- NOV. 1977
7. AUTHOR(s) H.F. Cooke, S. Hennies, W.W. Hooper		6. PERFORMING ORG. REPORT NUMBER
9. PERFORMING ORGANIZATION NAME AND ADDRESS Avantek, Inc. ✓ 3175 Bowers Avenue Santa Clara, CA 95051		8. CONTRACT OR GRANT NUMBER(s) N00014-75-C-1163 ✓
11. CONTROLLING OFFICE NAME AND ADDRESS Office of Naval Research Arlington, VA 22217		10. PROGRAM ELEMENT, PROJECT, TASK AREA & WORK UNIT NUMBERS 62762N; XF54581004; PMD-PME-107; 62762N; XF54545602; 63521N; X-0679-AA
14. MONITORING AGENCY NAME & ADDRESS (if different from Controlling Office) Naval Research Laboratory Washington, D.C. 20375		12. REPORT DATE
		13. NUMBER OF PAGES
		15. SECURITY CLASS. (of this report) Unclassified
16. DISTRIBUTION STATEMENT (of this Report) Unlimited is DISTRIBUTION STATEMENT A is Approved for public release; Distribution Unlimited		15a. DECLASSIFICATION/DOWNGRADING SCHEDULE
17. DISTRIBUTION STATEMENT (of the abstract entered in Block 20, if different from Report) Unlimited		
18. SUPPLEMENTARY NOTES		
19. KEY WORDS (Continue on reverse side if necessary and identify by block number) Microwave FET, Implantation, Noise Figure, J-Band, L.S.S. Distribution, Epitaxy, Source, Gate, Drain		
20. ABSTRACT (Continue on reverse side if necessary and identify by block number) FETs suitable for amplification through 18 GHz were developed with noise figures of 2.3 dB at 18 GHz. Using these FETs amplifiers covering 7 - 18 GHz and 10 - 18 GHz were successfully developed. All major specifications were met over the entire band.		

SECURITY CLASSIFICATION OF THIS PAGE(When Data Entered)



SECURITY CLASSIFICATION OF THIS PAGE(When Data Entered)

PREFACE

This report describes work performed at Avantek, Inc., under Contract Number N00014-75-C-1163. Funding for the program was provided by Naval Electronic Systems Command and Naval Air Systems Command. Mr. Eliot D. Cohen of Naval Research Laboratory was the Scientific Officer.

The results of the 29-month program are presented in this report. The objective of Phase I, the first 12 months, of this program was to develop both FETs and multistage amplifiers covering the 7-15 GHz frequency range. A 0.5 micron gate FET was successfully developed and the amplifiers were delivered on schedule. Work on this portion of the program is described in detail in the annual report issued in November 1976.

The objectives of Phase II were to develop both devices and multistage amplifiers capable of operating over the frequency ranges of 10.7-18 GHz and 7-18 GHz. A 0.5 x 300 micron GaAs FET with a noise figure of 2.5 dB and associated gain of 7 dB at 18 GHz was produced. In addition, all required amplifiers were delivered with most specifications met or exceeded.

SEARCHED		<input checked="" type="checkbox"/>
INDEXED	FILED	<input type="checkbox"/>
SERIALIZED		<input type="checkbox"/>
NOV 1976		
BY		
DISTRIBUTION/AVAILABILITY CODES		
Dist.	AVAIL.	and/or SPECIAL
A		

TABLE OF CONTENTS

	PAGE NO.
I. FET DEVELOPMENT	1
A. Introduction	1
B. Noise Figure Reduction	1
C. Mobility	14
D. Material Development	16
E. Design for Application	17
F. FET Performance	22
G. Device Modeling	24
II. ION IMPLANTATION	30
A. Si ₃ N ₄ Cap and Annealing	30
B. Qualification of Cr Doped Substrates	32
C. Ion Implantation	33
D. D.C. Evaluation	46
E. Performance Improvement Experiments	50
F. Conclusions	68
III. AMPLIFIER DEVELOPMENT	70
A. Introduction	70
B. FET Selection	73
C. Single-Ended Amplifiers	82
D. Balanced Gain Modules	88
E. Interconnections and Transitions	106
F. Limiter	109
G. Temperature Compensation	113
IV. 7 TO 18 GHz AMPLIFIERS	118
V. 10.7 TO 18 GHz AMPLIFIERS	133
VI. CONTRACT CHANGES	151

TABLE OF CONTENTS (Continued)

	<u>PAGE NO.</u>
VII. MEETINGS	152
VIII. REFERENCES	153
APPENDIX A - Temperature Measurements on 7 to 18 GHz Amplifiers	
APPENDIX B - Data on the Four 7 to 18 GHz Amplifiers which were Added onto the Contract	
APPENDIX C - Temperature Measurements on 10.7 to 18 GHz Amplifiers	
APPENDIX D - Portions of the Qualification Test Procedure and Functional Test Procedure for the Qualified 7 to 12 GHz Amplifier	

LIST OF ILLUSTRATIONS

FIGURE NO.	TITLE	PAGE NO.
1	FET Gate Geometry & Gate Resistance, r_m	5
2	M-104 FET Geometry	7
3	M-107 FET Geometry	8
4	M-103 FET Geometry	9
5	FET Cross-Section using Fukui's Notation	11
6	FET Gate Cross-Sections	12
7	Mobility and Capacitance Plots	15
8	Theoretical Effect of C on S_{21}	18
9	S_{21} vs. Frequency with N as a Parameter	20
10	Noise Figure and G_{NF} , Implanted FET	23
11	M-107 FET Equivalent Circuit	28
12	Silicon Nitride Deposition System	31
13	Surface Breakdown Voltage vs. Surface Doping of Cr-Doped GaAs Wafers after 900°C Anneal with Si_3N_4 Cap	35
14	Typical Impurity Profile of Cr-Doped GaAs Substrate Showing Conversion to N-type after 900°C Anneal with Si_3N_3 Cap	36
15	Typical Ion Implanted Profile Obtained with "Good" and "Bad" Cr-Doped Substrates after Annealing with Si_3N_4 Cap	37
16	Impurity Distribution of Se Implant, $\phi = 5 \times 10^{12}cm^{-2}$, E = 120 KeV	41
17	Impurity Distribution of Se Implant, $\phi = 4 \times 10^{12}cm^{-2}$, E = 240 KeV	42
18	Drain Characteristics of Se Implanted FETs (See Table IV)	45
19	Gaussian Distributions for Si and Se Implants, $\phi_{Si} = 6.2 \times 10^{12}cm^{-2}$, E = 50 KeV. $\phi_{Se} = 5 \times 10^{12}cm^{-2}$, E = 120 KeV. Dose and Energy Chosen so that the Peak Doping and Projected Range are Equal.	47

FIGURE NO.	TITLE	PAGE NO.
20	Typical Impurity Distribution for Si Implant, $\phi = 2 \times 10^{12}\text{cm}^{-2}$, $E = 120 \text{ KeV}$.	48
21	Drain Characteristics Typical of Si Implanted FET ($\phi = 2 \times 10^{12}\text{cm}^{-2}$, $E = 120 \text{ KeV}$, M-107).	49
22	G_m , C_{gs} , and μ_d vs. Gate Voltage for Si Implanted FET Run #361-C. Data obtained using the M-107 Fat-FET Structure.	51
23	G_m , C_{gs} , and μ_d vs. Gate Voltage for LPE FET run #363-C. Data obtained using the M-107 Fat-FET structure.	52
24	Resistance vs. Contact Spacing for Si Implanted FET Run #364-A. Data obtained using the M-107 Contact Test Pattern.	53
25	Schematic Representation of "Non-Selective" and "Selective" N^+ Implants.	54
26	Gaussian Distributions (LSS Theory) and Measured Impurity Profile for "Non-Selective" N^+/N Si Implanted FET run #360-B.	56
27	Drain Characteristics of Si Implanted FETs with "Non- Selective" N^+ Implanted Contacts.	57
28	Gaussian Distribution (LSS Theory) for Multiple Energy Si Implant Suitable for "Selective" N^+ Contact.	59
29	Gaussian Distribution (LSS Theory) for Multiple Energy Se Implant Suitable for "Selective" N^+ Contact	60
30	Resistance vs. Contact Spacing for the Multiple Energy Se N^+ Contact Implant of Fig. 29.	61
31	Resistance vs. Contact Spacing for the Multiple Energy Si N^+ Contact Implant of Fig. 28.	62
32	Schottky Diode Capacitance vs. Voltage for Si Implanted into a Qualified Cr-Doped Substrate and High Resistivity Buffer Layer ($\phi = 2 \times 10^{12}\text{cm}^{-2}$, $E = 120 \text{ KeV}$).	64

FIGURE NO.	TITLE	PAGE NO.
33	Drain Characteristics of Si Implanted FET. Implantation into High Resistivity Buffer Layer ($\phi = 2 \times 10^{12} \text{cm}^{-2}$, $E = 120 \text{ KeV}$).	66
34	G_m , C_{gs} , μ_d vs. Gate Voltage for Si Implanted FET Run #365-A. Implantation into High Resistivity Buffer Layer ($\phi = 2 \times 10^{12} \text{cm}^{-2}$, $E = 120 \text{ KeV}$).	67
35	Simplified FET Amplifier Circuit.	74
36	Effect of Impedance Mismatch on Output Mismatch Loss.	74
37	Single-Ended 7 to 18 GHz Amplifier	83
38	Single-Ended 10.7 to 18 GHz Amplifier	85
39	Maximum Impedance Transformation Using 4, 6 or 8 Element Networks.	86
40	Schematic Diagram of a Balanced Amplifier Module	89
41	Couplers	90
42	Through Loss for Two One Section 90° Hybrids Connected in Balanced Configuration.	91
43	Improvement in Return Loss & Frequencies	93
44	Coupler Measurements	94
45	Gain and Noise Figure for an M-104 Gain Module	96
46	Gain and Noise Figure for a 10.7 to 18 GHz M-107 Gain Module	99
47	Gain Response of 7 to 18 GHz Gain Modules	103
48	Gain vs. Drain Current	105
49	Compensated vs. Uncompensated Interconnections	107
50	Return Loss of Right Angle Hermetic Transition	108
51	Power in vs. Power out for the Two Diode Limiter	110
52	Temperature Compensation Circuit	114
53	7 to 18 GHz Amplifier	119
54	Swept Response of 7 to 18 GHz Amplifier Without Limiter	120
55	Complete 7 to 18 GHz Amplifier and Power Supply	123
56	Exploded View of 7 to 18 GHz Amplifier & Power Supply	124

FIGURE NO.	TITLE	PAGE NO.
57	Change in Gain & Phase with Temperature for 7 to 18 GHz Amplifier	130
58	Swept Response of 7 to 18 GHz Amplifiers	131
59	Noise Figure vs. Temperature, 7 to 18 GHz Amplifiers with Limiters	132
60	10.7 to 18 GHz Amplifiers	134
61	Swept Response of 10.7 to 18 GHz Amplifiers without Cables	135
62	Complete 10.7 to 18 GHz Amplifiers & Power Supply	139
63	Exploded View of 10.7 to 18 GHz Amplifier & Power Supply	140
64	Gain vs. Temperature 10.7 to 18 GHz Amplifier before Welding	146
65	Gain vs. Temperature of Completed 10.7 to 18 GHz Amplifiers	147
66	Power Output - 10.7 to 18 GHz Amplifiers	148
67	Outline Drawing - Microwave Amplifier with Integral Power Supply	149

LIST OF TABLES

NO.	TITLE	PAGE NO.
I	Effect of N on FET Parameters	19
II	Calculated S Parameters	29
III	Effect of Annealing on Surface Breakdown Voltage and Capacitance	34
IV	Summary Se Implanted FETs	40
V	Summary Si Implanted FETs on S.I.S.	45
VI	Summary Si Implanted FET on Buffers	65
VII	Amplifier Summary	71
VIII	FET Evaluation, M-104/R35A	76
IX	FET Evaluation, M-107/EXP-323D	77
X	FET Evaluation, M-107/EXP-323D	78
XI	FET Evaluation, M-107/EXP-338	79
XII	FET Evaluation, M-107/EXP-338	80
XIII	M-104 Gain Module, 10.7 to 18 GHz	94
XIV	10.7 to 18 GHz Gain Module	97
XV	7 to 18 GHz Module Phase Match, S/N 3	99
XVI	7 to 18 GHz Module Phase Match, S/N 4	100
XVII	7 to 18 GHz Module Phase Match	103
XVIII	Limiter 10.7 to 18 GHz, S/N 5	110
XIX	Limiters 7 to 18 GHz, S/N 10	112
XX	7 to 18 GHz Amplifier without Limiter, S/N 2	113
XXI	Temperature Comp. 10.7 to 18 GHz	114
XXII	Temperature Comp. 10.7 to 18 GHz	115
XXIII	7 to 18 GHz Amplifier without Limiter, S/N 2	119
XXIV	7 to 18 GHz Amplifier without Limiter, S/N 2	120
XXV	7 to 18 GHz Amplifier - Final Data	124
XXVI	7 to 18 GHz Amplifier - Phase Match, Final Data	125
XXVII	Comparison of Specified & Measured Data	126

NO.	TITLE	PAGE NO.
XXVIII	Change in Gain & Phase with Temperature	127
XXIX	10.7 to 18 GHz Amplifiers without Cables	134
XXX	10.7 to 18 GHz Amplifiers without Cables	135
XXXI	10.7 to 18 GHz Amplifiers without Cables	136
XXXII	10.7 to 18 GHz Amplifiers - Final Data	140
XXXIII	10.7 to 18 GHz Amplifiers - Final Data	141
XXXIV	Comparison of Specified & Measured Data	142

I. FET DEVELOPMENT

A. INTRODUCTION

During the first phase of this contract (June 1975 - June 1976), it was demonstrated that KU Band transistors were, indeed, feasible. By the end of the first year FETs with noise figures of 4.2 dB and 5 dB gain had been achieved at 18 GHz. At 9 GHz the noise figure was 2.8 dB with about 8 dB gain. This performance, while fairly impressive, was not adequate to build a 7-18 GHz amplifier which would meet all specifications at 18 GHz. Losses from couplers, limiters, cables, connectors, etc., are sufficient to increase the 4.2 dB noise figure to over 10 dB at the maximum temperature (+65°C).

By the end of Phase II (Nov. 1977), the noise figures at 18 GHz had been reduced to 3.2 dB and the net module gain had been increased to 8 dB. This resulted in an amplifier which had a noise figure between 5 and 6 dB at 18 GHz. Thus, the main thrust of the FET work in Phase II was devoted to reducing device noise figures and increasing gain. Due to the very heavy effort in this direction, particularly in implantation, it was necessary to reduce effort in others, such as the development of a dual gate FET. Feasibility of a dual gate FET was demonstrated in Phase I, when devices with over 30 dB agc range were built. The dual gate FET mask, however, was defective and a new mask would have been necessary if dual gate FETs were to be used in Phase II. Since our mask vendor has limited capability in sub-micron devices, we decided to concentrate on low noise, high gain, single gate FETs. An adequate leveler using PIN diodes was used in the final amplifiers.

B. NOISE FIGURE REDUCTION

In a paper by Hewitt, et al [1], Fukui developed an empirical equation for noise figure of FETs. The equation is particularly useful since it demonstrates the relative importance of how certain FET parameters affect noise figures. While we do not agree entirely on the exact form of the equation, it is still the only really useful one extant. All other forms are either too simplified, or else contain inaccessible parameters. The equation is as follows:

$$F = 1 + KfL^{5/6} \left(\frac{N}{a} \right)^{1/6} \left[\frac{3.3\omega^2\rho}{hL} + \frac{1.8L_{sg}}{Na_1} + \frac{0.18R_c}{Na_2} \right]^{1/2} \quad \text{Equation 1}$$

Where:

- K = noise coefficient, $\approx .033$ for good FETs
- f = frequency in GHz
- L = gate length in microns
- N = free carrier concentration, $\times 10^{16} \text{cm}^{-3}$ in active channel
- a = active layer thickness under gate in microns
- ω = unit gate width in mm
- ρ = gate metalization resistivity $\times 10^{-6} \Omega \text{cm}$
- h = gate metalization thickness in microns
- L_{sg} = spacing between gate and source in microns
- a_1 = thickness of channel between source and gate in microns
- R_c = specific contact resistivity, $\times 10^{-6} \Omega \text{cm}^2$ (for source and drain contacts)
- a_2 = thickness of channel under source in microns

The three terms inside the brackets can be identified as the gate metal loss, the source-to-gate channel resistance loss, and the contact resistance loss. For purposes of relating this equation to an equivalent circuit, Eq. 1 can be rearranged somewhat.

$$F = 1 + KfL^{5/6} \left(\frac{N}{a} \right)^{1/6} \omega^{1/2} \left[r_m + R_{sg} + R_{con} \right]^{1/2} \quad \text{Equation 1A}$$

Where:

$$r_m = \text{gate metal resistance} = \frac{\omega\rho}{3Lh} \quad \text{Equation 2}$$

R_{sg} = resistance of channel between source and gate

$$= \frac{L_{sg}}{q\mu N\omega a_1} = \frac{1.8 L_{sg}}{Na_1} ; \text{ if } \bar{\mu}_d = 3500 \quad \text{Equation 3}$$

$\bar{\mu}_d$ = average drift mobility

R_{con} = contact resistance

$$= \frac{1}{\omega} \sqrt{R_s R_c} = \frac{1}{\omega} \sqrt{\frac{R_c}{q\mu Na_2}}$$

$$= \frac{1}{\omega} \left[\frac{.18R_c}{Na_2} \right]; \text{ if } \bar{\mu}_d = 3500$$

Equation 4

Note several assumptions which do not appear in the reference.

1. Drift mobility (μ_d) is 3500
2. Gate resistance is for a gate ω wide with only one feed point

Our profiles of mobility indicate that 3500 is a reasonably good value for LPE mobility, but somewhat on the low side for implanted FETs. For devices with different gate feed systems r_m must be modified. A tee geometry requires that r_m be divided by 4, etc. Each of the terms in Fukui's equation will now be discussed.

The noise coefficient seems to be very close to a minimum value. We have observed numerous devices with values of K greater than 0.033, but very few with K's less than 0.033. The N/a term implies that light channel doping and thick channels are best for low noise. We do not believe that this term is correct. Our lowest noise devices have been built with $N > 10^{17}$ and a $< 0.15 \mu m$. It may be that there is less intervalley scattering in heavier doped channels, which in effect reduces K. K is determined by first measuring the noise figure, and then the accessible parameters, VIZ:

L	Microscopic examination, electronic micrometer (filar)
N	Profile of test pattern diode
a	Profile of test pattern diode
ρ	Measurement of test pattern
h	DeK-TAC measurement
L_{sg}	Microscopic examination, electronic micrometer
a_1, a_2	Same as "a"
R_c	Contact resistance test pattern

With these data plus the noise figure, a value for K can be inferred.

The metal resistance term is very important. It was investigated in considerable detail on an ECOM Program [2] which ran concurrently with Phase II of this program. If a gate has a single feed point, the resistance between the gate and the channel is:

$$\begin{aligned} r_m &= \frac{1}{3} \text{ (resistance from feed point to end of gate)} \\ &= \frac{1}{3} \left(\frac{\rho}{h} \cdot \frac{\omega}{L} \right) \end{aligned} \quad \text{Equation 5}$$

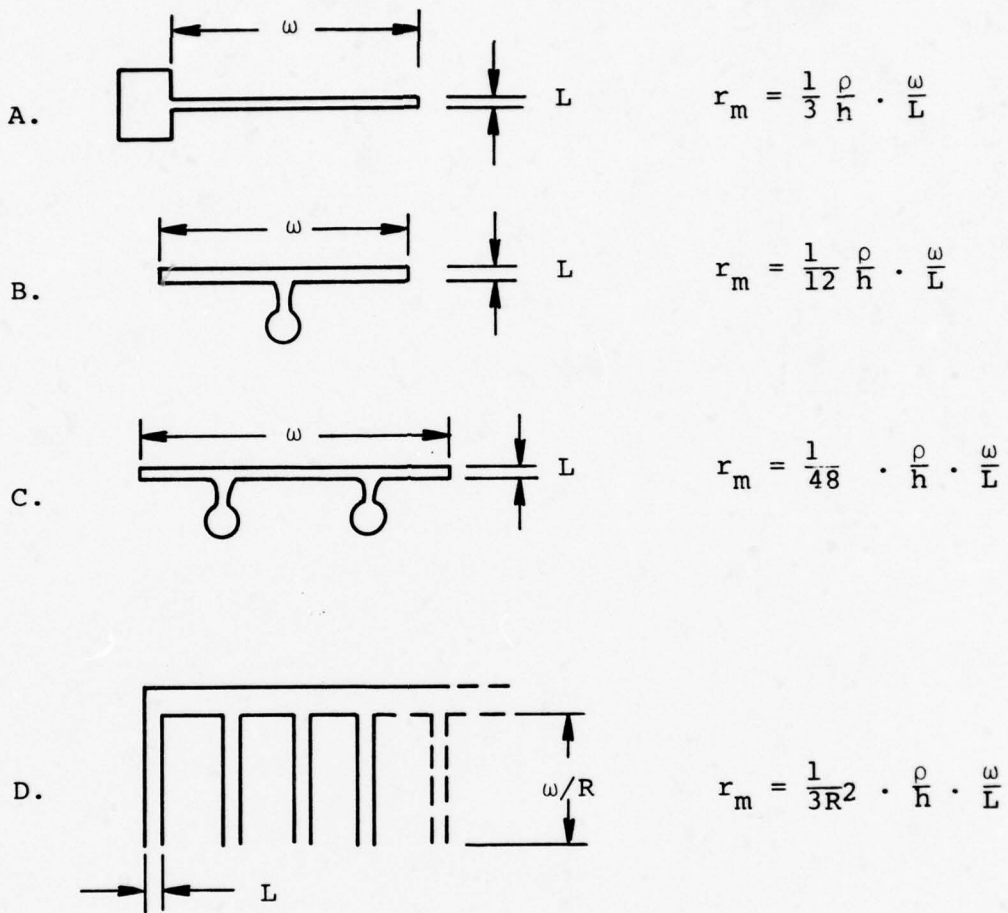
If there is more than one feed point, or more than one gate section, Eq. 2 must be modified. Figure 1 shows the appropriate equation for r_m , in several geometries.

As was pointed out in Phase I, the interdigitated geometry, Fig. 1D, can reduce r_m to an arbitrarily low value. Unfortunately, there are also some offsetting disadvantages to the interdigitated layout.

- Pad capacitance is high due to the interconnecting metal.
- Gate pad-to-source capacitance is higher since the source and gate metal are close. This was encountered with the M103 in Phase I.
- The isolated drains must be bonded individually, which results in a relatively complex and costly bonding scheme.

During Phase II we introduced two new geometries, the M104 (Fig. 1B) and the M107 (Fig. 1C). The reasons for adopting these geometries were the large parasitic capacitance associated with the gate pad in the M103. We can compare r_m as follows:

Figure 1
FET Gate Geometry & Gate Resistance, r_m



Gate is divided into R sections each of which is " L " long and $\frac{\omega}{R}$ wide

$$M103 \quad r_m = \frac{1}{3(6)^2} \cdot \frac{\rho}{h} \cdot \frac{360}{.5} = 6.67 \frac{\rho}{h}$$

$$M104 \quad r_m = \frac{1}{12} \frac{\rho}{h} \cdot \frac{150}{.5} = 25 \frac{\rho}{h}$$

$$M107 \quad r_m = \frac{1}{48} \frac{\rho}{h} \cdot \frac{300}{.5} = 12.5 \frac{\rho}{h}$$

Thus, for a given $\frac{\rho}{h}$, the M103 has an advantage in lower resistance. However, during the same interval, we investigated improving both ρ and h . The bulk conductivity of pure gold is about 4.1×10^{-5} mhos/cm. Plated gold, such as is used for gates, can vary in conductivity 40 to 90% of bulk or 1.64 to 3.7 mhos/cm. In general, "bright" gold is poorer in conductivity. Through experimentation, we were able to increase the conductivity from 40% to 70% bulk. At the same time, we increased h from $0.25 \mu\text{m}$ to $0.5 \mu\text{m}$. (We are presently increasing it still further to over $1 \mu\text{m}$.) If we now compare the 104 and 107 with new metal to the 103 with old metal, the resistance is as follows:

$$M103 \quad r_m = 6.67 \left(\frac{6.09 \times 10^{-6}}{.25 \times 10^{-4}} \right) = 1.49 \Omega$$

$$M104 \quad r_m = .25 \left(\frac{3.48 \times 10^{-6}}{.5 \times 10^{-4}} \right) = 1.74 \Omega$$

$$M107 \quad r_m = 12.5 \left(\frac{3.48 \times 10^{-6}}{.5 \times 10^{-4}} \right) = 0.87 \Omega$$

Therefore, by increasing the conductivity and metal thickness, we were able (in the case of the M107) to actually reduce r_m .

The M104 and M107 geometries are shown in Figs. 2 and 3. As shown in the calculation, the M104 has a $150 \times .5 \mu\text{m}$ gate and the M107 has a $300 \times 0.5 \mu\text{m}$ gate.

At this point, it will be necessary to digress slightly to explain in more detail the reasons for introducing the M104 and M107 geometries. During the early part of Phase I, measurements of the metal indicated the necessity for multiple gates and the first designs were of that type. However, the M103 (Fig. 4) and earlier designs always fell short on gain, particularly at higher frequencies. The problem was traced to parasitic gate capacitance of two kinds. Figure 4 shows how the gate metal is close to the source which introduces a parasitic capacitance of about .07 pFs in the M103. In addition, the gate pad has an area 60 times that of the active gate itself. It can be shown that the total gate capacitance is [2] as follows:

$$C_{\text{gate Total}} = C_{\text{gs}} \left[1 + \frac{A_p}{A_g} \left(\frac{N_{\text{buff}}}{N_{\text{active}}} \right)^{1/2} \right] + C_{\text{sw}} + C_{\text{misc}} \quad \text{Equation 6}$$

Where:

- A_p = area of gate pad
- A_g = area of active gate
- N_{buff} = doping level in region under gate pad
- N_{active} = doping level in region under active gate
- C_{sw} = side wall capacitance
- C_{misc} = metal capacitance, etc.

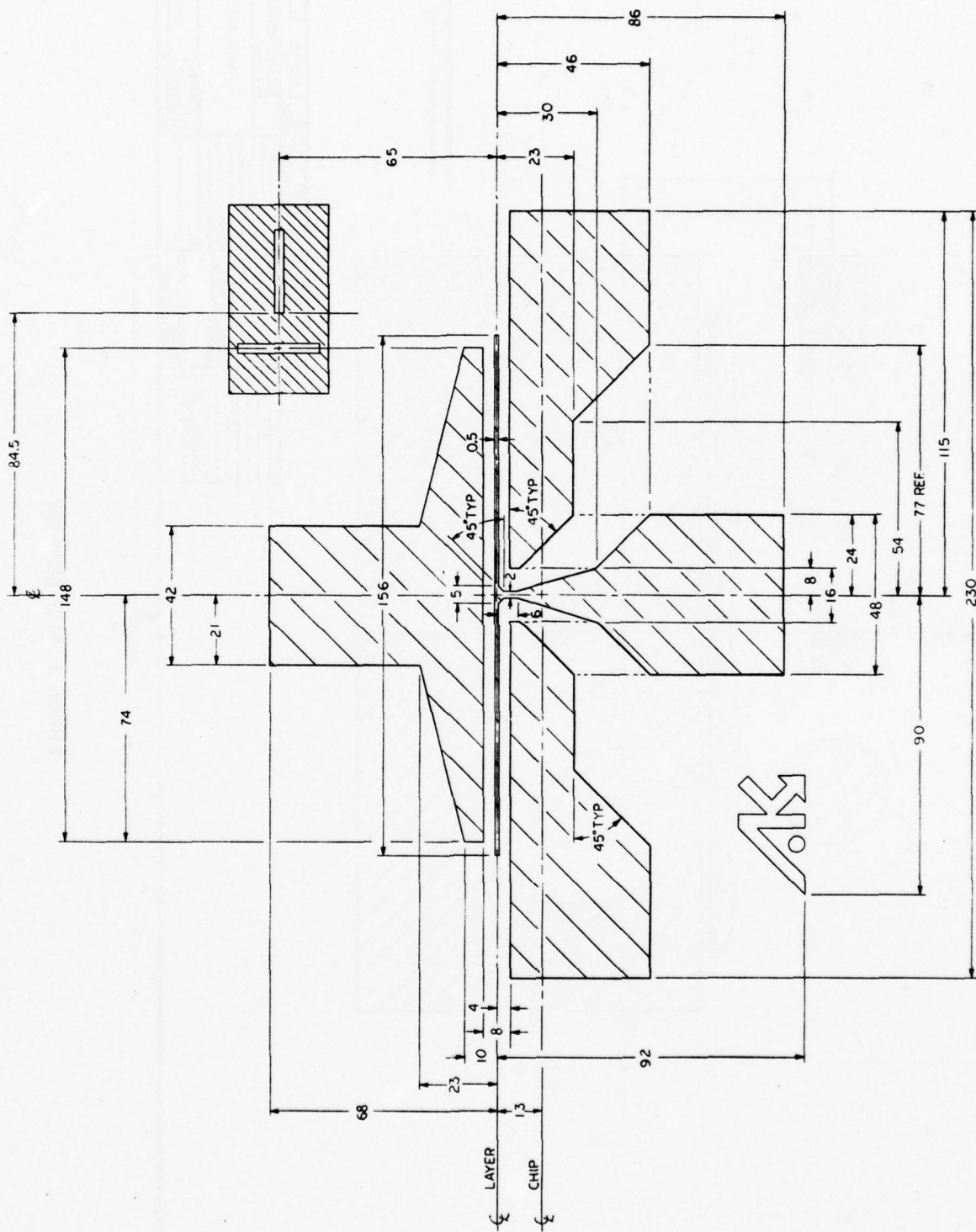


Figure 2 Composite Drawing of the MX-104
 Dimensions are in μM

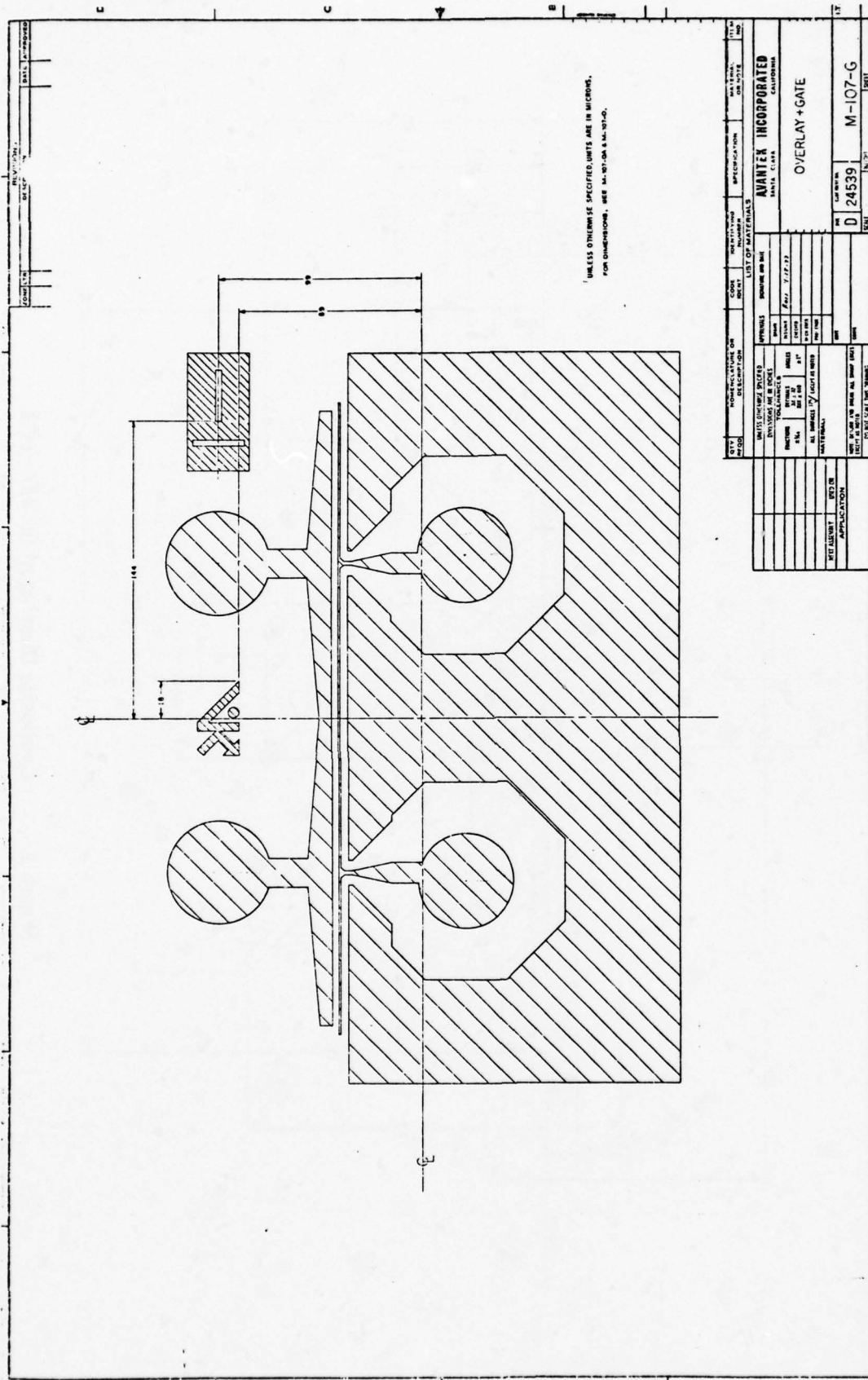
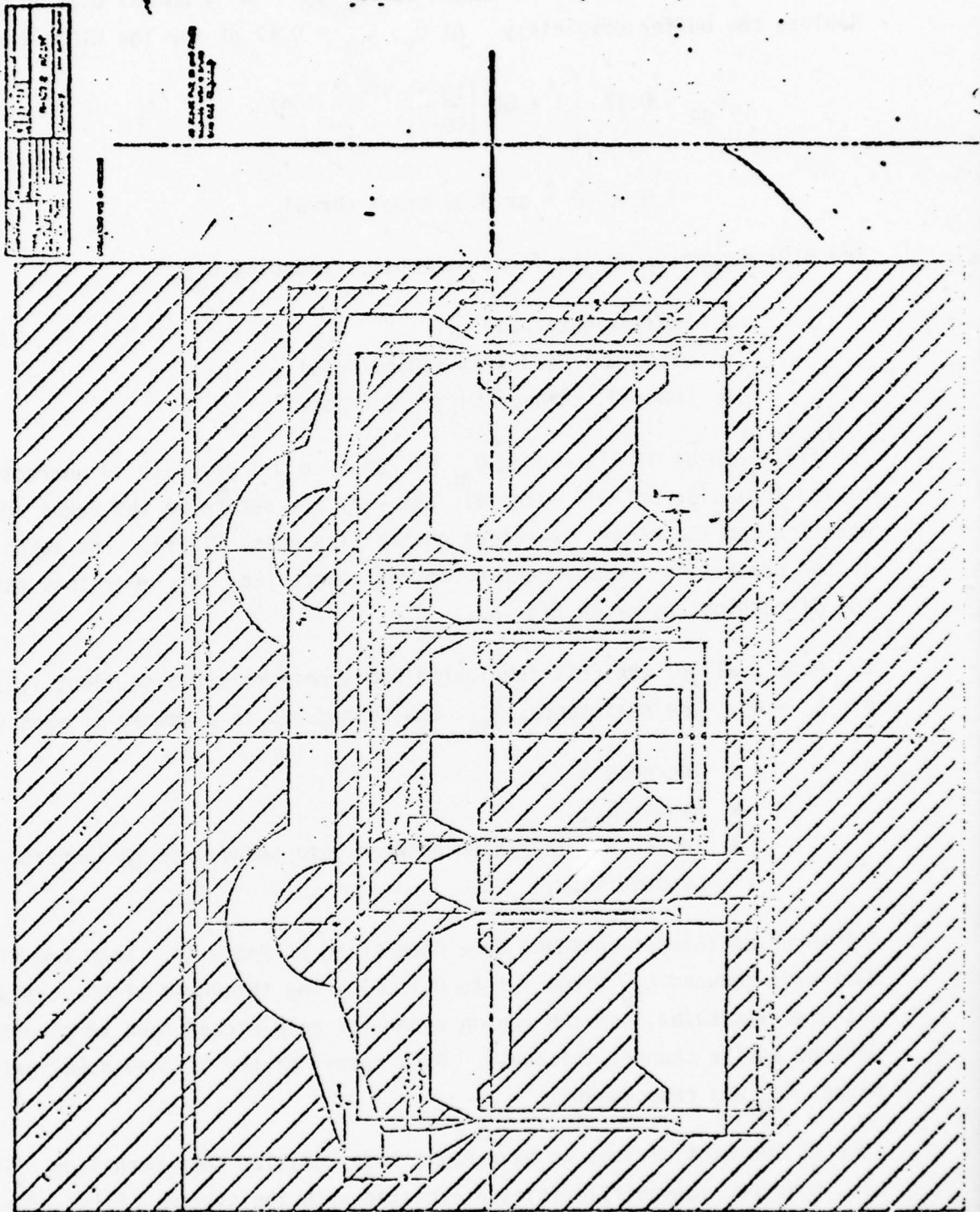


FIGURE 3 M107 GEOMETRY

FIGURE 4 M103 GEOMETRY



If the buffer is about 10 μm thick, and $N_{\text{buff}} \approx 10^{14}$, normal bias will not deplete the buffer completely. At 0_v , $C_{\text{gs}} = 0.17$ pF for the M103; then:

$$C_{\text{gs}} \approx 0.17 \left[1 + 60 \left(\frac{10^{14}}{10^{17}} \right)^{1/2} \right] + .07$$

$$= 0.56 \text{ pF} + \text{ or } 3.35 \text{ times normal.}$$

The M104 geometry was the first attempt at reducing C_{gs} .

- Smaller gate pad
- Gate separated from source metal
- Lower N, thinner buffer (or none)

The first run of M104's showed C_{gs} of close to 0.1 pF which is correct for a device that size on 10^{17} material. We will now return to the Fukui noise equation and the other parameters controlling noise figure. The second term in the bracket is the source-to-gate resistance (Eq. 1A). For this part of the discussion, refer to Fig. 5.

In Phase I all of the FETs fabricated had a uniform cross-section; i.e., $a = a_1 = a_2$. The resistance, R_{sg} , can be reduced in a number of ways.

- Increase a_1
- Reduce L_{sg}
- Increase N in region between gate and source to increase conductivity.

All three of these techniques have been tried in Phase II. Both the M104 and M107 have reduced L_{sg} (from 1.1 to 0.7 μm). The thickness of the channel (a_1) was also increased, and the region under the gate etched down to give the desired active channel thickness. As a result of the "etched-down" gate technique, R_{sg} was reduced 50%.

Some of the best devices we have built today utilize this technique. There are, however, some difficulties associated with the system. First of all, the proper etch system is important. Different etches result in different cross-sections (Fig. 6). The third system seems to work best, but absolutely accurate alignment is necessary. If the gate touches the sides of the trough,

Figure 5
FET Cross-Section Using Fukui's Notation

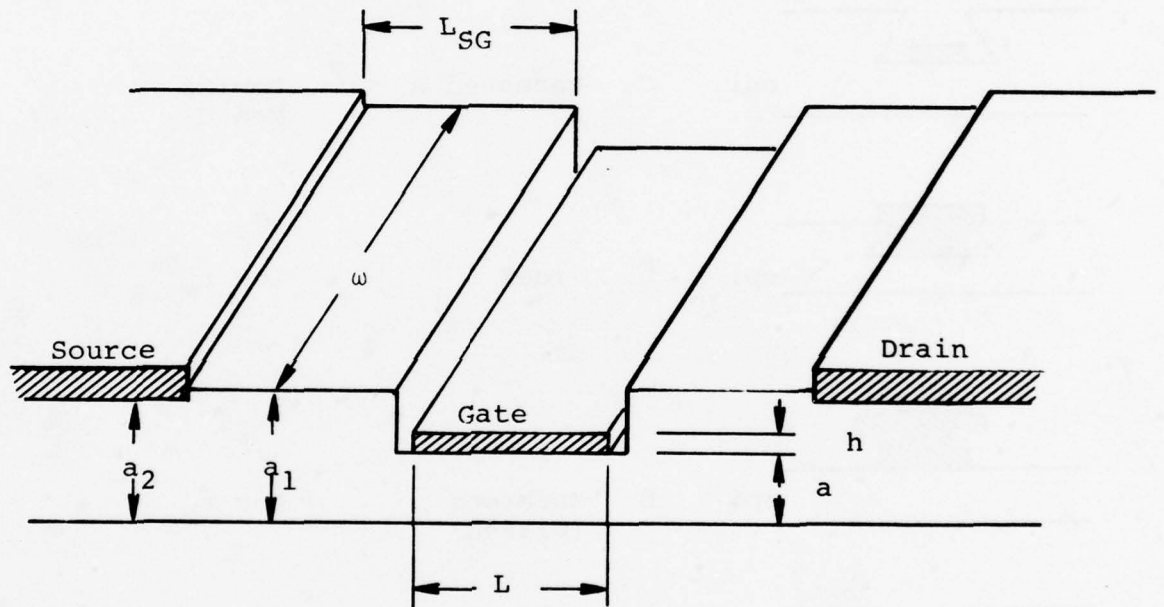
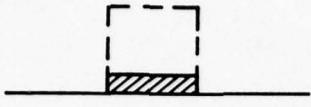

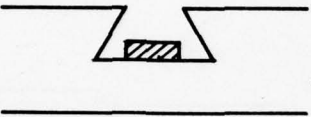
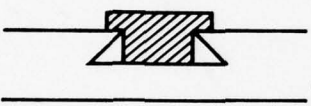
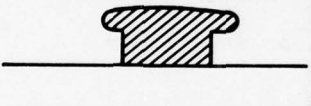
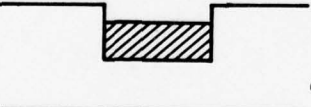



Figure 6
FET Gates

	<u>Type</u>	<u>Remarks</u>
 epi	A. Standard	Simple
 epi	B. "Vee"	High C _{gs} Low R _s
 epi	C. Recessed A	Low R _s Med C
 epi	D. "Tee"	Low r _m
 epi	E. Mushroom (plated)	Low r _m
 epi	F. Recessed B	High C Low R _s
 S.I. epi	G. Modified Vee	Med C _{gs} Short L _g

a large parasitic capacitance results which reduces gain and increases noise figure. Even when the gate is not touching the sides of the trough, the output capacitance, C_{gd} , is increased. This is because the total charge in the region next to the gate is increased. As a result, the gate-drain depletion layer is restrained from moving towards the drain. Devices with this type of gate show reduced noise figure and slightly reduced gain. It is possible that the increased C_{gd} results in negative feedback that reduces noise figure, particularly at lower frequencies. At 6 GHz, noise figures as low as 1.25 dB have been obtained with "etched down" gates.

The third term in the brackets in Eq. 1A is the contact resistance loss.

$$R_{con} = \frac{1}{\omega} \sqrt{\frac{R_c}{q\mu N a_2}} \quad \text{Equation 7}$$

Contact resistance can be improved by (ω kept constant):

- Increasing channel thickness, a_2
- Increasing N
- Increasing μ
- Reducing R_c , contact resistivity

The etched-down-gate process described earlier allows an increase in a_2 , which helps reduce contact resistance. What is not apparent from Eq. 4 is the effect of contact penetration. If the layer is very thin to begin with ($a_2 < 2\mu\text{m}$), the contact penetration may reach all the way to the buffer and contact is only through the sides of the contact. Thus, a thick layer under the source is doubly important.

Selective implantation and grown N^+ layers have both been used to increase N and reduce contact resistance. Both processes require that the region under the gate be etched away to get usable breakdowns. Etching is very critical, but the results can be worthwhile in terms of the superior performance.

The effect of mobility on contact resistance is probably a second order effect. No serious attempt was made to manipulate this parameter.

Contact resistivity is a major variable in FET performance. It is known to vary with:

- the metal system used
- the metal overlay used
- alloy time and temperature
- cleaning procedure used
- metal deposition method

Not all the variables in this system are perfectly understood as yet. The Ti/W-Au overlay on a Au/Ge contact will usually give a contact resistivity of $2 - 4 \times 10^{-6} \Omega \text{cm}^2$ on 10^{17} material. Contact resistivity is much more consistent on thick material, indicating the contact penetration may be the variable.

C. MOBILITY

The foregoing discussion based on Fukui's equation assumed a drift mobility of 3500. However, the all-important factor here is the mobility at the interface between the active layer and the layer underneath, whether it be a substrate or buffer. The role of mobility is explained as follows. For low noise operation, the drain diffusion noise of an FET varies inversely with the drain current, making low drain current desirable to reduce noise. However, as the active channel becomes pinched off, g_m will drop unless the mobility rises. Most epitaxial layers, both LPE and VPE, show a reduction in mobility as the device is pinched off. Figure 7 shows plots made from good and poor epitaxial material. The good device had a noise figure of 1.5 dB at 6 GHz, the poor device a noise figure of 3.0 dB at 6 GHz. A rising mobility characteristic has been most consistently achieved using implantation. Since implantation has been so important to this contract, the next major section will be mainly devoted to this subject. Although we have achieved a rising mobility characteristic on some epitaxial wafers, we have never seen the consistent high quality achieved with implantation.

The rising mobility characteristic, then means that g_m tends to remain constant as pinch-off is approached, and gain remains high even at low drain currents. There is an additional effect that is also important. When a device is biased

— Exp 338A, Implanted (good)
 -·-·- Reject Epi.

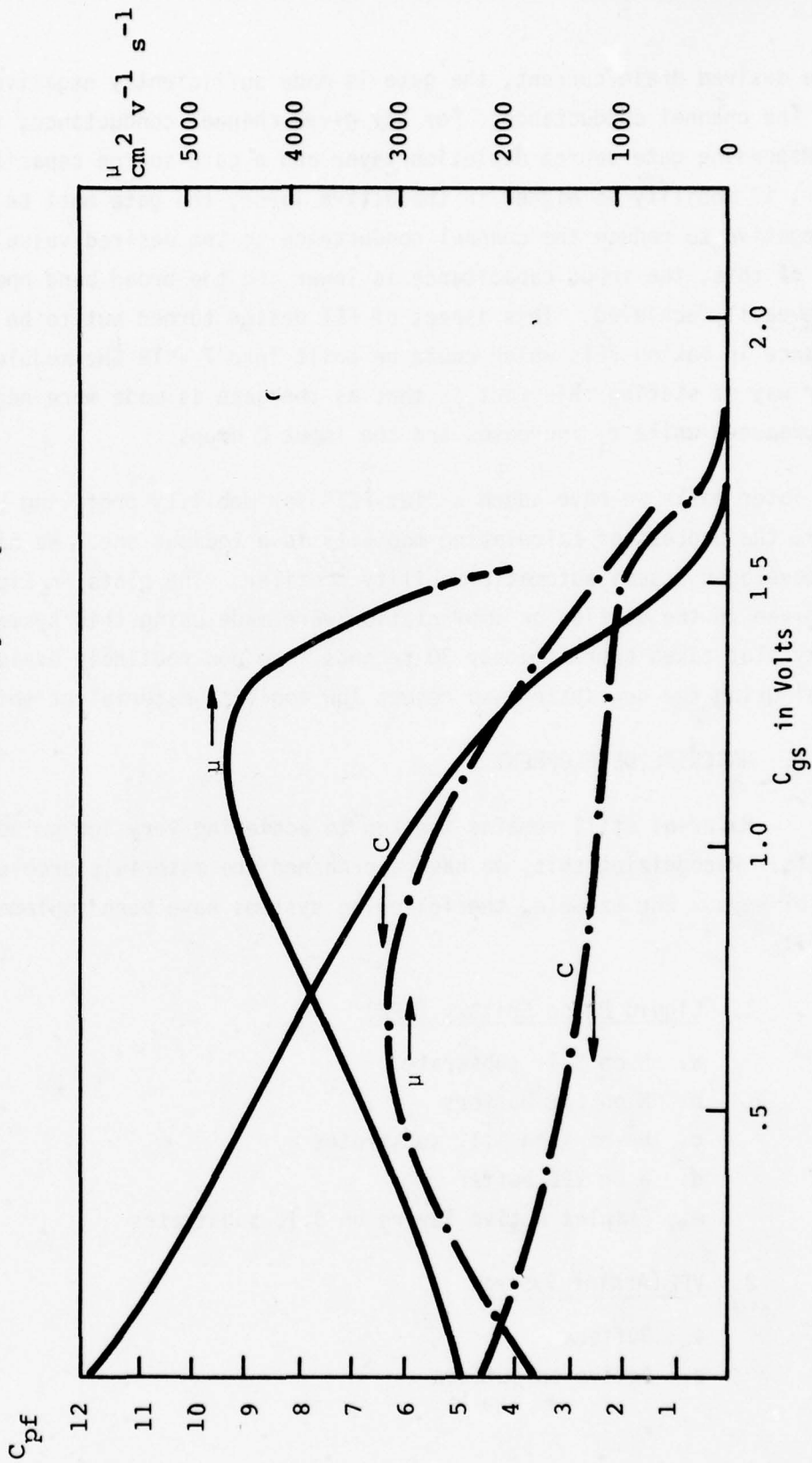


Figure 7
 Mobility & Capacitance Plots Taken From Two "Fat" FET Test Devices

to some desired drain current, the gate is made sufficiently negative to reduce the channel conductance. For any given channel conductance, there is a corresponding gate-source depletion layer and a gate source capacitance. However, if mobility is higher in the active layer, the gate must be made more negative to reduce the channel conductance to the desired value. As a result of this, the input capacitance is lower and the broad band operation is more easily achieved. This aspect of FET design turned out to be of major importance in making FETs which could be built into 7 - 18 GHz modules. Another way of stating this fact is that as the gate is made more negative, C_{gs} decreases, while r_i increases and the input Q drops.

In our later masks we have added a "fat-FET" for mobility profiling [3]. However, the process of calculating mobility is a tedious one. We have, therefore, developed a semi-automatic mobility profiler. The plots in Figure 7 and those given in the section on implantation were made using this system. A mobility plot takes approximately 30 seconds. We now routinely evaluate all material using the new system and reject low mobility material at this point.

D. MATERIAL DEVELOPMENT

Material still remains the key to achieving very low noise, high gain FETs. Recognizing this, we have approached the materials problem in a number of ways. For example, the following systems have been implemented in Phase II:

1. Liquid Phase Epitaxy (LPE)
 - a. N on S.I. substrate
 - b. N on LPE buffers
 - c. N^+ on N on S.I. substrates
 - d. N on VPE buffer
 - e. Complex active layers on S.I. substrates
2. VPE (Arsine System)
 - a. Buffers
 - b. Active on buffers

3. Implantation

- a. N on S.I. substrates
- b. N on VPE buffers
- c. N on LPE buffers
- d. N^+/N on buffer on S.I. substrates

As noted earlier, implantation has provided the most consistent high performance FETs. The section on implantation details the results of the various types of implantations tried. Excellent devices have also been built using all of the other schemes enumerated above, but the probability of achieving, say, a noise figure of <3.0 dB at 18 GHz is much lower than with implantation.

E. DESIGN FOR APPLICATION

It is our objective as device fabricators to design FETs to fit as closely as possible a specific application. An example of this was given earlier when it was pointed out that high mobility material could result in lower Q, larger bandwidth FETs.

We have been investigating the effects of device size and material on the suitability of an FET for a particular application. Noise figure of an FET is invariant with gate width, providing all parameters and parasitics scale linearly. However, S_{21} is not invariant with size (i.e., gate width), and it appears that there is an optimum size for any given frequency and material constants. The magnitude of S_{21} depends upon two factors:

1. The input match, i.e., S_{11}
2. The magnitude of the transfer coefficient (i.e., g_m)

Figure 8 shows a simplified equivalent circuit for calculating S_{21} . Note that S_{21} depends mainly on two factors:

- The fraction of the input voltage appearing across C, the input capacitance.
- The magnitude of g_m .

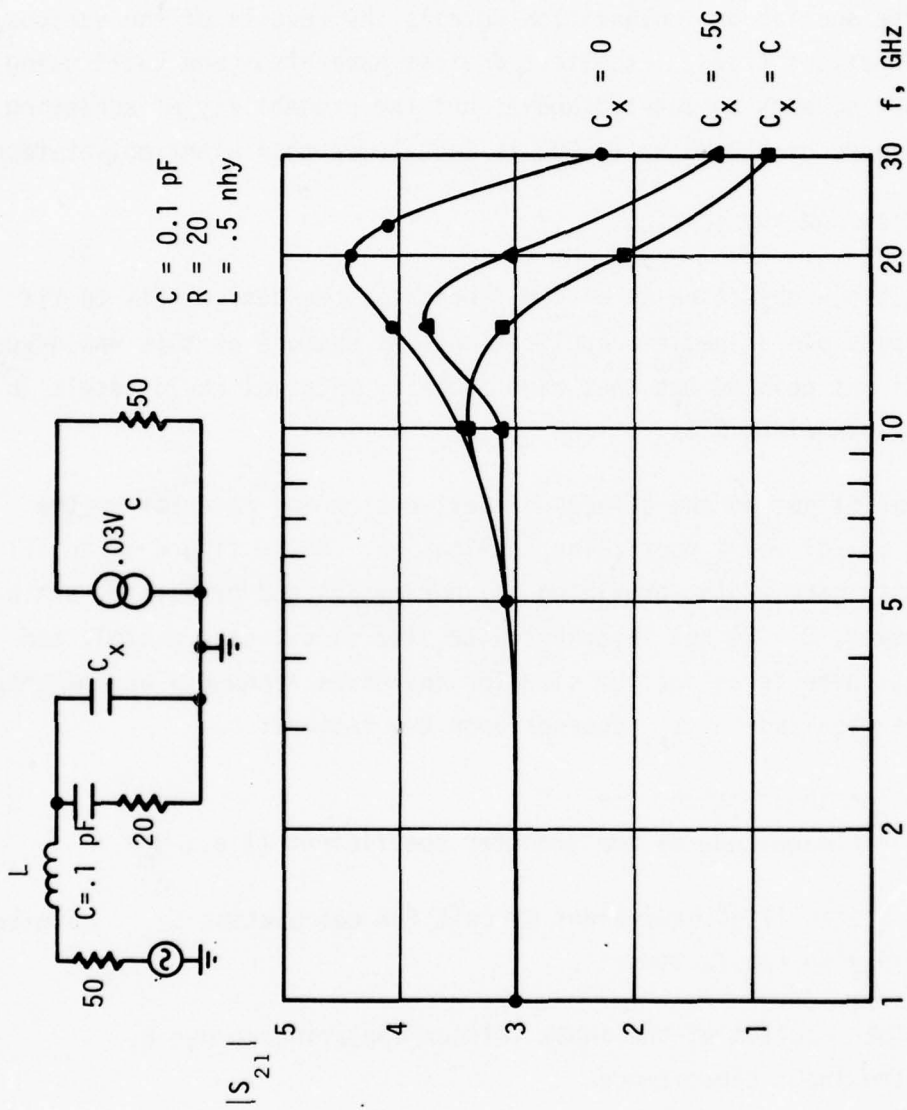


Figure 8
Theoretical Effect of C on S_{21}

From this equivalent circuit we can develop an approximate expression for S_{21} , with $Z_0 = 50\Omega$. For example:

$$|S_{21}| \cong \frac{100 g_m}{\left[(50+R)^2 (\omega C)^2 + \left\langle \left(\frac{f}{f_0} \right)^2 - 1 \right\rangle^2 \right]^{1/2}} \quad \text{Equation 8}$$

Where:

$$f_0 = \frac{1}{2\pi\sqrt{LC}}, \text{ is the input resonant frequency}$$

At very low frequencies, $(f/f_0)^2 \ll 1$ and $(\omega C)^2 \rightarrow 0$. Therefore:

$$S_{21} \Big|_{f=0} = 100 g_m$$

Using the M104 geometry, R , C and g_m were calculated for three different channel carrier concentrations. The results are given in Table I. The value of L is fixed at 0.5 nhy (one bonding wire) and the bias was adjusted to keep a constant drain current. Figure 8 shows three plots of S_{21} vs. frequency. These curves show that S_{21} always peaks below f_0 because the voltage across C is inversely proportional to frequency. These curves can be compared with Figure 9, which shows measured values of S_{21} vs. frequency for three FETs.

As will be shown in the circuit section, a low C , lower g_m FET is best for broadband operation. This is confirmed by the obviously wider band width of the low C device in Figure 8 and Table I.

TABLE I
EFFECT OF N ON FET PARAMETERS

($C_x = 0$)

N cm ⁻³	C pF	R ohms	g_m mmhos	f_0 , input GHz
1×10^{17}	0.1	20	25	22.5
2×10^{17}	0.15	15	30	18.4
5×10^{17}	0.20	10	35	15.91

Mx 104 ID \approx 10 ma
 S_{21} vs. N vs freq.

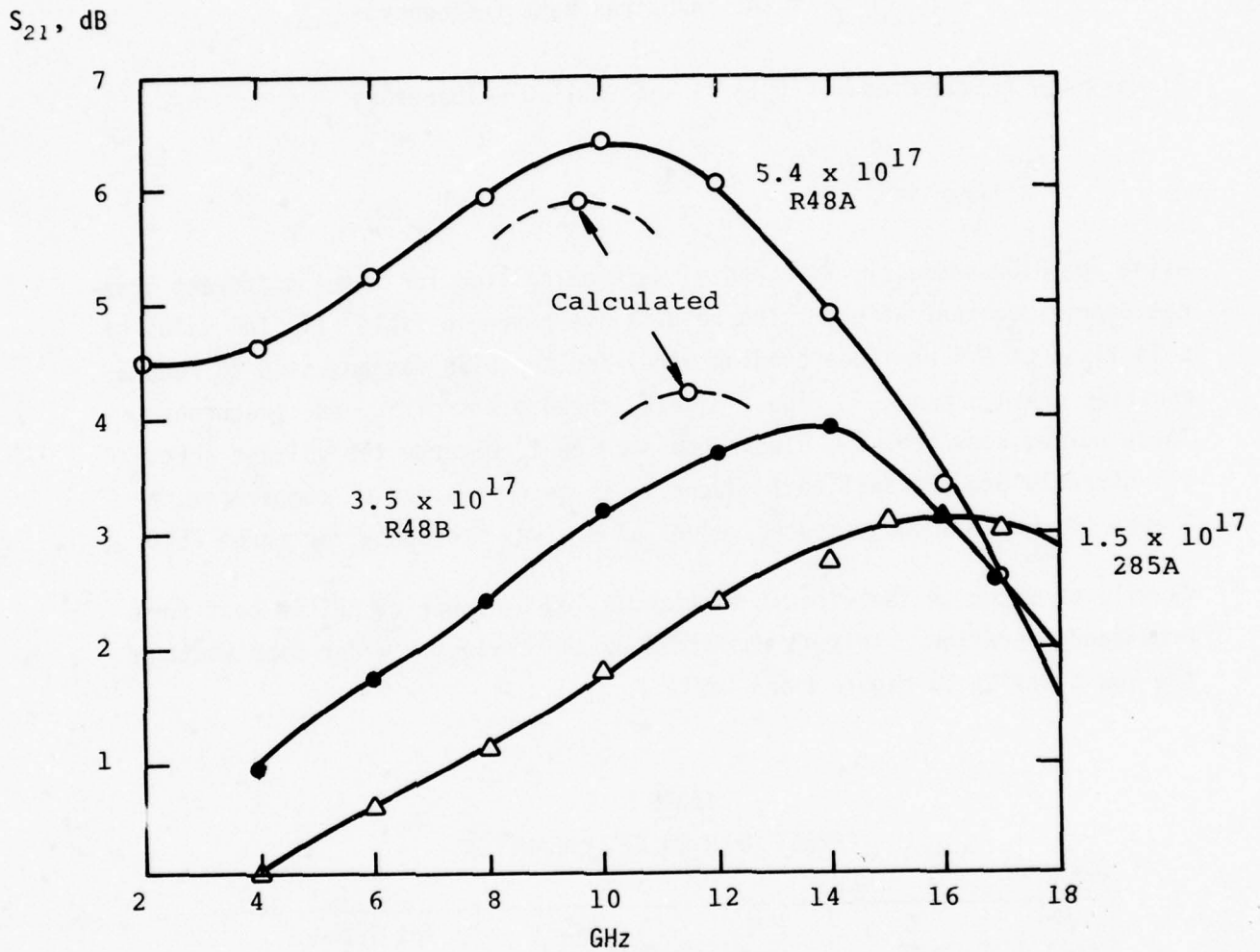


Figure 9
Mx 104
 S_{21} vs. frequency with N as a Parameter

This effect had a very real impact on our FET design for the amplifiers. The heavily doped device in Fig. 9 had the best X band value of S_{21} and noise figure of any device fabricated previously. However, as a KU band amplifier, it was definitely inferior to the lightest doped of the three FETs. As a matter of practical experience, it was found that the gate resonant frequency should be near the high end of the amplifier pass-band, but not too much higher. Devices with gate resonant frequencies near 25 GHz gave very flat, but low, gain in the amplifier modules. For the transistors shown in Fig. 9, which are MX104's, the optimum doping is near to 1.5×10^{17} . If the gate length were reduced to less than $0.5 \mu\text{m}$, N could be increased further, while still maintaining the same resonant frequency. Obviously this would result in an even better device for the application.

As a result of this study, we have been tailoring the implantation schedule for the M104 and M107 to keep gate resonances in the 16-18 GHz region. The result has been that the amplifier development group has made modules which are flat from 6-18 GHz.

The size of the FET is, of course, a major factor in wideband design. When the M104, $150 \mu\text{m}$, FET was introduced, we believed that the small device would favor operation at 18 GHz and, thus, be most desirable. This turned out to be only partially true. While excellent performance could be achieved at 18 GHz and higher, the device was extremely difficult to match in a broadband design, particularly at the low end near 7 GHz. The section on amplifiers indicates the results of a computer study which showed the desirability of a larger device to maintain low end performance. As a result of this study, the M107 was introduced which has a gate $300 \mu\text{m}$ wide and $0.5 \mu\text{m}$ long. It can be matched at the low end of the band much more easily.

The results above point out the general direction which should be taken to develop higher frequency FETs, i.e., 18-26 GHz and above. As the device is made smaller to facilitate matching at the higher frequencies, the channel doping should be increased to maintain a reasonable g_m . For broadband operation as much of the device gain as possible should come from S_{21} (i.e., g_m), and a lesser amount from impedance transformation. However, as the doping level N is increased, C_{gs} would also increase reducing the gate resonant

frequency. Therefore, the capacitance increase should be offset by:

- Shortening gates, reducing C_{gs}
- Shortening or eliminating input bond wires to reduce gate inductance

F. FET PERFORMANCE

In the section on amplifiers, the printout from the ANA will be used to show the type of S parameters which are characteristic of implanted FETs. These can be used to study the finer structure of S_{21} , S_{11} , etc. A noise figure vs. frequency curve is given in Fig. 10. This run was implanted with silicon as the donor species. The noise figure in the band of interest (7-18 GHz) is close to the state-of-the-art for FETs in general. We have achieved lower noise figures in S and C band using a larger, 500 μm , FET, but its KU band performance was not as good as the 300 or 150 μm FETs. The noise figure of the 500 μm FET was 1.0 and 1.25 dB at 4 and 6 GHz, respectively. Again, the performance was achieved by implantation.

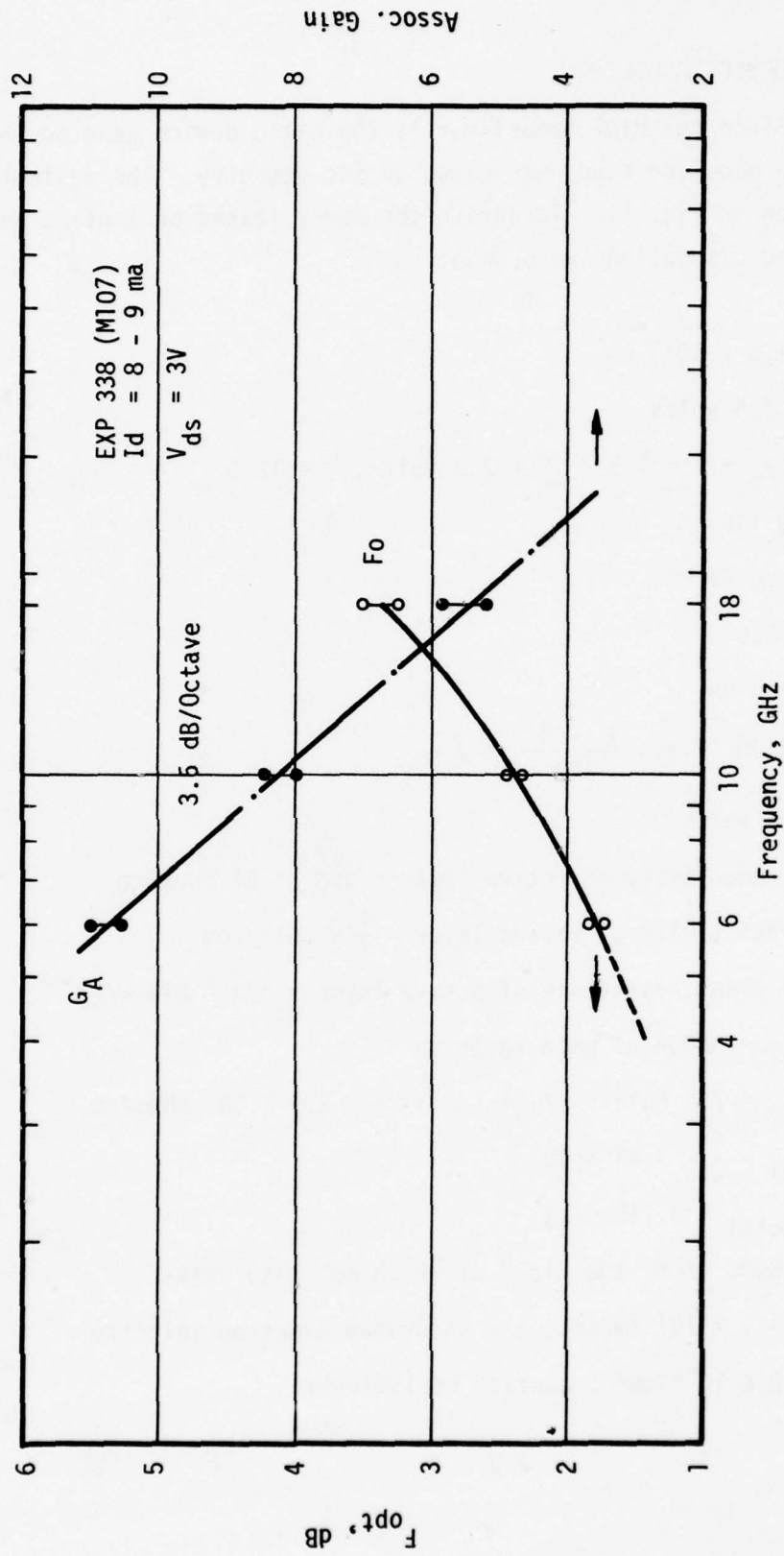


Figure 10
Noise Figure and G_{NF} , Implanted FET

G. DEVICE MODELING

Since the M107 transistor is the basic device used in the gain modules, the modeling study was based on its geometry. The equivalent circuit is given in Fig. 11. To derive the model (based on implant design), the following assumptions were made:

$$\bar{N} = 1.5 \times 10^{17} \text{ cm}^{-3}$$

$$V_p = 1.5 \text{ volts}$$

$$W_o = V_p + \phi = 1.5 + .8 = 2.3 \text{ volts}, \epsilon = 12.5$$

$$a = 0.146 \text{ } \mu\text{M}$$

$$L_{sg} = 0.75 \text{ } \mu\text{M}$$

$$L_g = 0.5 \text{ } \mu\text{M}$$

$$\omega = 300 \text{ } \mu\text{M}$$

$$\mu = 3500, \text{ i.e., } \frac{N^+ + N^-}{n} = 2$$

$$\phi = 0.8 \text{ volts}$$

$$\sigma = \text{conductivity of active layer} = q\mu N = 84 \text{ mhos/cm}$$

$$\rho = \text{resistivity of active layer} = \frac{1}{\sigma} = .012 \text{ } \Omega \text{ cm}$$

$$R_{sa} = \text{sheet resistance of active layer} = \rho/a = 815 \text{ } \Omega/\square$$

$$t_{\text{metal}} = 3000 \text{ \AA of gold} = 0.30 \text{ } \mu\text{M}$$

$$\sigma_{\text{metal}} = 70\% \text{ bulk} = .7 (4.1 \times 10^5) = 2.9 \times 10^5 \text{ mhos/cm}$$

$$\rho_{\text{metal}} = \frac{1}{\sigma} = 3.45 \times 10^{-6}$$

$$R_{sm \text{ metal}} = 0.115 \text{ } \Omega/\square$$

$$\epsilon_p = 5500 \text{ v/cm, the field at which mobility peaks}$$

$$V_{\text{sat}} = 1 \times 10^7 \text{ cm/sec, the saturated electron velocity}$$

$$\rho_c = 2 \times 10^{-6} \text{ } \Omega \text{ cm}^2, \text{ contact resistivity}$$

CALCULATION OF PARAMETERS FOR FIG. 11

$$R_{sg} = \frac{L_{sg} \times R_s}{\omega} = \frac{0.75 \times 10^{-4} \times 815}{.03} = 2.04\Omega \quad \text{Equation 9}$$

$$r_{con} = \frac{1}{\omega} \sqrt{R_s \rho_c} = \frac{1}{.03} \sqrt{815 \times 2 \times 10^{-6}} = 1.35\Omega \quad \text{Equation 10}$$

$$R_s = R_{sg} + r_{con} = 3.39 \quad \text{Equation 11}$$

$$R_{gate} = \frac{1}{48} R_s \cdot \frac{\omega}{L} = \frac{1}{48} (.115) \frac{(300)}{5} = 1.44\Omega \quad \text{Equation 12}$$

$$I_{dss} = qN V_{sat} \omega a \left[1 - \left(\frac{\phi + I_{dss} R_s + \epsilon p L}{\omega_0} \right)^{\frac{1}{2}} \right] \quad \text{Equation 13}$$

$$= 0.105 \left[1 - \left(\frac{1.075 + I_{dss} \times 3.4}{2.3} \right)^{\frac{1}{2}} \right]$$

$$= .03 = 30 \text{ ma}$$

$$g_m = V_{sat} \omega \sqrt{\frac{\epsilon \epsilon_0 q N}{2(\phi + I_{dss} R_s + \epsilon p L)}} \quad \text{at } I_{dss} \quad \text{Equation 14}$$

$$= .032 = 32 \text{ mmhos}$$

$$V_{ds(sat)} = .9 I_{dss} (R_s + R_d) + \epsilon p L = \text{saturation voltage} \quad \text{Equation 15}$$

$$= .9 (.03)(3.39 + 3.39) + 5500 (.5 \times 10^{-4})$$

$$= 0.46 \text{ volts}$$

$$C_{gs,0V} \approx \omega L \sqrt{\frac{q N \epsilon \epsilon_0}{2(I_{dss} R_s + .8)}} \quad \text{Equation 16}$$

$$= 0.149 \text{ pF}$$

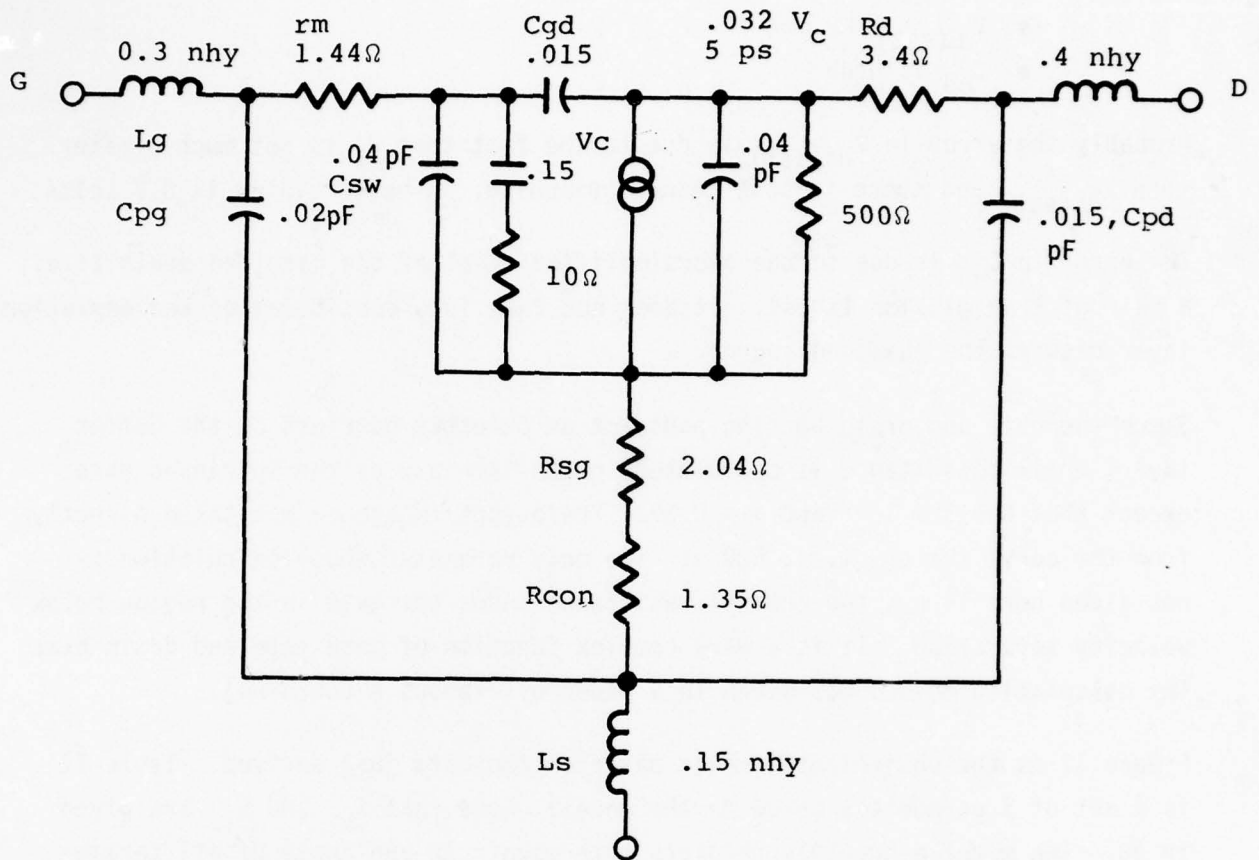
$$C_{sw} = .04 \text{ pF}$$

$$C_{gd} = .015, C_{ds} = .04 \text{ (from transmission line analog)}$$

$$C_{pad} = .02 \text{ pF, i.e., } N_{buff} \cong 5 \times 10^{12}$$

$$r_1 \cong 10 \text{ } \Omega \text{ at } I_{dss}$$

Figure 11
FET Equivalent Circuit (M107)



L_g , L_d , L_s = bonding wire inductances
 r_m = gate metal resistance
 C_{sw} = sidewall capacitance, gate-source junction
 R_{sg} = resistance of channel between gate and source
 R_{con} = source contact resistance
 R_D = drain resistance $\triangleq R_{gd} + R_{con}$ (drain)
 C_{pg} = gate pad capacitance
 C_{pd} = drain pad capacitance

The calculations give excellent agreement with measured values with the following exceptions:

- $V_{ds(sat)}$ is low
- C_{gd} is high

Probably the error in $V_{ds(sat)}$ is due to the fact that V_p is not much greater than $V_{ds(sat)}$ and there is some channel pinching. A better value is 0.7 volts.

The error in C_{gd} is due to the oversimplified model of the gate and drain (i.e., a pair of transmission lines). It does not take into consideration the depletion layer between the gate and source.

Since the gate and drain bonding pads act as Schottky barriers on the buffer layer, their capacitance is calculated in the same way as the intrinsic gate except that $N \cong 5 \times 10^{12}$ and $\phi = 0.5V$. The output impedance was taken directly from the curve tracer, i.e., 500Ω . The only parameter whose calculation is not given here is r_i , the channel resistance under the gate in the region below velocity saturation. It is a very complex function of both gate and drain bias. The calculation method was given in a paper by Gibbons & Cooke [4].

Figure 11 is the equivalent circuit based on the data just derived. Table II is a set of S parameters based on the model. Note that S_{21} and S_{12} are given in dB. The model accurately predicts both magnitude and angle of all parameters. It shows some minor differences from measured FET data given in the amplifier section. The differences are mainly due to variations in the doping level, N , and the channel thickness, a , compared to the model.

TABLE II
CALCULATED S PARAMETERS FROM EQUIVALENT CIRCUIT

F(GHz)	SPAR 11	SPAR 21	SPAR 21	SPAR 21	SPAR 12	SPAR 12	SPAR 22	SPAR 22	SPAR 22	MAG 11	K 11
4.000	0.91	-39.53	7.52	137.89	-29.22	74.13	0.81	0.81	-11.25	0.00	0.48
6.000	0.82	-59.42	7.14	117.93	-26.56	68.94	0.78	0.78	-16.35	0.00	0.72
8.000	0.72	-79.81	6.69	99.03	-25.05	66.95	0.75	0.75	-21.17	0.00	0.94
10.000	0.63	-101.20	6.20	81.24	-23.94	68.78	0.73	0.73	-26.06	13.16	1.10
12.000	0.56	-123.90	5.69	64.44	-22.68	73.71	0.70	0.70	-31.52	11.93	1.14
14.000	0.53	-147.41	5.20	48.42	-20.90	79.13	0.68	0.68	-38.15	12.00	1.03
16.000	0.53	-170.22	4.72	32.88	-18.65	82.12	0.65	0.65	-46.71	0.00	0.83
18.000	0.57	169.22	4.24	17.45	-16.22	81.32	0.62	0.62	-58.14	0.00	0.62
20.000	0.63	151.38	3.73	1.71	-13.84	76.69	0.58	0.58	-73.77	0.00	0.43
22.000	0.71	135.72	3.08	-14.71	-11.67	68.58	0.53	0.53	-95.42	0.00	0.29
24.000	0.80	121.43	2.17	-31.91	-9.86	57.49	0.50	0.50	-124.67	0.00	0.19
26.000	0.88	108.08	0.83	-49.40	-8.55	44.25	0.50	0.50	-160.04	0.00	0.12
28.000	0.93	95.87	-1.06	-65.96	-7.81	30.22	0.55	0.55	165.11	0.00	0.08
30.000	0.95	85.37	-3.50	-79.97	-7.61	16.89	0.63	0.63	136.47	0.00	0.09
32.000	0.95	76.84	-6.38	-90.10	-7.80	5.22	0.70	0.70	114.71	0.00	0.14
34.000	0.95	70.12	-9.53	-95.27	-8.21	-4.53	0.76	0.76	98.38	0.00	0.25
36.000	0.94	64.84	-12.75	-94.33	-8.74	-12.53	0.81	0.81	85.99	0.00	0.44
38.000	0.93	60.59	-15.63	-86.28	-9.30	-19.11	0.85	0.85	76.40	0.00	0.72
40.000	0.93	57.08	-17.49	-72.57	-9.86	-24.57	0.87	0.87	68.81	0.00	1.00

II. ION IMPLANTATION

Progress in ion implanted FETs at Avantek has been excellent during the period covered in this report and, in particular, during the past quarter. Implanted FETs are now fabricated routinely which show 6 GHz NF = 1.7 dB and gain >10 dB. These devices have shown NF = 2.5 dB @ 18 GHz, with >6 dB gain.

An obvious advantage of an implanted FET is reproducibility from run to run, as well as uniformity of the device characteristics. An additional benefit is the impurity profile shape which results in an FET with very low input capacitance and excellent high frequency performance. Recent performance indicates that this conclusion is borne out.

A. Si_3N_4 CAP AND ANNEALING

The high temperature behavior of the dielectric cap used for annealing the implanted GaAs wafer is undoubtedly the single most critical parameter in the FET implantation process. Such properties as index of refraction, stoichiometry, coefficient of expansion, and density are key factors in obtaining the highest possible electrical activity of the implanted layer. Changes in the physical properties of the GaAs surface under the annealing cap can cause totally unpredictable results with respect to the electrical properties of the annealed implanted layer. This is, of course, particularly true of low energy shallow implants.

During the course of this work we have concentrated on the use of a low temperature Si_3N_4 plasma deposition system [5] to provide the annealing cap used in the implanted FET process. The use of a low temperature (<500°C) Si_3N_4 deposition minimizes the loss of As from the GaAs surface during the deposition cycle. This advantage is particularly important where shallow implanted layers are concerned.

Figure 12 shows a schematic representation of such a Si_3N_4 deposition system. A silane (SiH_4) and nitrogen gas mixture is introduced into the gas manifold and ionized by the R.F. field applied between the manifold and substrate platform. Si_3N_4 is deposited at 200 - 400°C normally to a thickness of ~1000Å. The index of refraction, n, determined with an ellipsometer, is $2.03 \pm .01$.

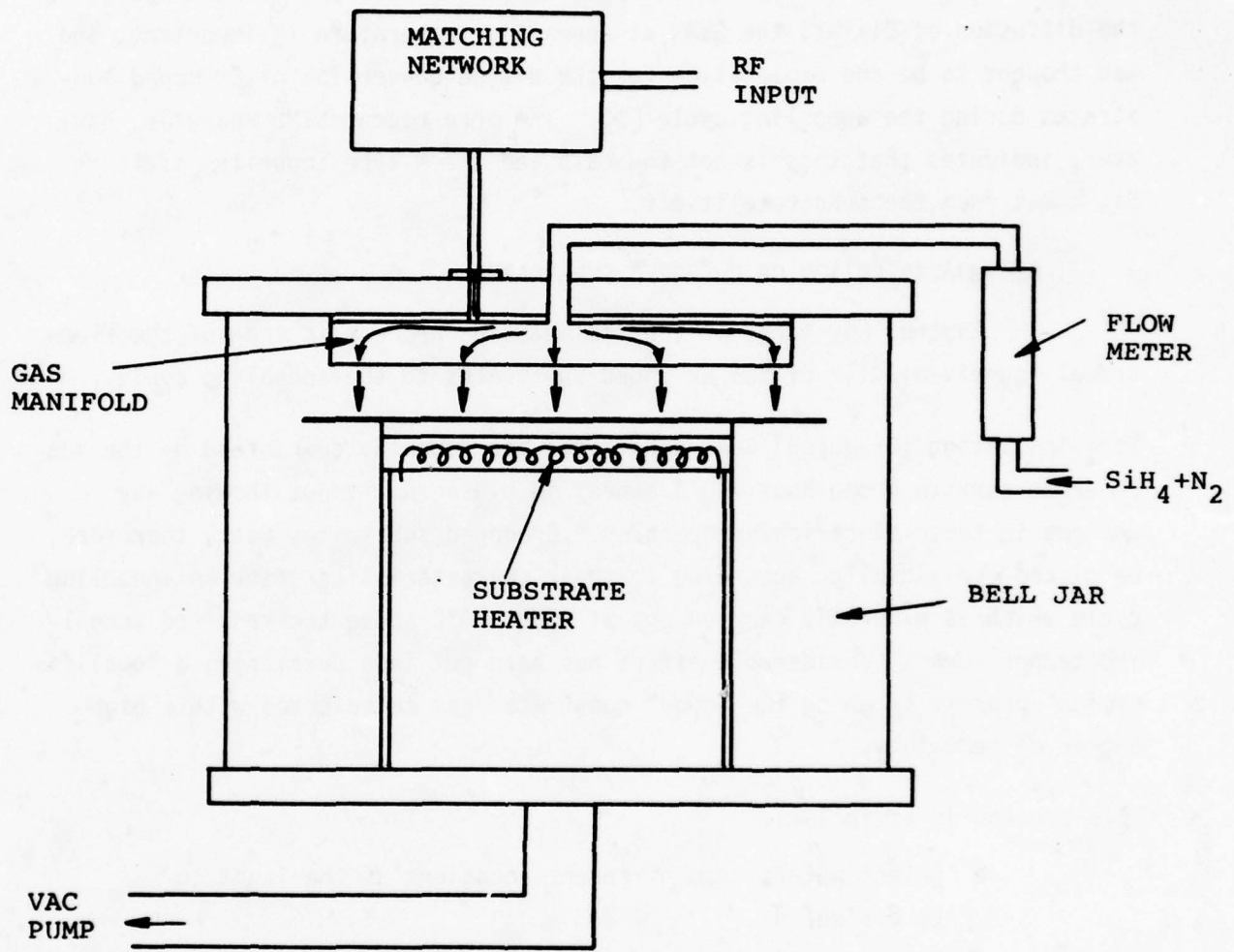


FIGURE 12
SILICON NITRIDE DEPOSITION SYSTEM

Analysis of these Si_3N_4 films by Auger and SIMS techniques [6] shows them to be perfectly stoichiometric and oxygen-free before and after annealing at temperatures as high as 1050°C . In addition, no in-diffusion of Si from the Si_3N_4 could be detected at the GaAs surface, or loss of Ga or As from the GaAs into the Si_3N_4 film. The possibility of the Si_3N_4 film providing a source for the diffusion of Si into the GaAs at annealing temperature is important, and was thought to be one explanation for the N-type conversion of Cr coped substrates during the annealing cycle [7]. The more recent SIMS analysis, however, indicates that this is not the case and the N-type impurity, if it is Si, comes from the substrate itself.

B. QUALIFICATION OF Cr DOPED SUBSTRATES

Another key facet of the implantation process is that of the electrical "survivability" of the Cr doped substrates to the annealing cycle.

Semi-insulating (Cr doped) GaAs substrates are normally guaranteed by the supplier to survive a one-hour 750°C anneal in hydrogen without showing any changes in their electrical properties. Cr doped substrates must, therefore, be picked individually, according to their characteristics after an annealing cycle which is generally carried out at least 50°C above the required annealing temperature. Considerable effort has been put into developing a "qualification" process by which the "good" substrates can be selected with a high degree of certainty.

This process is as follows:

- Select wafers from different locations of the ingot to be evaluated
- Measure surface breakdown voltage with 2-point probe and surface capacitance, C_S , with a Schottky diode ($V_B > 1500\text{V}$, $C_S < 0.1 \text{ pF}$)
- Deposit 1000\AA Si_3N_4 and anneal at desired temperature
- Remove the Si_3N_4 and remeasure the surface breakdown and capacitance (V_B must be $> 1000\text{V}$, $C_S < 0.5 \text{ pF}$)

Table III shows typical data obtained for several Cr doped GaAs ingots purchased from a leading GaAs supplier. From the surface capacitance, C_s , the surface doping is calculated using the expression:

$$N_s = \left(\frac{C_s}{A} \right)^2 \frac{2 V_{bi}}{qK} \quad \text{Equation 17}$$

Where A is the area of the Schottky diode, K is the dielectric constant of GaAs and V_{bi} is the built-in voltage (which is taken to be 0.7V). The choice of $V_B = 0.7V$ is only valid for $N_s \approx 10^{17} \text{cm}^{-3}$. For $N_s < 10^{16} \text{cm}^{-3}$ the actual value will be lower than the calculated value using $V_B = 0.7V$ (for $N_s = 10^{14} \text{cm}^{-3}$, $V_{bi} = 0.6V$). Since we are interested in the trend rather than absolute value, V_{bi} is assumed = 0.7V. Figure 13 shows a plot of measured surface breakdown vs. calculated surface doping, N_s . Data points were obtained from several different ingots annealed at 900°C. The lowering of surface breakdown voltage and increase in surface doping after annealing is always N-type in behavior. The dopant appears to be Si. Hall measurements indicate that $\mu = 1500\text{-}2000 \text{ cm}^2\text{V}^{-1}\text{sec}^{-1}$. A typical impurity distribution of such N-type conversion is shown in Fig. 14. It is evident that such a profile would make it impossible to fabricate an FET. Figure 15 depicts the implantation profile obtained with a "good" and "bad" Cr doped substrate.

We have found 100% correlation between the characteristics of the finished FET and the profile resulting from the qualification test.

C. ION IMPLANTATION

Ion implanted FETs have been fabricated for this program using Se and Si ions, with energy ranging from 50 KeV (Si) to 400 KeV (Se).

Substantial improvements have been achieved during the past six months in the Si_3N_4 capping process, as well as ohmic contact technology. As a result, overall performance of implanted FETs has continually improved. We have achieved excellent results using Si as the impurity. Si, because it is the lightest of the N-type dopants, gave us greater flexibility from a range point of view than Se.

TABLE III

Summary of surface breakdown voltage and capacitance before and after 900°C
1/2-hr. anneal. Surface protected with 1000Å Si_3N_4 during anneal.

GaAs Ingot	Before Anneal		After Anneal	
	V_B	C_s	V_B	C_s
20283	>1500	<0.1 pF	1300V	3.4 pF
285	"	"	110V	37.0 pF
311	"	"	350V	11.6 pF
312	"	"	1500V	3.8 pF
003	"	"	1400V	4.8 pF
004	"	"	60V	77.0 pF
009	"	"	1200V	4.3 pF
010	"	"	1300V	3.8 pF
011	"	"	1190V	5.3 pF
012	"	"	10V	480.0 pF
017	"	"	200V	26.0 pF
018	"	"	30V	152.0 pF

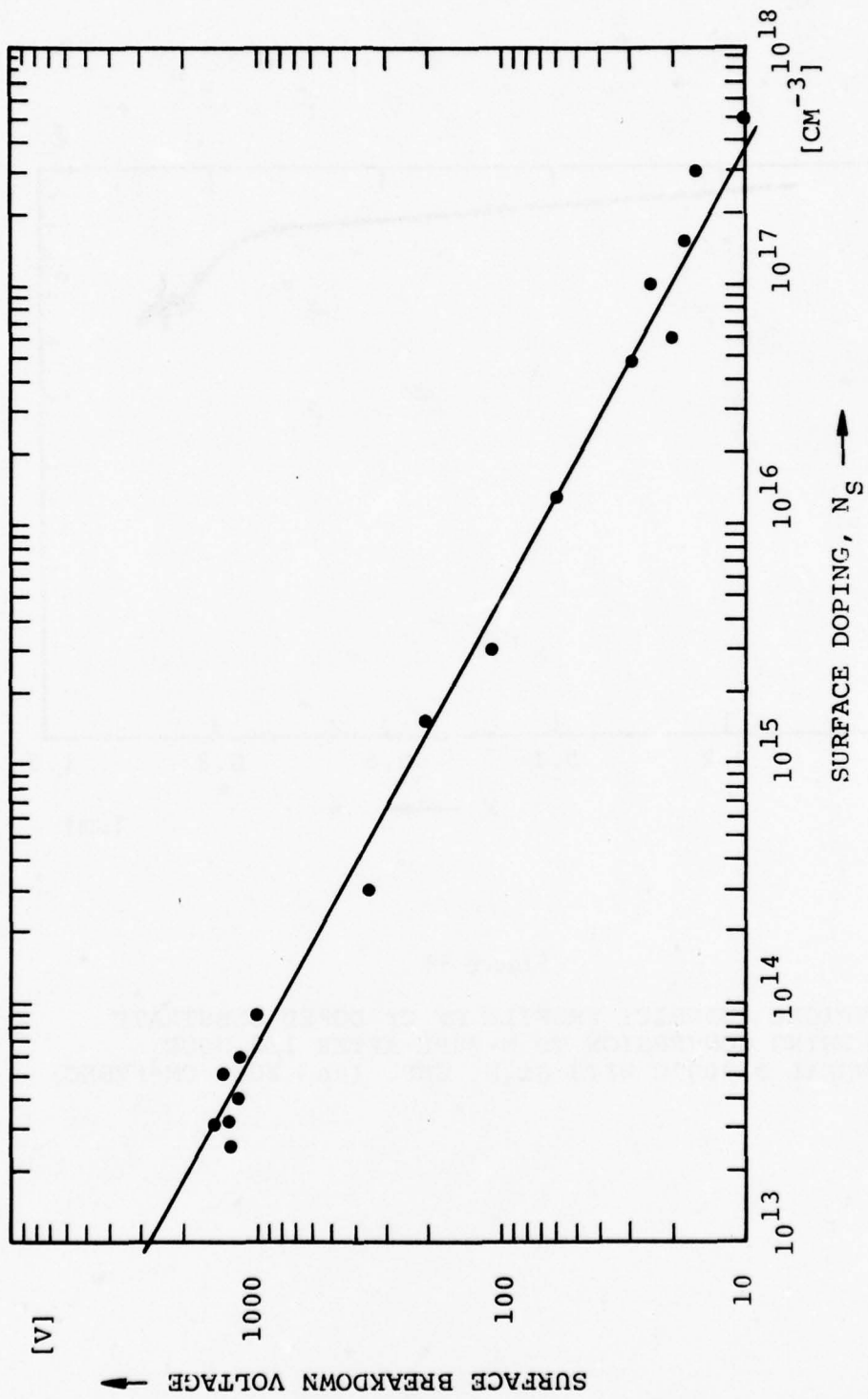


Figure 13
Surface Breakdown Voltage vs. Surface Doping

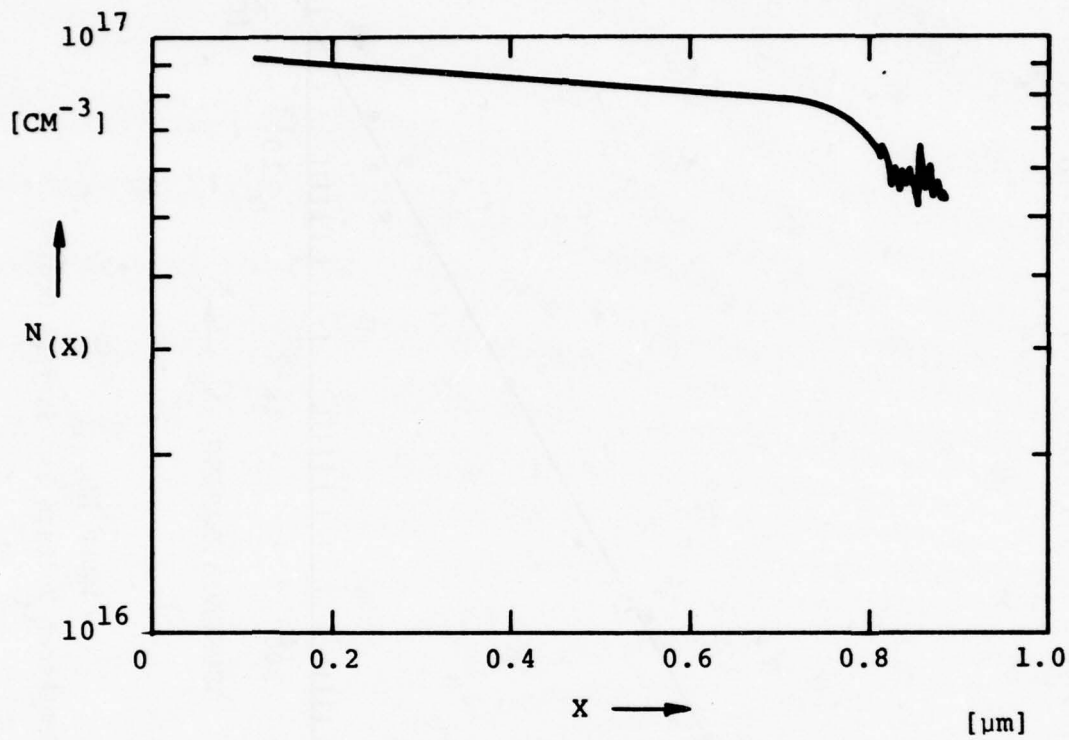


Figure 14

TYPICAL IMPURITY PROFILE OF Cr DOPED SUBSTRATE
 SHOWING CONVERSION TO N-TYPE AFTER 1/2 HOUR
 ANNEAL @ 900°C WITH Si_3N_4 CAP. ($\mu_n = 2000 \text{ CM}^2/\text{VSEC}$)

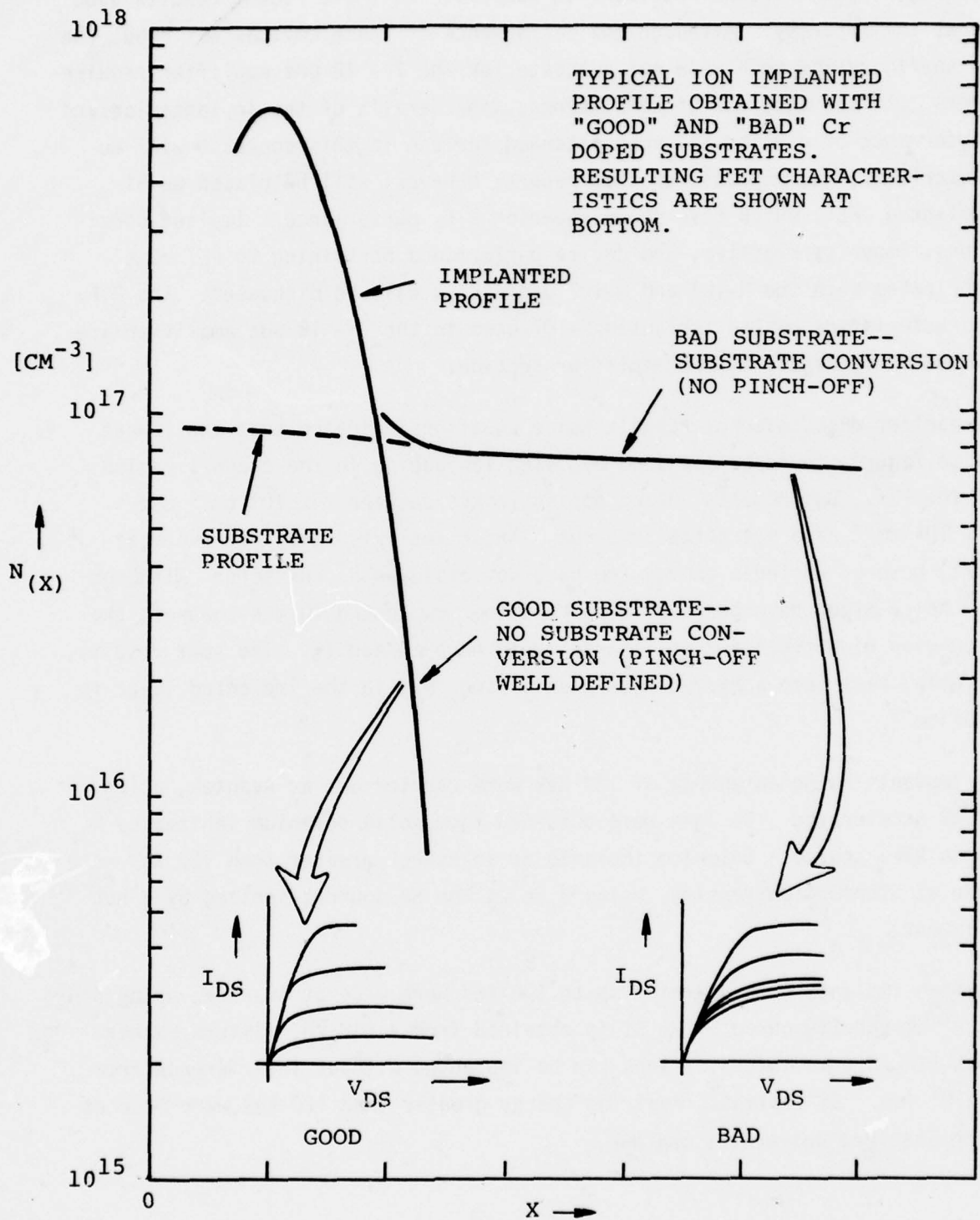


Figure 15

Typical Ion Implanted Profile Obtained with "Good" and "Bad" Cr-Doped Substrates after Annealing with Si_3N_4 Cap

The majority of our implants carried out prior to these recent results used Se as the impurity. Although the performance of these devices was good, the noise figure and gain were not adequate for the 7 - 18 GHz amplifier requirements. In the interest of completeness, the details of the implantation and performance of earlier FET runs intended for use in this contract will be summarized. The emphasis in this report, however, will be placed on Si implanted FETs which have shown superior R.F. performance. Implant conditions, impurity profiles, and device performance pertaining to FET runs fabricated with the M-104 and M-107 geometries will be discussed. The R.F. characteristics of the implanted M-107 used in the 7 - 18 GHz amplifier are discussed in detail in the amplifier section.

An earlier discussion of Fukui's noise equation indicated that the lowest noise figures could be obtained by using low doping in the channel region of the FET. Our results, using doping levels between $7 \times 10^{16} \text{cm}^{-3}$ and $2 \times 10^{18} \text{cm}^{-3}$ have not borne this out. These implants have, for the most part, been of a single energy and have not employed N^+ contacts. Although low noise might have been achieved by using low doping in the channel, the resulting higher contact resistance could have masked it. The best results, to date, have been achieved when peak doping, N_D , in the implanted layer is $>10^{17} \text{cm}^{-3}$.

Se implants using an energy of 120 KeV were carried out at Avantek, using a 60 KV accelerator. Se ions were obtained from solid selenium ionized by H_2 in an R.F. source. Selenium implants at an energy greater than 120 KeV were made at Stanford University, using H_2Se as the Se source, ionized by a hot filament.

Silicon implants with energies up to 120 KeV were made at Avantek, using SiH_4 in H_2 as the Si source. The Si is obtained from a SiH_4/H_2 mixture rather than SiH_4/N_2 , so that Si^{++} ions can be implanted without interference from the N^+ ion. Si implants requiring energy greater than 120 KeV were made at both Stanford University and NRL.

1. Selenium Implants

Table IV is a summary of Se implanted FET runs. In all cases these implants were of a single energy, carried out into "qualified" Cr doped substrates. The runs listed are for the M-104 and M-107 (1/2 μm) geometries (see Figs. 2 and 3) pertinent to this contract.

Additional FET performance summaries are presented in a later section covering FET performance improvement. In these cases, the implants were of multiple energies or heavy doses, which were later thinned by etching under the gate to achieve the required pinch-off voltage. Implantation into buffer layers will also be discussed.

Figure 16 shows the impurity profile obtained using Se^{++} ions implanted at 60 KV into a Cr doped substrate with a dose of $5 \times 10^{12} \text{cm}^{-2}$. The implant was made with the substrate at room temperature and tilted 7° to the impinging Se beam. The implanted layer was annealed at 850°C for 1/2 hour, using a 1000Å Si_3N_4 cap. Also shown is the Gaussian profile, based on LSS theory, for comparison. Because of the high leakage current encountered at this doping level, Schottky diode profiles of these low energy Se implanted layers were generally not possible to obtain. Our inability to profile shallow Se layers led us erroneously to the conclusion that these layers would not make good FETs. This, however, was not the case, and we abandoned the attempt to profile low energy Se implants prior to device fabrication. Although the performance of the FETs made using 120 KeV Se ions was reasonably good, the gate breakdown voltage was consistently low (1-3V). In particular, when the FET pinch-off voltage was $>3\text{V}$, the gate breakdown voltage was found to be substantially less than 3V. If, however, the pinch-off voltage was 1-2V, the gate breakdown voltage was substantially greater (5-7V). Effective control of this situation to maintain $V_{\text{Bgate}} \gg V_p$ is quite difficult. In order to achieve better control over pinch-off voltage as well as higher gate breakdown voltage, the energy of the Se implants was increased to 200 - 300 KeV.

Figure 17 shows the impurity profile obtained from a 240 KeV Se implant, ($\phi = 4 \times 10^{12} \text{cm}^{-2}$) carried out with the substrate at room temperature. Although the measured profile is not a very good fit to the Gaussian distribution,

TABLE IV
 RUN SUMMARY
 Se Implanted GaAs FETs (Cr Doped Substrates)

Run #	E(KeV)	$\phi(\text{CM}^{-2})$	Geom.	N.F. @ 6 GHz	G @ 6 GHz
291	240	6×10^{12}	M-104	2.9 dB	10.1 dB
291A	120	5×10^{12}	"	2.7	10.0
294	240	4×10^{12}	"	2.8	9.1
298	120	5×10^{12}	"	1.9	11.3
306	120	5×10^{12}	"	2.1	12.5
308A	120	5×10^{12}	"	2.4	11.1
332A	300	5×10^{12}	M-107	2.0	11.0
332B	300	5×10^{12}	"	2.6	9.1
334B	150	8×10^{12}	"	2.1	11.6
334C	150	8×10^{12}	"	2.7	10.4

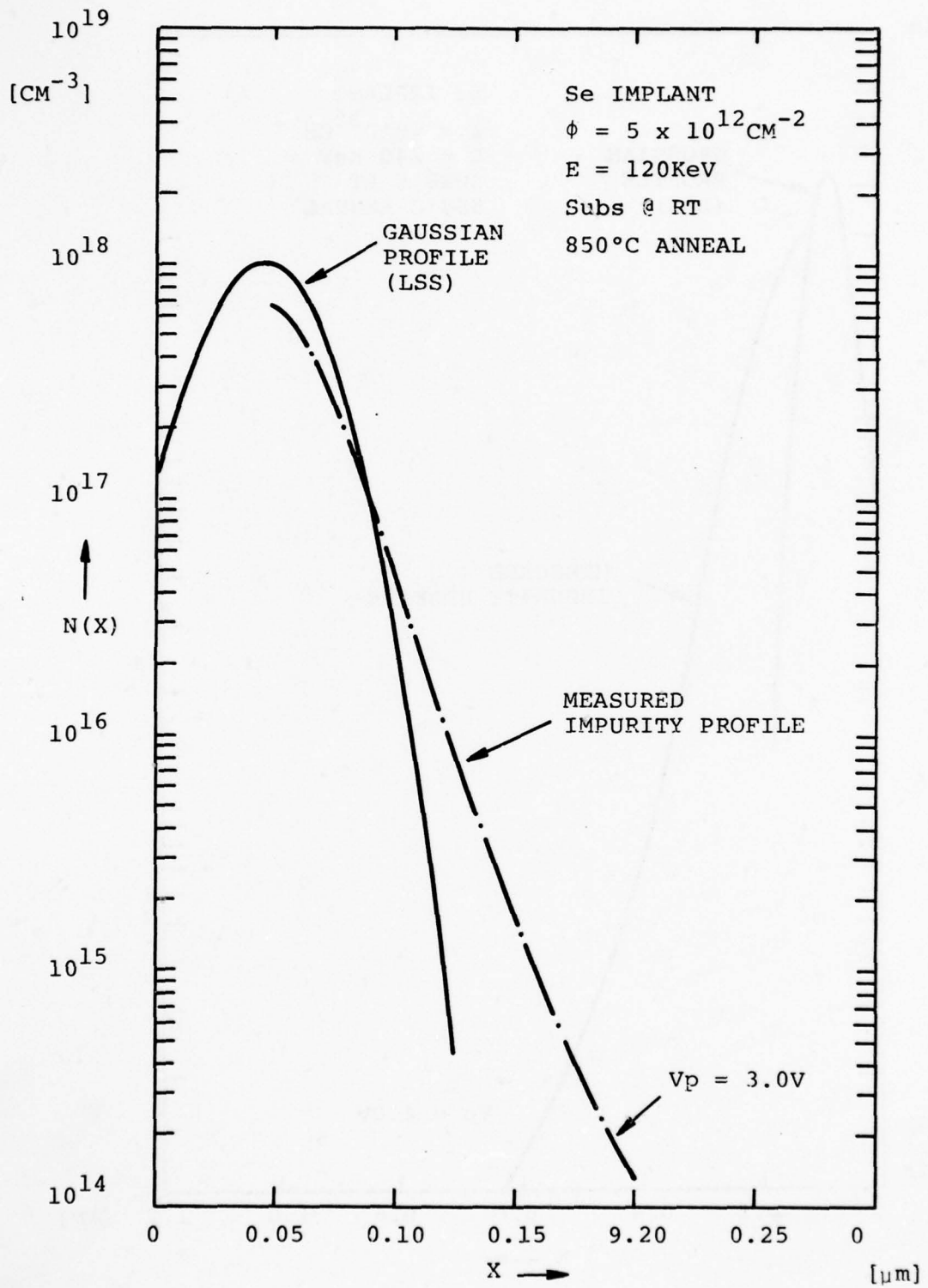


Figure 16

Impurity Distribution of Se Implant, $\phi = 5 \times 10^{12} cm^{-2}$, $E = 120 KeV$

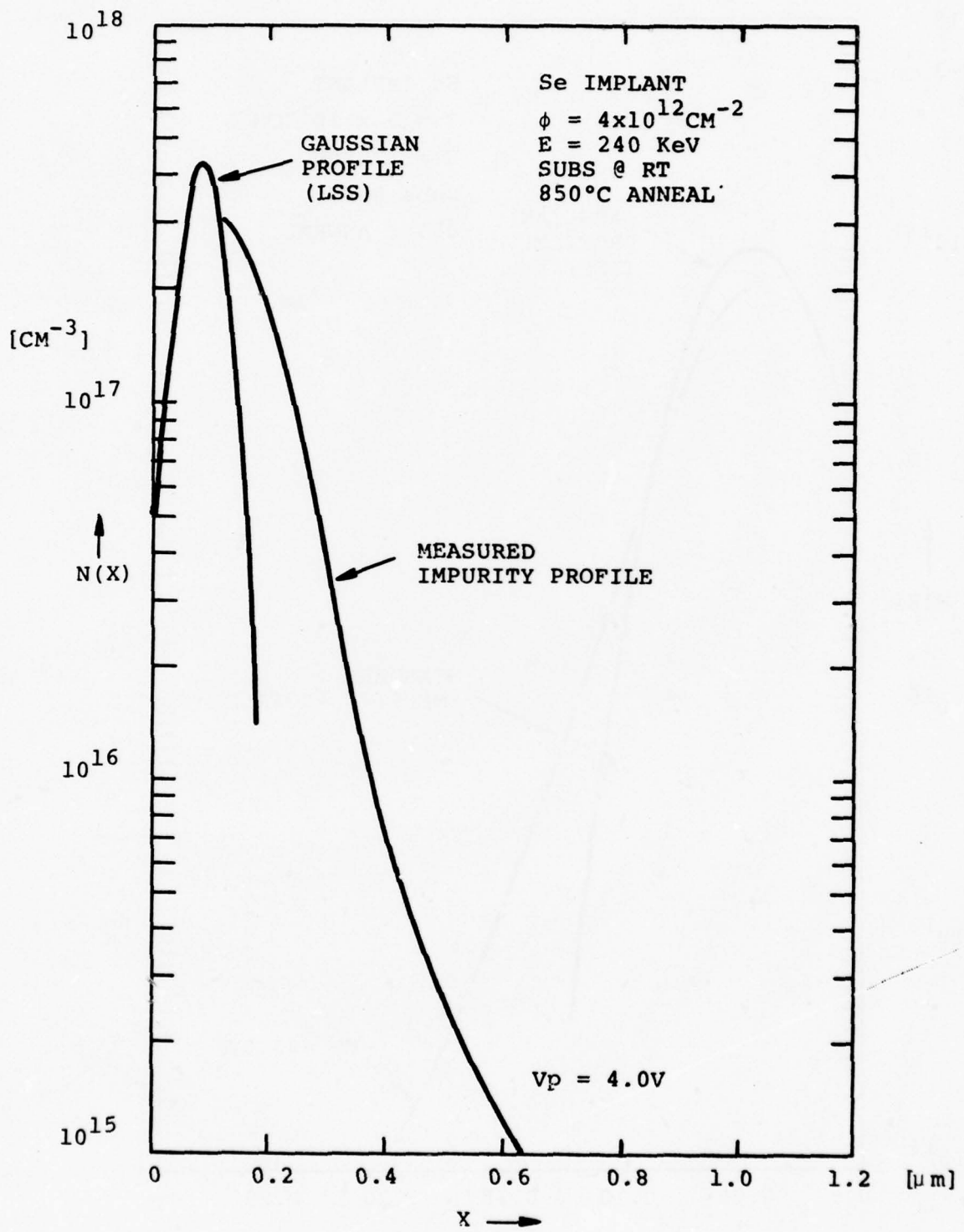


Figure 17
 Impurity Distribution of Se Implant, $\phi = 4 \times 10^{12} \text{cm}^{-2}$, $E = 240 \text{ KeV}$

the measured pinch-off voltage of 4.0V is in good agreement with the calculated value of 4.2V. A substantial improvement in gate breakdown voltage was obtained at this higher energy. V_B was found to be typically 8V, compared to 1 - 3V characteristic of the 120 KeV implants.

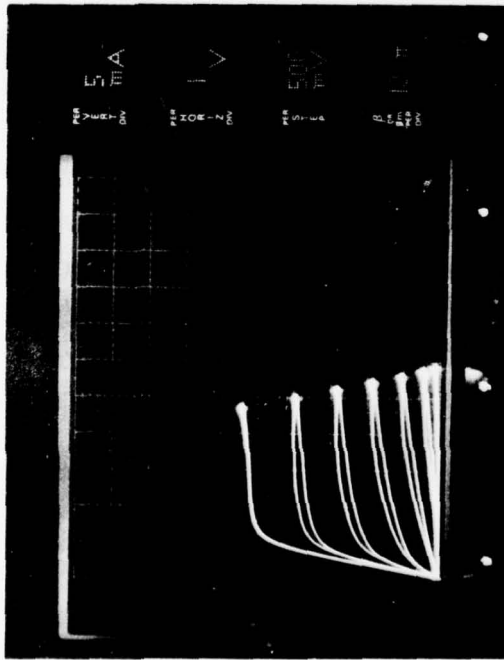
Figure 18 shows the drain characteristics of FET runs from Table IV; #294 (240 KeV, M-104 geometry), #298 (120 KeV, M-104), #334B (150 KeV, M-107), and #332A (300 KeV, M-107). A glance at Table IV shows that there is little, if any, trend in the 6 GHz noise figure with implantation energy. The lowest 6 GHz noise figures, however, were achieved with the lowest energy (i.e., run #298). This result is not consistent with the term in Fukui's noise equation which implies that low channel doping is required for best noise figure. As pointed out earlier, however, the contact resistance term in this equation can be compromised when attempting to lower the channel doping without using a special process to maintain high doping in the contact areas (i.e., N^+ contacts).

2. Silicon Implants

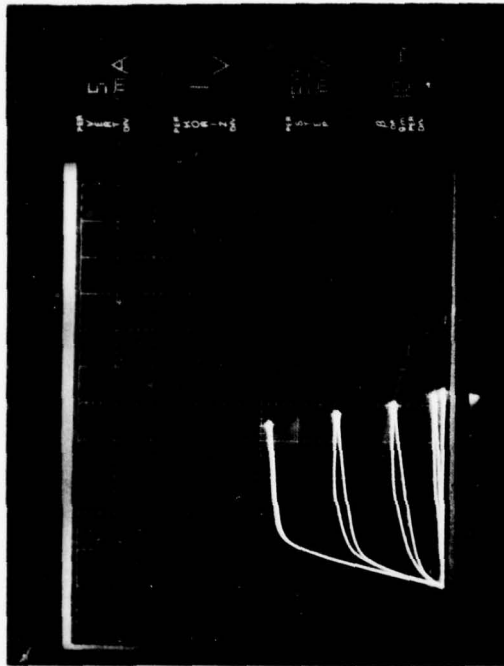
The previous experiments led us to believe that the 6 GHz noise figure could not be reduced substantially below 2 dB using Se implants. We felt that it was possible that a change to another impurity would give better results. Silicon seemed the best choice since it is the lightest of the N-type dopants, and gave the best range for our 60 KV capability. Doubly charged Si has an equivalent energy of 120 KeV, and a projected range of 1025\AA , equal to that of 300 KeV Se (1028\AA). Furthermore, since the standard deviation, σ_p , for Si is greater than that of Se (for the same projected range, R_p), one might expect the doping at the surface of the Si implant to be higher, resulting in lower contact resistance.

Table V is a summary of performance for Si implanted FETs. All runs presented here, except for #310A and 371C, D, and E, were fabricated using the M-107 geometry. In addition, all were implanted into qualified Cr doped substrates. 6 and 18 GHz gain and noise figure are shown for runs which showed performance suitable for the 7-18 GHz amplifier.

#294 - 240 KeV, M-104



#298 - 120 KeV, M-104



#334 - 150 KeV, M-107

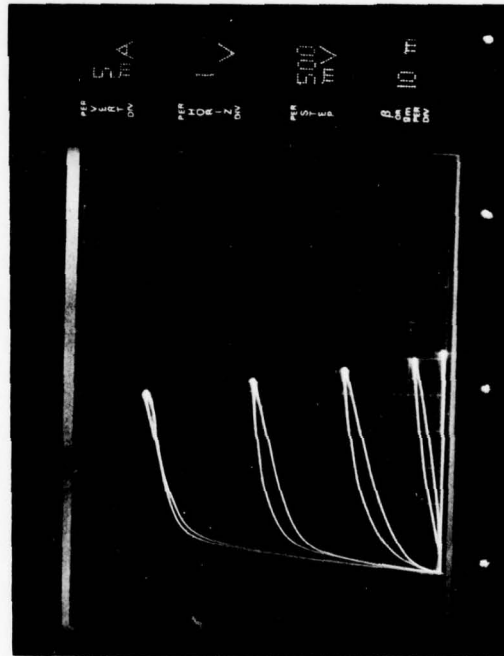


Figure 18
Drain Characteristics of Se Implanted FETs (See Table IV)

TABLE V
 RUN SUMMARY
 Si Implanted GaAs FETs (Cr Doped Substrates)

Run #	E (KeV)	ϕ (CM ⁻²)	Geom.	6 GHz		18 GHz	
				N.F.	G.	N.F.	G.
310A	50	5×10^{12}	M-104	2.6	10.8		
338	120	2×10^{12}	M-107	1.8	11.0	3.2	5.9
346-A	120	"	"	1.8	10.3		
349-C	"	"	"	1.8	8.9		
350-3A	"	"	"	1.8	10.6		
350-3B	"	"	"	1.7	11.0		
351-1A	"	"	"	1.9	10.0		
351-1B	"	"	"	1.9	10.1		
353-A	"	"	"	2.0	11.5		
361-B	"	"	"	1.7	9.0		
361-C	"	"	"	1.7	9.0		
368-C	"	"	"	1.6	11.5	2.4	6.0
362-A	"	"	"	1.6	10.8		
362-B	"	"	"	1.5	10.1		
362-C	"	"	"	1.6	10.8		
371-D	"	"	M-104	2.1	10.3	2.8	5.8
371-E	"	"	"	2.2	10.1		
371-C	"	"	"	2.1	10.9	2.7	6.8

The first Si implant, run #310A, was made with an energy of 50 KeV, chosen to give the same projected range, R_p , as for the 120 KeV Se implants of Table IV. The dose was chosen to give the same peak doping as for the 120 KeV Se implant based on the relationship:

$$\hat{n} = \frac{\phi}{\sigma_p \sqrt{2\pi}} \approx \frac{\phi}{\sigma_p} \quad \text{Equation 18}$$

Where \hat{n} is the peak impurity density, ϕ is the ion dose/cm², and σ_p is the standard deviation in the projected range. For a 120 KeV Se dose of 5×10^{12} cm⁻², $\hat{n} = 9.7 \times 10^{17}$ cm⁻³.

This peak doping requires a dose of 6.2×10^{12} cm⁻² using 50 KeV Si ions. The estimate does not take into account the differences in doping efficiency between Si and Se, but it is a good first order approximation. Figure 19 shows, for comparison, the LSS distributions for 120 KeV Se and 50 KeV Si. The balance of the FET runs included in Table V were done with 120 KeV Si, $\phi = 2 \times 10^{12}$ cm⁻². Figure 20 shows the measured profile, typical of all the Si implants using this energy and dose. This particular implantation schedule has consistently given the best fit to the LSS distribution, has been the most reproducible, and given the best R.F. performance.

Figure 21 shows the drain characteristic typical of the 120 KeV, 2×10^{12} cm⁻² Si implanted FET. These D.C. parameters (as well as R.F.) are very reproducible from run to run.

D. D.C. EVALUATION

The M-107 mask includes a long-gate FET (referred to as the "Fat-FET") and an ohmic contact test pattern. The "Fat-FET" is an FET which has a gate length, L_g , much larger than the source-to-gate and gate-to-drain spacing. Since $L_g \gg L_{sd}$ and L_{gd} , the effect of extrinsic resistances on the FET transfer characteristics can be neglected. Using this type of FET structure, Pucel [3] has shown that one can determine the carrier drift mobility using the ratio of transconductance to gate-source capacitance, G_m/C_{gs} .

Using the "Fat-FET" with this measurement technique we have measured the drift mobility and impurity profiles of our ion implanted as well as LPE

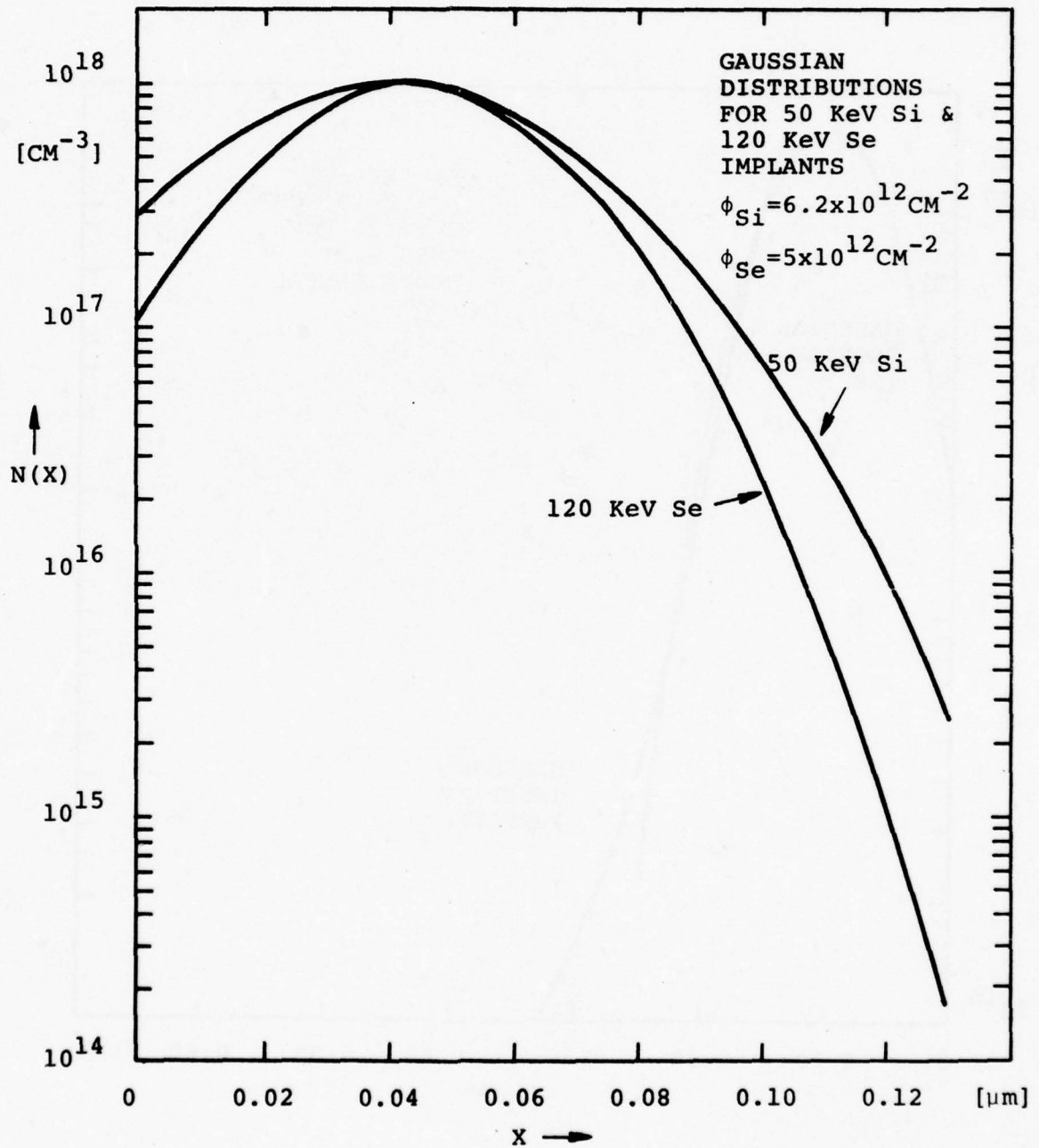


Figure 19

Gaussian Distributions for Si and Se Implants
 $\phi_{Si} = 6.2 \times 10^{12} \text{cm}^{-2}$, $E = 50 \text{ KeV}$. $\phi_{Se} = 5 \times 10^{12} \text{cm}^{-2}$, $E = 120 \text{ KeV}$

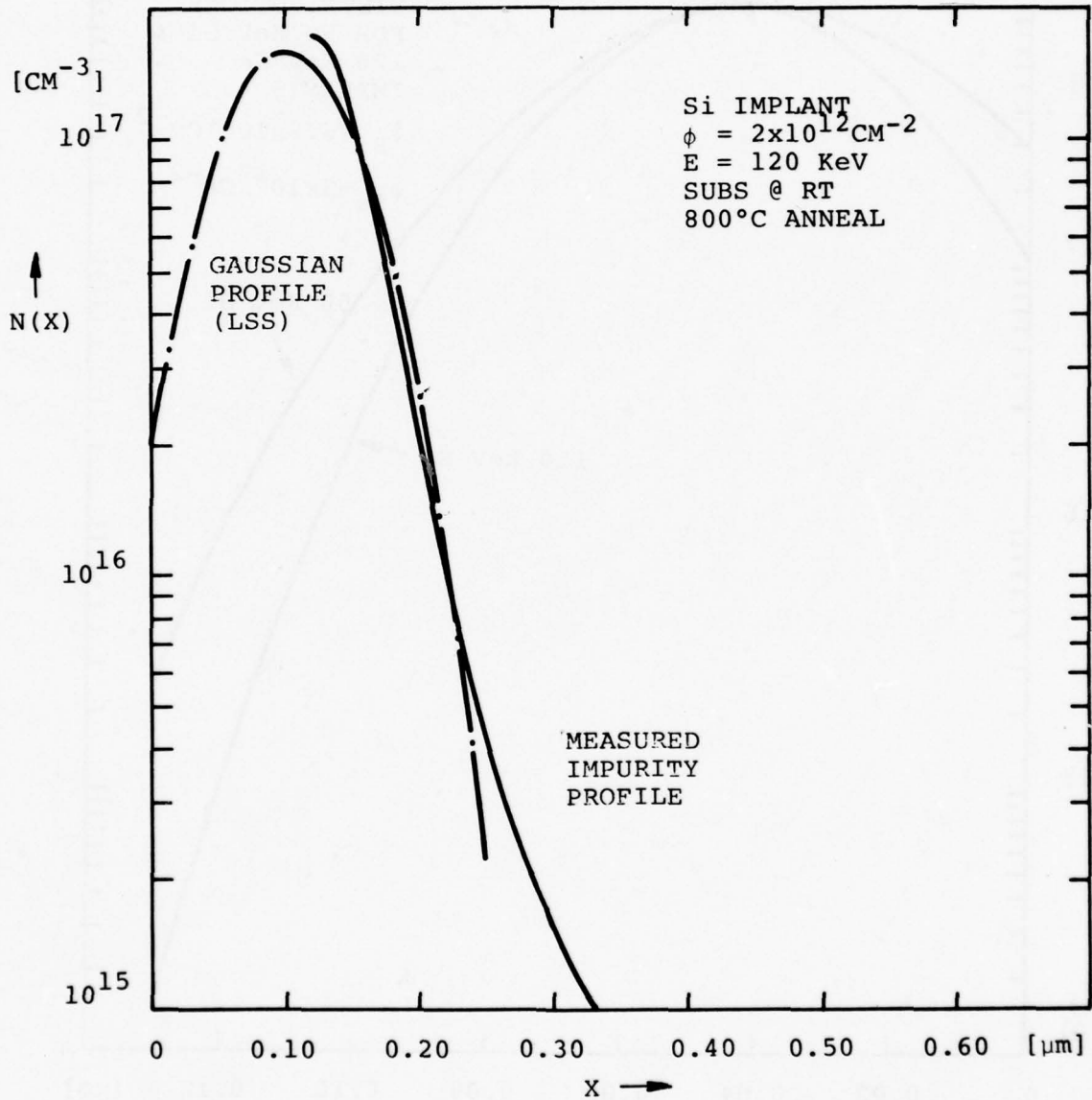


Figure 20

Typical Impurity Distribution for Si Implant
 $\phi = 2 \times 10^{12} cm^{-2}$, $E = 120 KeV$

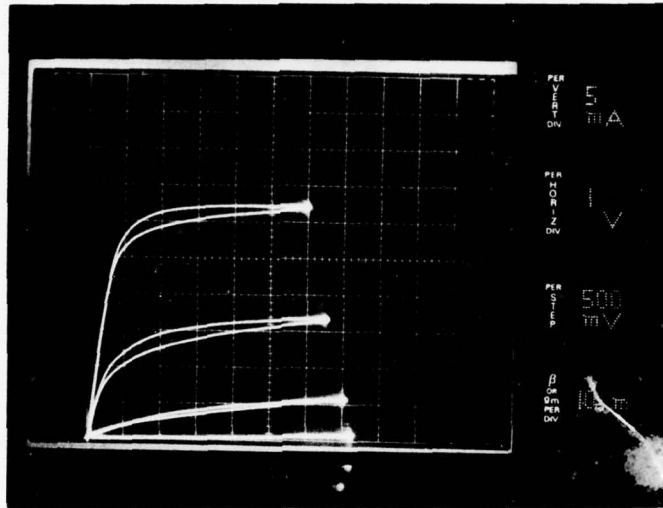


Figure 21
 Drain Characteristics Typical of Si Implanted FET
 ($\phi = 2 \times 10^{12} \text{cm}^{-2}$, $E = 120 \text{ KeV}$, M-107)

FETs. It is of particular interest to compare the G_m and μ_d plots of the Si implanted vs. LPE runs. Figure 22 shows C_{gs} , G_m , and μ_d obtained from the "Fat-FET" of a typical 120 KeV, $2 \times 10^{12} \text{cm}^{-2}$ Si implanted FET run (implant directly into the Cr doped substrate). Figure 23 shows the same parameters obtained from the "Fat-FET" of a typical LPE run. In all cases the transconductance and mobility of the implanted layers is superior to that of the LPE layers. Drift mobility is seen to increase with gate bias and peak very near the pinch-off voltage in the implanted layers, to drop continuously in the LPE layers. This improved transconductance and mobility are key to the excellent R.F. performance we are achieving with ion implantation.

Figure 24 shows typical contact resistance data for the Si implanted FETs. The test structure which is included in the M-107 geometry consists of four ohmic contacts spaced as indicated in the figure. The specific contact resistance is found to be $\approx 1 \times 10^{-6} \Omega \text{cm}^2$.

E. PERFORMANCE IMPROVEMENT EXPERIMENTS

1. N^+ Contacts

The discussion of ion implanted FETs has so far been restricted to devices fabricated into Cr doped substrates using a single energy implant for the active layer. Further improvement in gain and noise figure is expected by the use of an N^+ implant to reduce the contact resistance [8]. Earlier attempts (see Phase I Annual Report on this contract) to use Se in an N^+ implanted contact were not successful due to early problems with the lack of reproducibility of the Si_3N_4 capping process. Improvements in the capping process as well as in the FET fabrication (contacts, cleaning, surface preparation, etc.) now make this approach feasible.

Two methods for obtaining an N^+ contact have been used. The first referred to as "non-selective" is that of implanting the entire surface of the active layer with a shallow N^+ dose. Prior to evaporation of the gate metal, the N^+ layer is etched away to expose the active channel region. This situation is depicted in Fig. 25a. The main disadvantage of this structure is that the N^+ region must be sufficiently steep and thin that it does not "tail" into the active region.

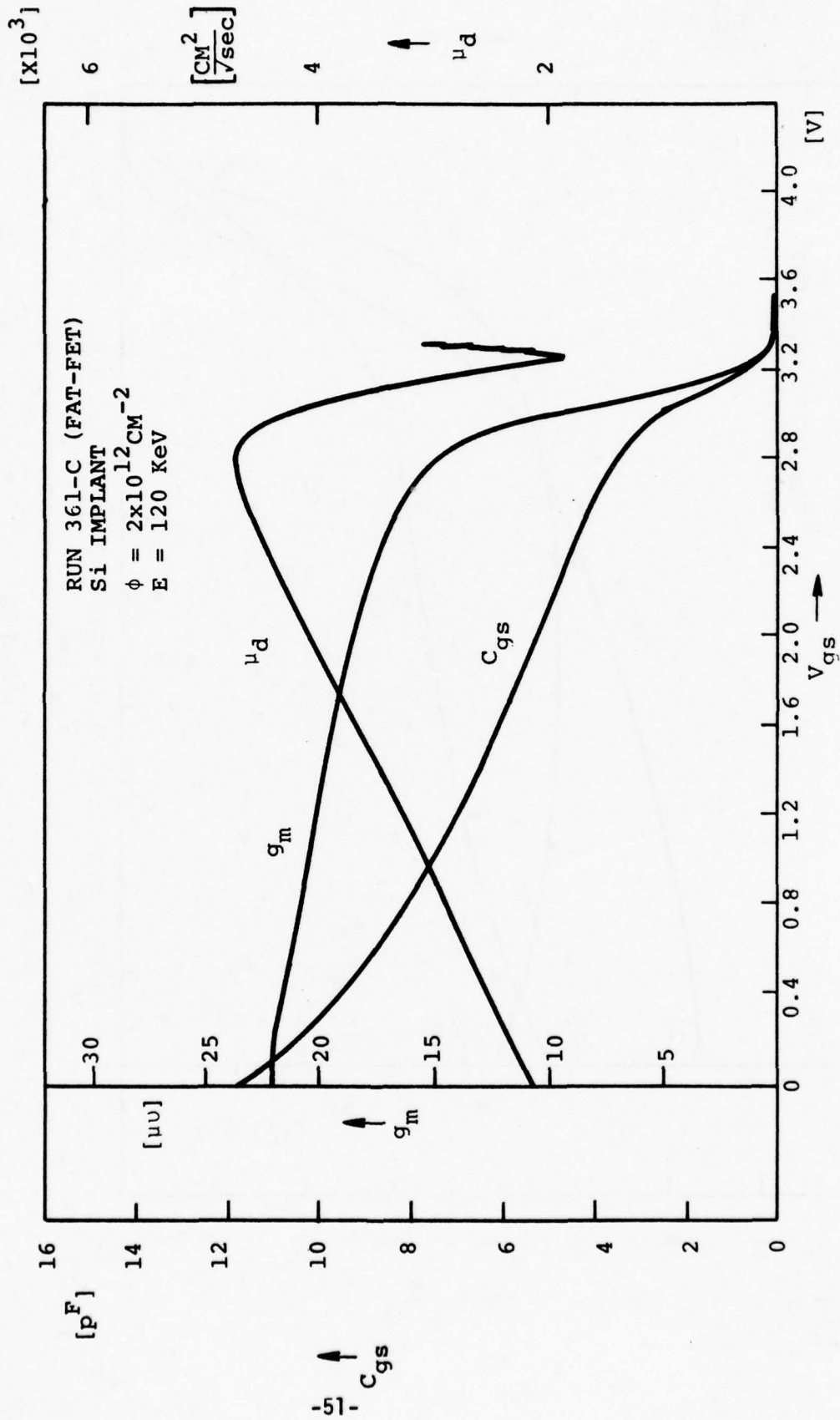


Figure 22
 g_m , C_{gs} , and μ_d vs. Gate Voltage for Si Implanted FET Run #361-C.

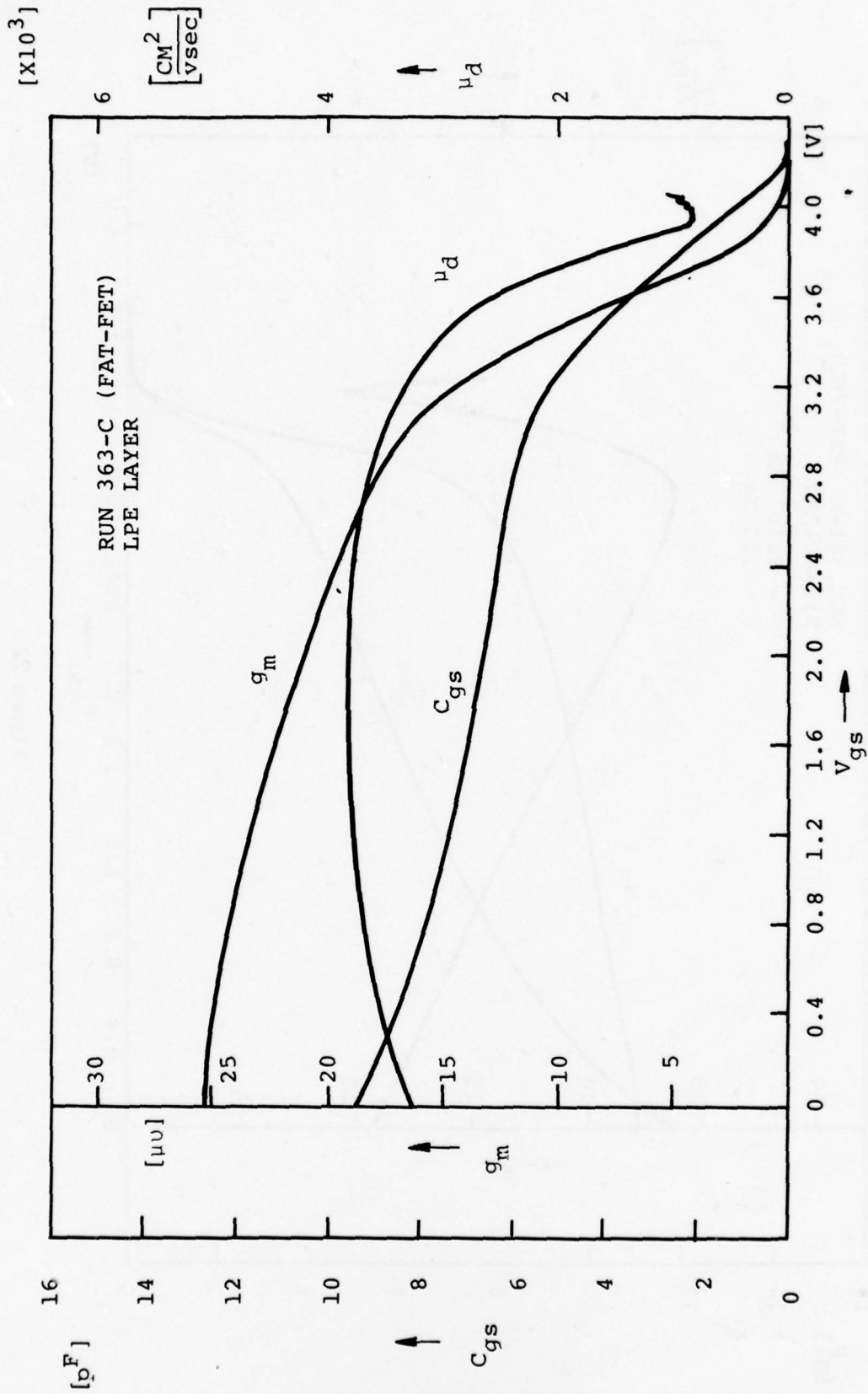


Figure 23
 g_m , C_{gs} , and μ_d vs. Gate Voltage for LPE FET Run #363-C

FET RUN 346-A
Si IMPLANT, 120 KeV

CONTACT TEST PATTERN (M-107)

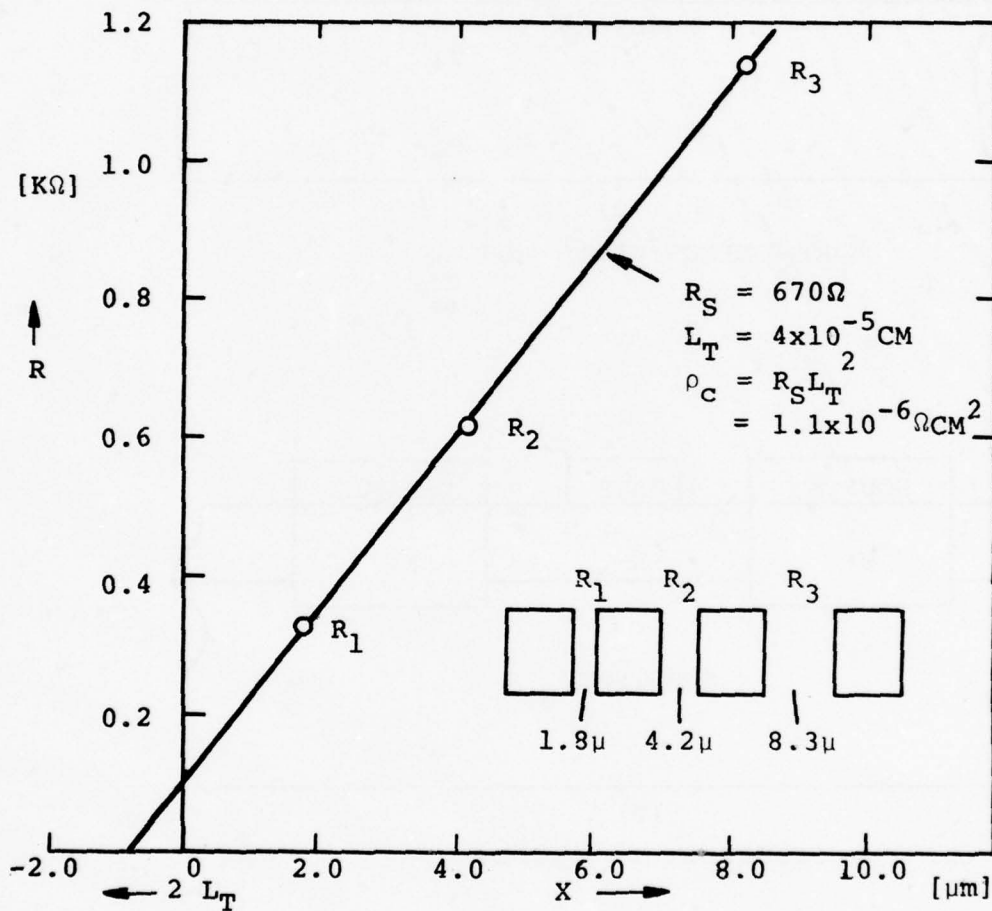
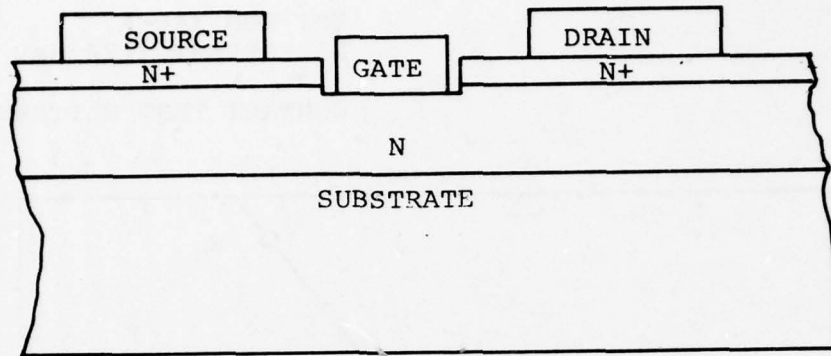
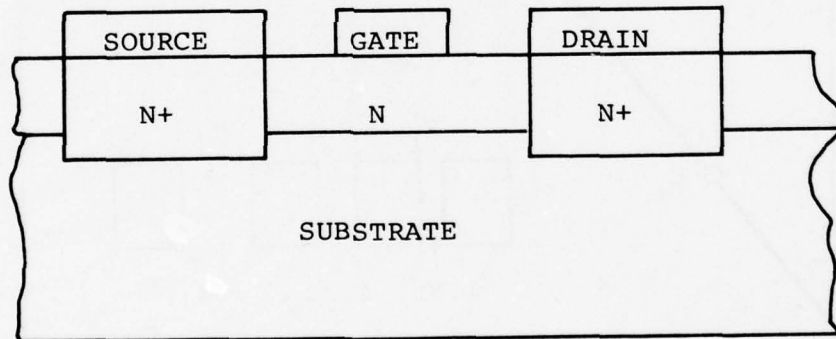


Figure 24
Resistance vs. Contact Spacing for Si Implanted FET Run #364-A



(a)

NON-SELECTIVE N^+ IMPLANT



(b)

SELECTIVE N^+ IMPLANT

Figure 25
Schematic Representation of "Non-Selective" and "Selective" N^+ Implants

Contact improvement, therefore, relies mostly on the surface concentration of this implant rather than the combination of surface concentration and thickness ($N \times W$). In a case where the active layer is very lightly doped and thick, the implantation depth of the N^+ contact can be greater than it could for a more heavily doped, shallow active layer.

The second contact improvement method uses selective implantation into the contact areas through a mask such as Al [8] or photoresist. The active channel is protected against the N^+ implant by the mask. The structure is shown in Fig. 25b. In this case the choice of depth of the N^+ region is not limited by the active layer thickness. This is the preferable situation since by this method the charge under the contact ($N \times W$) can be made sufficiently large that its sheet resistance is negligible compared to that of the active region.

(a) Non-Selective N^+ Implant

"Non-selective" N^+ contact implants were carried out using 50 KeV Si ions ($\phi = 3.3 \times 10^{13} \text{cm}^{-2}$) for the N^+ layer and 300 KeV Si ($\phi = 1.7 \times 10^{12} \text{cm}^{-2}$) ions for the active layer. Figure 26 shows the LSS distribution for the N^+/N combination, along with the measured impurity distribution determined from the "Fat-FET." Implants were made directly into Cr doped substrates. For the purpose of comparison, a control run was processed with the N active layer only (300 KeV, $1.7 \times 10^{12} \text{cm}^{-2}$). In the " N^+ " case, the region under the gate was etched away to achieve the required pinch-off voltage.

Figure 27 shows the drain characteristic typical of devices from the N^+ implanted and control runs. Although gain and noise figure were not the best we have seen, slightly improved gain and noise figure were observed in the N^+ contacted run, compared to that of the control run.

(b) Selective N^+ Implant

"Selective" implants have been carried out using both photoresist and aluminum as the masking material. In the case where photoresist was used as a mask, the maximum energy was 40 KeV, with a dose of $5 \times 10^{13} \text{cm}^{-2}$ Si ions implanted into the M-107 contact areas defined on LPE active layers. Gain and noise figure were 10.5 dB and 1.9 dB, respectively,

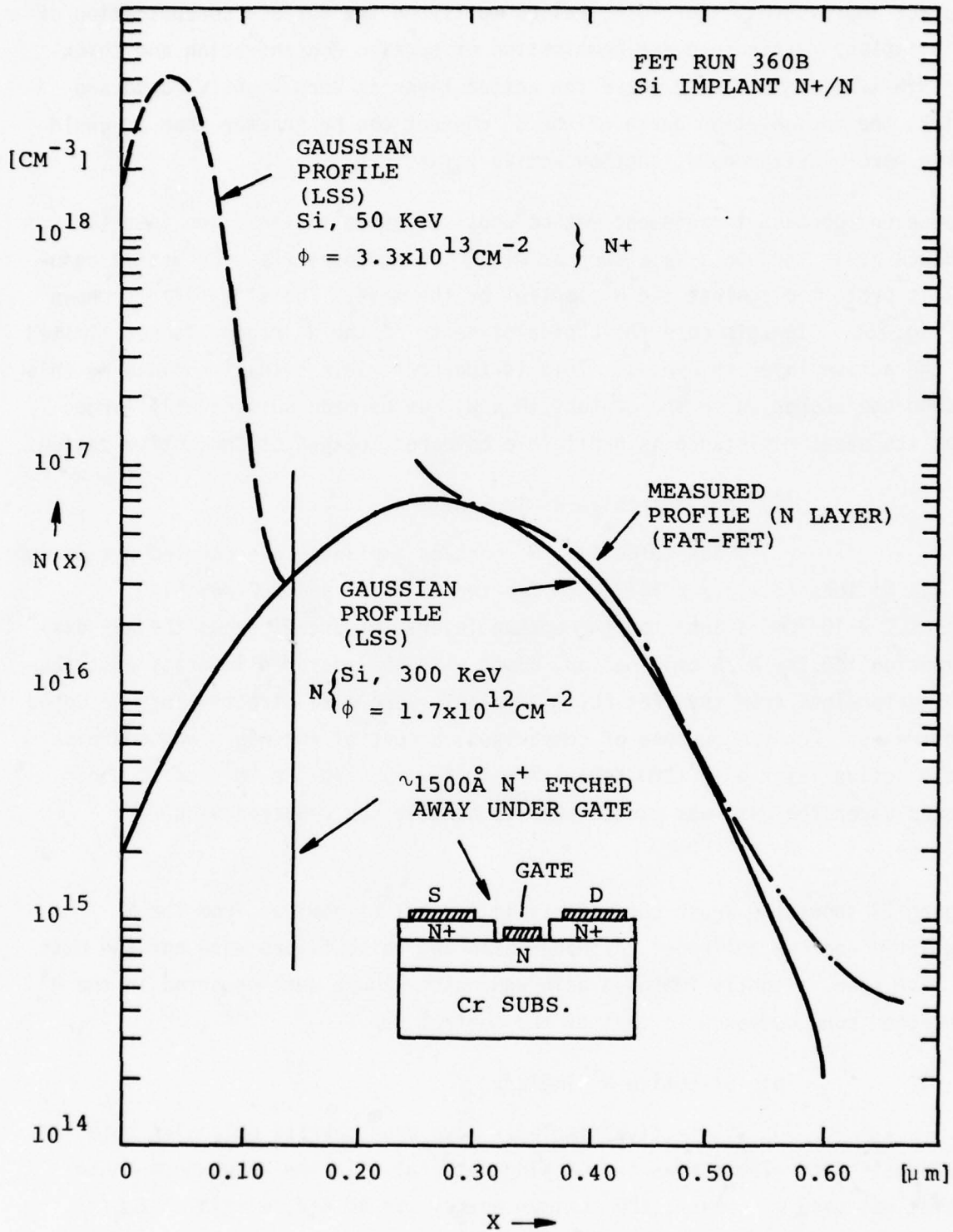
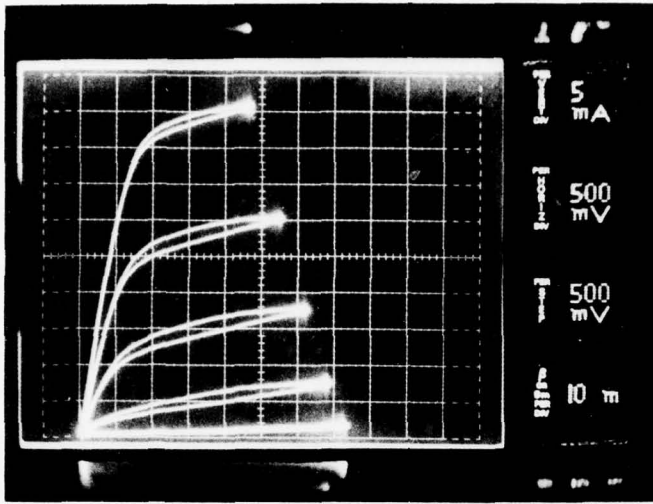


Figure 26

Gaussian Distributions (LSS Theory) and Measured Impurity Profile for "Non-Selective" N⁺/N Si Implanted FET Run #360-B

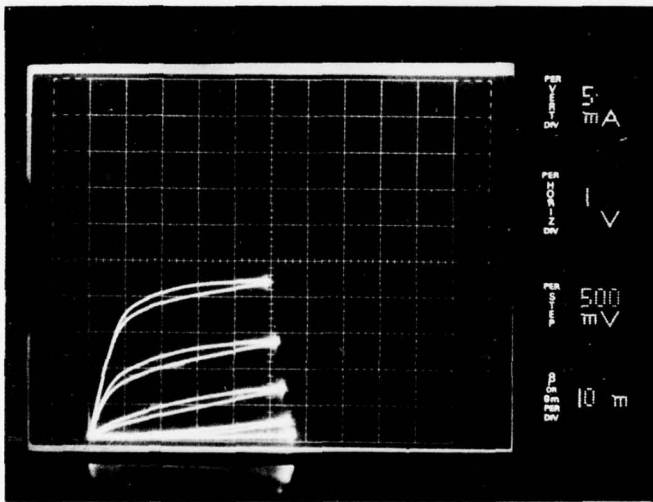


360B-N+, $\phi=3 \times 10^{13} \text{cm}^{-2} \text{Si}$ @ 50 KeV
 $N, \phi=1.7 \times 10^{12} \text{cm}^{-2} \text{Si}$ @ 300 KeV

N.F. = 2.0 dB

G. = 8.9 dB

f = 6 GHz



360D-N, $\phi=1.7 \times 10^{12} \text{cm}^{-2} \text{Si}$ @ 300 KeV

N.F. = 2.4 dB

G. = 8.8 dB

f = 6 GHz

N(CONTROL)

Figure 27
 Drain Characteristics of Si Implanted FETs with
 "Non-Selective" N^+ Implanted Contacts

at 6 GHz. Typical 6 GHz values for M-107 gain and noise figure using single layer LPE material are 10.0 dB and 2.3 dB. This is, therefore, the best 6 GHz data we have seen for the M-107 using LPE material.

The maximum benefit from the selective N^+ implant is achieved by making the implanted layer deep while maintaining high surface concentration. Such an implant is represented in Fig. 28. Plotted is the LSS distribution for a three-energy Si implant with energy/dose conditions adjusted to give a flat profile with maximum concentration $\approx 5 \times 10^{18} \text{cm}^{-3}$. Figure 29 shows a three-energy Se implant with doses adjusted to give the same peak doping. A maximum doping of $5 \times 10^{18} \text{cm}^{-3}$ was chosen since it is compatible with a maximum annealing temperature of 850°C . (Activation of a higher doping level would require an annealing temperature $> 850^\circ\text{C}$, in which case we find a high incidence of substrate failures.) The N^+ implants of Fig. 28 and 29 were evaluated using a contact test pattern which consists of 5 contact pads spaced as shown in Fig. 24. For evaluation purposes, the entire surface of the Cr doped substrate was implanted and metalized with the test pattern. Figure 30 shows the resistance data for the Se N^+ implant of Fig. 29. The median value of sheet resistance was found to be $185 \Omega/\square$, in good agreement with an estimated value of $180 \Omega/\square$ based on 40% electrical activity. Specific contact resistance is calculated to be $8 \times 10^{-7} \Omega \text{cm}^2$; in reasonable agreement with the expected value of ρ_c for $N_d \approx 10^{18} \text{cm}^{-3}$.

Figure 31 shows the resistance data for the Si- N^+ implant of Fig. 28. In this case, the sheet resistance was found to be $60 \Omega/\square$, very close to the predicted value of $57 \Omega/\square$. Under the same conditions of maximum energy = 120 KeV, the Si implant appears to be the preferred choice. The specific contact resistance is $4 \times 10^{-7} \Omega \text{cm}^2$, and the contact resistance R_c (at $x = 0$) is 0.1 compared to 0.5 Ω for the Se implant. FET runs using the "selective N^+ " approach and the Si implantation schedule of Fig. 28 will be fabricated. Evaporated Al will be used to protect the channel region from the implantation.

2. Implantation into Buffer Layers

The performance of epitaxial GaAs FETs has been shown to be substantially improved by the use of a high purity buffer layer grown on a Cr doped substrate prior to the growth of the active layer. The arguments

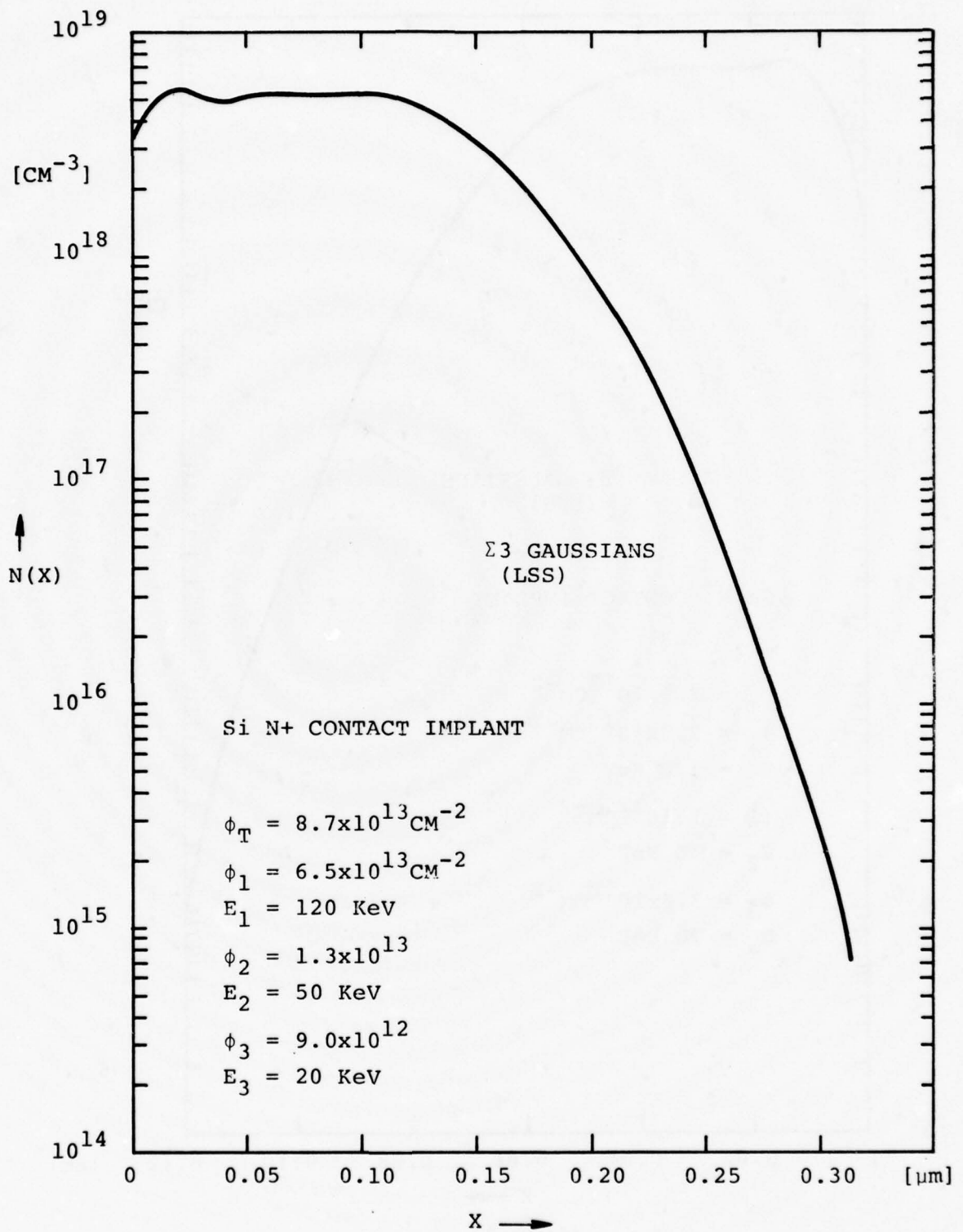


Figure 28
 Gaussian Distribution (LSS Theory) for Multiple Energy
 Si Implant Suitable for "Selective" N⁺ Contact

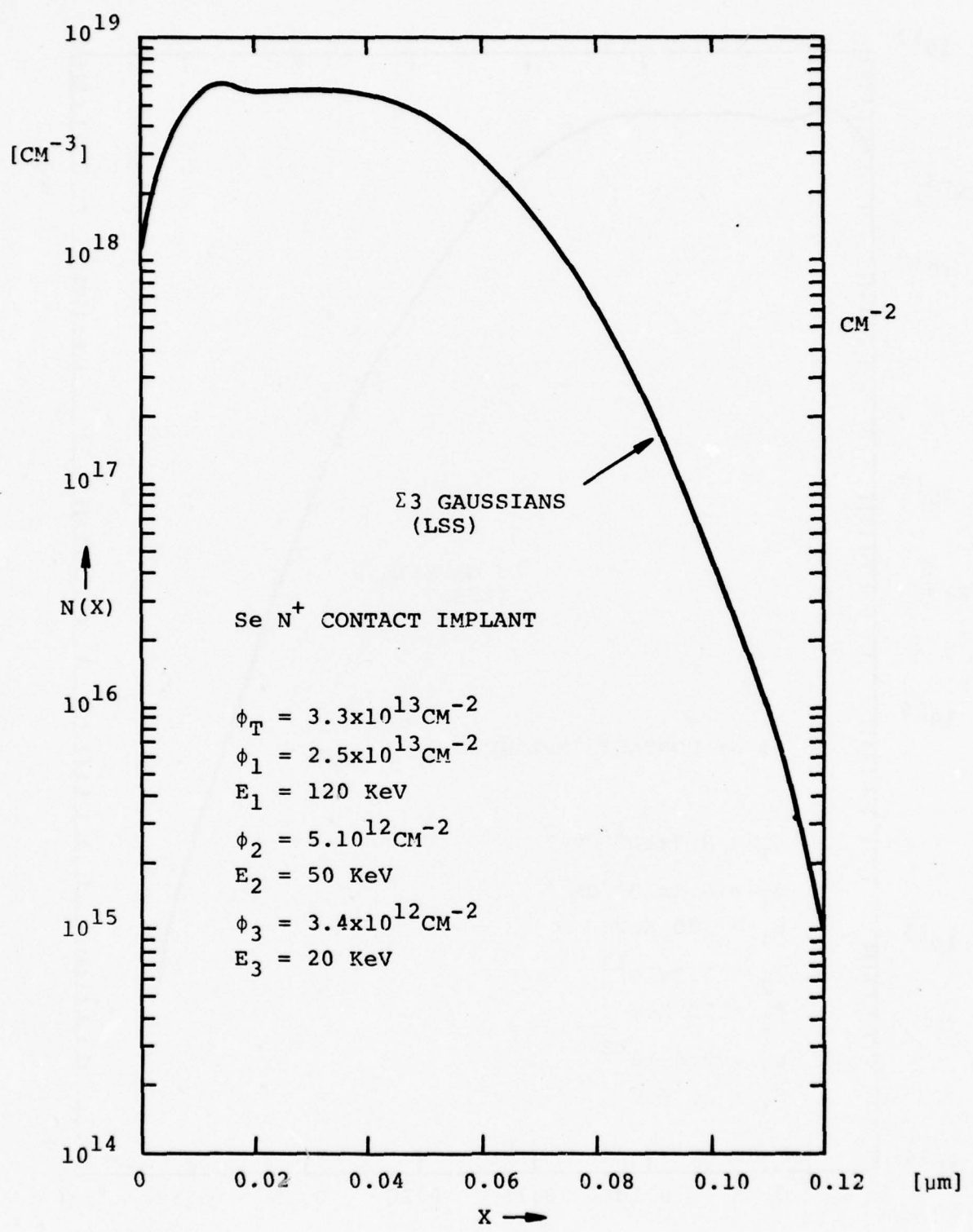


Figure 29
 Gaussian Distribution (LSS Theory) for Multiple Energy
 Se Implant Suitable for "Selective" N⁺ Contact

N⁺ CONTACT IMPLANT
 Si, $\phi_T = 8.7 \times 10^{13} \text{CM}^{-2}$

(CONTACT TEST PATTERN)

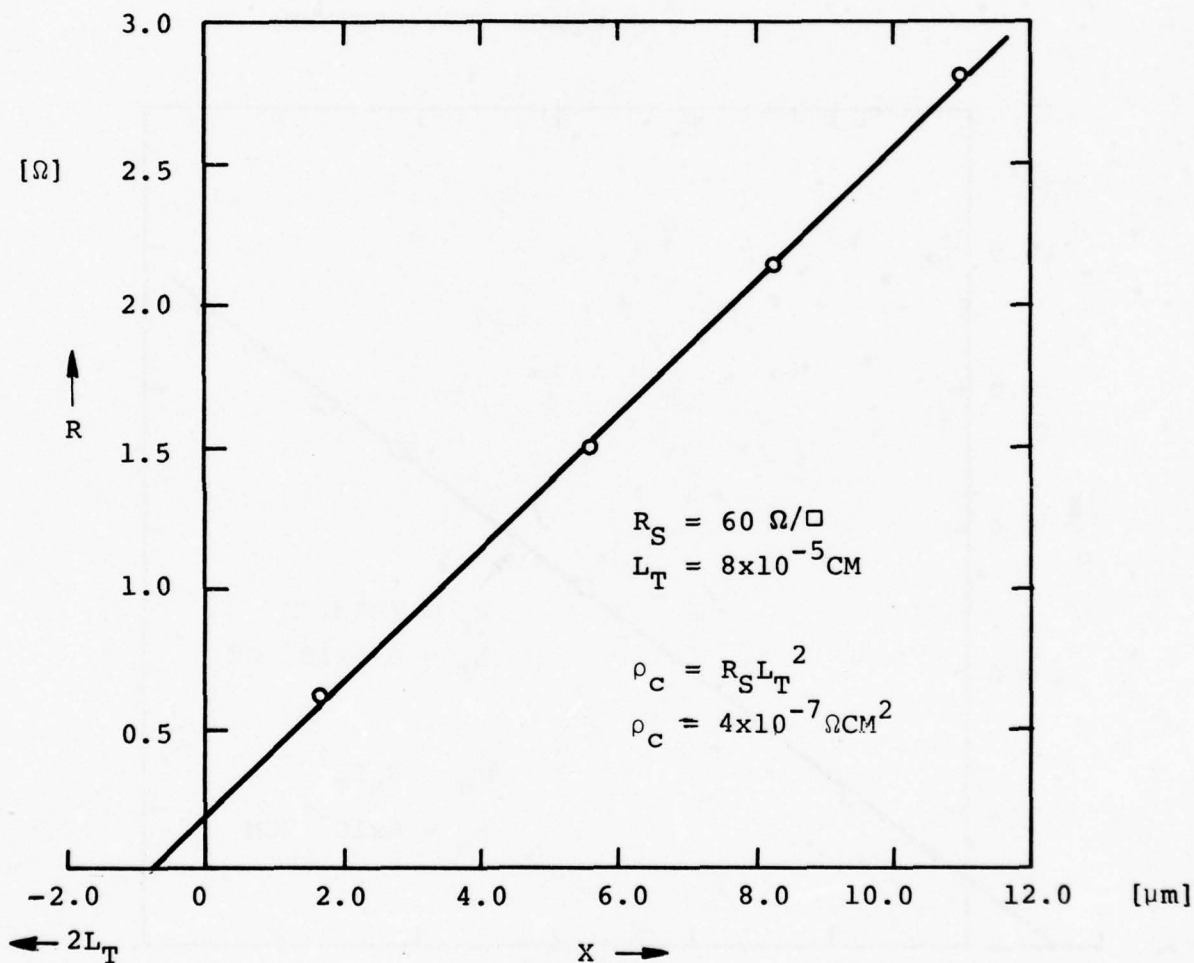


Figure 30

Resistance vs. Contact Spacing for the Multiple Energy
 Se N⁺ Contact Implant of Fig. 29

N^+ CONTACT IMPLANT
 $Se, \phi_T = 3.3 \times 10^{13} \text{CM}^{-2}$
 (CONTACT TEST PATTERN)

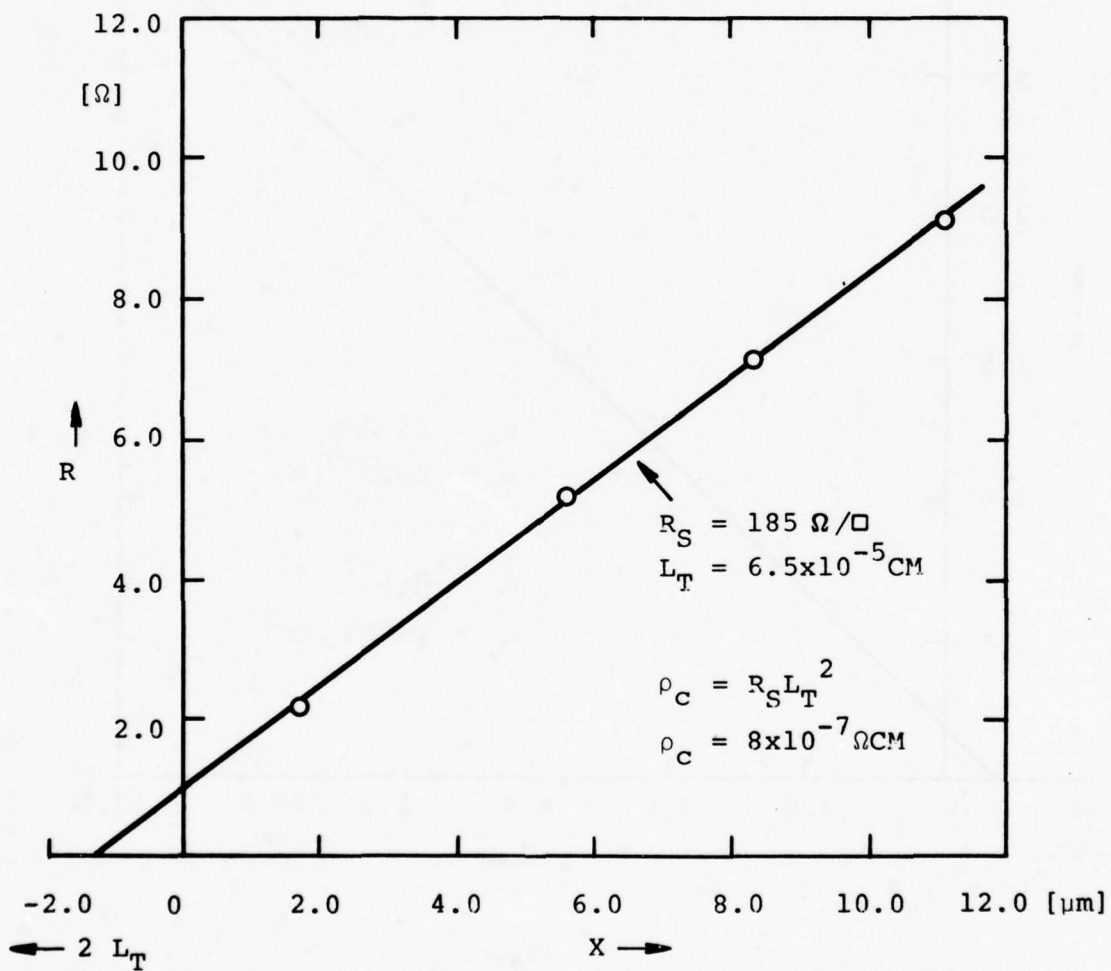


Figure 31
 Resistance vs. Contact Spacing for the Multiple Energy
 Si N^+ Contact Implant of Fig. 28

in favor of the use of a buffer layer in an epitaxial structure, should, in principle, apply to ion implantation.

Earlier attempts at ion implantation into LPE buffer layers did not give device results comparable to those obtained by implantation into the Cr doped substrate. High resistivity ($N_D \approx 5 \times 10^{14}$) LPE layers were grown making use of the "notch" effect [9]. High resistivity layers achieved by this technique are closely compensated, and the relatively large number of donors and acceptors results in a film with poor mobility. Room temperature mobility for these layers was $\approx 6000 \text{cm}^2 \text{v}^{-1} \text{sec}^{-1}$, and liquid nitrogen mobility $\approx 40,000 \text{cm}^2 \text{v}^{-1} \text{sec}^{-1}$, rather than the expected value of $150 - 200,000 \text{cm}^2 \text{v}^{-1} \text{sec}^{-1}$. Furthermore, when these buffer layers were implanted and annealed at $800 - 900^\circ \text{C}$, a p-type conversion of the buffer layer was observed. FET performance under these conditions was very poor compared to non-buffered devices.

The buffer layer program has since that time been approached using vapor phase epitaxy. N-type buffer layers can now be grown routinely which have room temperature mobility in excess of $8000 \text{cm}^2 \text{v}^{-1} \text{sec}^{-1}$, and liquid nitrogen mobility approaching $200,000 \text{cm}^2 \text{v}^{-1} \text{sec}^{-1}$, at doping level of $\approx 10^{13} \text{cm}^{-3}$. These layers are grown using the AsH_3/HCl technique.

Figure 32 shows the Schottky diode capacitance vs. voltage for Si implanted into a qualified Cr doped substrate, as well as into a buffer layer ($\phi = 2 \times 10^{12} \text{cm}^{-2}$, $E = 120 \text{ KeV}$). We have consistently found that the C-V plots for the buffer layers do not pinch off to zero capacitance as the non-buffered samples do. At pinch-off there is a residual capacitance which appears to be due to a thin p-layer at the interface between the buffer layer and Cr doped substrate. This residual capacitance may affect the high frequency performance of the FET.

Table VI shows a performance summary of buffer-layered Si implanted FETs, and Fig. 33 shows typical drain characteristics. Notable is the absence of the looping which is characteristic of non-buffered devices. Table VI shows that run #365-A gave the lowest 6 GHz N.F. of all Si implanted FETs. The noise figure at 18 GHz, however, was not as low as that of the non-buffered run #368-C (see Table V). Figure 34 shows C_{gs} , G_m and μ_d for run #365-A obtained

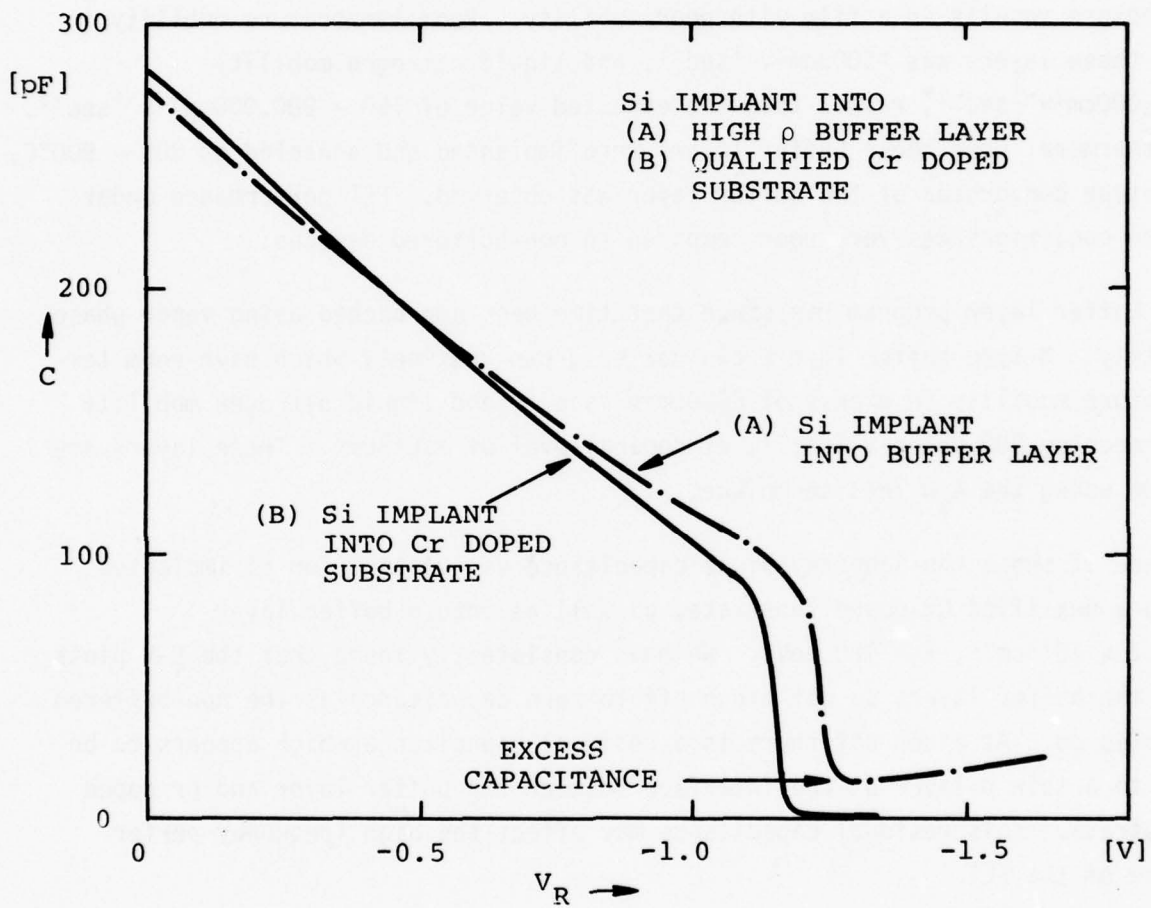


Figure 32
 Schottky Diode Capacitance vs. Voltage for Si Implanted
 into a Qualified Cr-Doped Substrate and High Resistivity
 Buffer Layer ($\phi = 2 \times 10^{12} \text{cm}^{-2}$, $E = 120 \text{ KeV}$)

TABLE VI
 RUN SUMMARY
 Si Implanted GaAs FETs (Buffer Layer)

Run #	Buffer Layer		E (KeV)	ϕ (cm ⁻²)	Geom.	6 GHz		18 GHz	
	N _D (cm ⁻³)	t (μm)				NF (dB)	G (dB)	NF (dB)	G (dB)
348-A			120	2 x 10 ¹²	M-107	2.3	10.0		
350-1A			"	"	"	1.8	10.5		
355-B			"	"	"	1.6	10.5		
355-D			"	"	"	1.7	9.8		
356-A			"	"	"	3.1	8.1		
356-B			"	"	"	1.7	10.9		
358-A			"	"	"	1.7	9.6		
365-A			"	"	"	1.4	10.9	2.8	6.0
365-B			"	"	"	1.8	10.5	3.9	5.7
365-C			"	"	"	1.6	10.6	2.8	5.5
366-C			"	"	"	1.7	11.1		

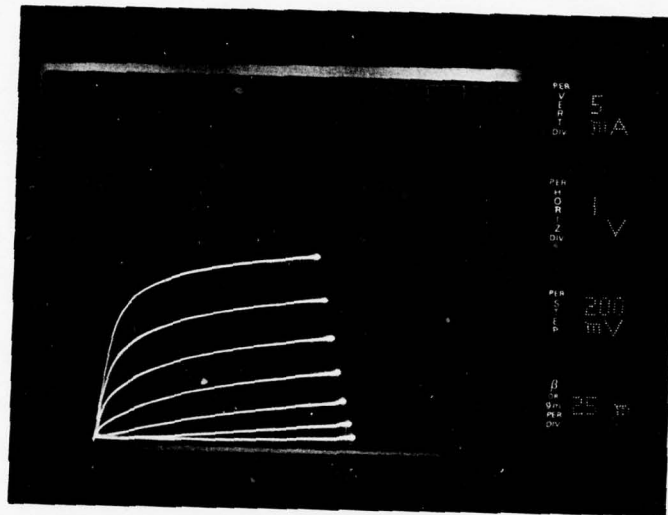


Figure 33
 Drain Characteristics Typical of Si Implanted Buffer
 Layer FET ($\phi = 2 \times 10^{12} \text{cm}^{-2}$, $E = 120 \text{KeV}$, M-107)

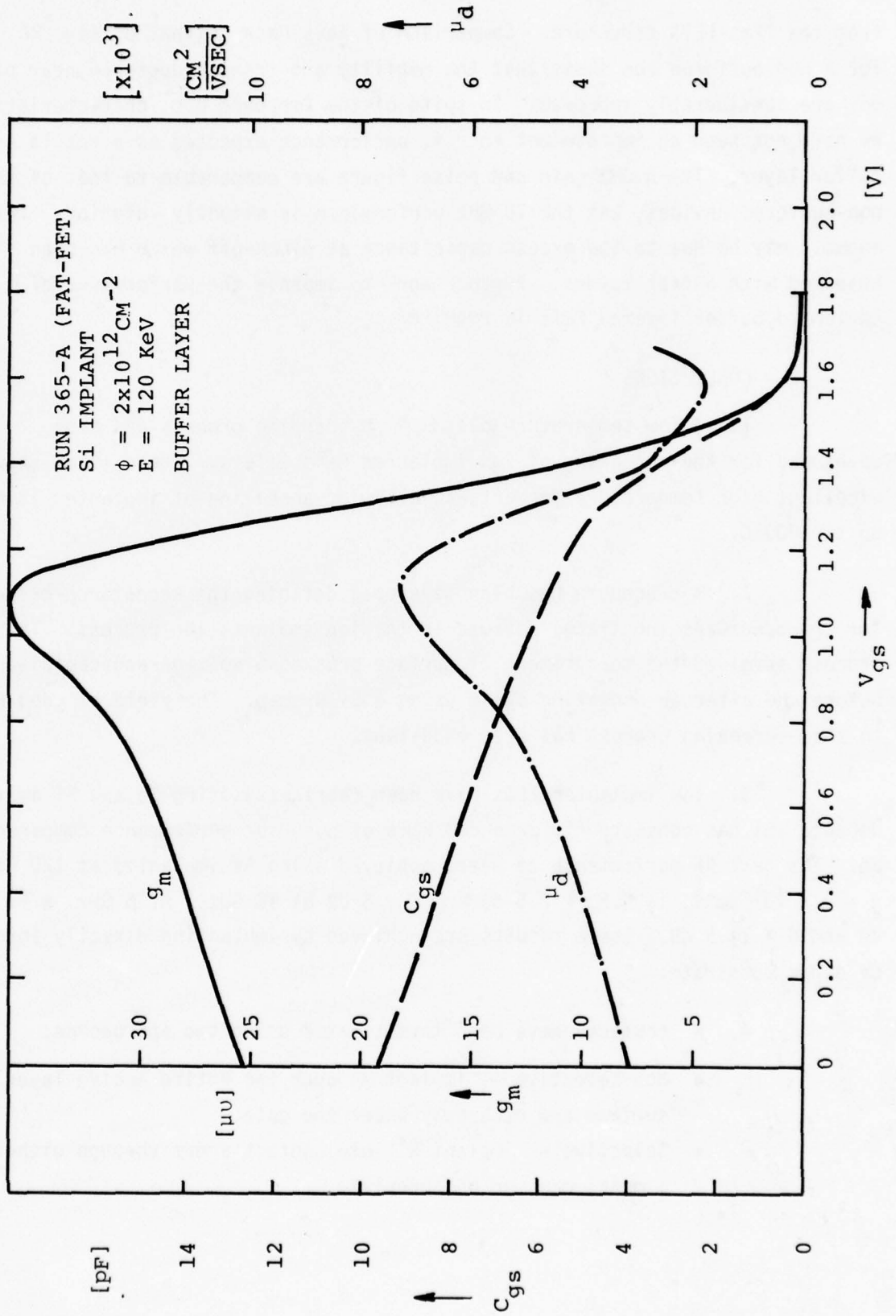


Figure 34
 g_m , C_{gs} , μ_d vs. Gate Voltage for Si Implanted FET Run #365-A

from the "Fat-FET" structure. Comparison of this data to that of Fig. 22 for a non-buffered run shows that the mobility and transconductance near pinch-off are considerably improved. In spite of the improved d.c. characteristics, we have not seen an improvement in r.f. performance expected as a result of the buffer layer. The 6 GHz gain and noise figure are comparable to that of the non-buffered devices, but the 18 GHz performance is slightly inferior. This anomaly may be due to the excess capacitance at pinch-off which has been observed with buffer layers. Further work to improve the performance of implanted buffer layered FETs is required.

F. CONCLUSIONS

1. A low temperature plasma Si_3N_4 capping process has been developed for the annealing of ion implanted GaAs wafers. These films show excellent high temperature properties, allowing annealing of implanted layers up to 1000°C .

2. A procedure has been developed defining the acceptance criteria for Cr doped GaAs substrates for use in the ion implantation process. This process involves the measurement of surface breakdown voltage and capacitance before and after an annealing cycle using a Si_3N_4 cap. The yield of good FETs to this screening process has been excellent.

3. Ion implanted FETs have been fabricated using Se and Si as the dopant. Si has consistently produced FETs of superior performance compared to Se. The best RF performance to date, achieved using Si implanted at 120 KeV, $\phi = 2 \times 10^{12}\text{cm}^{-2}$, is N.F. = 2.5 dB and G = 6 dB at 18 GHz. At 6 GHz, N.F. = 1.6 dB and G = 11.5 dB. These results are achieved by implanting directly into the Cr doped substrate.

4. N^+ contacts have been investigated using two approaches:
- Non-selective — implant N^+ over the entire active layer surface and etch away under the gate.
 - Selective — implant N^+ into contact areas through either a metal mask or photoresist.

The "non-selective" technique has not given performance as good as the single energy implant. The "selective" technique has not yet been evaluated.

5. Buffer layers are now routinely produced, using the A_5H_3/HCl method which have liquid nitrogen mobility $\approx 200,000\text{cm}^2\text{v}^{-1}\text{sec}^{-1}$, and doping $N_D \approx 10^{13}\text{cm}^{-3}$. Implantation into these buffer layers produces FETs with no looping and excellent D.C. characteristics. RF performance is found to be equivalent to that of the non-buffered devices at 6 GHz ($G \approx 11.0$ dB, N.F. ≈ 1.5 dB), but poorer at 18 GHz. This may be due to a residual excess capacitance resulting from a p-layer at the buffer layer-Cr substrate interface.

III. AMPLIFIER DEVELOPMENT

A. INTRODUCTION

The various amplifiers delivered on the contract are summarized in Table VII, as well as some of the characteristics of the gain modules and FETs used in these amplifiers. The data in the table shows that improvements in the FETs and circuits over the period of the contract resulted in higher module gain and power output and lower module noise figure. Also, over the period of the contract the Maximum Available Gain of the FETs at 18 GHz and the corrected noise figure were improved by very significant amounts.

All of the gain modules in the amplifiers are balanced amplifiers (2 FETs per module). Each gain module contains its own source and drain resistors and bypass capacitors, FET input and output matching networks, and low VSWR input and output Lange [9] couplers. These gain modules can be selected for particular characteristics and then connected together in any order. The ribbons which connect the microstrip lines of one gain module to the microstrip lines of the next module are compensated by capacitive tabs to reduce reflections and, therefore, "bumps" in the gain curve.

The input and output of each amplifier is a 90°, hermetically sealed, SMA-to-microstrip adapter. These adapters have a VSWR of 1.2 or less through 18 GHz. To reduce reverse gain and possible oscillation, the region above the gain modules in an assembled amplifier is a below-cutoff waveguide within the specified frequency range. At frequencies above the cutoff frequency of this waveguide where the forward gain may be over 20 dB (for a 40 dB gain amplifier), lossy material is placed in the waveguide to reduce reverse gain.

On this contract the amplifiers were assembled in stainless steel cases. The two halves of the case are welded to form a hermetically sealed amplifier. The amplifiers can be placed in larger packages with integral power supplies. Two such amplifier pairs with integral power supplies were delivered on the contract. The 10.7 to 18 GHz amplifiers were in a 2 x 2 x 11, TWT equivalent package. The 7 to 18 GHz amplifiers were mounted on a smaller AvanteK standard power supply.

TABLE VII
Amplifier Summary

AMPLIFIER			GAIN MODULE				FET CHARACTERISTICS AT 3V, 10 mA						
TOTAL GAIN DB	NUMBER OF MODULES	GAIN PER MODULE	AT HIGHEST FREQ. F_{∞} DB	1 DB PWR DBM	MASK/SLICE	INPUT C	INPUT R	OUTPUT C	OUTPUT R	MAG DB	18 GHz F _{COR} DB	GA DB	
20	6	3.5	7.8	13	EXP-130B	.21	10.4	.11	400	4.6			
25 with Limiter	6	4.5	8.5	12	EXP-150B	.26	9.4	.12	400	3.8			
10	4	2.5	9.5	10	M-103 EXP-182D	.32	9.9	.14	490	3.2			
40 with Limiter & Temp Comp	10	5	8.6	10	M-104 R35A	.18	20	.056	1050	6.0			
29 with Limiter	6	5	6.3	15	M-107 EXP-323D	.18	16	.071	460	6.2	4.4	5.5	
29 with Limiter	6	5	5.9	15	M-107 EXP-338	.22	18	.086	390	6.5	3.4	5.5	

Final tests on the 7 to 18 GHz amplifiers indicated that these amplifiers met all specifications in the original statement of work except those shown in the following table.

	<u>Specification</u>	<u>Measured</u>
Phase Deviation	$\pm 10^\circ$ max	+20, -30
Phase Matching	$\leq 5^\circ$	$< 5.3^\circ$
Safe Input Power	+50 dBm	+50 dBm
	10% Duty	1% Duty

The phase deviation was high due to the use of a 6-element FET input matching network to obtain a flat gain response down to less than 7 GHz. The peak pulse power handling ability of the input signal limiter is limited by the power dissipation of the diodes which are presently available.

Final tests on the 10.7 to 18 GHz amplifiers indicated that these amplifiers met all specifications over temperature except those shown in the following table.

	<u>Specification</u>	<u>Measured</u>
Gain Variation	0.5 dB over 0.5 GHz band	0.8 dB over 0.5 GHz band (0°C to 65°C)
Phase Deviation	$\pm 10^\circ$ max	$\pm 14^\circ$
Phase Matching	$\leq 5^\circ$	$< 8^\circ$ (0°C to 65°C)
Safe Input Power	+50 dBm	+50 dBm
	10% Duty	1% Duty

The calculated curves of gain and mismatch loss in the following sections were obtained through the use of Avantek computer simulation and circuit synthesis programs.

B. FET SELECTION

A detailed model or equivalent circuit for an M-107 FET is shown in Fig. 11. This actual equivalent circuit is more complicated than necessary to get approximate element values for the FET matching networks from a circuit synthesis program. The equivalent circuit of the FET is, therefore, simplified to be as shown in Fig. 35. This simplified equivalent circuit is accurate only over a narrow frequency range and for either S-parameter or simultaneous match. After the values of the elements in both the input and output matching networks have been determined from the synthesis program, the complete amplifier circuit may be simulated on a computer program which uses measured S-parameters or the equivalent of the complete and accurate FET model.

The matching networks are initially designed using the element values of the simplified FET equivalent circuit; conversely, FETs may be selected for use in a circuit on the basis of their simplified equivalent circuit element values. FETs with approximately the same element values can be used in similar amplifier circuits.

The minimum gate bonding inductance and the frequency range of the amplifier determine the maximum allowable FET input capacity, or vice versa. Since the physical layout of the circuit determines the gate bonding inductance, every effort was made to keep this inductance as small as possible without resorting to a "flip-chip" design. Table VII shows that the FET input capacity should be approximately 0.2 pF for the physical layout of either the 7 to 18 GHz or 10.7 to 18 GHz gain modules. Since the gain of the M-107 circuits in the 10.7 to 18 GHz amplifiers fell off too rapidly above 17 GHz to meet the 0.5 dB gain change per 0.5 bandwidth specification, the FETs selected for use in these circuits should have had a smaller input capacity. For a given bandwidth as determined by Fano's equation [10] (see Fig. 35), the RC product of the FET input circuit must be greater than or equal to some value. In other words, the Q of the input circuit has a maximum usable value.

Similarly, the maximum FET output capacity is determined by the drain bonding inductance and the frequency range. The bonding inductance is determined by

$$\int_0^{\infty} \frac{1}{\omega^2} \ln \left| \frac{1}{\rho} \right| d\omega = \pi RC$$

$$Q = \frac{1}{\omega RC}$$

$$\int_0^{\infty} \ln \left| \frac{1}{\rho} \right| d\omega = \frac{\pi}{RC}$$

$$Q = \omega RC$$

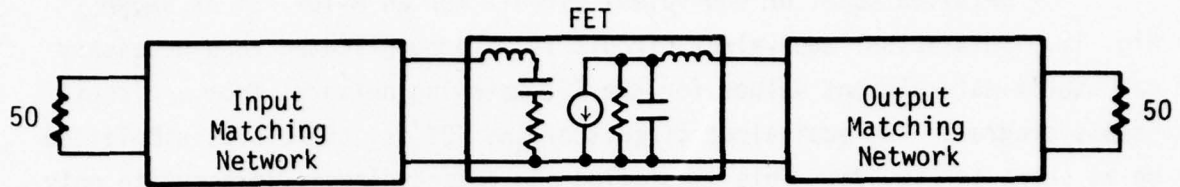


Figure 35
Simplified FET Amplifier Circuit

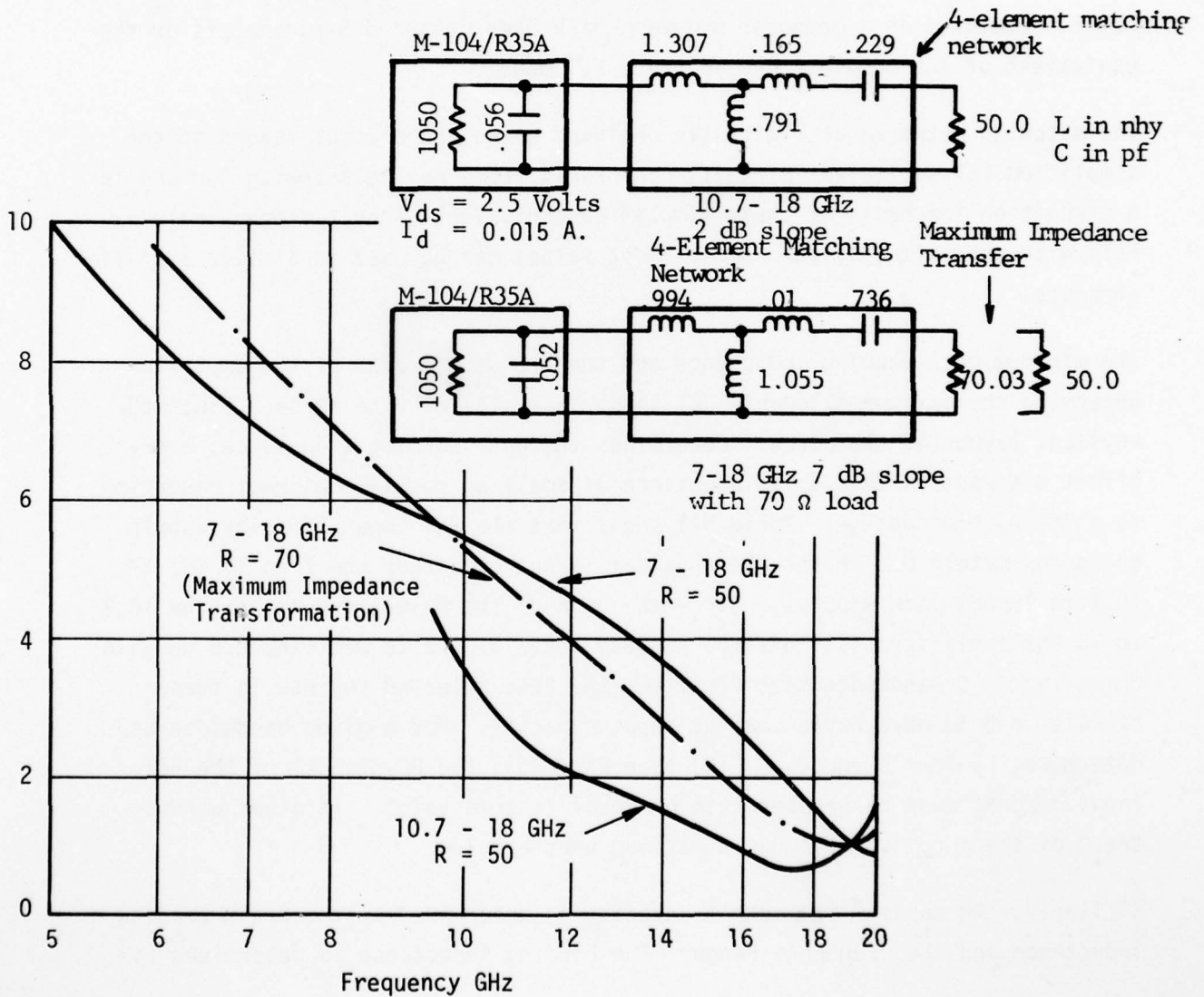


Figure 36
Effect of Impedance Mismatch on Output Mismatch Loss

the physical layout of the circuit. For a given bandwidth as determined by Fano's equation, both the RC product and the Q of the FET output circuit must be less than or equal to a particular value.

All of the gain modules used 4-element FET output matching circuits. The impedance transforming ability of a 4-element matching circuit is limited [10]. Therefore, for a small ripple in the gain curve (small impedance mismatch), the bandwidth of the M-104/R35A FETs were limited by the impedance transforming ability of the 4-element matching network. These FETs could not be used for the 7 to 18 GHz amplifiers. In Table VII the output resistance of the M-104/R35A FET is seen to be approximately twice the output resistance of the other wider gate FETs. As an example, Fig. 36 shows a plot of the mismatch loss for the M-104/R35A FET for two different output matching circuits. For the 10.7 to 18 GHz frequency range, the 4-element matching circuit has a 2 dB slope and is able to match 1050 ohms to 50 ohms. For the 7 to 18 GHz frequency range and 7 dB slope, the maximum impedance transformation is from 1050 ohms to only 70 ohms. One curve shows the relatively straight line slope for this matching network with a 70 ohm termination. Another curve shows the high ripple in the mismatch curve if the termination is changed from 70 to 50 ohms with no other changes in the circuit. Any ripples in the mismatch loss curve appear as ripples in the gain curve.

Tables VIII through XII show Automatic Network Analyzer (ANA) listings for the 3 different FETs used in the final 10.7 to 18 GHz and 7 to 18 GHz amplifiers. The data in Table VIII was taken at high current (near I_{DSS}) where the M-104 was normally used. The data in Tables IX and XI was taken on M-107's at low current where the noise figure was near optimum. The data in Tables X and XII was taken at higher currents where the M-107's were used for high gain and power output.

RPZ
2/9/77

TABLE VIII

FET EVALUATION
M-104/K35A

SER NO. 1

BIAS= 2.50 VOLTS, 20.00 MA

S -- MAGN AND ANGLES:

FREQ	11 RAT10	11 DB	21 DB	12 DB	22 RAT10
2000.00	.976	-17.2	3.487	161.3-37.834	83.3 .917 -4.9
3000.00	.952	-23.2	3.420	154.0-33.714	75.3 .907 -7.4
4000.00	.929	-29.5	3.467	146.5-31.245	77.1 .908 -8.6
5000.00	.878	-38.1	3.517	137.5-29.647	77.5 .890 -9.4
6000.00	.821	-48.9	3.544	128.7-28.861	80.7 .886 -12.0
7000.00	.788	-58.3	3.613	120.6-28.778	81.4 .871 -14.0
8000.00	.729	-70.8	3.447	110.6-28.848	75.0 .873 -16.0
9000.00	.675	-82.3	3.365	100.1-28.560	72.7 .864 -19.1
10000.00	.612	-94.8	3.108	91.4-28.331	68.1 .848 -21.6
11000.00	.582	-109.9	3.025	83.4-27.584	69.9 .851 -24.4
12000.00	.546	-124.1	2.929	73.9-26.312	67.0 .836 -27.1
13000.00	.512	-140.2	2.801	64.0-25.748	66.4 .809 -30.2
14000.00	.480	-158.4	2.480	56.4-26.374	60.7 .790 -31.5
15000.00	.490	-176.8	2.554	44.6-24.856	60.8 .796 -38.8
16000.00	.532	167.0	2.310	32.3-24.087	49.9 .790 -45.1
17000.00	.541	151.1	2.066	22.4-23.178	41.3 .779 -50.9
17999.99	.561	132.9	1.660	13.1-21.908	30.3 .724 -53.6

REF PLANES = 3.09 3.09 6.18

FREQ MHZ	S21 DB	MSG DB	K	MAG DB	MASON U DB
2000.00	3.49	20.66	.26	\$\$\$\$\$\$	31.55
3000.00	3.42	18.57	.45	\$\$\$\$\$\$	21.72
4000.00	3.47	17.36	.44	\$\$\$\$\$\$	25.03
5000.00	3.52	16.58	.61	\$\$\$\$\$\$	23.23
6000.00	3.54	16.20	.67	\$\$\$\$\$\$	\$\$\$\$\$\$
7000.00	3.61	16.20	.81	\$\$\$\$\$\$	28.50
8000.00	3.45	16.15	1.04	14.96	19.54
9000.00	3.37	15.96	1.24	13.03	17.36
10000.00	3.11	15.72	1.58	11.26	14.37
11000.00	3.03	15.30	1.42	11.45	15.56
12000.00	2.93	14.62	1.42	10.77	15.03
13000.00	2.80	14.27	1.61	9.69	13.08
14000.00	2.48	14.43	2.07	8.53	10.79
15000.00	2.55	13.71	1.55	9.33	12.61
16000.00	2.31	13.20	1.37	9.56	13.61
17000.00	2.07	12.62	1.29	9.42	13.87
17999.99	1.66	11.78	1.39	8.05	11.79

REF PLANES = 3.09 3.09 6.18

TABLE IX

SA
JULY 13, 1977

FET EVALUATION
M-107/CAF 325D

SER NO. 1

BRS= 2.00 VOLTS, 12.00 MA

S -- MAGN AND ANGLES:

FREQ		11		21		12		22
2000.00	.981	-17.7	1.609	161.9	.922	93.1	.773	-6.2
3000.00	.954	-25.1	1.555	154.2	.933	90.4	.761	-6.6
4000.00	.942	-32.0	1.564	147.3	.941	79.2	.746	-8.1
5000.00	.899	-39.0	1.547	139.6	.948	78.0	.727	-9.2
6000.00	.877	-47.9	1.571	132.0	.954	77.2	.711	-12.0
7000.00	.849	-55.6	1.570	123.6	.960	74.5	.698	-16.7
8000.00	.806	-64.9	1.565	115.9	.964	72.7	.685	-21.3
9000.00	.759	-73.8	1.546	105.9	.968	69.2	.663	-26.1
10000.00	.710	-83.6	1.487	99.7	.961	69.7	.629	-29.2
11000.00	.697	-92.2	1.491	91.0	.971	71.8	.645	-33.3
12000.00	.670	-103.2	1.468	82.5	.977	65.7	.671	-42.4
13000.00	.612	-115.3	1.394	74.9	.962	63.7	.607	-46.8
14000.00	.612	-128.1	1.443	65.6	.984	68.6	.609	-53.4
15000.00	.618	-140.5	1.401	55.7	.993	60.8	.595	-62.6
16000.00	.629	-150.5	1.374	46.0	.997	56.4	.571	-71.0
17000.00	.590	-162.2	1.329	34.9	.105	49.5	.545	-79.8
17999.99	.557	-176.6	1.278	26.3	.123	43.8	.533	-85.6

REF PLANES = 3.09 3.09 6.18

FREQ MHZ	S21 DB	NSC DB	K	MAG DB	MASON U DB
2000.00	4.13	18.55	.24	*****	29.12
3000.00	3.33	16.78	.35	*****	21.62
4000.00	3.88	15.78	.47	*****	22.16
5000.00	3.79	15.12	.70	*****	16.58
6000.00	3.92	14.60	.72	*****	20.02
7000.00	3.92	14.16	.83	*****	18.30
8000.00	3.89	13.89	.94	*****	17.60
9000.00	3.78	13.59	1.14	11.29	14.94
10000.00	3.94	13.34	1.61	9.25	11.81
11000.00	3.47	13.24	1.38	9.77	13.91
12000.00	3.34	12.79	1.21	10.00	15.33
13000.00	2.88	13.54	2.16	7.45	9.97
14000.00	3.19	12.33	1.41	8.52	12.65
15000.00	2.93	11.76	1.32	8.41	13.09
16000.00	2.75	11.50	1.30	8.21	12.81
17000.00	2.97	11.04	1.45	7.06	10.50
17999.99	2.13	10.17	1.39	6.46	9.97

REF PLANES = 3.09 3.09 6.18

TABLE X

SH
JULY 13, 1977

FET EVALUATION
M-107/ ERF 323D

SEP NO. 1

BIAS= 2.00 VOLTS; 20.00 MA

S -- HIGH AND HIGLES:

FREQ	11	21	12	22
2000.00	.980 -18.5	1.812 161.6	.019 84.0	.785 -45.8
3000.00	.950 -26.2	1.746 153.7	.027 81.5	.773 -46.0
4000.00	.933 -33.4	1.752 147.1	.034 80.1	.759 -47.3
5000.00	.890 -40.7	1.726 138.7	.039 81.1	.740 -48.3
6000.00	.865 -49.9	1.747 131.5	.044 81.4	.725 -49.7
7000.00	.826 -57.9	1.734 123.1	.048 80.1	.713 -49.0
8000.00	.793 -67.3	1.724 115.3	.051 79.6	.703 -49.4
9000.00	.747 -76.2	1.700 106.4	.054 77.9	.684 -48.7
10000.00	.702 -86.9	1.623 99.6	.048 81.6	.648 -47.2
11000.00	.685 -95.6	1.627 90.8	.058 84.8	.669 -46.5
12000.00	.657 -107.4	1.607 82.4	.063 79.2	.705 -48.8
13000.00	.607 -119.2	1.521 74.8	.052 82.3	.642 -46.8
14000.00	.601 -131.7	1.563 65.7	.075 84.6	.645 -49.9
15000.00	.613 -143.8	1.515 55.8	.084 76.7	.637 -48.9
16000.00	.625 -153.9	1.484 46.1	.090 72.6	.614 -46.1
17000.00	.586 -165.4	1.433 35.3	.097 64.4	.588 -45.5
17999.99	.556 -179.7	1.366 26.5	.116 57.9	.577 -48.2

REF PLANES = 3.09 3.09 6.18

FREQ MHz	S21 DB	M5G DB	F	MAG DB	MASON D DB
2000.00	5.16	19.82	.24	*****	34.10
3000.00	4.84	18.07	.47	*****	22.94
4000.00	4.87	17.07	.46	*****	24.62
5000.00	4.74	16.48	.75	*****	20.13
6000.00	4.85	15.99	.78	*****	21.73
7000.00	4.78	15.55	.91	*****	19.82
8000.00	4.73	15.28	1.00	*****	19.42
9000.00	4.61	14.96	1.21	12.22	16.67
10000.00	4.21	13.26	1.72	10.32	13.14
11000.00	4.23	14.50	1.37	10.68	15.51
12000.00	4.12	14.06	1.18	11.52	18.21
13000.00	3.64	14.70	2.11	6.71	10.91
14000.00	3.88	13.20	1.31	9.85	14.15
15000.00	3.61	12.55	1.17	10.09	15.39
16000.00	3.43	12.17	1.13	10.00	15.01
17000.00	3.13	11.69	1.29	8.47	11.99
17999.99	2.71	10.62	1.19	7.98	11.69

REF PLANES = 3.09 3.09 6.18

THIS PAGE IS BEST QUALITY PRACTICABLE
FROM COPY FURNISHED TO DDC

SH
AUG 2, 1977

TABLE XI

FET EVALUATION
M-107 EXP-338

SER NO. 1

BIAS= 2.00 VOLTS, 12.00 MA

S -- MAGN AND ANGLES:

FREQ	11	21	12	22
2000.00	.979 -15.3	1.714 163.6	.018 85.5	.792 -5.8
3000.00	.950 -21.2	1.653 156.5	.026 84.9	.778 -6.2
4000.00	.936 -26.9	1.672 149.4	.033 85.1	.769 -7.8
5000.00	.893 -33.0	1.678 143.6	.038 85.4	.748 -10.0
6000.00	.862 -40.5	1.711 134.8	.043 84.3	.750 -13.9
7000.00	.834 -46.7	1.691 126.6	.047 87.0	.723 -18.5
8000.00	.777 -58.0	1.687 119.8	.048 87.9	.717 -21.9
9000.00	.736 -65.2	1.628 110.2	.052 87.7	.728 -26.4
10000.00	.683 -75.1	1.592 103.0	.054 89.2	.706 -31.9
11000.00*	1.175 -86.4	1.409 96.8	.055 94.6	.713 -36.3
12000.00	.620 -91.6	1.528 88.5	.063 92.5	.714 -42.1
13000.00	.573 -104.5	1.490 79.0	.067 92.4	.698 -44.5
14000.00	.525 -117.3	1.406 72.6	.068 94.2	.698 -46.9
15000.00	.536 -129.6	1.396 63.4	.086 91.8	.723 -52.9
16000.00*	.537 -139.5	1.310 50.3	.090 81.4	*1.351 -61.3
17000.00	.494 -149.5	1.332 48.6	.106 84.8	.701 -60.9
17999.99	.464 -163.7	1.338 40.4	.116 76.9	.711 -64.9

REF PLANES = 3.09 3.09 6.18

FREQ MHZ	S21 DB	MSG DB	K	MAG DB	MASON U DB
2000.00	4.68	19.70	.26	*****	30.09
3000.00	4.36	18.09	.49	*****	22.67
4000.00	4.47	17.11	.50	*****	25.63
5000.00	4.50	16.46	.71	*****	20.76
6000.00	4.67	15.98	.76	*****	22.18
7000.00	4.56	15.58	.86	*****	22.84
8000.00	4.54	15.46	1.07	13.90	18.88
9000.00	4.23	14.97	1.14	12.71	18.40
10000.00	4.04	14.69	1.36	11.10	15.44
11000.00*	2.98	14.10	-1.75	*****	*****
12000.00	3.68	13.84	1.30	10.56	15.71
13000.00	3.47	13.45	1.46	9.43	13.19
14000.00	2.96	13.14	1.66	8.38	11.09
15000.00	2.90	12.12	1.12	10.00	14.78
16000.00*	2.35	11.65	-3.08	*****	*****
17000.00	2.49	11.00	1.10	9.05	12.74
17999.99	2.53	10.63	1.01	10.04	13.87

REF PLANES = 3.09 3.09 6.18

* Bad Data

SH
AUG 2, 1977

TABLE XII

FET EVALUATION
M-107 EXP-338

SER NO. 1

BIAS= 2.00 VOLTS, 20.00 MA

S -- MAGN AND ANGLES:

FREQ	11	21	12	22
2000.00	.978 -16.4	2.011 162.9	.016 85.6	.797 -5.6
3000.00	.944 -22.8	1.933 155.6	.023 85.8	.784 -5.9
4000.00	.928 -28.9	1.952 148.7	.028 86.7	.773 -7.3
5000.00	.876 -35.7	1.951 142.4	.033 87.8	.752 -9.4
6000.00	.854 -44.0	1.974 133.5	.037 88.6	.756 -13.2
7000.00	.803 -53.5	1.934 125.2	.040 90.5	.729 -17.5
8000.00	.762 -60.4	1.924 118.5	.042 95.7	.721 -20.6
9000.00	.710 -69.2	1.846 108.9	.045 97.2	.736 -24.9
10000.00	.655 -79.6	1.797 101.4	.049 99.9	.715 -30.2
11000.00	.628 -87.6	1.743 94.4	.055 104.8	.723 -34.5
12000.00	.588 -98.0	1.704 85.9	.060 103.6	.729 -40.5
13000.00	.541 -110.3	1.649 77.7	.066 103.4	.713 -42.7
14000.00	.496 -123.5	1.553 71.7	.068 105.1	.715 -45.1
15000.00	.510 -135.6	1.532 62.5	.086 101.2	.744 -51.0
16000.00	.513 -145.6	1.490 55.2	.094 97.3	.730 -56.1
17000.00	.473 -155.6	1.453 48.0	.106 92.3	.729 -59.5
17999.99	.441 -170.5	1.453 39.5	.118 84.6	.741 -62.9

REF PLANES = 3.09 3.09 6.18

FREQ MHZ	S21 DB	MSG DB	K	MAG DB	MASON U DB
2000.00	6.07	20.94	.26	*****	32.94
3000.00	5.72	19.33	.50	*****	24.43
4000.00	5.81	18.39	.51	*****	28.82
5000.00	5.80	17.78	.77	*****	22.02
6000.00	5.91	17.28	.73	*****	31.26
7000.00	5.73	16.83	.94	*****	22.90
8000.00	5.68	16.60	1.05	15.25	22.46
9000.00	5.33	16.08	1.13	13.89	21.12
10000.00	5.09	15.68	1.34	12.22	17.15
11000.00	4.83	15.04	1.21	12.27	18.25
12000.00	4.63	14.53	1.18	11.94	17.66
13000.00	4.34	13.99	1.31	10.64	14.51
14000.00	3.82	13.58	1.45	9.59	12.32
15000.00	3.71	12.49	.94	*****	17.11
16000.00	3.47	11.99	.92	*****	16.03
17000.00	3.24	11.35	.91	*****	14.99
17999.99	3.25	10.89	.82	*****	17.07

REF PLANES = 3.09 3.09 6.18

To summarize, the following FET characteristics must be specified if the FET is to be useful in a particular physical circuit:

- C_{in} and C_{out} - maximum values which depend upon upon bonding inductance
- $(RC)_{input}$ - minimum value depends upon bandwidth
- $(RC)_{output}$ - maximum value depends upon bandwidth
- R_{in} and R_{out} - minimum value of R_{in} and maximum value of R_{out} which depend on impedance transforming ability of matching network
- MAG - (desired gain) + (input and output mismatch loss)
+ (circuit losses)

C. SINGLE-ENDED AMPLIFIERS

The gain of an amplifier is equal to the maximum available gain minus the sum of the mismatch losses of the input and output matching networks.

$$\text{Gain} = \text{MAG} - (\text{MMLS}_{11} \text{ and } \text{MMLS}_{22})$$

For a flat gain response over the bandwidth of the amplifier the right hand side of the equation must be a constant. Since MAG decreases with increasing frequency at about 6 dB/octave, the sum of the mismatch losses should decrease with increasing frequency at the same rate of about 6 dB/octave. In addition, to have the highest gain at the high frequency end of the desired band the sum of the mismatch losses must be as small as possible at that frequency.

The mismatch loss of a circuit is:

$$\text{Loss} = 1/(1 - |\rho|^2)$$

For a given input or output FET RC product Fano's equation (Fig. 35) shows that the narrower the bandwidth, the higher must be the term, $\text{Ln } |1/\rho|$. Or, the narrower the bandwidth, the smaller will be ρ and the mismatch loss. Also, the wider the bandwidth, the higher will be ρ and the mismatch loss. The FET RC product determines the maximum bandwidth obtainable from a particular type of matching network.

Figure 37 shows the calculated mismatch loss for two different input matching networks for an M-107 type FET over the 5 to 20 GHz frequency range. The upper curve is for a 4-element matching network and the lower curve is for the 6-element matching network that was used in the 7 to 18 GHz amplifiers. At 7 GHz the loss for the 4-element network is about 0.5 dB higher than the loss for the 6-element network. Since 6 gain modules were used in the 7 to 18 GHz amplifier, this 0.5 dB loss per matching network would have corresponded to a 3 dB loss in gain at 7 GHz for a complete amplifier. The ripple in the mismatch loss curves must be kept low so that the total ripple in the gain curve for a single, balanced gain module is only ± 0.2 dB maximum. Many gain modules may then be connected together with a low resultant amplifier gain ripple.

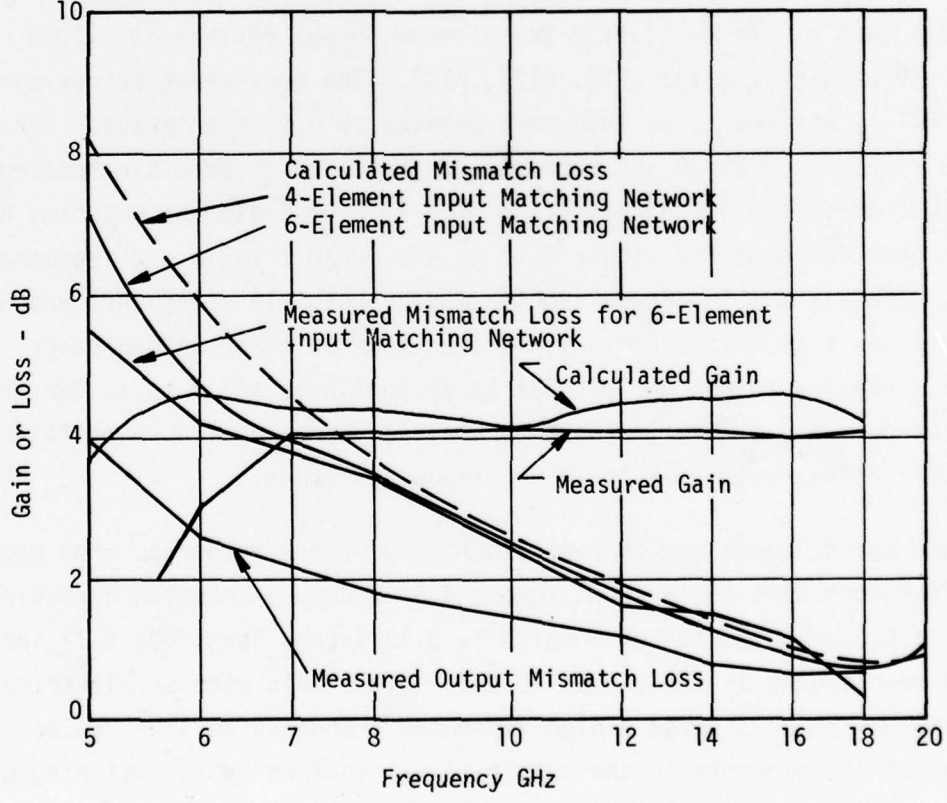
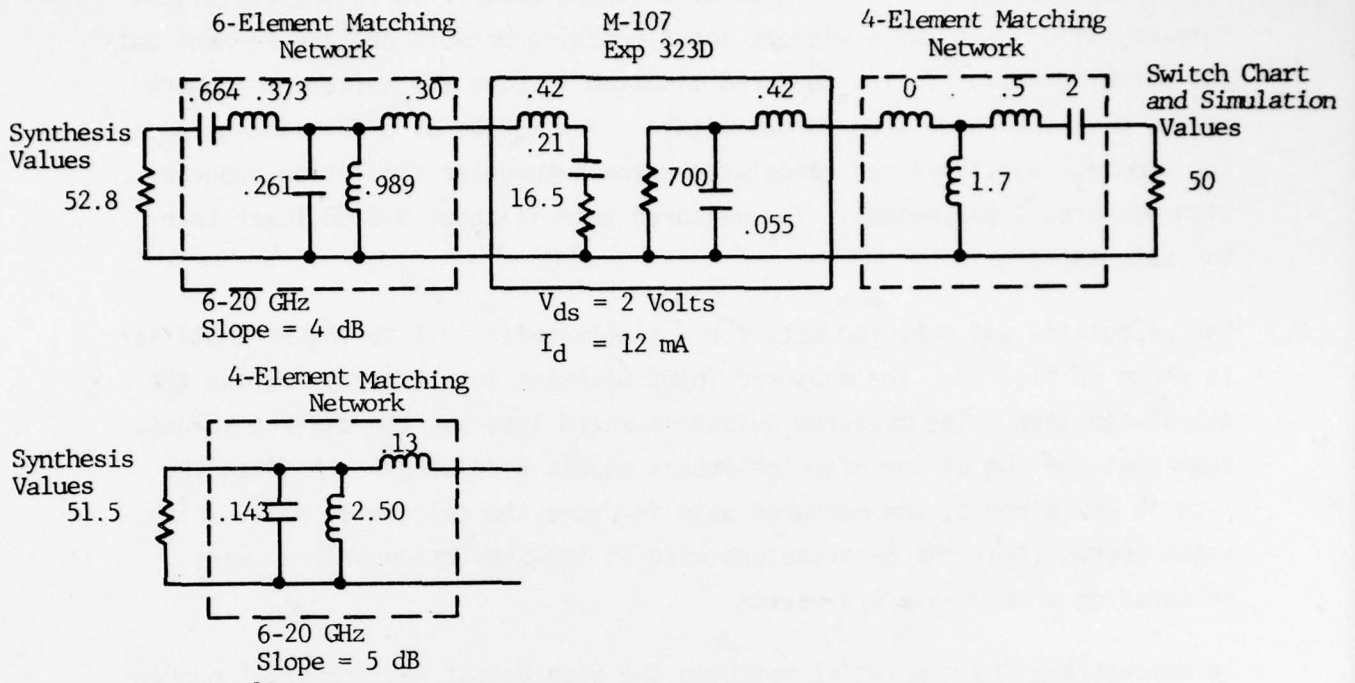


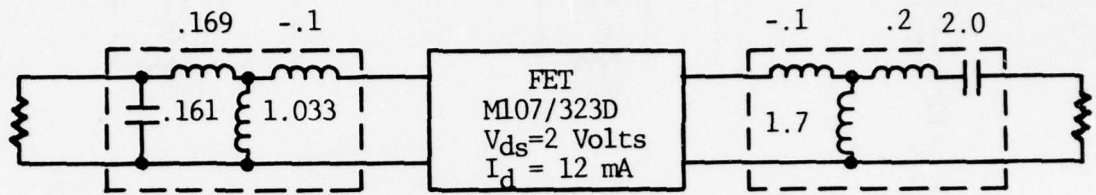
Figure 37
Single Ended 7 to 18 GHz Amplifier

Also shown in Fig. 37 are the data on a single-ended 7 to 18 GHz amplifier. This amplifier used the 6-element input matching network and a 4-element output matching network. The measured mismatch loss on the 6-element network agrees with the calculated values within a few tenths of a dB. The gain of the complete amplifier was calculated using a computer simulation program with measured S-parameters. The measured gain is about 0.5 dB lower than the calculated gain.

The calculated and measured data for a single-ended 10.7 to 18 GHz amplifier is shown in Fig. 38. The measured input mismatch loss closely follows the calculated loss. The measured output mismatch loss has the desired values, such that the sum of the mismatch losses equals 6 dB/octave. As with the 7 to 18 GHz circuit, the measured gain is above the calculated gain, which might suggest that the S-parameters used in the simulation program were measured on a below-average device.

To demonstrate the problem of matching the high output resistance of narrow gate FETs such as the M-104, the transformed output resistance values in Fig. 39 were calculated [11], [12], [13]. The equivalent output circuit of the FET is assumed to be 1000 ohms shunted by 0.03 picofarads. For an assumed ripple of 0.25 dB and zero slope, the circuits were synthesized. After synthesis, the output resistance for 4, 6 or 8-element matching networks are all over 400 ohms for either 7 to 18 GHz or 10.7 to 18 GHz frequency ranges. The maximum impedance transformation possible using the L-connected inductors was then calculated. It is seen that at least an 8-element network is necessary to match 1000 ohms to 50 ohms over the 7 to 18 GHz frequency range. A 4-element network can be used to match 1000 ohms to 50 ohms over the narrower 10.7 to 18 GHz frequency range.

There are special problems in realizing any of these networks. For example, a low frequency wire table shows that a 4.5 nanohenry inductance requires a length of 0.5 mil diameter wire which is 0.12 inches long; but 0.12 inches is 0.18 wavelengths in the air at 18 GHz. Since this wire is electrically long, it must be considered a high impedance transmission line. Also, the location of the elements on the substrate as required by the matching network compared to the location of RF grounds and FET and coupler terminals make some matching networks difficult to achieve.



9-20 GHz
3 dB slope from
synthesis

Smith Chart and
Simulation

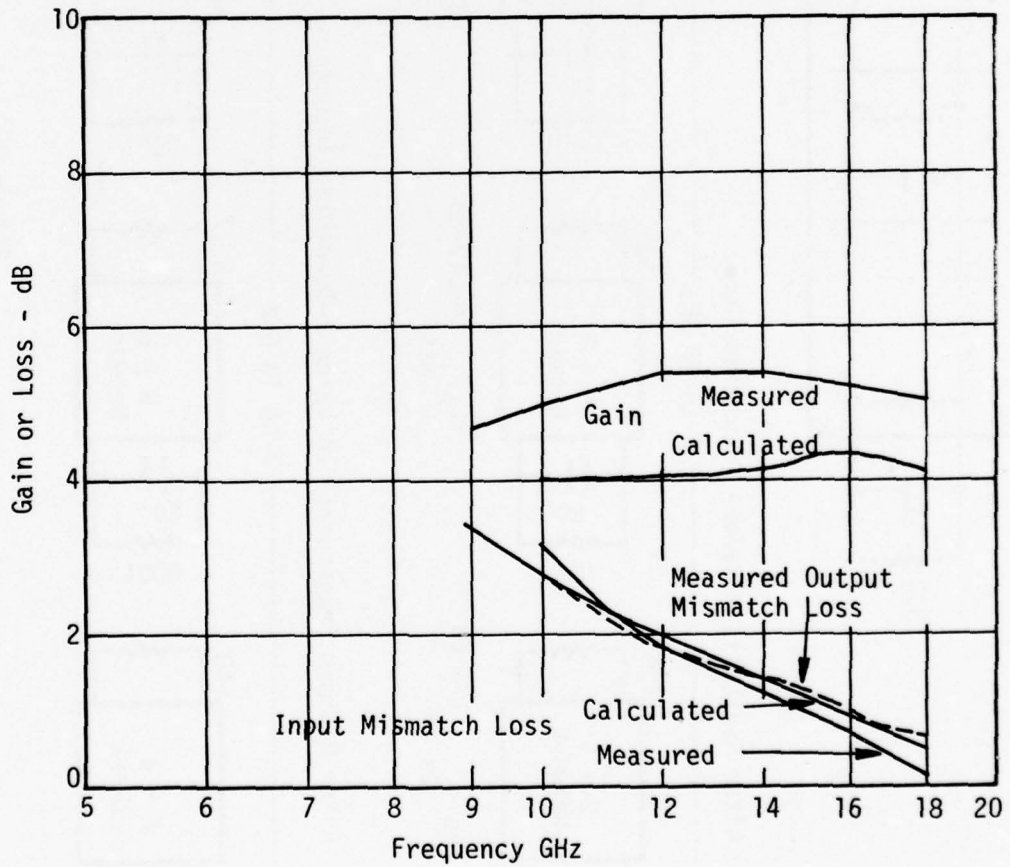
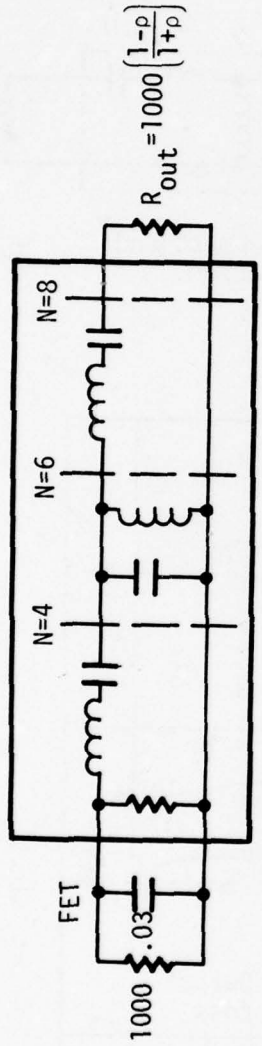


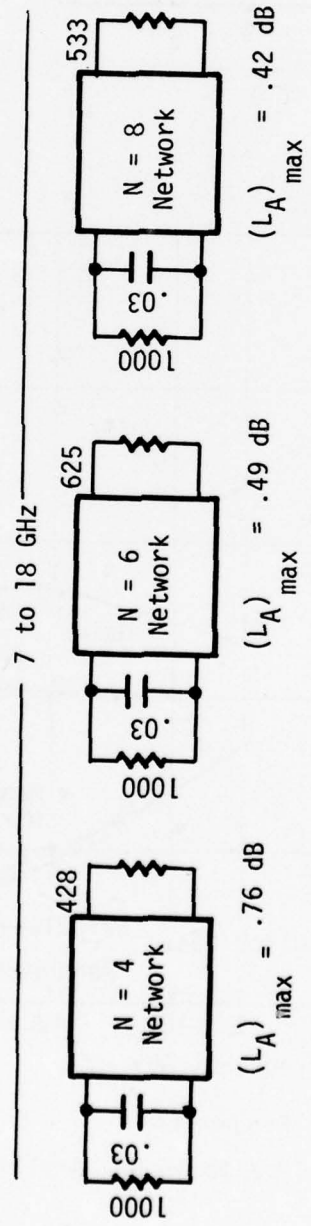
Figure 38
Single Ended 10.7 to 18 GHz Amplifier

Possible Bandpass Matching Networks



N=4 and N=8
 $|\rho|^2 = 1 - \frac{1}{(L_A)_{\max}}$
 N=6
 $|\rho|^2 = 1 - \frac{1}{(L_A)_{\min}}$
 $(L_A)_{\max} = (L_A)_{\min} + \text{Ripple}$

After Synthesis - Before Transformation



After Maximum Transformation using L-Connected Inductors

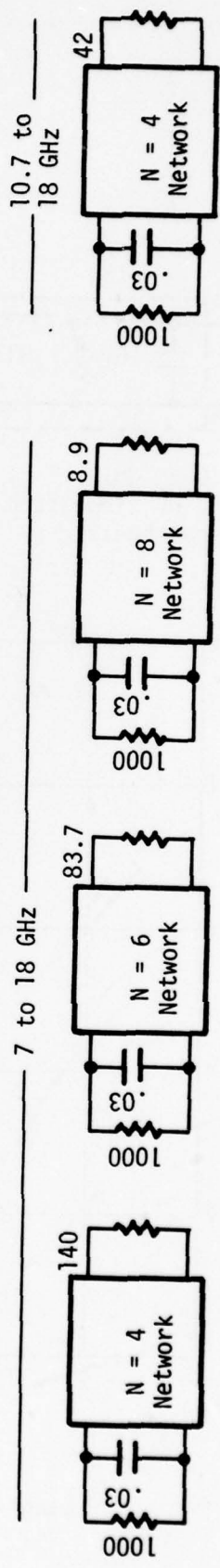


Figure 39

Maximum Impedance Transformation using 4, 6, or 8 Element Networks

Several sources of error in circuit synthesis and simulation are: (1) the inaccuracy of the S-parameter data, (2) the reference planes error (or bonding inductance), (3) the overly-simplified FET equivalent circuit is not accurate over the entire frequency range, and (4) the equivalent resistance and capacitance of the FET should correspond to those for simultaneous match rather than unilateral match near the high frequency edge of the band.

D. BALANCED GAIN MODULES

A schematic diagram of a balanced amplifier module is shown in Fig. 40 [14]. An input signal applied at ①, splits and appears at ③ and ④. The two signals at those points are now 90° out of phase because of the hybrid coupler. The two signals are amplified by A1 and A2 which are made as identical as possible. The two signals are then recombined by the output hybrid coupler.

The phasing is such that they appear at ⑦ in phase and at ⑧, 180° out of phase. If the coupling of the hybrids is exactly 3 dB at a particular frequency, then the two signals cancel at ⑧ and the gain of the balanced amplifier from ① to ⑦ is that of the individual stages A1 or A2, minus any losses in the hybrids. At frequencies where the coupling is not 3 dB, there will be a reduction in gain from ① to ⑦ equal to $2k\sqrt{1-k^2}$ where k^2 is the coupling of the coupled port. ($k^2 = 0.5$ for 3 dB coupling.)

The deviation of coupling from 3 dB will cause mismatch loss and ripple in the balanced amplifier (see Fig. 42). A coupler with 3 dB of coupling at midband would cause significant loss (~0.3 dB) at the band edges of a 7 to 18 GHz amplifier. By overcoupling the design at midband, some loss occurs at midband but bandpass response of the amplifier is significantly increased. A 2.4 dB coupling seemed to be the best compromise for the 7 to 18 GHz band since it caused less than 0.1 dB of degradation in gain from 6.5 to 18.5 GHz. Likewise, 2.8 dB coupling was selected for the 10.7 to 18 GHz band.

The most significant reason for using balanced construction, however, is the improvement in VSWR which is gained over that of a single-ended amplifier. Again referring to Fig. 40, any reflections at ③ and ④ due to a signal at ① are again split by the input hybrid. If the amplifiers have identical reflection coefficients, and the coupling is 3 dB at that particular frequency, the reflections will be in phase at ② and will be absorbed by the 50 ohm termination. The reflections will cancel at ① and make the amplifier appear to have unity VSWR. For frequencies where the coupling is not 3 dB, the improvement return loss over that of the single-ended stages will be $(2k^2-1)$. Figure 41 shows the coupler dimensions.

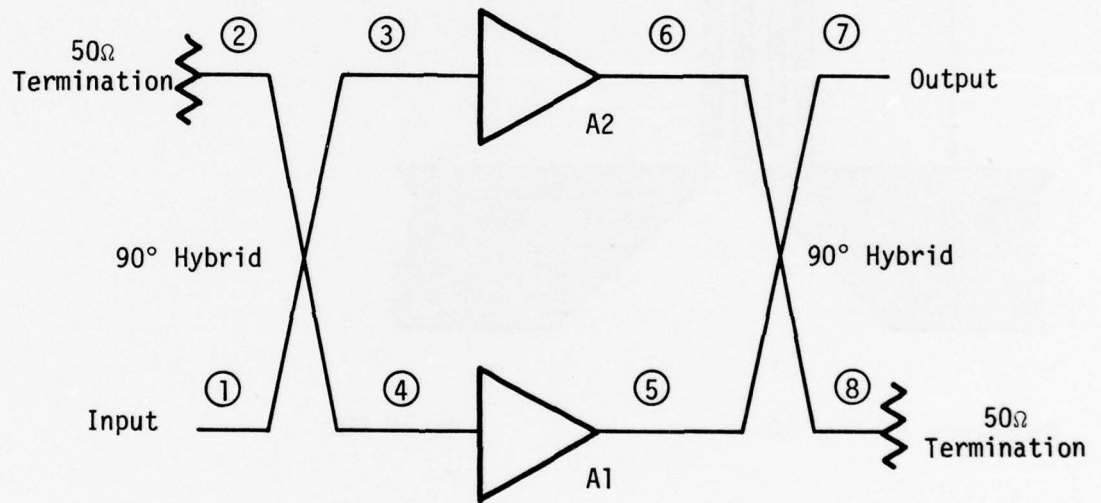
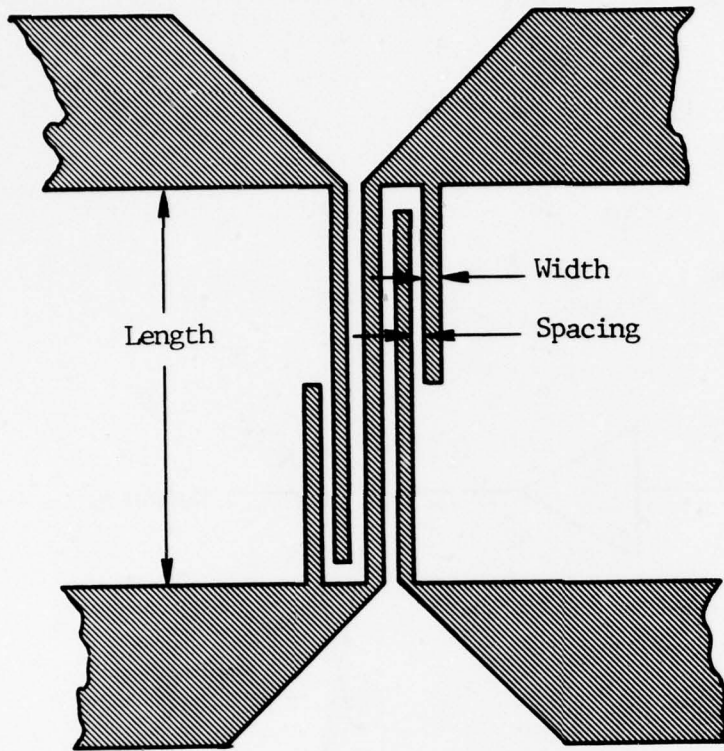


Figure 40
Schematic Diagram of a Balanced Amplifier Module



Material: .015 inch
Thick Alumina

Frequency 10.7 to 18

7 to 18 GHz

K 2.4

2.8 dB

W .00122

.00140 inches

S .00063

.00096 inches

L .0945

.0823 inches

Figure 41 Couplers

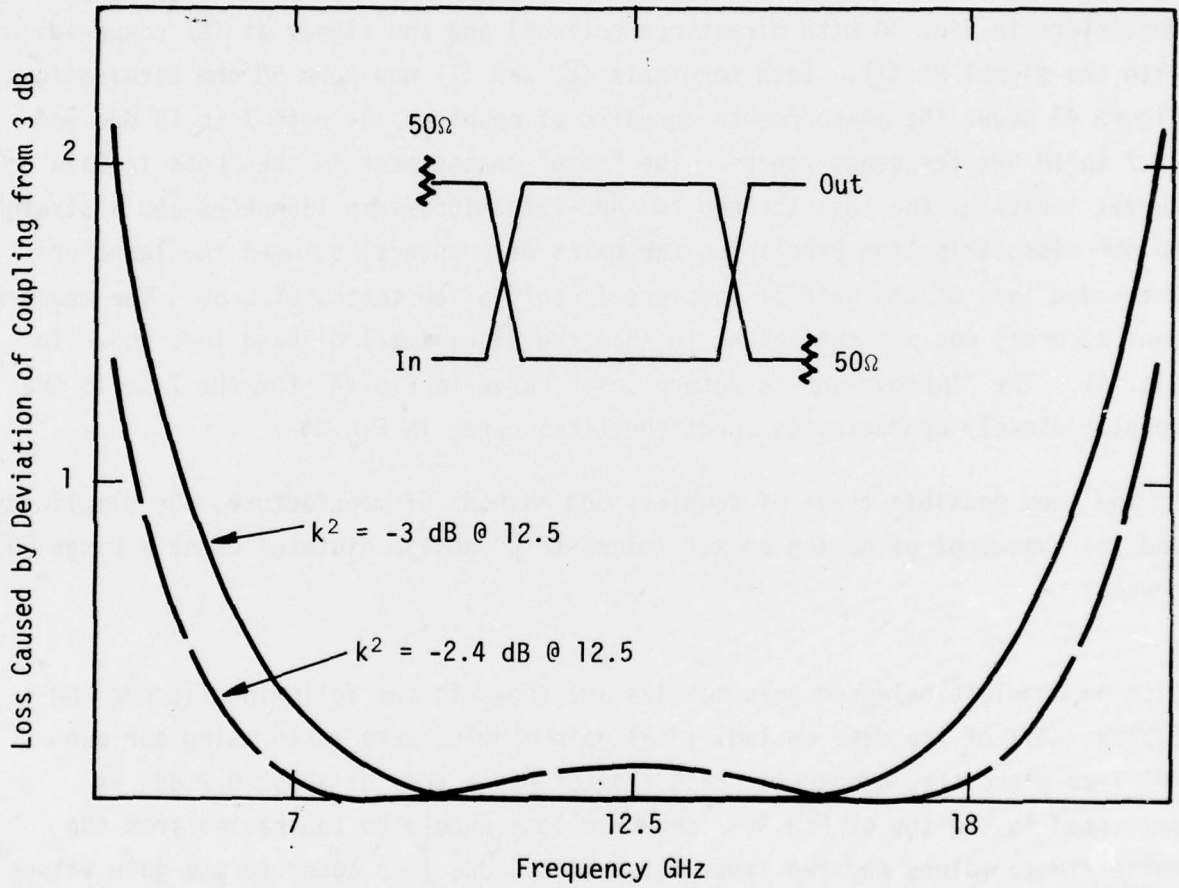


Figure 42

Through Loss for 2-Single Section 90° Hybrids
Connected in Balanced Configuration

Figure 43 shows the improvement in return loss vs. frequency for a 2.4 and 3.0 dB single section coupler.

The theoretical midband improvement in return loss is 16 dB for a 2.4 dB coupler and 26 dB for 2.8 dB coupler. A 16 dB improvement corresponds to a VSWR = 1.38 maximum and 26 dB corresponds to a VSWR = 1.1 maximum when ③ and ④ are connected to unity reflection coefficient. This improvement in return loss can be measured approximately if two couplers are placed back-to-back (replacing the amplifiers in Fig. 40 with direct connections) and the signal at ⑧ compared with the signal at ①. Both terminals ② and ⑦ now have 50 ohm terminations. Figure 43 shows the measurements on pairs of couplers for both 7 to 18 GHz and 10.7 to 18 GHz frequency ranges. The "thru" measurement in the "Loss in Gain" curves indicates the loss through two APC-7-to-microstrip launchers and a straight 50 ohm microstrip line (replacing the pairs of couplers) between the launchers. The added loss of the pair of couplers is only a few tenths of a dB. The measurement accuracy was not sufficient to show the extra small midband loss shown in Fig. 41. The "Improvement in Return Loss" curve in Fig. 44 for the 7 to 18 GHz coupler closely approximates the theoretical curve in Fig. 43 .

Of the many possible types of couplers and methods of manufacture, the simplicity and the advantage of having an all "microstrip" design dictated using a Lange [9] coupler.

Data on complete balanced gain modules are shown in the following figures and tables. All of the data on individual gain modules were taken using our own APC-7-to-microstrip adaptors. Each adaptor has a loss of about 0.2 dB, as indicated in the top of Fig. 44, and this loss should be subtracted from the noise figure values and two times this, or 0.4 dB, loss added to the gain values shown. The reflections in these adaptors will affect the VSWR values shown. The gain modules have parameters which change slowly with frequency, so that any abrupt changes shown on an ANA listing indicates a poor ANA calibration at that frequency.

Data on the 10.7 to 18 GHz gain modules using the M-104/R35A FETs are shown in Table XIII and Fig. 45. Table XIII is an ANA listing which shows the low VSWR

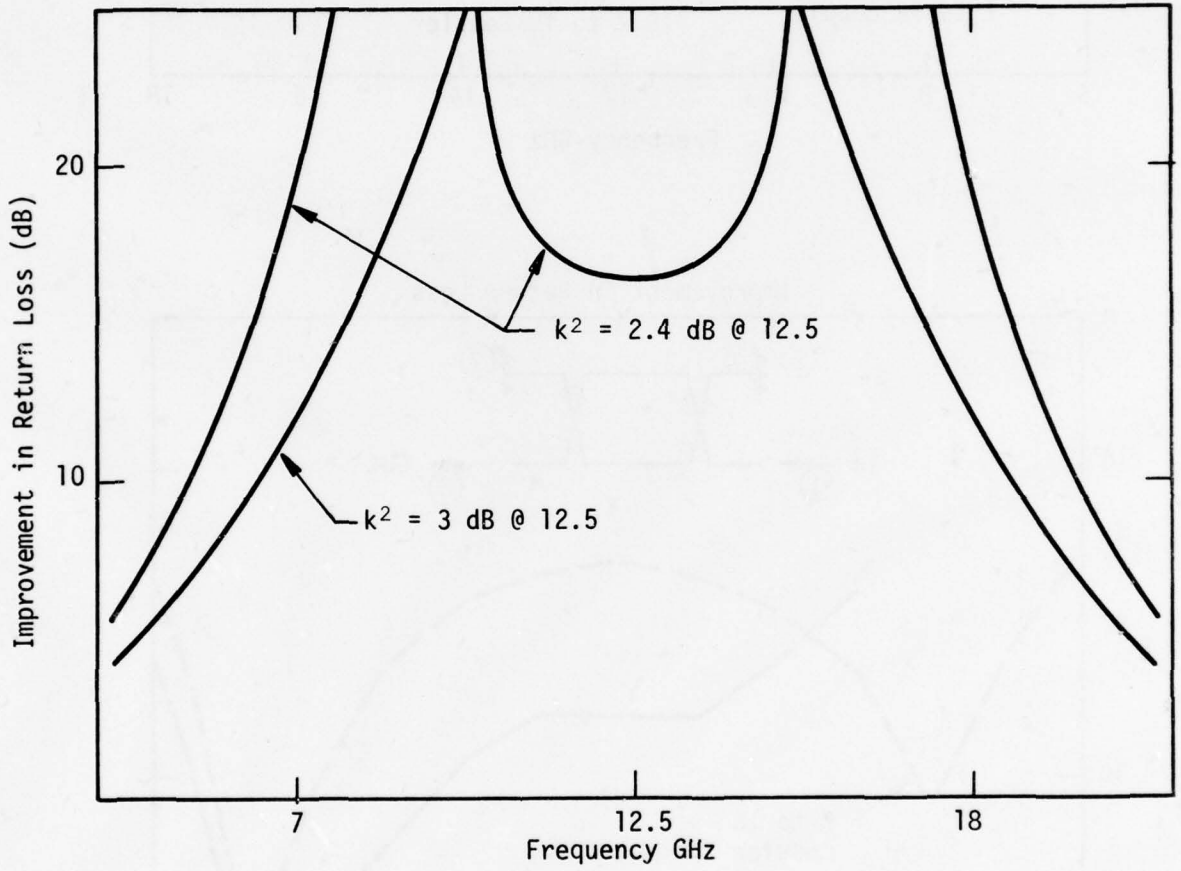


Figure 43
Improvement in Return Loss vs. Frequency

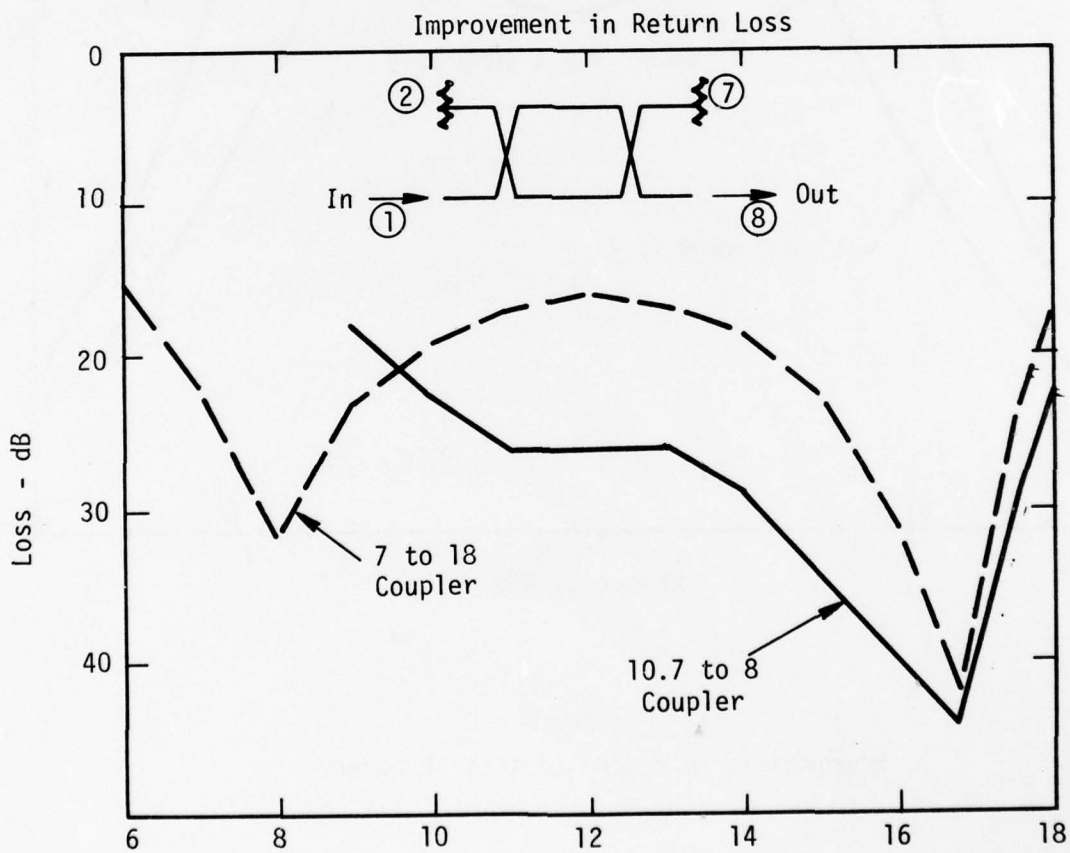
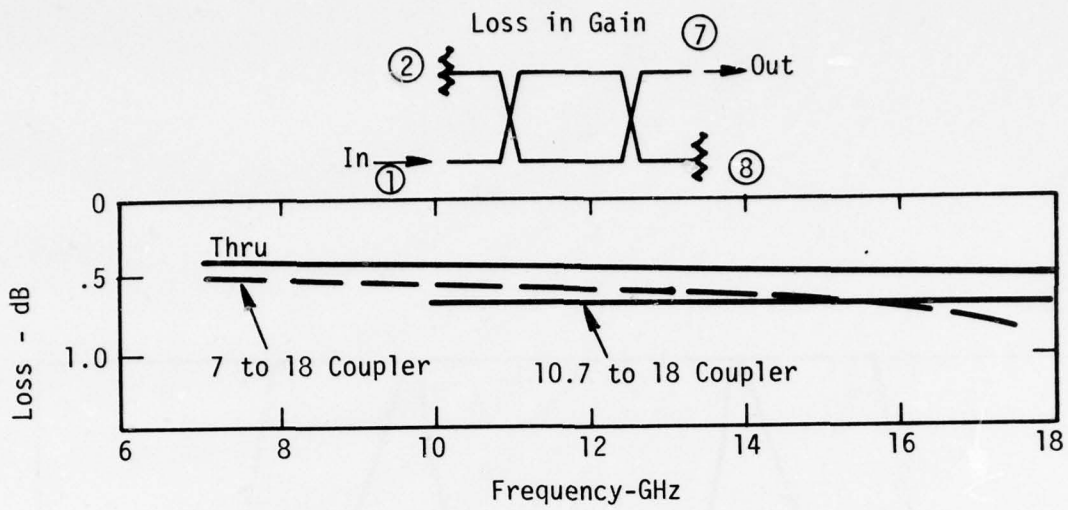


Figure 44
Coupler Measurements

TABLE XIII

SH
MAR 14, 1977M-104 GAIN MODULE
10.7 TO 18 GHz
S/N B 8 B10

FREQ MHz	USNR IN	GAIN dB	FLAT dB	PHASE DEG	PHASE DEV	GPDEL NSEC	ISOL dB	USNR OUT
9000.0	1.22	5.51		-142.63		.00	23.23	1.74
9200.0	1.19	5.71		-165.71		.34	22.87	1.71
9400.0	1.17	5.75		168.28		.34	22.65	1.64
9600.0	1.16	5.92		144.90		.33	22.43	1.60
9800.0	1.16	5.86		120.79		.34	22.31	1.55
10000.0	1.15	5.99		96.30		.33	22.06	1.46
10200.0	1.16	5.94		73.47		.32	21.91	1.41
10400.0	1.15	5.94		49.75		.32	21.86	1.37
10600.0	1.15	5.87	-.15	27.60	2.39	.31	21.77	1.31
10800.0	1.16	5.77	-.05	5.03	1.12	.31	21.75	1.28
11000.0	1.17	5.76	-.04	-17.50	-1.10	.31	21.65	1.27
11200.0	1.17	5.60	.10	-39.86	-1.15	.30	21.54	1.21
11400.0	1.18	5.60	.10	-60.73	-.71	.30	21.54	1.25
11600.0	1.19	5.60	.10	-83.00	-1.67	.30	21.57	1.25
11800.0	1.21	5.54	.16	-103.23	-.60	.30	21.46	1.25
12000.0	1.22	5.42	.28	-126.42	-2.49	.33	21.33	1.27
12200.0*	1.22	4.44	1.26	-150.24	-5.01	.29	21.79	1.25
12400.0	1.23	5.38	.33	-168.08	-1.54	.28	21.18	1.30
12600.0	1.25	5.40	.30	170.10	-2.06	.29	21.18	1.39
12800.0	1.26	5.42	.29	150.51	-.34	.29	21.12	1.28
13000.0	1.27	5.27	.43	128.20	-1.35	.29	21.06	1.31
13200.0	1.29	5.40	.30	108.69	.43	.28	21.00	1.25
13400.0	1.30	5.36	.34	87.77	.82	.30	20.94	1.19
13600.0	1.30	5.45	.26	66.10	.46	.29	20.74	1.18
13800.0	1.30	5.50	.21	45.39	1.06	.29	20.60	1.16
14000.0	1.30	5.60	.11	24.18	1.15	.29	20.51	1.10
14200.0	1.29	5.66	.05	3.25	1.52	.29	20.27	1.08
14400.0	1.28	5.71	.00	-17.95	1.62	.29	20.05	1.08
14600.0	1.25	5.71	.00	-38.64	2.23	.29	20.15	1.08
14800.0	1.24	5.75	-.03	-60.20	1.97	.29	19.92	1.07
15000.0	1.21	5.82	-.10	-80.46	3.01	.30	19.84	1.10
15200.0	1.18	5.92	-.20	-103.18	1.59	.30	19.55	1.11
15400.0	1.15	5.97	-.26	-123.48	2.59	.30	19.19	1.10
15600.0	1.13	5.98	-.26	-146.08	1.29	.30	19.07	1.15
15800.0	1.10	6.06	-.35	-166.98	1.69	.29	18.79	1.07
16000.0	1.09	6.02	-.31	172.58	2.56	.31	18.64	1.08
16200.0	1.09	6.03	-.31	148.89	.17	.31	18.40	1.10
16400.0	1.09	6.05	-.33	128.65	1.24	.29	18.23	1.11
16600.0	1.10	6.00	-.28	106.68	.58	.31	18.19	1.03
16800.0	1.10	6.03	-.32	84.14	-.66	.30	17.74	1.15
17000.0	1.11	6.06	-.34	63.56	.05	.29	17.68	1.03
17200.0	1.11	6.04	-.32	41.78	-.41	.31	17.35	1.02
17400.0	1.11	6.29	-.57	19.59	-1.30	.31	17.53	1.30
17600.0	1.10	5.98	-.26	-2.90	-2.48	.31	17.21	1.10
17800.0	1.10	5.80	-.08	-24.95	-3.23	.31	17.18	1.35
18000.0	1.11	5.74	-.02	-47.46	-4.45	.00	17.00	1.22

LINEAR-
IZATION
RANGE

10600.0	10600.0
10	10
18000.0	18000.0

* Bad Data

THIS PAGE IS BEST QUALITY PRACTICAL
FROM COPY FURNISHED TO DDG

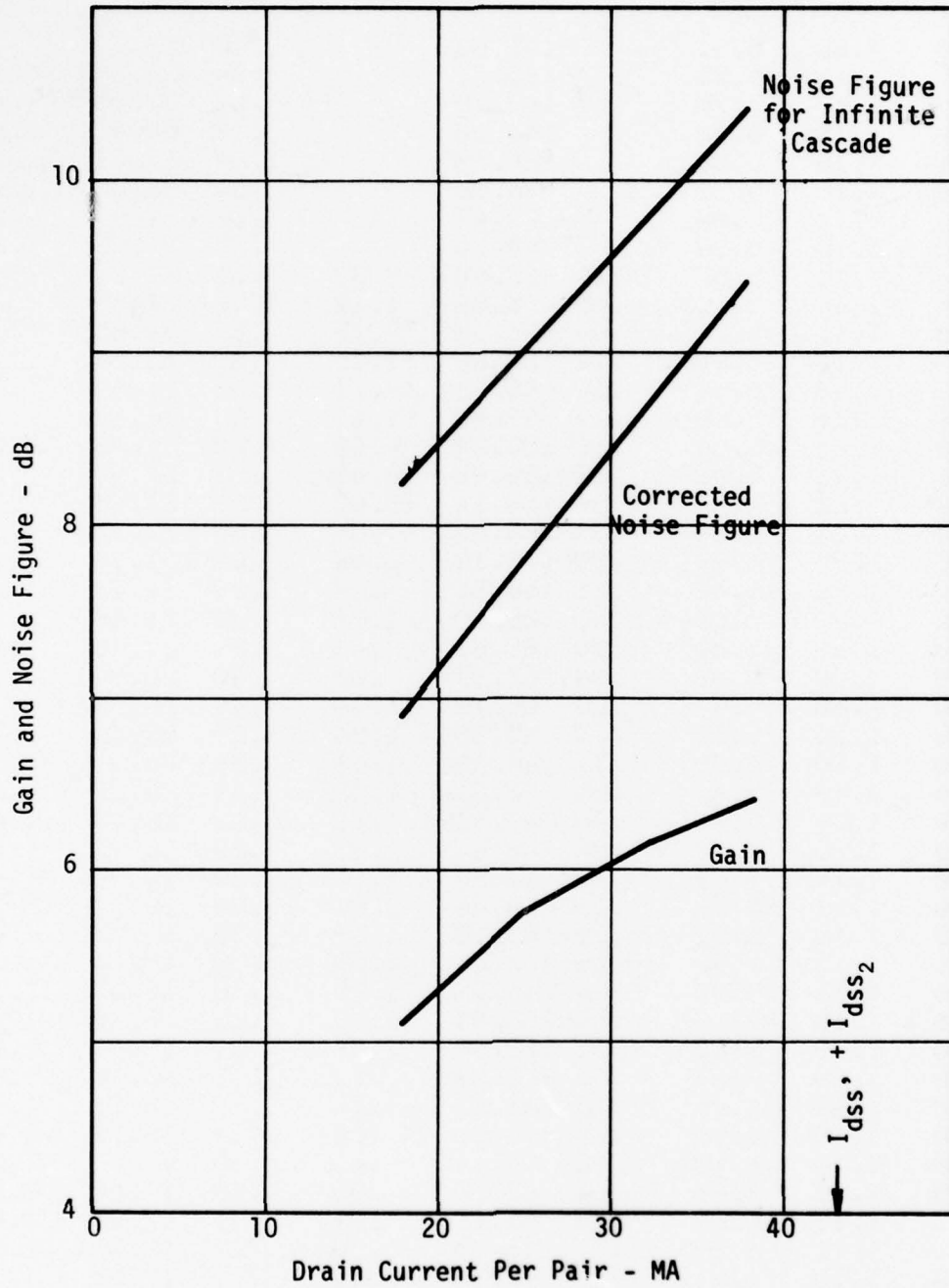


Figure 45
Gain and Noise Figure for an M-104 Gain Module

expected from the use of couplers and a balanced amplifier design. The gain varies from about 5.4 to 6 dB across the band. The M-104 gain modules in particular were tuned to have an increasing gain with frequency to overcome the loss in the input signal limiter. The phase deviation follows the expected curve which is slightly positive near 10.7 and slightly negative near 18 GHz. The phase deviation data is somewhat erratic which indicates that the data is near the resolution of the ANA. Figure 44 shows the gain, corrected noise figure, and noise figure for an infinite cascade* of these modules. Because of the high noise figure for this particular slice of M-104 transistors, the M-104 gain modules were placed near the middle of the amplifier where they could supply 6 dB gain without affecting the amplifier noise figure. The power output at 1 dB gain compression of an M-104 gain module at 18 GHz is approximately +10 dBm.

Data on the 10.7 to 18 GHz gain module using the M-107/323D FET is shown in the ANA listing of Table XIV. The VSWR is quite low. The module current was adjusted for good noise figure, so that the gain is only 4.6 near 10.7 GHz to near 4.0 at 18 GHz. Over the center of the band the gain variation or "Flatness" is very small. For drain currents near I_{DSS} the gain increases to near 7 dB. The phase deviation is only 1 or 2 degrees over most of the band. Figure 46 is for a single-ended M-107 circuit but shows noise figure data similar to Fig. 45. For a total module current of 25 mA (12.5 mA in Fig. 46) the infinite cascade noise figure is 7.1 dB which compares to 9 dB for the older M-104. The power output at 1 dB gain compression of the M-107 gain module is near +15 dBm.

Data on two, 7 to 18 GHz gain modules which use the M-107/338 FET are shown in the ANA listings in Tables XV and XVI. The VSWR's, again, are very low. The gain of both modules is near 5 dB with the gain increasing with frequency.

* The noise figure of an infinite cascade (F_{∞}) of amplifiers having individual noise figures of F, and Gains, G, is:

$$F_{\infty} = F + \frac{F-1}{G-1}$$

TABLE XIV

SH
JULY 25, 1977

16.7 TO 18 GAIN MODULE
M-107 EXP-3230 FBI
5-N CH3 L65

FREQ MHz	USMR dB	GAIN dB	FLHT dB	FRASE DEV	CPDEL MSEC	ISOL dB	USMR dB	NOISE FIC Corrected
10000.0	1.63	4.51			.00	19.74	1.02	4.8
10200.0	1.63	4.74			.25	19.66	1.04	
10400.0	1.63	4.68			.25	19.58	1.07	
10600.0	1.61	4.64	-1.45	.57	.25	19.51	1.09	
10800.0	1.59	4.60	-1.41	-1.40	.25	19.45	1.11	
11000.0	1.56	4.49	-1.30	.25	.25	19.43	1.12	
11200.0	1.54	4.43	-1.24	-1.31	.25	19.28	1.13	
11400.0	1.51	4.42	-1.25	-1.61	.25	19.26	1.14	
11600.0	1.47	4.29	-1.10	-1.53	.25	19.27	1.14	
11800.0	1.44	4.35	-1.16	-1.10	.25	19.16	1.15	
12000.0	1.40	4.23	-1.04	-2.06	.25	19.05	1.14	4.6
12200.0*	1.35	5.09	-1.50	3.68	.27	18.82	1.13	
12400.0	1.34	4.26	-1.07	-1.29	.31	18.58	1.12	
12600.0	1.33	4.25	-1.06	-1.51	.29	18.55	1.11	
12800.0	1.31	4.15	.04	-1.61	.27	18.31	1.08	
13000.0	1.28	4.17	.01	.15	.27	18.73	1.07	
13200.0	1.26	4.15	.04	.23	.29	18.63	1.06	
13400.0	1.23	4.23	-1.04	-1.07	.25	18.55	1.05	
13600.0	1.20	4.16	.02	.52	.27	18.53	1.05	
13800.0	1.18	4.13	.06	.25	.28	18.39	1.09	
14000.0	1.16	4.15	.03	.37	.28	18.29	1.11	4.7
14200.0	1.13	4.14	.04	.65	.28	18.16	1.14	
14400.0	1.10	4.13	.06	.68	.25	18.08	1.18	
14600.0	1.08	4.12	.07	.61	.27	17.97	1.21	
14800.0	1.06	4.07	.11	1.60	.25	17.86	1.23	
15000.0	1.03	4.19	.00	.29	.29	17.55	1.25	
15200.0	1.02	4.13	.05	.72	.27	17.52	1.27	
15400.0	1.04	4.07	.11	1.32	.27	17.43	1.29	
15600.0	1.07	4.15	.03	1.59	.29	17.20	1.30	
15800.0	1.11	4.16	.02	.47	.25	16.96	1.31	
16000.0	1.14	4.13	.05	1.00	.25	16.95	1.34	5.6
16200.0	1.18	4.21	-1.01	1.27	.25	16.79	1.33	
16400.0	1.21	4.22	-1.03	.99	.29	16.64	1.33	
16600.0	1.24	4.07	.11	.40	.25	16.43	1.34	
16800.0	1.26	4.13	.05	.77	.25	16.33	1.35	
17000.0	1.29	4.17	.01	.50	.29	16.22	1.34	
17200.0	1.32	4.16	.02	-1.74	.29	16.11	1.35	
17400.0	1.33	4.10	.09	-1.56	.25	16.02	1.36	
17600.0	1.33	4.01	.17	-1.32	.29	15.78	1.38	
17800.0	1.33	3.94	.24	-2.60	.29	15.61	1.38	
18000.0*	1.35	2.65	1.54	-3.14	.00	15.38	1.43	5.3

LINEAR- 10000.010000.0
IZATION 10 10
RANGE 10000.010000.0

* Bad Data

THIS PAGE IS BEST QUALITY PRACTICABLE
FROM COPY FURNISHED TO DDC

Frequency = 18 GHz
FET: M-107, EXP 323D
 $V_{ds} = 2$ Volts

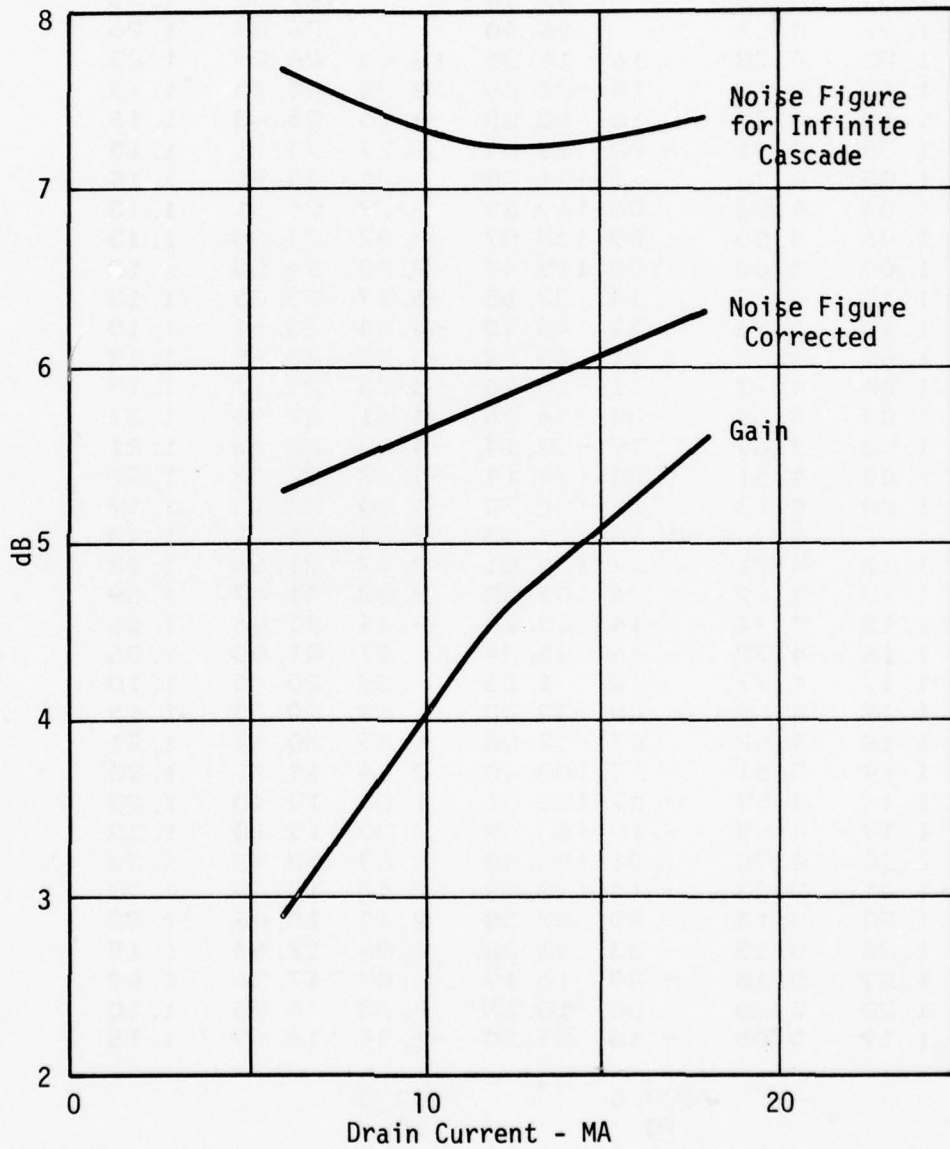


Figure 46
Gain and Noise Figure for a 10.7 to 18 GHz M-107 Gain Module

CH
SEPT 20, 1977

TABLE XV

7 TO 18 MODULE
PHASE MATCH
S/N 3

FREQ MHZ	VSWR IN	GAIN DB	FLAT DB	PHASE DEG	PHASE DEV	ISOL DB	VSWR OUT	NOISE FIG
5000.0	2.11	1.38		-75.48		34.23	1.88	
5333.3	1.84	3.01		-124.38		31.35	1.73	
5666.7	1.62	3.86		-174.23		29.33	1.58	
6000.0	1.44	4.17		141.75		28.37	1.43	
6333.3	1.34	4.56		97.18		27.52	1.33	
6666.7	1.27	4.69		56.40		26.84	1.26	
7000.0	1.22	4.73	.16	16.31	13.03	26.29	1.22	
7333.3	1.18	4.78	.10	-22.86	8.33	25.75	1.18	
7666.7	1.13	4.78	.10	-60.25	5.36	25.48	1.16	
8000.0	1.08	4.91	-.02	-98.24	1.79	25.11	1.15	
8333.3	1.05	4.76	.13	-134.20	.26	24.96	1.14	
8666.7	1.04	4.83	.06	-169.69	-.79	24.61	1.13	
9000.0	1.06	4.80	.09	153.87	-2.82	24.38	1.13	
9333.3	1.09	4.80	.08	119.47	-2.80	24.05	1.12	
9666.7	1.10	4.75	.14	82.55	-5.29	23.85	1.13	
10000.0	1.10	4.76	.12	48.98	-4.44	23.61	1.15	
10333.3	1.09	4.78	.11	13.72	-5.27	23.48	1.17	
10666.7	1.06	4.77	.11	-20.70	-5.26	23.17	1.19	
11000.0	1.04	4.69	.20	-54.46	-4.61	22.94	1.21	
11333.3	1.03	4.69	.19	-89.14	-4.85	22.58	1.21	
11666.7	1.05	4.61	.26	-122.14	-3.43	22.49	1.21	
12000.0	1.03	4.73	.15	-157.73	-4.60	22.13	1.19	
12333.3*	1.11	5.05	-1.16	167.93	-2.52	21.11	1.15	
12666.7	1.12	4.71	.17	136.01	-2.02	21.66	1.13	
13000.0	1.13	4.62	.26	103.02	-.53	21.47	1.09	
13333.3	1.15	4.74	.14	68.74	-.44	21.06	1.06	
13666.7	1.16	4.72	.16	35.84	.57	21.00	1.06	
14000.0	1.17	4.77	.12	1.23	.89	20.70	1.10	
14333.3	1.18	4.89	.00	-33.20	.88	20.23	1.16	
14666.7	1.18	4.82	.07	-67.06	1.45	20.11	1.21	
15000.0	1.19	5.01	-.12	-100.40	2.54	19.71	1.25	
15333.3	1.19	4.99	-.07	-135.51	1.85	19.43	1.30	
15666.7	1.19	4.99	-.10	-168.49	3.30	19.10	1.32	
16000.0	1.20	4.90	-.01	156.43	2.63	18.92	1.33	
16333.3	1.21	5.03	-.14	122.85	3.47	18.48	1.28	
16666.7	1.22	5.14	-.25	87.58	2.64	18.08	1.22	
17000.0	1.22	5.23	-.33	52.88	2.36	17.64	1.15	
17333.3	1.22	5.18	-.29	16.19	.09	17.36	1.09	
17666.7	1.20	5.20	-.30	-18.66	-.33	16.95	1.10	
18000.0	1.19	5.05	-.16	-54.20	-1.44	16.49	1.16	
LINEAR- IZATION RANGE			7000.0 TO 18000.0		7000.0 TO 18000.0			

* Bad Data

THIS PAGE IS BEST QUALITY PRACTICABLE
FROM COPY FURNISHED TO DDC

TABLE XVI

SH
SEPT 20, 19777 TO 18 MODULE
PHASE MATCH
S/N 4

FREQ MHZ	VSWR IN	GAIN DB	FLAT DB	PHASE DEG	PHASE DEV	ISOL DB	VSWR OUT	NOISE FIG
5000.0	2.11	1.35		-78.69		37.07	1.93	
5333.3	1.86	2.78		-127.41		32.73	1.76	
5666.7	1.66	3.54		-176.46		30.16	1.60	
6000.0	1.49	3.77		140.53		28.96	1.44	
6333.3	1.40	4.15		96.85		27.99	1.34	
6666.7	1.33	4.33		56.77		27.20	1.27	
7000.0	1.27	4.41	.51	17.11	11.70	26.65	1.21	
7333.3	1.23	4.51	.41	-21.47	7.52	26.07	1.16	
7666.7	1.17	4.56	.37	-58.75	4.63	25.81	1.13	
8000.0	1.12	4.74	.18	-96.52	1.25	25.52	1.10	
8333.3	1.08	4.64	.28	-132.32	-.15	25.31	1.08	
8666.7	1.04	4.72	.20	-167.73	-1.18	25.02	1.06	
9000.0	1.01	4.70	.22	155.98	-3.08	24.85	1.07	
9333.3	1.03	4.72	.20	121.54	-3.13	24.60	1.09	
9666.7	1.04	4.64	.28	84.91	-5.37	24.37	1.13	
10000.0	1.04	4.67	.25	51.45	-4.44	24.28	1.17	
10333.3	1.04	4.67	.25	16.36	-5.14	24.16	1.20	
10666.7	1.05	4.68	.24	-17.74	-4.84	24.01	1.24	
11000.0	1.07	4.69	.33	-51.37	-4.08	23.83	1.26	
11333.3	1.09	4.63	.29	-65.61	-3.93	23.51	1.27	
11666.7	1.12	4.67	.35	-118.62	-2.45	23.40	1.28	
12000.0	1.14	4.71	.21	-153.95	-3.60	22.97	1.27	
12333.3*	1.17	6.09	-1.16	173.52	-1.63	21.94	1.22	
12666.7	1.18	4.77	.15	139.76	-1.00	22.57	1.21	
13000.0	1.19	4.72	.20	106.92	.54	22.49	1.17	
13333.3	1.21	4.87	.05	72.35	.35	22.02	1.13	
13666.7	1.22	4.87	.05	39.05	1.44	21.91	1.09	
14000.0	1.23	4.94	-.01	4.85	1.63	21.55	1.07	
14333.3	1.24	5.07	-.13	-29.77	1.39	21.04	1.07	
14666.7	1.23	5.04	-.11	-63.81	1.75	20.80	1.10	
15000.0	1.21	5.22	-.29	-97.46	2.49	20.32	1.13	
15333.3	1.20	5.21	-.28	-132.57	1.78	19.97	1.16	
15666.7	1.16	5.23	-.30	-165.77	2.98	19.51	1.19	
16000.0	1.13	5.15	-.22	159.20	2.33	19.02	1.19	
16333.3	1.12	5.25	-.32	125.11	2.63	18.53	1.16	
16666.7	1.12	5.34	-.41	89.97	1.88	18.04	1.12	
17000.0	1.12	5.43	-.50	55.18	1.48	17.46	1.08	
17333.3	1.14	5.37	-.44	18.46	-.83	17.23	1.07	
17666.7	1.15	5.40	-.47	-16.09	-1.00	16.72	1.10	
18000.0	1.16	5.36	-.43	-51.48	-2.00	16.31	1.15	
LINEAR- IZATION RANGE			7000.0 TO 18000.0		7000.0 TO 18000.0			

* Bad Data

The gain variation is near ± 0.2 dB if the gain slope is ignored (see Fig.47). The phase deviation is near 5 degrees except near 7 GHz. This phase deviation is much larger than for the 10.7 to 18 GHz gain modules. The larger phase deviation is due to the increased bandwidth and the required use of a 6-element input matching network.

Figure 47 shows the swept gain response of these two 7 to 18 GHz gain modules from 4 to 23 GHz. The gain from 7 to 18 GHz compares well with the calculated gain curve in Fig. 37. The out-of-band gain (below 6 GHz and above 20 GHz) for these two gain modules has been adjusted so that they are nearly equal. Table XVII shows a listing, calculated from the ANA data, which shows the gain and phase of each amplifier and the difference in gain (DG12) and phase (DP12) between the two modules. The difference in phase (DP12) of these modules starts at near 1 degree at 7 GHz and remains less than 4 degrees through 18 GHz.

Gain for a 7 to 18 GHz module as a function of total module drain current is shown in Fig. 48. For 19 mA total current, the gain is from 4 to 4.5 dB across the band. At 18 GHz the corrected noise figure is 5 dB and the noise figure for an infinite cascade is 6.4 dB. These noise figures for the M-107/338 in a 7 to 18 GHz module are much better than the M-107/323D in the 10.7 to 18 GHz module. (See Fig. 46.) For the total module current equal to I_{DSS} of the FETs, the gain is near 7 dB from 7 to 18 GHz.

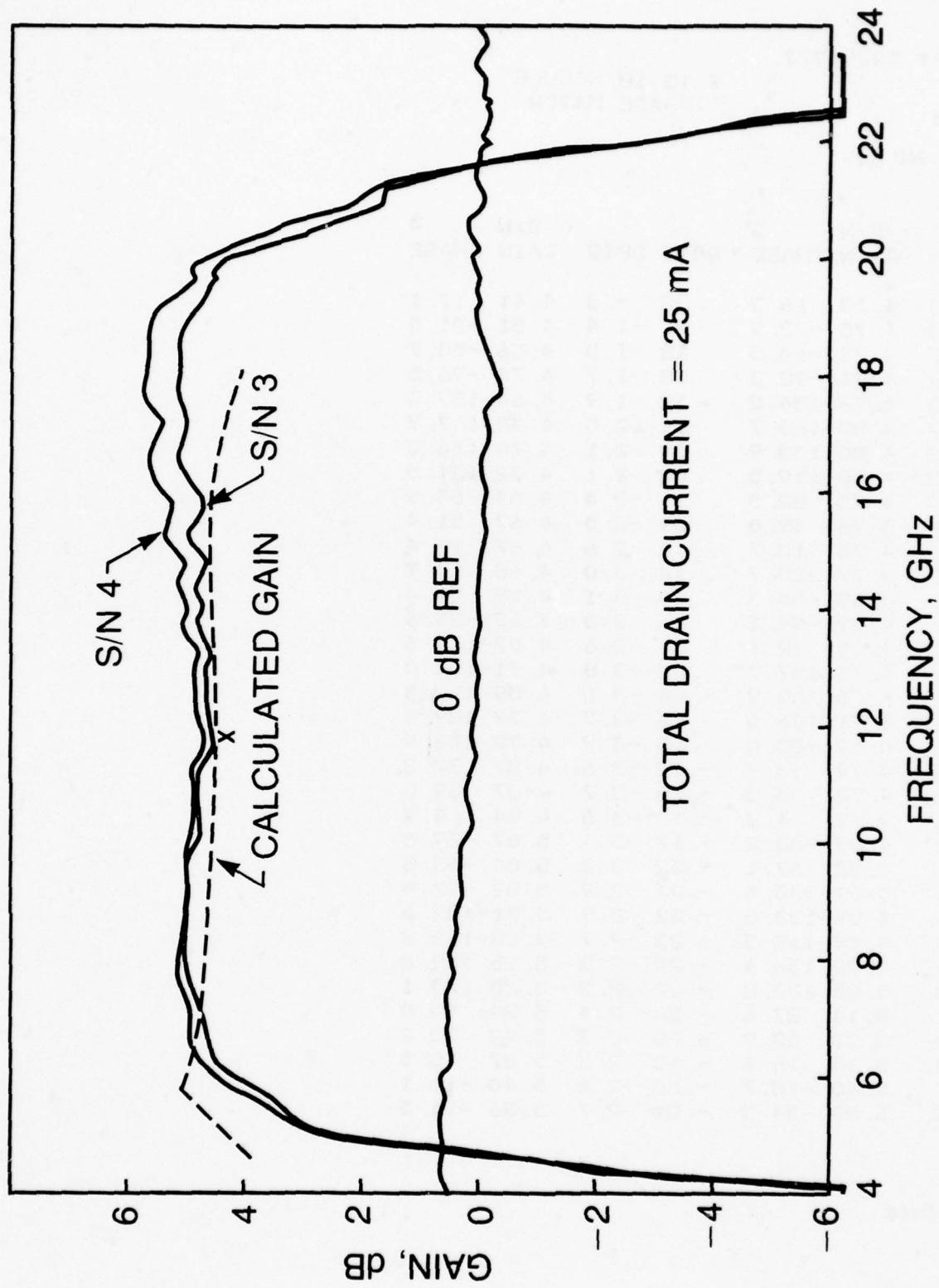


Figure 47
Gain Response of 7 to 13 Gain Modules

TABLE XVII

SH
SEPT 20, 1977

7 TO 18 MODULE
PHASE MATCH

S21 IN DB

FREQ	S/N 3		DG12	DP12	S/N 4	
	GAIN	PHASE			GAIN	PHASE
7000.0	4.73	16.3	.32	-.8	4.41	17.1
7333.3	4.78	-22.9	.27	-1.4	4.51	-21.5
7666.7	4.78	-60.3	.23	-1.5	4.56	-58.7
8000.0	4.91	-98.2	.18	-1.7	4.74	-96.5
8333.3	4.76	-134.2	.12	-1.9	4.64	-132.3
8666.7	4.83	-169.7	.11	-2.0	4.72	-167.7
9000.0	4.80	153.9	.09	-2.1	4.70	156.0
9333.3	4.80	119.5	.08	-2.1	4.72	121.5
9666.7	4.75	82.5	.11	-2.4	4.64	84.9
10000.	4.76	49.0	.09	-2.5	4.67	51.4
10333.	4.78	13.7	.10	-2.6	4.67	16.4
10667.	4.77	-20.7	.10	-3.0	4.68	-17.7
11000.	4.69	-54.5	.10	-3.1	4.59	-51.4
11333.	4.69	-89.1	.06	-3.5	4.63	-85.6
11667.	4.61	-122.1	.04	-3.6	4.57	-118.5
12000.	4.73	-157.7	.02	-3.8	4.71	-154.0
12333.*	6.06	169.9	-.04	-3.6	6.09	173.5
12667.	4.71	136.0	-.06	-3.7	4.77	139.8
13000.	4.62	103.0	-.10	-3.9	4.72	106.9
13333.	4.74	68.7	-.13	-3.6	4.87	72.3
13667.	4.72	35.3	-.15	-3.7	4.87	39.0
14000.	4.77	1.2	-.17	-3.6	4.94	4.9
14333.	4.89	-33.2	-.17	-3.4	5.07	-29.8
14667.	4.82	-67.1	-.22	-3.2	5.04	-63.3
15000.	5.01	-100.4	-.21	-2.9	5.22	-97.5
15333.	4.99	-135.5	-.22	-2.9	5.21	-132.6
15667.	4.99	-168.5	-.23	-2.7	5.23	-165.8
16000.	4.90	156.4	-.25	-2.8	5.15	159.2
16333.	5.03	122.8	-.22	-2.3	5.25	125.1
16667.	5.14	87.6	-.20	-2.4	5.34	90.0
17000.	5.23	52.9	-.20	-2.3	5.43	55.2
17333.	5.18	16.2	-.18	-2.3	5.37	18.5
17667.	5.20	-18.7	-.20	-2.6	5.40	-16.1
18000.	5.05	-54.2	-.31	-2.7	5.36	-51.5

* Bad Data

THIS PAGE IS BEST QUALITY PRACTICABLE
FROM COPY FURNISHED TO DDC

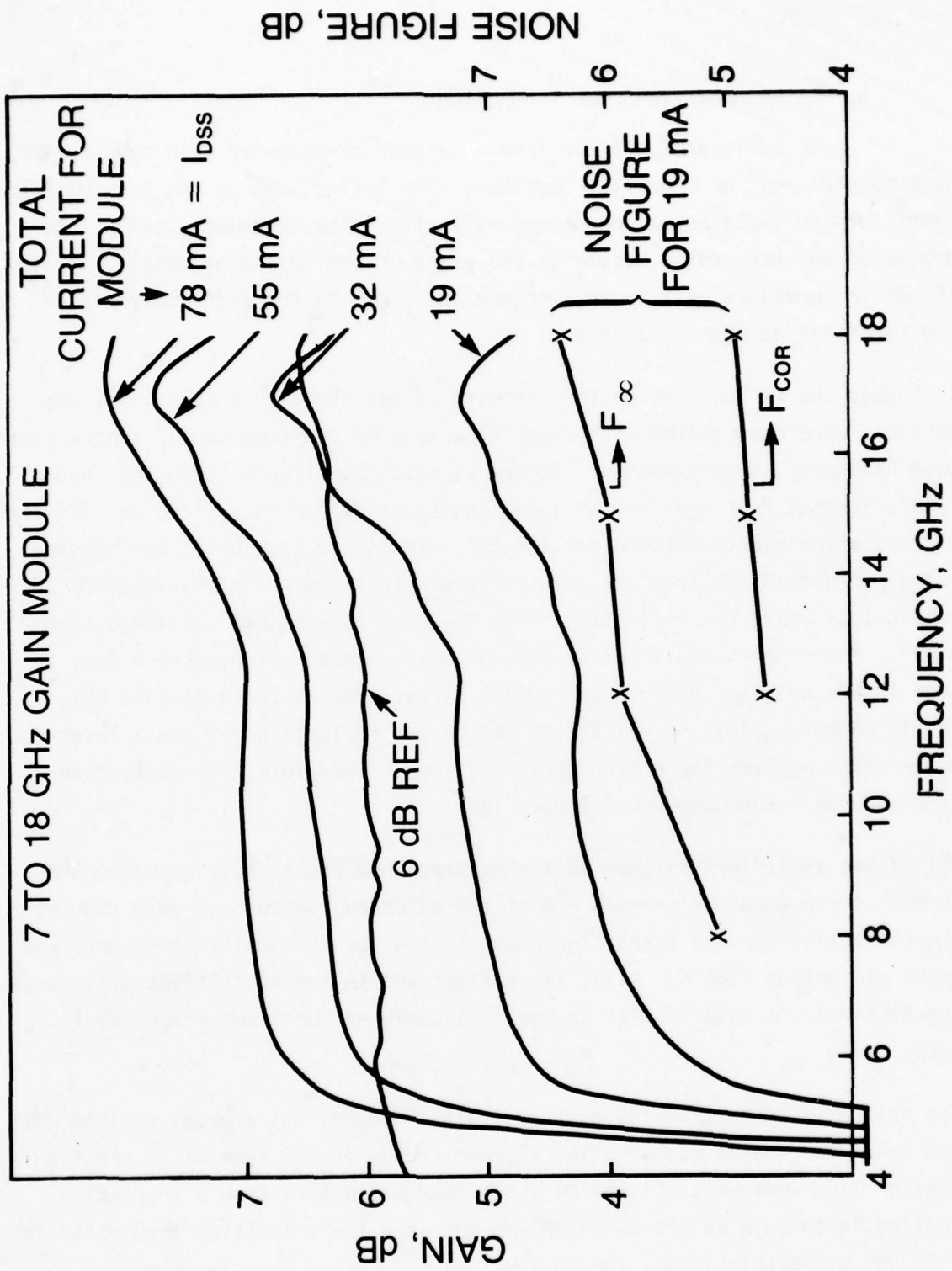


Figure 48
Gain vs. Drain Current

E. INTERCONNECTIONS AND TRANSITIONS

To build an amplifier from a cascade of balanced gain modules the gain modules must be connected together. Any reflections in the transmission lines forming these interconnections will affect the impedance seen by the drains of the preceding module or the gates of the following module. This change in impedance will cause a change or "bump" in the gain and phase of the amplifier at some frequency.

To reduce the reflections on the connections between gain modules, the connections were compensated with capacitive tabs in the same manner that a micro-wave connector is compensated. Figure 49 shows the transmission loss and return loss of four one-quarter inch lengths of 50 ohm microstrip on .025 inch thick alumina placed between our APC-7-to-microstrip adapters. The uncompensated microstrip sections are seen to have large "bumps" in transmission and return loss where the reflections from the interconnections reinforce each other. The compensated interconnections have a smooth transmission loss to near 18 GHz and the return loss remains higher than 18 dB to near 18 GHz. The 18 dB return loss ($\rho = .125$) is due to the reflections of the 3 interconnections between the 4 microstrip sections. Therefore, the reflection from any one interconnection is very low.

All of the amplifiers shipped on the contract had right-angle hermetic SMA-to-microstrip adaptors on each end of the cascaded limiter and gain modules. The reflections in the transitions must be low for the amplifier to have low input and output VSWR's. Also, any reflections in the transitions will cause the amplifier to have ripples in the gain curve as the input frequency is swept.

The design of these transitions was straightforward, but a great deal of care was taken to provide compensation at each change in the type of 50 ohm transmission line employed. Figure 50 shows the return loss from a transition looking in through an APC-7-to-SMA-adapter with the transition terminated in a 50 ohm microstrip load. The 50 ohm load had better than 30 dB return loss. The return loss of the adapter is seen to be greater than 19 dB at all frequencies.

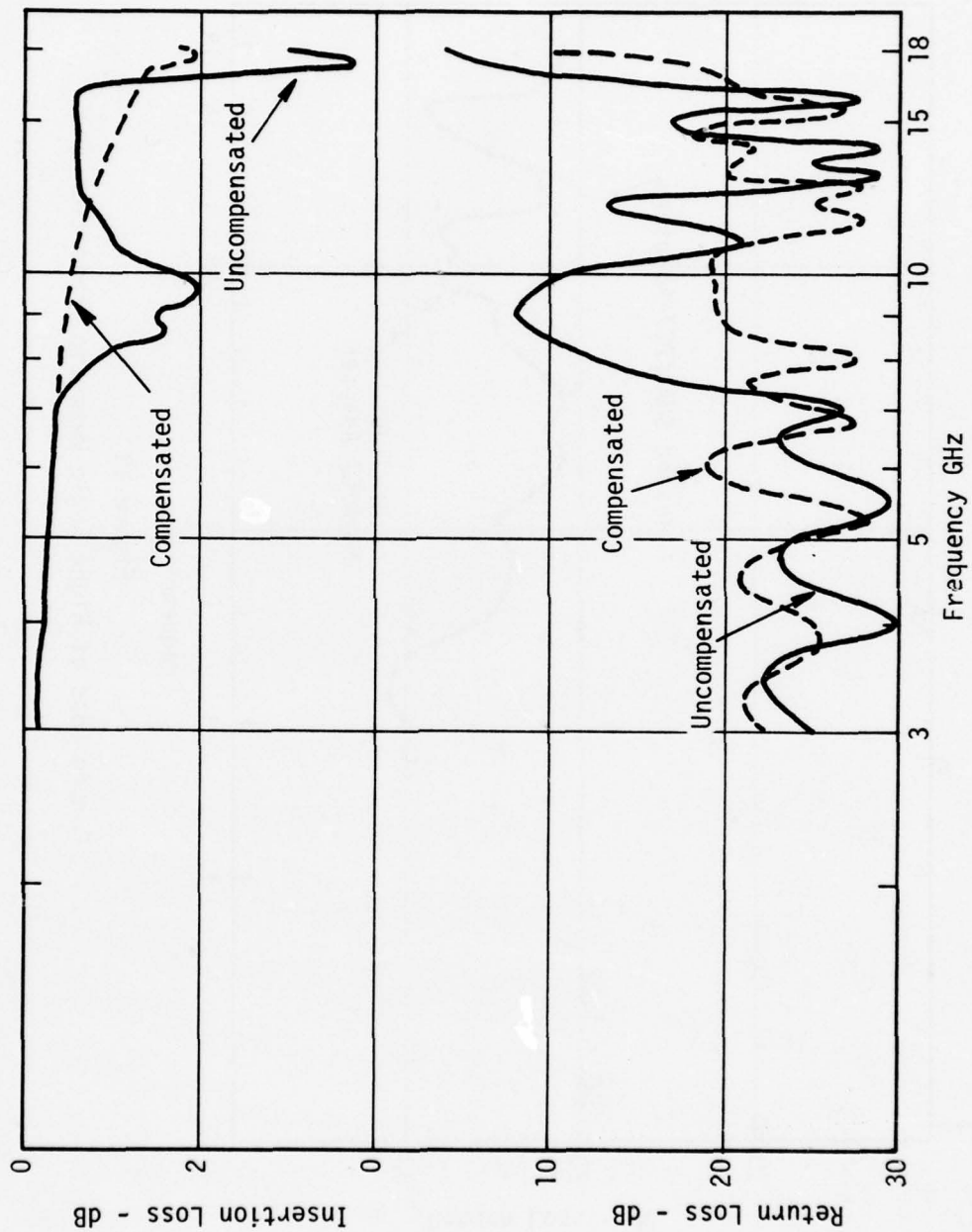


Figure 49
Compensated vs. Uncompensated Interconnections

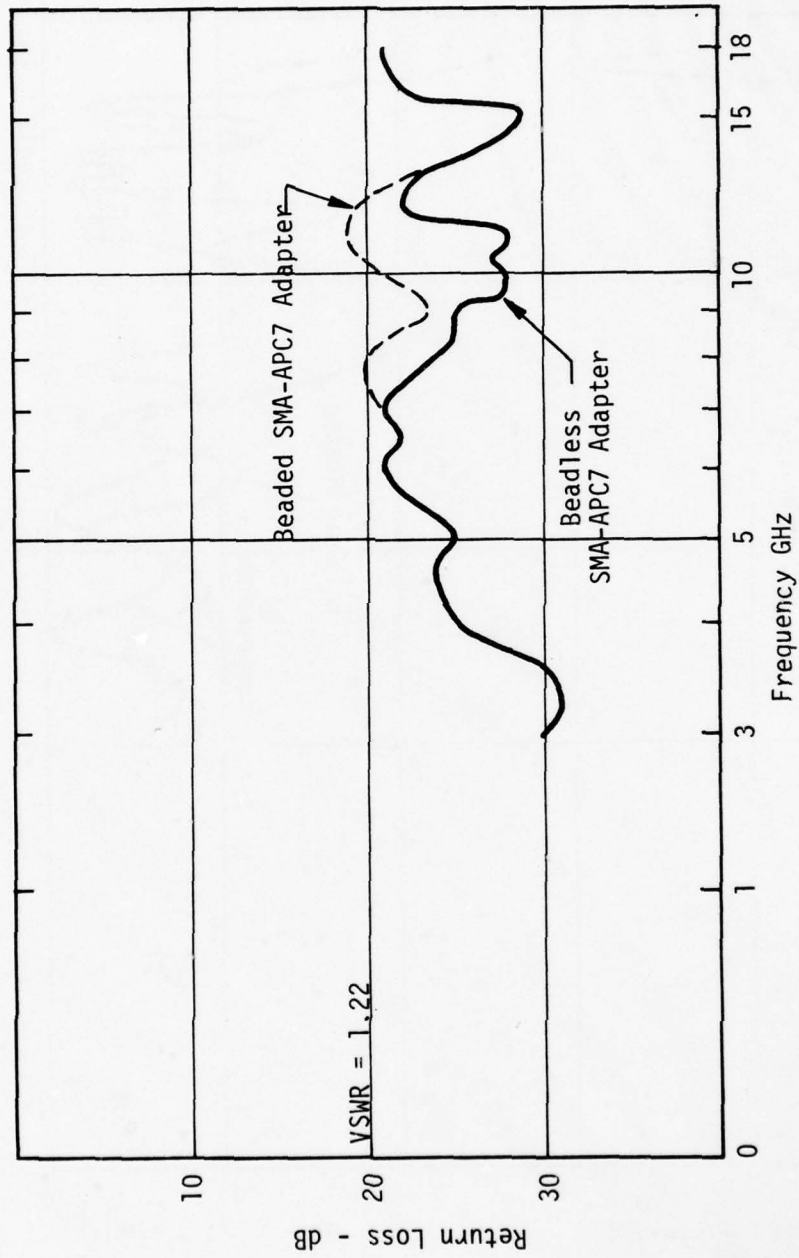


Figure 50
Return Loss of Right Angle Hermetic Transition

The curve marked "Beaded SMA-APC-7 Adaptor" is for a standard commercial adaptor where the SMA center conductor is supported by a teflon bead. The curve marked "Beadless SMA-APC-7" is for a special adaptor where the entire center conductor is supported by a single APC-7 bead.

F. LIMITER

The input signal limiter circuit has two fast PIN diodes in a low pass filter circuit. The PIN diodes conduct heavily on CW or pulse signals greater than +10dBm. The output of the limiter is well below the level where the transistors in the following gain modules could be damaged. Figure 51 shows curves of power output as a function of power input for both CW and pulse signals.

When the limiter is not limiting a signal, it is desirable that the circuit be "transparent;" i.e., that will not degrade low level gain and noise figure. Tables XVIII and XIX show ANA listings for similar limiters over the 10.7 to 18 and 7 to 18 GHz frequency ranges. The VSWR's are very low and the loss increases from 0.7 dB at 7 GHz to 1.7 dB at 18 GHz. This VSWR and loss data include the reflections and loss of a pair of APC-7-to-microstrip adaptors. The "FLAT" listing is the difference between the loss at that frequency and the average "LOSS." The "LOSS DEV" listing is the deviation from a least-squares-line thru the "LOSS" data and is the portion of the loss remaining after the gain modules have been tuned to remove the slope.

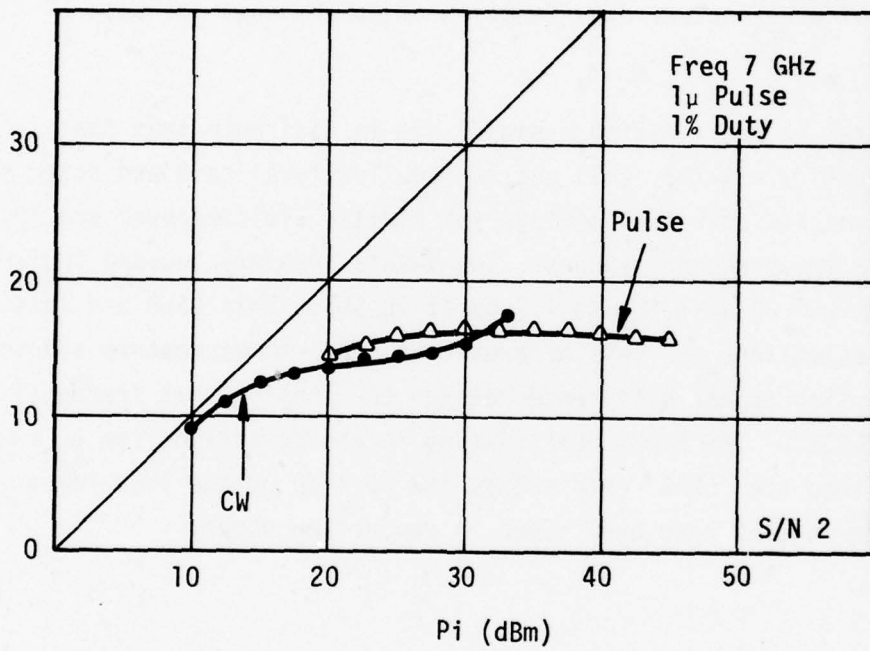
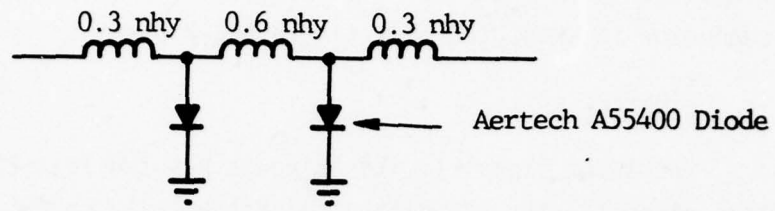


Figure 51
Power in vs. Power out for the
Two-Diode Limiter

TABLE XVIII

AUG 19, 1977

LIMITER
10.7 TO 18 GHZ
S/N 5

FREQ MHZ	VSWR IN	LOSS DB	FLAT DB	LOSS DEV	PHASE DEG	PHASE DEV	GPDEL NSEC	ISOL DB	VSWR OUT
10000.0	1.06	.72			-129.33		.00	.72	1.05
10200.0	1.06	.80			-147.62		.25	.80	1.04
10400.0	1.06	.83			-164.95		.24	.81	1.05
10600.0	1.07	.76	-.50	.00	177.59	-1.18	.25	.75	1.05
10800.0	1.08	.76	-.51	-.03	158.68	-2.01	.25	.78	1.05
11000.0	1.09	.86	-.40	.04	141.17	-1.42	.24	.89	1.05
11200.0	1.10	.82	-.44	-.02	124.05	-.46	.24	.87	1.06
11400.0	1.11	.85	-.41	-.02	105.98	-.46	.26	.87	1.06
11600.0	1.11	.86	-.40	-.03	86.74	-1.61	.25	.88	1.06
11800.0	1.12	.94	-.33	.00	70.59	.32	.24	1.00	1.06
12000.0	1.11	.95	-.31	.00	52.10	-.08	.26	.98	1.05
12200.0	1.10	1.47	.19	.48	33.13	-.98	.25	1.28	1.05
12400.0	1.10	1.01	-.25	.00	15.89	-.14	.24	1.00	1.06
12600.0	1.09	1.01	-.25	-.02	-1.70	.34	.25	1.01	1.06
12800.0	1.08	1.03	-.23	-.02	-19.92	.21	.25	1.02	1.05
13000.0	1.08	1.09	-.17	.00	-37.55	.65	.26	1.06	1.05
13200.0	1.06	1.06	-.21	-.06	-56.89	-.60	.25	.98	1.05
13400.0	1.07	1.11	-.16	-.03	-74.05	.31	.24	1.08	1.06
13600.0	1.07	1.16	-.11	-.01	-91.25	1.19	.25	1.13	1.07
13800.0	1.06	1.08	-.18	-.11	-109.58	.94	.26	1.10	1.06
14000.0	1.07	1.23	-.04	.00	-128.07	.53	.25	1.22	1.08
14200.0	1.07	1.23	-.03	-.02	-145.86	.82	.24	1.21	1.08
14400.0	1.07	1.21	-.06	-.07	-162.41	2.35	.25	1.25	1.08
14600.0	1.07	1.23	-.03	-.07	178.55	1.39	.26	1.24	1.08
14800.0	1.06	1.36	.09	.02	159.97	.88	.25	1.34	1.09
15000.0	1.05	1.35	.08	.00	143.03	2.02	.24	1.39	1.07
15200.0	1.04	1.33	.06	-.05	124.78	1.86	.26	1.36	1.05
15400.0	1.02	1.39	.11	-.03	105.58	.75	.26	1.34	1.04
15600.0	1.01	1.52	.25	.07	88.02	1.26	.25	1.50	1.05
15800.0	1.03	1.44	.17	-.02	69.73	1.06	.25	1.42	1.05
16000.0	1.06	1.46	.19	-.03	51.70	1.10	.26	1.45	1.06
16200.0	1.08	1.48	.20	-.05	32.70	.19	.25	1.46	1.08
16400.0	1.11	1.47	.20	-.08	15.03	.60	.25	1.51	1.10
16600.0	1.12	1.57	.29	-.01	-3.60	.04	.25	1.54	1.11
16800.0	1.14	1.62	.35	.01	-21.57	.15	.26	1.59	1.13
17000.0	1.15	1.62	.35	-.01	-40.57	-.76	.26	1.50	1.13
17200.0	1.15	1.62	.34	-.04	-58.71	-.82	.25	1.66	1.13
17400.0	1.14	1.60	.32	-.09	-77.03	-1.05	.25	1.71	1.10
17600.0	1.13	1.67	.40	-.04	-95.04	-.97	.26	1.66	1.09
17800.0	1.12	1.77	.49	.02	-115.05	-2.89	.27	1.71	1.08
18000.0*	1.09	2.18	.91	.41	-133.80	-3.58	.00	1.73	1.08
LINEAR- IZATION RANGE			10600.0	10600.0		10600.0			
			TO	TO		TO			
			18000.0	18000.0		18000.0			

* Bad Data

TABLE XIX

11/11/77

 LIMITERS
 7 TO 18 GHZ
 S/N 10

FREQ MHZ	VSWR IN	LOSS DB	LOSS DEV	FLAT DB	PHASE DEG	PHASE DEV	ISOL DB	VSWR OUT
2000.0	1.73	.87			54.73		.87	1.69
3000.0	1.58	.62			8.21		.64	1.71
4000.0	1.54	.60			-18.75		.59	1.72
4500.0	1.50	.66			-30.74		.65	1.65
5000.0	1.45	.70			-41.57		.68	1.56
5500.0	1.40	.78			-50.86		.73	1.47
6000.0	1.37	.31			-60.72		.29	1.43
6500.0	1.28	.73			-70.73		.71	1.34
7000.0	1.20	.69	-.02	-.31	-79.43	-.72	.65	1.23
7500.0	1.14	.71	-.03	-.29	-90.08	-2.24	.57	1.17
8000.0	1.08	.79	.02	-.20	-97.84	-.89	.82	1.14
9000.0	1.03	.77	-.05	-.22	-116.07	-.89	.74	1.08
10000.0	1.03	.75	-.13	-.24	-132.59	.81	.76	1.03
11000.0	1.05	.94	.00	-.06	-150.23	1.41	.99	1.03
12000.0	1.05	.84	-.15	-.15	-168.36	1.52	.80	1.06
13000.0	1.06	1.14	.09	.14	173.56	1.67	1.15	1.09
14000.0	1.12	1.35	.24	.35	156.35	2.70	1.34	1.17
15000.0	1.10	1.36	.19	.35	136.72	1.32	1.36	1.16
16000.0	1.05	1.44	.21	.43	117.55	.38	1.50	1.11
17000.0	1.19	1.71	.43	.70	97.94	-.99	1.66	1.14
18000.0*	1.17	.52	-.80	-.47	76.63	-4.08	1.62	1.33

LINEAR-
 IZATION
 RANGE

	7000.0	7000.0	7000.0
	TD	TD	TD
	18000.0	18000.0	18000.0

REF PLANES = 2.46 2.46 5.92

* Bad Data

G. TEMPERATURE COMPENSATION

The temperature compensation circuit used in the 10.7 to 18 GHz amplifiers consisted of two variable attenuators (A_1 and A_2 in Fig. 40) between Lange couplers. The use of a balanced circuit with couplers provide a circuit with variable attenuation and with low input and output VSWR. The variable attenuators consisted of PIN diodes. The amount of attenuation is determined by the current flowing through the diodes. This current is derived from a temperature sensitive source mounted on the substrate.

Table XX shows an ANA listing for a temperature compensation circuit with a nominal 6.5 dB loss. The VSWR is low. The loss increases with frequency, about 1 dB over the band, but "LOSS DEV" shows that the loss is within a few tenths of a dB from a straight line.

Tables XXI and XXII show the difference between two circuits set for the same loss. Table XXI is with the circuits set for minimum loss. The difference in loss (DG12) is within a few tenths of a dB and the difference in phase (DP12) is within a few degrees. Table XXII shows the same two circuits adjusted for about 6.5 dB loss at midband. The differences in loss and phase remain low even though the magnitude of the loss and phase have both changed. Since the difference in phase remains low, these circuits can be used in phase matched amplifiers.

Figure 52 shows a schematic of the temperature compensation section.

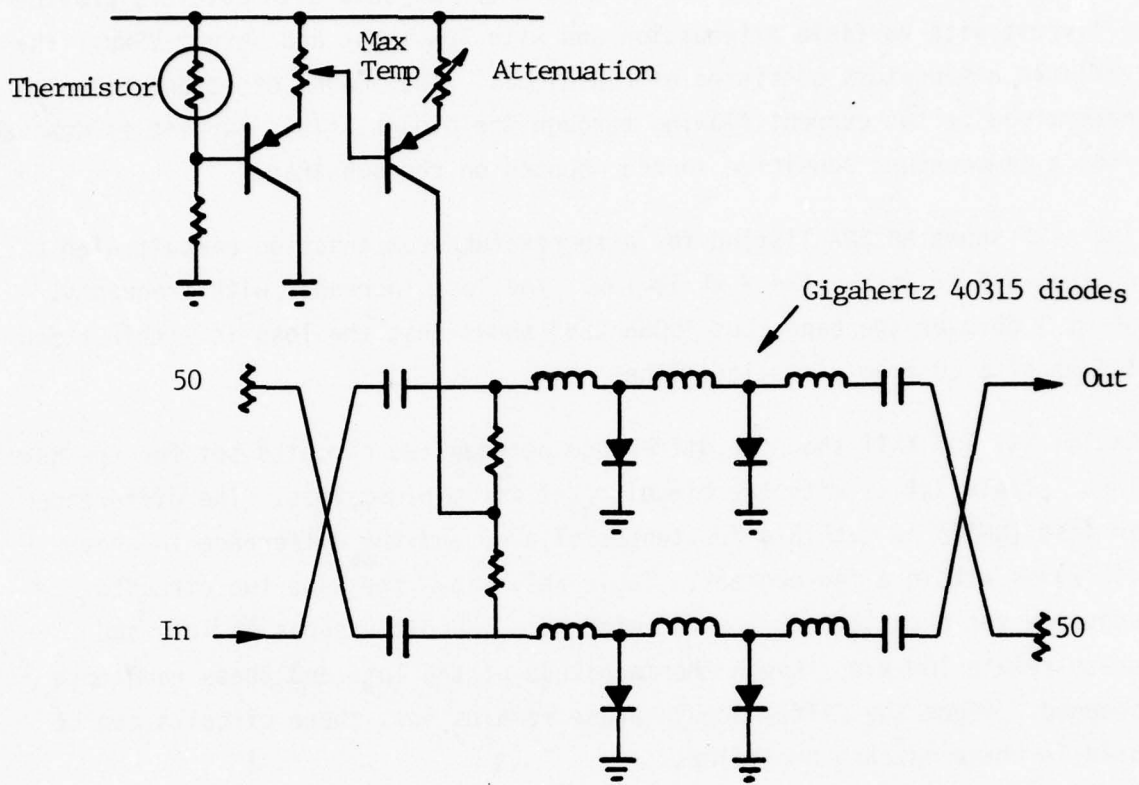


Figure 52

Temperature Compensation Circuit

TABLE XX

AUG 19, 1977

TEMP COMP
10.7 TO 18 GHZ
S/N 2

FREQ MHZ	VSWR IN	LOSS DB	FLAT DB	LOSS DEV	PHASE DEG	PHASE DEV	GPDEL NSEC	ISOL DB	VSWR OUT
10000.0	1.07	5.98			-151.65		.00	5.97	1.22
10200.0	1.05	6.01			-171.52		.26	5.97	1.22
10400.0	1.04	6.01			170.57		.25	5.96	1.22
10600.0	1.04	5.94	-.48	.13	152.02	-.66	.26	5.91	1.22
10800.0	1.05	5.97	-.45	.12	132.43	-1.30	.27	5.98	1.22
11000.0	1.07	6.05	-.37	.17	113.14	-1.66	.26	6.03	1.21
11200.0	1.08	5.96	-.45	.05	95.46	-.40	.26	5.99	1.21
11400.0	1.10	6.01	-.41	.06	76.34	-.58	.27	6.01	1.20
11600.0	1.11	6.03	-.39	.05	56.65	-1.33	.26	6.06	1.19
11800.0	1.13	6.16	-.26	.15	38.90	-.14	.26	6.17	1.18
12000.0	1.14	6.14	-.27	.10	19.82	-.28	.25	6.15	1.18
12200.0	1.15	6.38	-.04	.30	2.64	1.47	.26	6.14	1.19
12400.0	1.16	6.14	-.28	.03	-17.34	.44	.27	6.15	1.22
12600.0	1.17	6.20	-.22	.05	-36.55	.18	.27	6.14	1.21
12800.0	1.18	6.16	-.26	-.01	-55.60	.06	.26	6.14	1.21
13000.0	1.19	6.19	-.23	-.01	-73.78	.82	.26	6.16	1.21
13200.0	1.20	6.11	-.31	-.12	-93.72	-.16	.27	6.06	1.20
13400.0	1.21	6.19	-.23	-.08	-112.17	.32	.26	6.19	1.21
13600.0	1.22	6.24	-.17	-.06	-130.51	.92	.26	6.21	1.21
13800.0	1.21	6.16	-.26	-.18	-149.43	.94	.27	6.15	1.20
14000.0	1.21	6.20	-.22	-.17	-169.33	.00	.27	6.19	1.20
14200.0	1.20	6.30	-.12	-.10	172.28	.54	.25	6.28	1.19
14400.0	1.20	6.27	-.15	-.16	154.76	1.96	.26	6.33	1.17
14600.0	1.20	6.32	-.10	-.15	135.32	1.46	.28	6.28	1.15
14800.0	1.20	6.32	-.10	-.18	114.98	.07	.26	6.28	1.14
15000.0	1.20	6.38	-.04	-.15	97.64	1.66	.26	6.42	1.13
15200.0	1.21	6.36	-.06	-.21	78.21	1.18	.27	6.40	1.12
15400.0	1.22	6.42	.00	-.18	58.84	.75	.27	6.40	1.13
15600.0	1.24	6.45	.03	-.18	39.45	.30	.27	6.45	1.15
15800.0	1.26	6.45	.03	-.21	20.46	.26	.26	6.50	1.18
16000.0	1.27	6.50	.07	-.21	1.45	.19	.27	6.49	1.21
16200.0	1.27	6.50	.07	-.24	-17.89	-.19	.27	6.56	1.26
16400.0	1.28	6.58	.15	-.19	-37.77	-1.12	.27	6.53	1.30
16600.0	1.25	6.77	.34	-.03	-57.25	-1.67	.26	6.68	1.33
16800.0	1.23	6.87	.44	.02	-75.49	-.97	.27	6.84	1.35
17000.0	1.19	6.92	.49	.04	-95.47	-2.00	.27	6.91	1.39
17200.0	1.17	7.24	.81	.33	-113.73	-1.33	.25	7.23	1.42
17400.0	1.18	7.25	.83	.31	-131.29	.04	.24	7.25	1.41
17600.0	1.19	7.11	.68	.13	-148.38	1.89	.26	7.15	1.40
17800.0	1.18	7.06	.64	.05	-169.18	.03	.29	7.02	1.38
18000.0	1.16	7.79	1.36	.74	170.11	-1.72	.00	7.01	1.39
LINEAR- IZATION RANGE			10600.0	10600.0	10600.0	10600.0			
			TO	TO	TO	TO			
			18000.0	18000.0	18000.0	18000.0			

TABLE XXI

AUG 19, 1977

TEMP COMP
10.7 TO 18 GHZ

S21 IN DB

FREQ	S/N 100		DG12	DP12	S/N 200	
	GAIN	PHASE			GAIN	PHASE
10600.	-1.30	150.9	-.06	-.3	-1.24	151.3
10800.	-1.32	131.2	-.09	-.2	-1.23	131.4
11000.	-1.43	111.6	-.12	.0	-1.31	111.6
11200.	-1.37	93.9	-.13	.2	-1.24	93.7
11400.	-1.42	74.7	-.13	.3	-1.29	74.3
11600.	-1.42	55.0	-.11	.6	-1.31	54.4
11800.	-1.52	36.8	-.09	.6	-1.42	36.2
12000.	-1.49	17.4	-.06	.6	-1.43	16.8
12200.	-1.65	.1	.06	.4	-1.72	-.3
12400.	-1.52	-20.3	-.09	-.0	-1.43	-20.3
12600.	-1.57	-39.7	-.14	.2	-1.43	-39.9
12800.	-1.51	-58.9	-.13	.4	-1.37	-59.3
13000.	-1.56	-77.3	-.13	.5	-1.42	-77.8
13200.	-1.49	-97.4	-.14	.4	-1.35	-97.9
13400.	-1.57	-116.2	-.16	.4	-1.42	-116.6
13600.	-1.65	-134.7	-.19	.5	-1.46	-135.2
13800.	-1.56	-153.8	-.21	.7	-1.36	-154.5
14000.	-1.60	-173.5	-.23	.9	-1.38	-174.5
14200.	-1.66	168.1	-.22	1.3	-1.44	166.9
14400.	-1.61	150.3	-.19	1.5	-1.42	148.9
14600.	-1.63	130.8	-.18	1.6	-1.45	129.1
14800.	-1.62	110.1	-.16	1.7	-1.46	108.3
15000.	-1.65	92.6	-.13	1.8	-1.52	90.7
15200.	-1.62	72.6	-.11	1.8	-1.51	70.7
15400.	-1.67	53.2	-.09	1.9	-1.58	51.2
15600.	-1.69	33.1	-.07	1.9	-1.62	31.2
15800.	-1.69	14.3	-.00	1.9	-1.68	12.4
16000.	-1.72	-5.1	-.01	2.0	-1.72	-7.1
16200.	-1.76	-24.4	.01	2.0	-1.77	-26.3
16400.	-1.81	-44.2	.04	2.2	-1.85	-46.4
16600.	-1.88	-63.7	.13	2.3	-2.02	-66.0
16800.	-1.89	-82.3	.20	2.1	-2.09	-84.4
17000.	-1.83	-102.7	.30	1.7	-2.13	-104.5
17200.	-2.02	-121.9	.44	1.0	-2.46	-122.9
17400.	-2.00	-141.4	.46	-.5	-2.46	-141.0
17600.	-2.03	-160.0	.33	-1.7	-2.36	-158.3
17800.	-2.15	179.1	.16	358.	-2.31	-179.1
18000.	-2.78	158.1	.18	-1.7	-2.96	159.8

TABLE XXII

AUG 19, 1977

TEMP COMP
10.7 TO 18 GHZ

S21 IN DB

FREQ	S/N 150		DG12	DP12	S/N 258	
	GAIN	PHASE			GAIN	PHASE
10600.	-6.12	151.6	-.18	-.4	-5.94	152.0
10800.	-6.15	132.0	-.19	-.4	-5.97	132.4
11000.	-6.30	112.8	-.25	-.3	-6.05	113.1
11200.	-6.23	95.3	-.27	-.1	-5.96	95.5
11400.	-6.28	76.4	-.27	.0	-6.01	76.3
11600.	-6.29	56.8	-.25	.1	-6.03	56.6
11800.	-6.40	39.0	-.25	.1	-6.16	38.9
12000.	-6.39	20.0	-.25	.2	-6.14	19.8
12200.	-6.61	2.5	-.23	-.1	-6.38	2.6
12400.	-6.45	-17.4	-.30	-.1	-6.14	-17.3
12600.	-6.54	-36.3	-.34	.2	-6.20	-36.6
12800.	-6.50	-55.1	-.34	.5	-6.16	-55.6
13000.	-6.51	-73.2	-.32	.6	-6.19	-73.8
13200.	-6.42	-93.2	-.31	.5	-6.11	-93.7
13400.	-6.54	-111.7	-.35	.5	-6.19	-112.2
13600.	-6.62	-129.8	-.37	.7	-6.24	-130.5
13800.	-6.55	-148.7	-.39	.7	-6.16	-149.4
14000.	-6.62	-168.2	-.42	1.1	-6.20	-169.3
14200.	-6.72	173.9	-.42	1.6	-6.30	172.3
14400.	-6.62	156.7	-.35	1.9	-6.27	154.8
14600.	-6.63	137.2	-.31	1.8	-6.32	135.3
14800.	-6.64	116.7	-.32	1.7	-6.32	115.0
15000.	-6.70	99.7	-.31	2.0	-6.38	97.6
15200.	-6.62	80.2	-.26	2.0	-6.36	78.2
15400.	-6.68	60.8	-.26	2.0	-6.42	58.8
15600.	-6.71	41.0	-.25	1.5	-6.45	39.4
15800.	-6.70	22.7	-.25	2.2	-6.45	20.5
16000.	-6.71	3.9	-.22	2.4	-6.50	1.4
16200.	-6.70	-15.3	-.20	2.6	-6.50	-17.9
16400.	-6.71	-35.0	-.13	2.8	-6.58	-37.8
16600.	-6.81	-54.2	-.04	3.0	-6.77	-57.3
16800.	-6.81	-72.5	.05	2.9	-6.87	-75.5
17000.	-6.72	-93.0	.20	2.5	-6.92	-95.5
17200.	-6.91	-111.6	.33	2.1	-7.24	-113.7
17400.	-6.88	-130.9	.37	.4	-7.25	-131.3
17600.	-6.89	-149.4	.22	-1.0	-7.11	-148.4
17800.	-7.01	-170.2	.06	-1.0	-7.06	-169.2
18000.	-7.73	168.9	.06	-1.2	-7.79	170.1

IV. 7 TO 18 GHz AMPLIFIERS

The 7 to 18 GHz amplifiers consist of a limiter followed by 6 balanced gain modules and a voltage regulator. A block diagram of the amplifier is shown in Fig. 53. Since the first two gain modules are operated at low drain current to give good noise figure, their gain is approximately 4.5 dB. The remaining four gain modules have approximately 5.5 dB gain each.

Figure 54 and Tables XXIII and XXIV show data on amplifier serial No. 2 without a limiter and before the amplifier was tuned to phase match serial No. 1. The data in the figure and the two tables do not agree since the amplifier in Fig. 54 has been retuned to have a gain slope which increases with frequency to overcome the limiter loss. Figure 54 shows that the amplifier gain is smooth and without "bumps" and small ripples due to reflections at the interconnections or transitions. Ignoring the slope in the gain curve, the gain variation is approximately ± 1 dB from 7 to 18 GHz.

Tables XXIII and XXIV show the same ANA data except that the "FLAT" and "PHASE DEV" are linearized over 7 to 18 GHz in Table XXIII and 8 to 18 GHz in Table XXIV. The phase deviation over 8 to 18 GHz in Table XXIV is seen to be much lower than the 7 to 18 GHz data. The tables show VSWR's less than 1.5, an average gain of 31.3 dB, reverse isolation data which is probably at the noise level of the ANA, a maximum noise figure of 6.7 dB, and a power output at 1 dB gain compression increasing from 11.2 dB at 7 GHz to 15.6 dB at 17 GHz.

Figure 55 is a photograph of one of the 7 to 18 GHz amplifiers assembled to a heat sink on top of our PS-46 power supply. Figure 56 is a picture of the disassembled amplifier and power supply. The figure shows the various carriers which hold the transitions, limiter, gain modules, and regulator in the amplifier. The power supply has been potted with Sylgard.

The following figures and tables show data on the completed amplifiers. These amplifiers are serial Nos. 1 and 2. They have been final-tuned for best gain shape with limiters, best noise figure, and phase matched. The amplifier cases have been welded and mounted on the power supply as shown in Fig. 55.

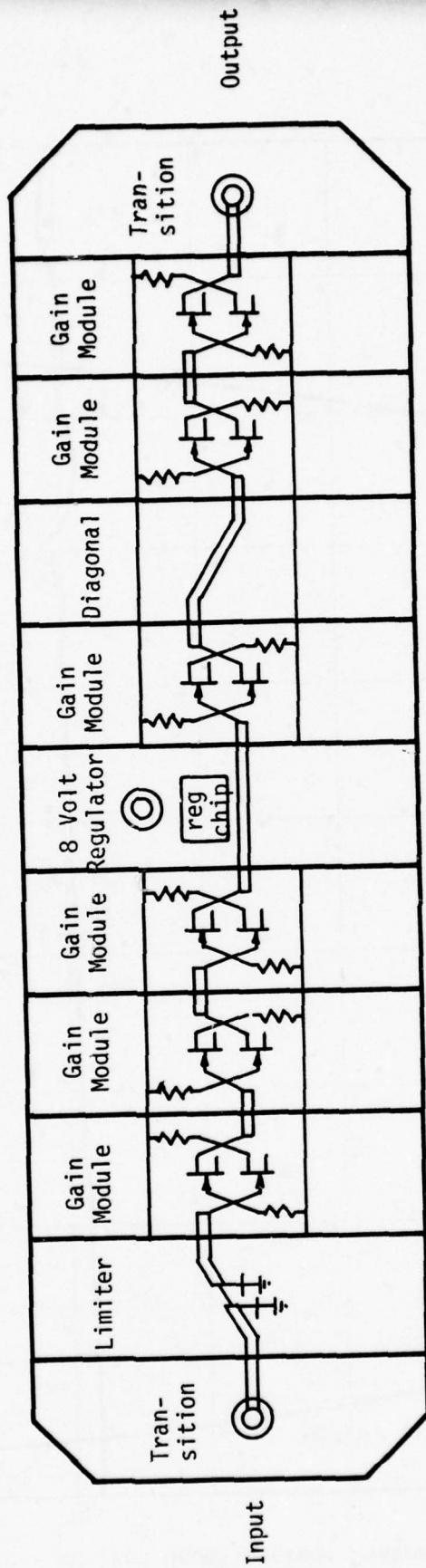


Figure 53
7 to 18 GHz Amplifier

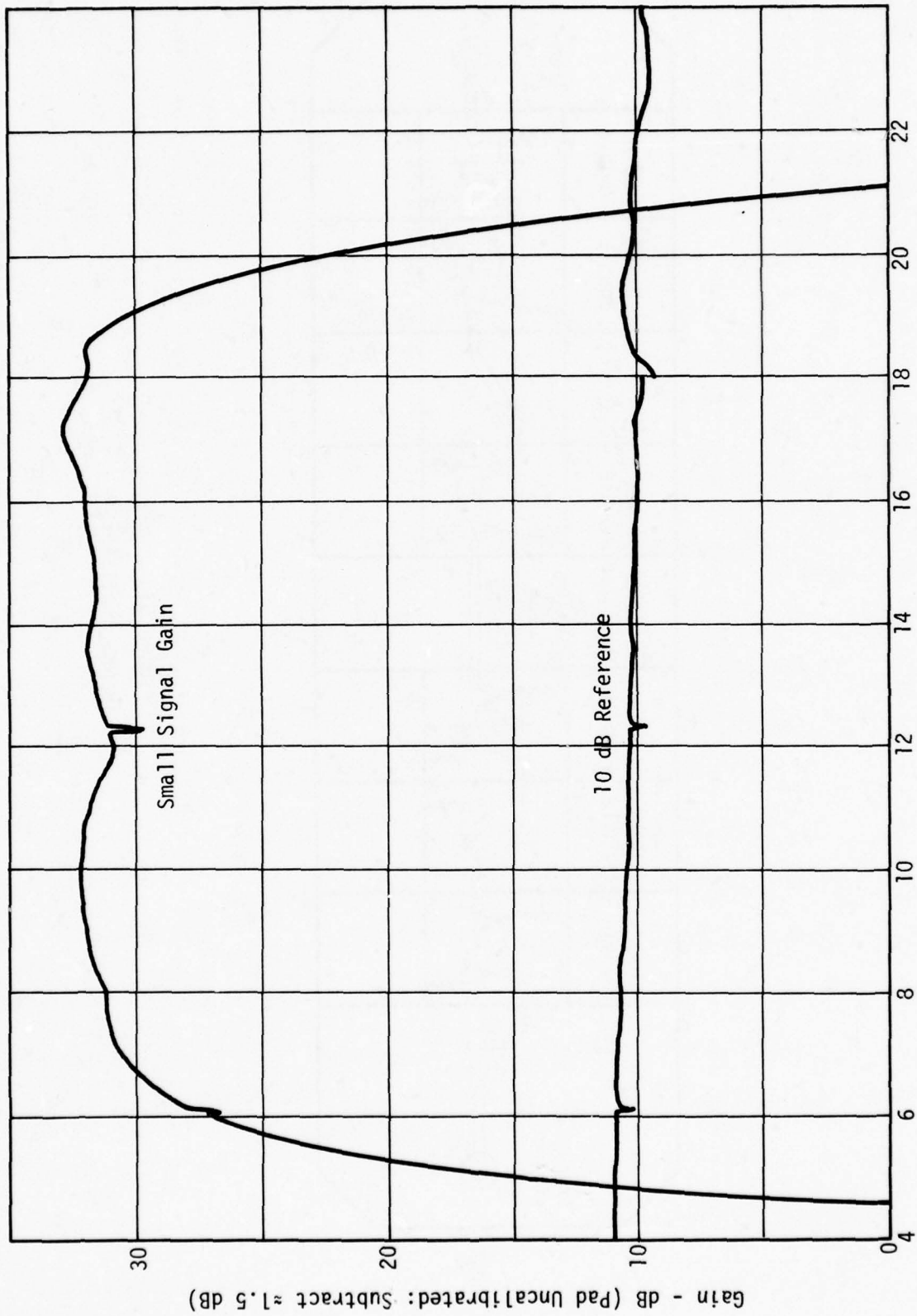


Figure 54
Swept Response of 7 to 18 GHz Amplifier without Limiter

TABLE XXIII

OCT 19, 1977

7 TO 18 GHZ AMPLIFIER
WITHOUT LIMITER
S/N 2

FREQ MHZ	VSWR IN	GAIN DB	FLAT DB	PHASE DEG	PHASE DEV	ISOL DB	VSWR OUT	1DBPWR DBM	NOISE FIG
6000.0	1.50	25.43		-67.08		88.95	1.50		6.7
6250.0	1.47	27.27		151.99		89.77	1.46		
6500.0	1.45	28.70		15.29		81.66	1.43	5.0	6.3
6750.0	1.42	29.62		-116.19		91.10	1.36		
7000.0	1.38	30.39	.91	114.77	79.13	77.76	1.32	11.2	6.2
7250.0	1.30	30.82	.48	-10.60	58.49	86.77	1.31		
7500.0	1.21	31.02	.28	-133.10	40.71	85.91	1.26		
7750.0	1.14	31.14	.16	109.74	28.29	88.94	1.21		
8000.0	1.07	31.22	.08	-7.70	15.55	81.47	1.21	12.2	6.0
8250.0	1.03	31.40	-.09	-120.19	7.79	80.87	1.20		
8500.0	1.04	31.62	-.31	125.95	-1.33	83.13	1.17		
8750.0	1.05	31.78	-.47	16.16	-6.40	79.69	1.18		
9000.0	1.08	31.97	-.66	-95.02	-12.84	95.75	1.19	13.1	5.9
9250.0	1.07	32.20	-.89	156.35	-16.75	86.83	1.16		
9500.0	1.07	32.24	-.93	46.87	-21.52	86.24	1.16		
9750.0	1.04	32.31	-1.00	-61.39	-25.05	78.34	1.23		
10000.0	1.04	32.25	-.94	-168.16	-27.10	84.31	1.23	13.2	6.1
10250.0	1.06	32.26	-.95	85.65	-28.56	87.69	1.24		
10500.0	1.06	32.24	-.93	-20.21	-29.69	77.21	1.32		
10750.0	1.09	32.17	-.86	-126.14	-30.89	80.13	1.34		
11000.0	1.09	31.86	-.55	129.25	-30.78	80.70	1.32	14.0	6.4
11250.0	1.10	31.75	-.44	24.98	-30.32	85.05	1.35		
11500.0	1.13	31.42	-.11	-76.76	-27.33	86.74	1.37		
11750.0	1.19	31.21	.09	-179.58	-25.43	89.19	1.27		
12000.0	1.22	30.85	.45	78.55	-22.57	85.76	1.18	13.9	6.7
12250.0	1.30	31.25	.05	-22.24	-18.65	86.59	1.21		
12500.0	1.31	30.59	.71	-121.62	-13.32	80.31	1.11		
12750.0	1.27	30.79	.51	136.55	-10.43	79.47	1.10		
13000.0	1.24	30.77	.53	34.61	-7.65	82.87	1.16	14.6	5.6
13250.0	1.26	30.98	.32	-67.53	-5.07	83.53	1.11		
13500.0	1.22	31.07	.23	-169.10	-1.91	78.73	1.23		
13750.0	1.19	31.13	.17	86.82	-1.27	92.21	1.29		
14000.0	1.18	30.98	.32	-15.69	.93	81.92	1.25	14.4	5.5
14250.0	1.17	30.84	.46	-118.20	3.14	96.50	1.34		
14500.0	1.17	30.72	.58	141.08	7.15	86.67	1.40		
14750.0	1.20	30.61	.69	38.51	9.30	88.99	1.33		
15000.0	1.17	30.68	.62	-63.65	11.87	85.65	1.28	15.5	5.9
15250.0	1.16	30.69	.61	-166.46	13.79	89.29	1.27		
15500.0	1.20	30.80	.50	90.98	15.95	84.69	1.16		
15750.0	1.18	30.77	.53	-12.60	17.09	79.26	1.12		
16000.0	1.17	30.94	.36	-116.92	17.49	83.38	1.15	15.2	6.5
16250.0	1.22	30.98	.32	140.23	19.36	80.78	1.14		
16500.0	1.23	31.34	-.03	35.02	18.86	79.34	1.15		
16750.0	1.21	31.59	-.28	-69.91	18.66	85.88	1.23		
17000.0	1.21	31.66	-.35	179.74	13.03	87.15	1.24	15.6	6.4
17250.0	1.22	31.79	-.48	72.21	10.22	77.71	1.22		
17500.0	1.32	31.51	-.20	-39.37	3.36	71.50	1.23		
17750.0	1.37	31.30	.00	-152.00	-4.52	72.68	1.35		
18000.0	1.47	30.63	.67	97.05	-10.76	79.76	1.47	14.5	6.7

TABLE XXIV

OCT 19, 1977

 7 TO 18 GHZ AMPLIFIER
 WITHOUT LIMITER
 S/N 2

FREQ MHZ	VSWR IN	GAIN DB	FLAT DB	PHASE DEG	PHASE DEV	ISOL DB	VSWR OUT	1DBPWR DBM	NOISE FIG
6000.0	1.50	25.43		-67.08		88.95	1.50		6.7
6250.0	1.47	27.27		151.99		89.77	1.46		
6500.0	1.45	28.70		15.29		81.66	1.43	5.0	6.3
6750.0	1.42	29.62		-116.19		91.10	1.36		
7000.0	1.38	30.39		114.77		77.76	1.32	11.2	6.2
7250.0	1.30	30.82		-10.60		86.77	1.31		
7500.0	1.21	31.02		-133.10		85.91	1.26		
7750.0	1.14	31.14		109.74		88.94	1.21		
8000.0	1.07	31.22	.12	-7.70	37.09	81.47	1.21	12.2	6.0
8250.0	1.03	31.40	-.05	-120.19	28.50	80.87	1.20		
8500.0	1.04	31.62	-.27	125.95	18.55	83.13	1.17		
8750.0	1.05	31.78	-.43	16.16	12.65	79.69	1.18		
9000.0	1.08	31.97	-.62	-95.02	5.38	95.75	1.19	13.1	5.9
9250.0	1.07	32.20	-.85	156.35	.65	86.83	1.16		
9500.0	1.07	32.24	-.89	46.87	-4.93	86.24	1.16		
9750.0	1.04	32.31	-.96	-61.39	-9.29	78.34	1.23		
10000.0	1.04	32.25	-.90	-168.16	-12.16	84.31	1.23	13.2	6.1
10250.0	1.06	32.26	-.91	85.65	-14.45	87.69	1.24		
10500.0	1.06	32.24	-.89	-20.21	-16.40	77.21	1.32		
10750.0	1.09	32.17	-.82	-126.14	-18.43	80.13	1.34		
11000.0	1.09	31.86	-.51	129.25	-19.14	80.70	1.32	14.0	6.4
11250.0	1.10	31.75	-.40	24.98	-19.50	85.05	1.35		
11500.0	1.13	31.42	-.07	-76.76	-17.34	86.74	1.37		
11750.0	1.19	31.21	.13	-179.58	-16.27	89.19	1.27		
12000.0	1.22	30.85	.49	78.55	-14.23	85.76	1.18	13.9	6.7
12250.0	1.30	31.25	.09	-22.24	-11.14	86.59	1.21		
12500.0	1.31	30.59	.75	-121.62	-6.63	80.31	1.11		
12750.0	1.27	30.79	.55	136.55	-4.56	79.47	1.10		
13000.0	1.24	30.77	.57	34.61	-2.61	82.87	1.16	14.6	5.6
13250.0	1.26	30.98	.36	-67.53	-.86	83.53	1.11		
13500.0	1.22	31.07	.27	-169.10	1.47	78.73	1.23		
13750.0	1.19	31.13	.21	86.82	1.28	92.21	1.29		
14000.0	1.18	30.98	.36	-15.69	2.67	81.92	1.25	14.4	5.5
14250.0	1.17	30.84	.50	-118.20	4.06	96.50	1.34		
14500.0	1.17	30.72	.62	141.08	7.24	86.67	1.40		
14750.0	1.20	30.61	.73	38.51	8.57	88.99	1.33		
15000.0	1.17	30.68	.66	-63.65	10.31	85.65	1.28	15.5	5.9
15250.0	1.16	30.69	.65	-166.46	11.40	89.29	1.27		
15500.0	1.20	30.80	.54	90.98	12.75	84.69	1.16		
15750.0	1.18	30.77	.57	-12.60	13.06	79.26	1.12		
16000.0	1.17	30.94	.40	-116.92	12.63	83.38	1.15	15.2	6.5
16250.0	1.22	30.98	.36	140.23	13.68	80.78	1.14		
16500.0	1.23	31.34	.00	35.02	12.35	79.34	1.15		
16750.0	1.21	31.59	-.24	-69.91	11.32	85.88	1.23		
17000.0	1.21	31.66	-.31	179.74	4.88	87.15	1.24	15.6	6.4
17250.0	1.22	31.79	-.44	72.21	1.24	77.71	1.22		
17500.0	1.32	31.51	-.16	-39.37	-6.44	71.50	1.23		
17750.0	1.37	31.30	.04	-152.00	-15.15	72.68	1.35		
18000.0*	1.47	30.63	.71	97.05	-22.21	79.76	1.47	14.5	6.7

* Bad Data

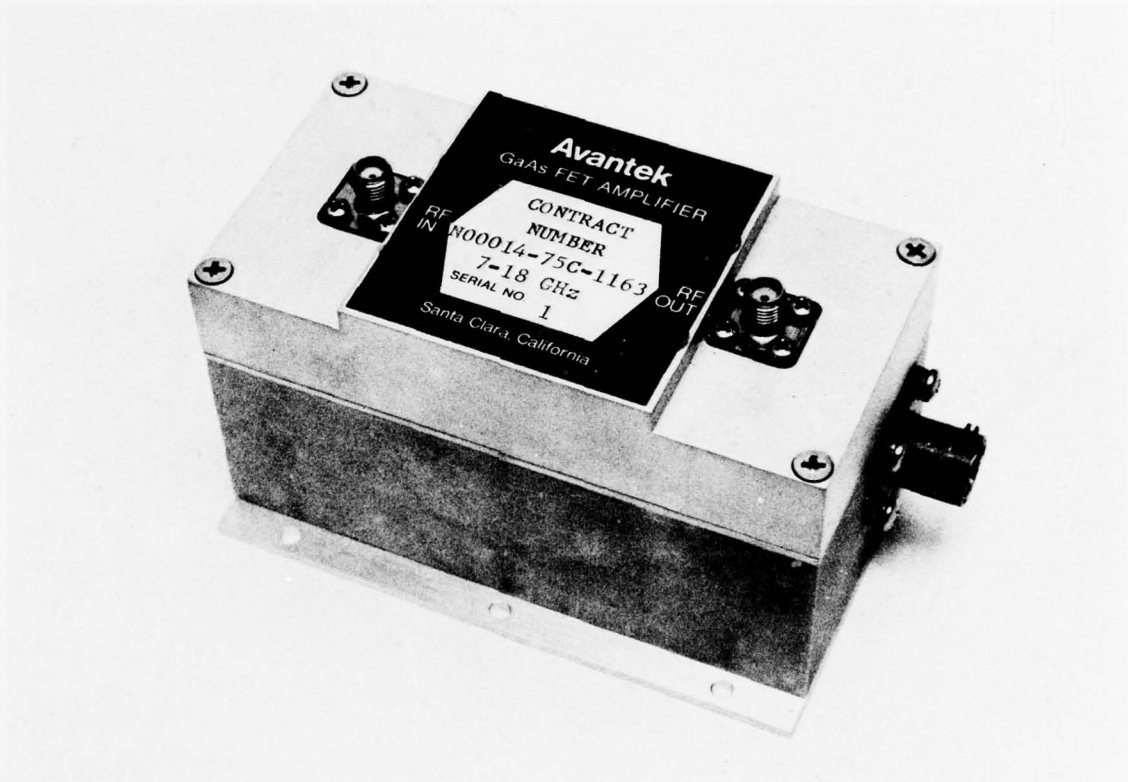


Figure 55
Complete 7 to 18 Amplifier and Power Supply

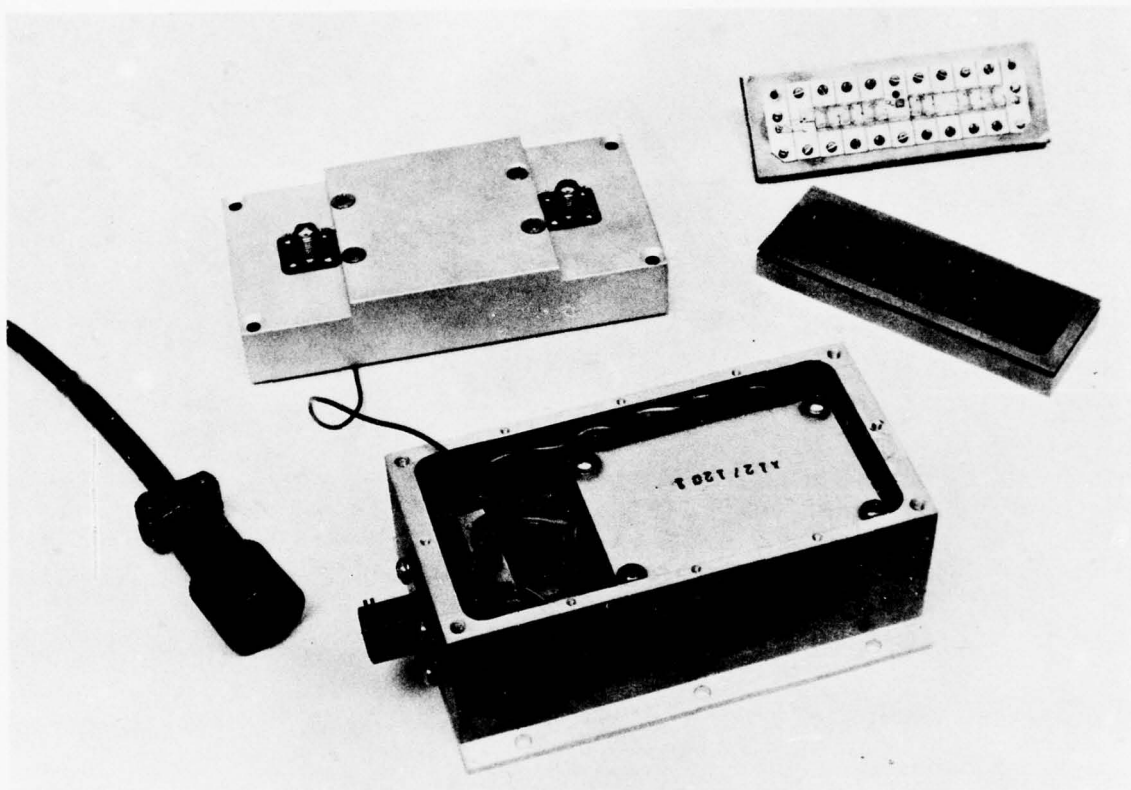


Figure 56
Exploded View of 7 to 18 GHz Amplifier and Power Supply

Final ANA data, power output at 1 dB gain compression, and noise figure on the amplifiers is shown in Table XXV. Table XXVI shows the difference in gain (DG12) and difference in phase (DP12) between the two amplifiers. Excluding the ANA data at 18 GHz, the two tables show that these two amplifiers have met all the required specifications except for phase deviation, perhaps phase match, and safe power input power which is 1% duty and not the specified 10% duty. Measured data compared to specification requirements are summarized in Table XXVII. Phase deviation data is shown for several amplifiers in Table XXIII and Appendix D. Ignoring the peaks in phase deviation at the band edges, the phase deviation linearized from 7 to 18 GHz is seen to be approximately -30° near 10.5 GHz and $+20^\circ$ near 15.5 GHz. During the temperature run on these amplifiers, the maximum difference in phase measured was near 16 degrees, but a short length of transmission line could correct this phase difference to approximately 8 degrees (see Fig.57). Measurement accuracy and SMA connector repeatability are not good enough to determine the actual phase match of the amplifiers. In our proposal we stated that we expected the phase match to be less than 10° . The reverse isolation measurement on the ANA is probably just measuring the noise level of the ANA, so that the reverse isolation is greater than that value listed for the particular frequency.

Figure 58 shows the swept frequency response of the two amplifiers. Note that there are no "bumps" or small ripples due to reflections in the interconnections or transitions. In addition, there is no tendency to oscillate at frequencies above 20 GHz where the waveguide formed by the lid on the amplifier is no longer below cutoff.

The effect of temperature on gain and phase is summarized in Table XXVIII and plotted in Fig. 57. Table XXVIII and Fig.57 show that the gain and phase changes with temperature; however, the difference in gain and phase between the two amplifiers is small enough to be determined to a large extent by measurement accuracy and connector repeatability. The noise figure increases with temperature as seen in Fig. 59 to about 10 dB at 18 GHz at $+70^\circ\text{C}$. The solid lines in Fig.59 are drawn to be parallel with the room temperature data taken at many frequencies in the laboratory. Complete temperature test data is given in Appendix A.

TABLE XXV

NOV 21, 1977

7 TO 18 GHZ AMPLIFIER
FINAL DATA
S/N 1

FREQ MHZ	VSWR IN	GAIN DB	FLAT DB	PHASE DEC	PHASE DEV	ISOL DB	VSWR OUT	1DBPWR DBM	NOISE FIO	FREQ MHZ	VSWR IN	GAIN DB	FLAT DB	PHASE DEC	PHASE DEV	ISOL DB	VSWR OUT	1DBPWR DBM	NOISE FIO	
7000.0	1.41	28.64	1.17	88.28	72.76	92.02	1.10	14.2	6.6	7000.0	1.32	28.64	.72	90.33	71.67	81.66	1.10	11.8	6.5	
7250.0	1.52	28.94	.87	-36.75	54.13	84.98	1.10			7250.0	1.35	28.74	.62	-35.22	52.61	88.19	1.16			
7500.0	1.59	27.37	.44	-158.85	38.42	84.84	1.09			7500.0	1.40	29.00	.36	-157.67	36.65	79.19	1.26			
7750.0	1.46	29.50	.31	83.81	27.47	83.78	1.08			7750.0	1.31	29.01	.35	85.12	25.94	83.70	1.29			
8000.0	1.31	29.69	.12	-34.66	15.40	83.33	1.07			8000.0	1.20	29.16	.20	-33.13	14.19	84.79	1.36			6.1
8250.0	1.28	30.02	-.20	-149.59	6.88	88.65	1.07			8250.0	1.21	29.47	-.10	-148.00	5.80	91.70	1.42			
8500.0	1.32	29.99	-.17	95.65	-1.48	95.46	1.07			8500.0	1.29	29.42	-.05	97.36	-2.33	95.94	1.45			
8750.0	1.31	30.33	-.51	-16.65	-7.39	85.60	1.09			8750.0	1.31	29.70	-.33	-14.81	-8.00	89.12	1.50			6.3
9000.0	1.26	30.67	-.80	-126.96	-11.31	92.84	1.11			9000.0	1.27	29.95	-.58	-124.41	-11.12	86.77	1.49			
9250.0	1.20	30.67	-.85	119.35	-18.60	89.63	1.11			9250.0	1.20	30.00	-.63	122.91	-17.30	93.31	1.47			
9500.0	1.35	30.95	-1.04	10.61	-20.94	90.97	1.12			9500.0	1.21	30.19	-.82	14.95	-18.77	82.50	1.43			
9750.0	1.37	30.75	-.93	-97.45	-22.60	83.28	1.15			9750.0	1.28	30.14	-.77	-92.34	-19.37	87.90	1.43			
10000.0	1.33	30.91	-1.09	152.03	-26.59	90.03	1.15			10000.0	1.28	30.35	-.98	157.81	-22.97	92.60	1.26			6.3
10250.0	1.23	30.97	-1.15	45.40	-26.97	88.81	1.15			10250.0	1.18	30.52	-1.15	51.18	-23.07	84.35	1.31			
10500.0	1.17	30.65	-1.04	-62.44	-28.41	83.02	1.16			10500.0	1.05	30.53	-1.16	-56.52	-24.28	99.69	1.27			
10750.0	1.16	30.82	-1.00	-170.40	-27.98	78.91	1.18			10750.0	1.01	30.64	-1.27	-165.24	-26.50	99.98	1.23			
11000.0	1.18	30.45	-.63	84.43	-28.71	89.28	1.22			11000.0	1.06	30.39	-1.02	88.92	-25.85	87.38	1.29			6.9
11250.0	1.27	30.23	-.41	-22.07	-28.67	88.25	1.25			11250.0	1.26	30.19	-.82	-17.85	-26.14	84.59	1.27			
11500.0	1.33	30.04	-.82	-126.37	-26.73	83.70	1.29			11500.0	1.46	30.05	-.68	-122.14	-23.93	82.41	1.32			
11750.0	1.34	29.71	-.10	129.82	-24.20	79.47	1.32			11750.0	1.47	29.84	-.47	135.03	-20.26	83.26	1.28			
12000.0	1.26	29.68	.13	26.35	-21.26	78.99	1.40			12000.0	1.31	29.93	-.56	31.67	-17.14	82.47	1.26			7.1
12250.0	1.31	29.82	.49	-65.51	-27.74	74.38	1.43			12250.0	1.25	29.72	-.55	-81.50	-23.81	78.41	1.23			
12500.0	1.33	29.17	.64	-177.75	-12.09	81.56	1.43			12500.0	1.39	29.52	-.15	-177.69	-13.50	79.74	1.22			
12750.0	1.29	29.37	.44	81.91	-6.53	96.48	1.43			12750.0	1.35	29.54	-.17	70.05	-11.28	97.58	1.25			6.7
13000.0	1.14	29.44	.37	-20.93	-2.96	92.56	1.50			13000.0	1.14	29.56	-.19	-27.76	-10.59	82.33	1.42			
13250.0	1.10	29.73	.03	-123.94	.42	97.93	1.51			13250.0	1.04	29.35	.01	-135.24	-11.57	83.31	1.42			
13500.0	1.07	30.13	-.31	131.41	2.14	85.25	1.50			13500.0	1.16	29.46	-.09	120.69	-9.16	77.26	1.43			
13750.0	1.09	30.01	-.19	24.33	1.45	76.77	1.42			13750.0	1.12	28.99	.37	17.03	-6.33	81.86	1.52			6.7
14000.0	1.25	29.60	.01	-79.73	3.79	77.50	1.40			14000.0	1.05	28.63	.73	-82.92	.19	77.37	1.55			
14250.0	1.43	29.65	.25	177.97	7.57	78.56	1.50			14250.0	1.24	28.45	.91	178.21	7.81	77.49	1.57			
14500.0	1.43	29.58	.25	71.77	8.09	77.05	1.22			14500.0	1.34	28.51	.85	72.80	8.90	80.83	1.64			
14750.0	1.39	29.79	.32	-50.69	12.03	83.65	1.16			14750.0	1.31	28.52	.84	-50.44	12.15	83.75	1.59			
15000.0	1.06	29.54	.27	-131.07	15.02	80.93	1.21			15000.0	1.09	28.75	.61	-133.83	15.24	81.50	1.60			7.2
15250.0	1.12	29.64	.17	118.78	14.28	83.79	1.29			15250.0	1.09	29.06	.30	117.85	13.43	82.06	1.45			
15500.0	1.24	29.61	.20	13.49	15.37	76.31	1.43			15500.0	1.28	29.17	.19	13.52	15.99	78.14	1.40			
15750.0	1.19	29.42	.39	-93.33	14.95	77.64	1.53			15750.0	1.24	29.10	.26	-92.31	16.25	77.74	1.27			
16000.0	1.20	29.56	.25	160.03	14.69	81.82	1.56			16000.0	1.14	29.37	.00	162.59	17.64	75.96	1.09			7.5
16250.0	1.20	29.44	.37	53.98	15.04	80.59	1.44			16250.0	1.13	29.08	.48	50.98	18.25	76.04	1.25			
16500.0	1.14	29.41	.40	-53.60	13.05	77.94	1.41			16500.0	1.24	28.88	.48	-50.98	17.05	70.50	1.41			
16750.0	1.04	29.56	.35	-193.83	15.01	87.41	1.32			16750.0	1.28	29.04	.32	-157.28	17.25	81.22	1.55			
17000.0	1.18	29.50	.31	90.99	11.22	74.23	1.32			17000.0	1.10	29.16	.20	92.23	13.26	71.52	1.74			7.5
17250.0	1.18	29.24	.57	-19.19	7.42	79.09	1.18			17250.0	1.20	29.05	.31	-21.06	6.45	81.69	1.79			
17500.0	1.20	29.59	.42	-126.85	6.16	76.04	1.08			17500.0	1.42	28.74	.62	-130.98	3.03	85.19	1.47			
17750.0	1.15	29.50	.31	114.95	-5.64	68.15	1.03			17750.0*	1.46	28.11	1.25	112.46	-7.02	64.32	2.04			
18000.0	1.13	29.13	.68	-.53	-14.78	69.27	1.20			18000.0*	1.31	27.98	1.38	4.11	-8.88	70.58	2.34			7.6

NOV 21, 1977

7 TO 18 GHZ AMPLIFIER
FINAL DATA
S/N 2

* Bad Data

TABLE XXVI

NOV 21, 1977
 7 TO 18 GHZ AMPLIFIER
 PHASE MATCH - FINAL DATA

521 IN DB

FREQ	S/N	GAIN	PHASE	1	2	DP12	DF12	S/N	2		
7000	0	29	11	82	5	-55	-1.2	29	66	83	7
7333	3	29	61	-83	0	-26	-6	29	87	-82	4
7666	7	30	04	116	1	-04	-9	30	09	117	1
8000	0	30	42	-41	8	.03	-1.4	30	38	-40	4
8333	3	30	71	164	4	.04	-1.9	30	67	166	3
8666	7	31	02	12	7	.18	-1.8	30	65	14	5
9000	0	31	17	-137	8	.24	-2.5	30	92	-135	3
9333	3	31	32	75	1	.26	-3.3	31	06	78	5
9666	7	31	40	-71	5	.21	-4.2	31	19	-67	3
10000	31	48	143	3	.10	-4.9	31	37	148	1	
10333	31	49	-	8	-04	-3.2	31	52	4	4	
10667	31	33	-145	1	-19	-5.3	31	51	-139	8	
11000	30	98	73	0	-27	-4.9	31	24	77	8	
11333	30	66	-68	5	-34	-4.6	31	00	-63	8	
11667	30	28	151	4	-52	-4.8	30	80	156	3	
12000	29	97	15	8	-81	-3.7	30	78	19	4	
12667	29	88	102	7	-75	1.5	30	64	101	1	
13000	30	22	-34	5	-55	3.2	30	77	-37	7	
13333	30	47	-174	1	-12	4.0	30	59	-178	1	
13667	30	47	46	5	.33	2.7	30	14	43	8	
14000	30	45	-93	7	.59	-2.2	29	87	-93	5	
14333	30	26	126	3	.51	-2.7	29	75	129	1	
14667	30	18	-11	7	.32	-3.6	29	86	-8	1	
15000	30	15	-151	3	.15	-3.9	30	00	-147	4	
15333	30	11	67	8	-05	-4.2	30	16	72	0	
15667	29	75	-73	4	-20	-3.9	29	93	-69	4	
16000	29	80	145	3	-17	-3.7	29	97	149	1	
16333	29	81	2	1	-11	-3.2	29	92	5	3	
16667	29	61	-140	8	.10	-4.3	29	91	-136	5	
17000	29	61	75	9	-16	-4.1	29	76	80	1	
17333	29	60	-70	4	-02	-3.5	29	62	-66	9	
17667	29	47	138	3	.40	-3.6	29	07	141	8	
18000	*28	95	-15	6	1.10	-8.5	27	85	-7	0	

* Probably Bad Data

Comparison of Specified and Measured Data*

Table XXVII

Frequency Range of Operation:	7.0 - 18.0 GHz
Input and Output Impedance:	50 ohms
AC Coupling at Input and Output:	
Stability:	Amplifier did not oscillate with input and/or output open or short circuited.

	<u>Specification</u>	<u>Measurement</u>	
		<u>S/N 1</u>	<u>S/N 2</u>
Gain:	25 dB (min)	28.64 dB (min)	28.11 dB (min)
Gain Variation:	±1.5 dB (max)	±1.16 dB (max)	±1.26 dB (max)
Noise Figure:	10 dB (max)	8.1 dB (max)	7.6 dB (max)
Power Output:	+6 dBm	13.1 dBm (min)	11.8 dBm (min)
Phase Deviation from Linear:	±10° (max)	+20° (max) -30°	+20° (max)** -30°
Input VSWR:	2.5:1 (max)	1.44:1 (max)	1.47:1 (max)
Output VSWR:	2.5:1 (max)	1.56:1 (max)	2.04:1 (max)
Phase Matching Between Amplifier Pairs	≤5°		+4.0° -5.3°
Reverse Isolation:	50 dB (min)	>68 dB (min)	>64 dB (min)
Safe Input Power CW, RF:	+30 dBm (min)	+30 dBm	+30 dBm
10% Duty - Peak Pulse:	+50 dBm (min)	+50 dBm 1%	+50 dBm 1%

* Ignores 18 GHz data in Tables XXV and XXVI.

**See Table XXIII and Appendix B.

TABLE XXVIII

CHANGE IN GAIN AND PHASE WITH TEMPERATURE

SERIAL NO. 2

NOV 22, 1977
7 TO 18 GHZ AMPLIFIER
TEMPERATURE TEST

S21 IN DB

SERIAL NO. 1

NOV 22, 1977
7 TO 18 GHZ AMPLIFIER
TEMPERATURE TEST

S21 IN DB

FREQ	AT -28°C			AT 30°C			AT 70°C			AT 70°C			
	S/N	DP12	DP13	S/N	DP12	DP13	S/N	DP12	DP13	S/N	DP23	DP13	
7000.0	33.28	-50.1	5.14	16.7	28.13	-66.8	3.95	10.0	0.24	18	-76.8	9.10	26.7
7333.3	33.92	153.5	5.13	16.9	28.79	136.6	3.91	10.0	0.24	88	126.6	9.04	26.9
7666.7	34.23	2.4	5.05	16.9	29.18	-14.5	3.85	10.2	0.25	32	-24.7	8.90	27.1
8000.0	34.49	-145.2	4.94	17.4	29.56	-162.6	3.78	10.6	0.25	78	-173.2	8.72	28.0
8333.3	34.57	73.6	4.85	18.4	29.72	55.3	3.72	11.1	0.26	00	44.1	8.57	29.5
8666.7	34.91	-68.7	4.73	18.4	30.17	-87.1	3.68	11.3	0.26	50	-98.4	8.41	29.7
9000.0	35.11	153.8	4.65	19.5	30.46	134.3	3.66	11.1	0.26	80	123.2	8.31	30.5
9333.3	35.29	14.9	4.61	19.9	30.67	-5.0	3.55	11.9	0.27	12	-16.9	8.17	31.8
9666.7	35.35	-120.7	4.54	20.2	30.80	-141.0	3.49	12.4	0.27	31	-153.3	8.03	32.6
10000.0	35.32	103.4	4.48	20.6	30.85	82.8	3.48	13.0	0.27	37	69.7	7.96	33.7
10333.3	35.11	-30.1	4.29	22.0	30.82	-52.0	3.48	13.4	0.27	34	-65.4	7.77	35.4
10667.0	34.94	-162.0	4.39	23.0	30.58	175.0	3.44	13.8	0.27	13	161.2	7.83	36.8
11000.0	34.85	66.2	4.31	23.6	30.55	42.6	3.40	14.1	0.27	15	28.5	7.70	37.7
11333.3	34.40	-63.4	4.35	24.5	30.05	-87.9	3.36	14.8	0.26	69	-102.7	7.70	39.3
11667.0	33.94	168.2	4.31	24.9	29.64	143.3	3.31	15.2	0.26	33	128.1	7.62	40.1
12000.0	33.53	41.6	4.17	25.7	29.36	16.0	3.27	15.9	0.25	79	1.1	7.74	41.6
12667.0	33.79	152.6	4.18	28.1	29.50	124.5	3.27	17.4	0.26	33	107.1	7.45	45.5
13000.0	34.08	24.8	4.15	28.9	29.93	-4.0	3.22	17.4	0.26	71	-21.5	7.37	46.3
13333.3	34.33	-104.6	4.14	30.6	30.19	-135.1	3.18	18.2	0.27	01	-153.4	7.32	48.8
13667.0	34.91	126.5	4.22	29.9	30.69	96.5	3.14	18.9	0.27	55	77.6	7.37	48.9
14000.0	34.56	-2.8	4.15	30.5	30.41	-33.3	3.15	19.3	0.27	26	-52.6	7.30	49.8
14333.3	34.23	-134.1	4.04	32.4	30.19	-166.5	3.07	20.0	0.27	12	173.5	7.11	52.4
14667.0	34.99	99.7	4.10	32.8	30.19	66.9	3.10	20.9	0.27	09	46.1	7.21	53.7
15000.0	33.99	-31.2	4.06	33.9	29.93	-65.2	3.06	21.7	0.26	87	-86.9	7.12	55.7
15333.3	33.95	160.9	3.95	34.4	29.99	164.7	3.07	22.5	0.26	92	143.2	7.04	56.9
15667.0	33.89	71.5	3.95	35.3	29.94	36.1	2.93	23.7	0.27	00	13.5	6.88	58.0
16000.0	33.60	-99.6	3.85	36.3	29.75	-95.9	2.90	23.3	0.26	89	-119.1	6.75	59.5
16333.3	33.46	169.1	3.77	38.6	29.69	130.5	2.79	24.5	0.26	90	106.0	6.56	63.1
16667.0	33.32	35.0	3.58	40.0	29.74	-5.0	2.93	25.8	0.26	80	-30.8	6.51	65.8
17000.0	33.30	-94.8	3.60	42.8	29.69	-137.6	2.83	27.6	0.26	87	-165.2	6.43	70.4
17333.3	33.57	131.1	3.70	45.0	29.87	86.1	2.83	29.3	0.27	04	56.8	6.53	74.2
17667.0	33.41	-8.2	3.77	47.0	29.64	-55.1	2.92	30.9	0.26	73	-86.0	6.68	77.9
18000.0*	32.84	-148.8	3.97	50.2	28.87	161.0	2.96	31.3	0.25	91	129.7	6.93	81.5

* Bad Data

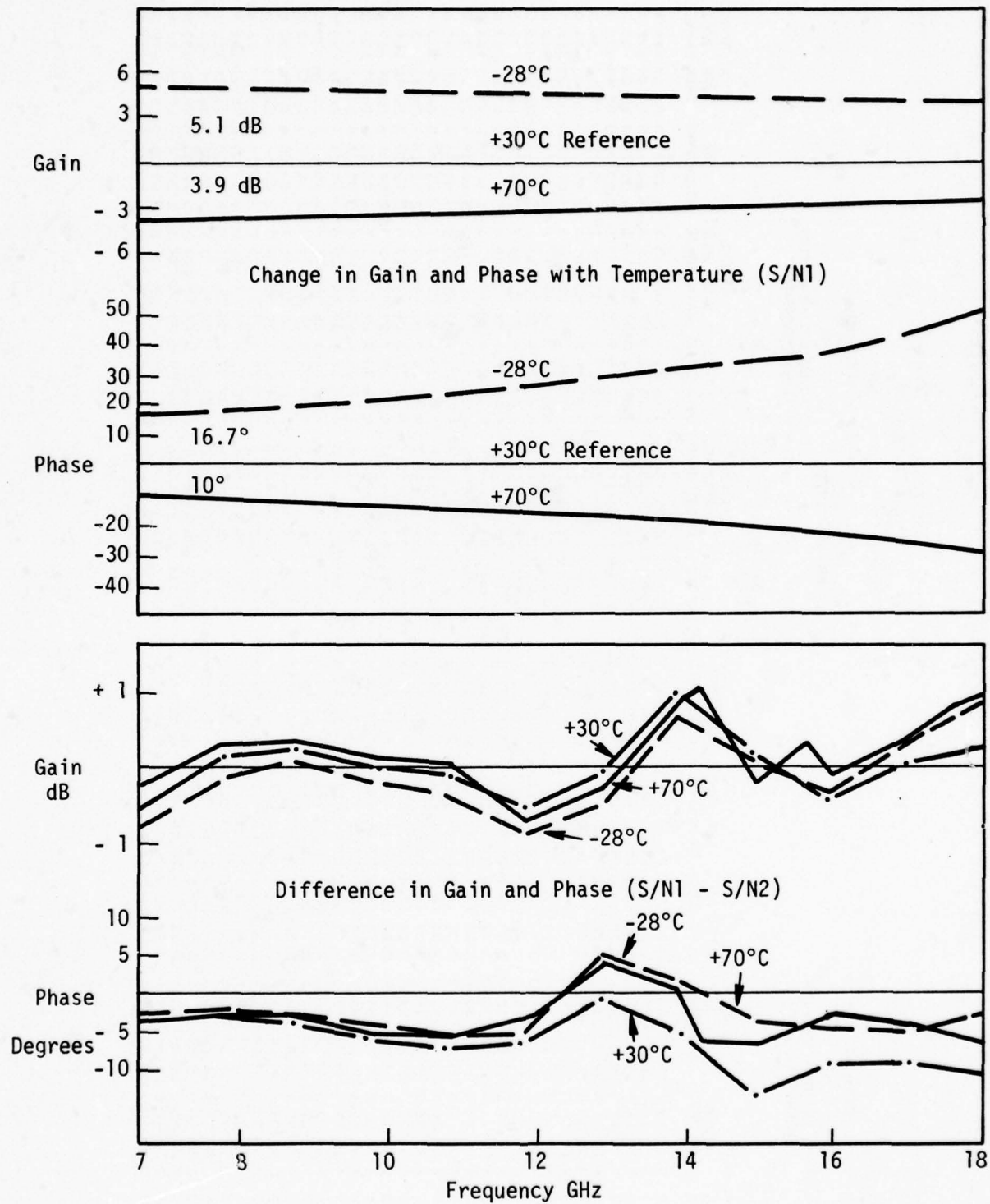


Figure 57
 Change in Gain and Phase with Temperature
 for 7 to 18 GHz Amplifier

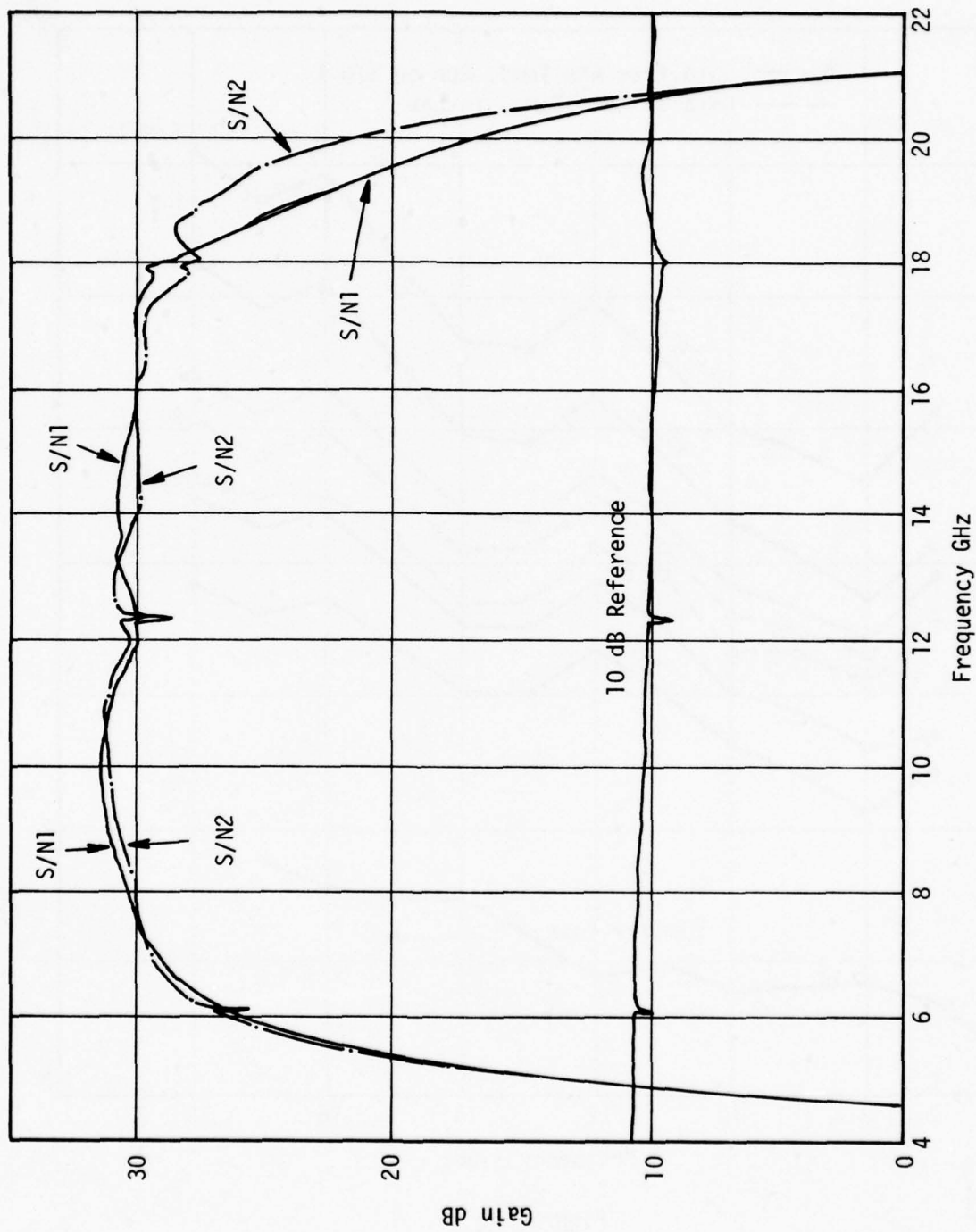


Figure 58
Swept Response of 7 to 18 GHz Amplifiers

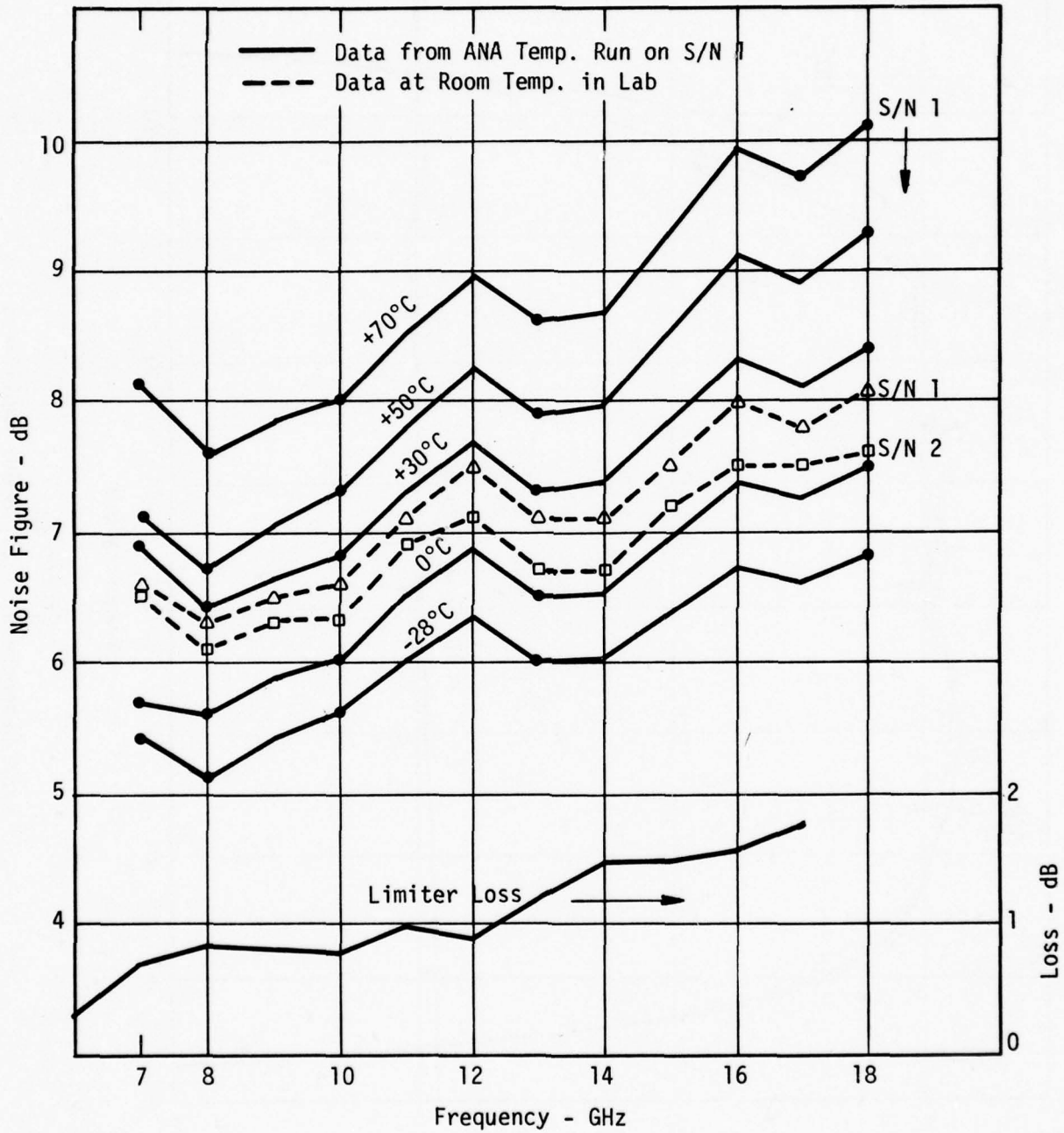


Figure 59
 Noise Figure vs. Temperature
 7 to 18 GHz Amplifiers with Limiters

V. 10.7 TO 18 GHz AMPLIFIERS

The 10.7 to 18 GHz amplifier consists of 10 balanced gain modules, a limiter, a temperature compensation module, and a voltage regulator as shown in Fig. 60. As with the 7 to 18 GHz amplifiers, the first two gain modules are operating at low current to give a gain of about 4.5 dB and good noise figure. The remaining gain modules have approximately 5.5 dB gain each to give an overall gain above 50 dB at 18 GHz. Since approximately 10 dB is lost in the limiter and temperature compensation module at room temperature, the nominal overall gain is near 40 dB.

Data on the completed amplifiers without cables is shown in Fig. 61 and Tables XXIX through XXXI. Figure 61 shows the swept frequency response of both amplifiers from 8 to 21 GHz. The gain curves are smooth without "bumps" or small ripples due to interconnections or transactions. Also, there was no tendency to oscillate above 20 GHz where the waveguide above the gain modules is no longer below cutoff. Both the figure and tables show a slightly sloped gain response to overcome the cable loss. Tables XXIX and XXX show very low VSWR's except where the output VSWR of serial No. 1 reaches 1.62 at 16.2 GHz. The phase difference (DP12) in Table XXXI shows that the phase of serial No. 1 is always several degrees greater than serial No. 2. This phase difference can be centered around zero degrees by making the cables to one amplifier slightly longer than the cables to the other amplifier.

Figure 62 shows the finished amplifier in the 2 x 2 x 11 chassis. Figure 62 shows the amplifier with the lid of the 2 x 2 x 11 chassis removed. The coaxial cables between the lid and the amplifier may be seen. The components of the power supply mounted on the printed-circuit board have been potted in Sylgard. The spark-gap, large resistor and other components to protect the power supply from high voltage power line transients can be seen. During assembly the amplifier heat sink shown in Fig. 63 is screwed to the 2 x 2 x 11 chassis. The remaining space within the 2 x 2 x 11 chassis is filled with a combination of foam and Sylgard. The lid is then screwed onto the chassis.

The following figures and tables show data on the completed 10.7 to 18 GHz amplifiers. The cables between the amplifier and the lid have been selected, installed, and the chassis potted. The units appear as in Fig. 62 .

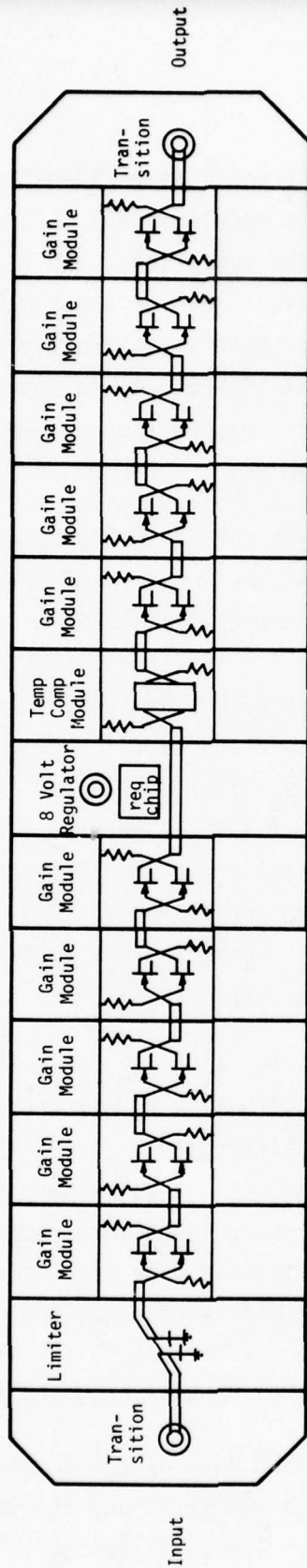


Figure 60
10.7 to 18 GHz Amplifier

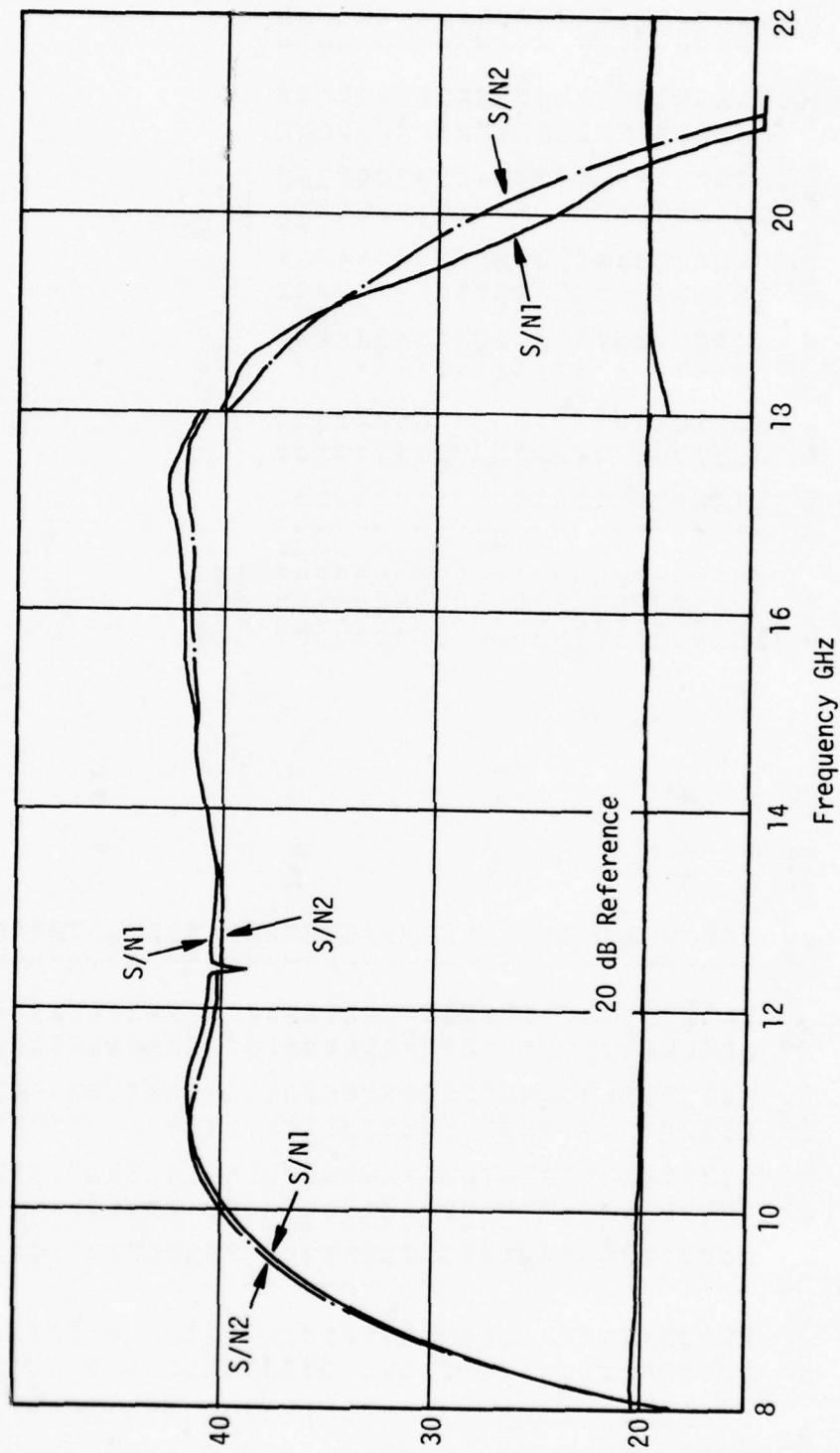


Figure 61
Swept Response of 10.7 to 18 GHz Amplifiers without Cables

TABLE XXIX

SEPT 29, 1977
10.7 TO 18 GHz AMPLIFIER
WITHOUT CABLES
S/N 1

FREQ MHZ	VSWR IN	GAIN DB	FLAT DB	PHASE DEG	PHASE DEV	ISOL DB	VSWR OUT	1DBPWR DBM	NOISE FIG	FREQ MHZ	VSWR IN	GAIN DB	FLAT DB	PHASE DEG	PHASE DEV	ISOL DB	VSWR OUT	1DBPWR DBM	NOISE FIG
10700.0	1.13	41.89	-31	-65.95	24.34	81.97	1.15	14.5	7.7	15600.0	1.26	41.96	-38	149.31	10.47	85.47	1.40		
10800.0	1.16	41.99	-41	-132.41	19.41	85.77	1.14			15700.0	1.24	42.04	-46	84.77	11.45	95.05	1.54		
10900.0	1.17	42.03	-45	163.12	16.48	84.19	1.12			15800.0	1.21	42.07	-49	22.23	10.45	81.20	1.39		
11000.0	1.18	42.01	-43	97.15	12.04	79.29	1.11	15.3	8.0	15900.0	1.15	41.93	-35	-38.37	11.38	83.49	1.51	14.8	8.2
11100.0	1.20	42.05	-47	30.50	6.92	93.73	1.10			16000.0	1.18	42.27	-69	-99.99	11.28	93.62	1.31		
11200.0	1.23	42.05	-47	-34.81	3.13	80.13	1.08			16100.0	1.13	42.28	-70	-162.82	9.98	84.27	1.43		
11300.0	1.23	41.93	-33	-98.74	7.73	79.67	1.08			16200.0	1.10	42.46	-88	136.02	10.35	91.30	1.62		
11400.0	1.24	41.91	-33	-162.70	-1.68	92.14	1.06			16300.0	1.10	42.42	-84	73.96	9.82	78.98	1.62		
11500.0	1.26	41.79	-21	133.83	-3.63	86.82	1.07			16400.0	1.09	42.50	-92	11.49	8.87	79.39	1.49		
11600.0	1.26	41.70	-12	68.47	-7.45	83.76	1.07			16500.0	1.15	42.66	-1.08	-51.06	7.85	84.39	1.42		
11700.0	1.25	41.57	00	5.94	-8.46	81.01	1.06			16600.0	1.08	42.56	-98	-113.41	7.02	86.65	1.42		
11800.0	1.25	41.56	01	-57.63	-10.50	79.03	1.05			16700.0	1.15	42.44	-86	-176.62	5.36	78.72	1.44		
11900.0	1.25	41.41	16	-120.35	-11.70	85.13	1.05	14.6	7.2	16800.0	1.12	42.53	-95	122.48	5.98	78.15	1.52		
12000.0	1.23	41.37	20	177.84	-11.98	80.50	1.05			16900.0	1.21	42.13	-55	58.37	3.39	81.11	1.45	15.0	7.9
12100.0	1.24	41.86	-28	117.25	-11.05	75.92	1.05			17000.0	1.16	42.38	-80	-5.48	1.06	72.05	1.37		
12200.0*	1.16	40.38	1.19	57.08	-9.70	72.60	1.03			17100.0	1.15	42.36	-78	-69.31	-1.23	76.24	1.41		
12300.0	1.20	40.97	60	-6.97	-12.22	78.10	1.05			17200.0	1.18	42.29	-71	-132.01	-2.40	76.15	1.39		
12400.0	1.17	40.67	90	-59.01	-12.72	86.73	1.08			17300.0	1.18	42.23	-65	164.63	-4.22	71.29	1.36		
12500.0	1.17	40.67	90	-130.31	-12.50	86.11	1.06			17400.0	1.17	42.49	-91	102.25	-5.08	85.93	1.54		
12600.0	1.13	40.49	1.08	169.53	-11.13	93.29	1.04			17500.0	1.17	42.12	-54	36.27	-9.53	72.26	1.33		
12700.0	1.07	40.53	1.04	107.28	-11.85	85.51	1.03			17600.0	1.18	41.82	-24	-26.38	-10.65	90.64	1.32		
12800.0	1.07	40.57	1.00	47.18	-10.42	85.07	1.03			17700.0	1.20	41.52	01	-91.39	-14.13	73.77	1.35		
12900.0	1.04	40.56	1.01	-13.93	-10.00	85.88	1.03			17800.0	1.17	41.52	05	-155.63	-16.85	77.39	1.31		
13000.0	1.04	40.66	91	-74.82	-9.36	91.07	1.01			17900.0	1.16	41.60	-02	139.81	-19.88	78.31	1.31		
13100.0	1.04	40.54	1.03	-134.02	-7.05	89.59	1.02			18000.0	1.17	41.34	23	72.62	-25.53	73.56	1.28	14.3	8.7
13200.0	1.05	40.53	1.04	164.40	-7.09	85.74	1.02			LINEAR- IZATION RANGE									
13300.0	1.10	40.65	92	103.61	-6.26	85.76	1.04			10700.0									
13400.0	1.13	40.64	93	43.59	-4.85	83.19	1.04			18000.0									
13500.0	1.15	40.74	83	-16.87	-3.78	83.80	1.08			TO									
13600.0	1.18	40.83	74	-77.14	-2.52	86.55	1.07			18000.0									
13700.0	1.21	40.72	85	-137.03	-8.88	79.30	1.09			10700.0									
13800.0	1.23	40.81	76	161.68	-6.65	82.64	1.10			TO									
13900.0	1.26	40.98	59	100.97	15	102.02	1.09			18000.0									
14000.0	1.28	40.99	58	40.86	1.58	85.79	1.12			* Bad Data									
14100.0	1.28	41.06	51	-20.21	2.04	88.19	1.12												
14200.0	1.30	41.08	49	-79.46	4.32	69.58	1.13												
14300.0	1.32	41.14	41	-141.94	3.37	87.66	1.13												
14400.0	1.32	41.31	26	156.48	3.32	94.39	1.15												
14500.0	1.34	41.36	21	97.42	5.78	83.03	1.17												
14600.0	1.35	41.42	15	35.75	9.64	84.62	1.20												
14700.0	1.35	41.49	08	-25.26	6.15	92.47	1.21												
14800.0	1.36	41.35	22	-85.34	7.61	87.38	1.24												
14900.0	1.36	41.61	-03	-146.62	7.86	89.57	1.24												
15000.0	1.35	41.76	-18	152.42	8.42	87.40	1.26												
15100.0	1.34	41.71	-13	90.47	7.99	93.17	1.28												
15200.0	1.35	41.77	-18	29.80	8.84	98.79	1.30												
15300.0	1.32	41.77	-19	-31.78	8.79	86.22	1.30												
15400.0	1.33	41.83	-25	-92.34	9.78	82.99	1.33												
15500.0	1.28	41.93	-35	-154.03	9.60	82.59	1.45												

TABLE XXX

SEPT 29, 1977
10.7 TO 18 GHz AMPLIFIER
WITHOUT CABLES
S/N 2

FREQ MHZ	VSWR IN	GAIN DB	FLAT DB	PHASE DEG	PHASE DEV	ISOL DB	VSWR OUT	1DBPWR DBM	NOISE FIG	FREQ MHZ	VSWR IN	GAIN DB	FLAT DB	PHASE DEG	PHASE DEV	ISOL DB	VSWR OUT	1DBPWR DBM	NOISE FIG	
10700.0	1.28	42.16	-59	-70.96	23.26	85.44	1.10	15.1	7.0	15700.0	1.21	41.84	-27	76.24	9.34	77.77	1.20			
10800.0	1.29	42.18	-61	-137.70	18.10	95.80	1.11			15800.0	1.19	41.77	-20	13.78	8.46	86.77	1.11			
10900.0	1.30	42.14	-57	157.55	14.93	84.08	1.11			15900.0	1.21	41.59	-02	-46.64	9.62	78.01	1.20	15.0	8.2	
11000.0	1.28	42.04	-47	91.59	10.54	77.98	1.12	15.8	7.4	16000.0	1.21	41.92	-35	-108.14	9.69	86.08	1.17			
11100.0	1.28	42.02	-45	24.92	5.46	93.32	1.12			16100.0	1.21	41.86	-29	-170.65	8.75	83.13	1.08			
11200.0	1.29	41.98	-41	-40.39	1.72	81.24	1.13			16200.0	1.22	42.02	-45	128.37	9.36	77.95	1.23			
11300.0	1.27	41.79	-22	-104.08	-39	86.00	1.12			16300.0	1.20	42.00	-43	67.17	9.73	79.58	1.17			
11400.0	1.27	41.73	-16	-167.87	-2.59	86.62	1.13			16400.0	1.20	42.09	-52	4.98	9.11	86.90	1.14			
11500.0	1.27	41.62	-05	128.87	-4.28	87.52	1.12			16500.0	1.17	42.30	-73	-57.18	8.53	78.55	1.09			
11600.0	1.26	41.51	05	63.75	-7.82	89.30	1.11			16600.0	1.24	42.21	-64	-119.19	8.11	76.86	1.02			
11700.0	1.24	41.38	18	1.38	-8.62	95.36	1.12			16700.0	1.21	42.18	-61	177.46	6.34	79.81	1.08			
11800.0	1.24	41.37	19	-62.12	-10.54	80.45	1.12			16800.0	1.18	42.38	-81	116.50	7.06	78.11	1.03			
11900.0	1.24	41.22	34	-124.75	-11.59	92.68	1.13	15.2	6.7	16900.0	1.30	42.01	-44	52.69	4.73	75.38	1.06	15.2	7.9	
12000.0	1.23	41.19	37	173.36	-11.90	79.04	1.13			17000.0	1.24	42.30	-73	-11.08	2.54	75.77	1.12			
12100.0	1.19	40.40	02	113.11	-10.58	78.97	1.13			17100.0	1.24	42.35	-78	-75.05	1.4	81.99	1.08			
12200.0	1.23	40.77	79	-11.09	-11.63	86.69	1.12			17200.0	1.24	42.31	-74	-137.45	-2.73	79.56	1.09			
12300.0	1.22	40.54	1.02	-72.12	-11.09	88.97	1.12			17300.0	1.28	42.30	-73	158.92	-2.73	78.77	1.11			
12400.0	1.24	40.53	1.03	-132.84	-10.23	93.21	1.11			17400.0	1.23	42.55	-98	96.47	-3.60	89.37	1.07			
12500.0	1.23	40.38	1.18	166.02	-9.79	97.50	1.11			17500.0	1.26	42.23	-66	30.30	-8.20	85.97	1.12			
12600.0	1.20	40.45	1.11	103.96	-10.26	102.94	1.11			17600.0	1.27	42.02	-45	-32.97	-9.89	83.06	1.14			
12700.0	1.22	40.47	1.09	44.17	-8.48	89.52	1.09			17700.0	1.27	41.72	-15	-98.64	-13.99	80.39	1.09			
12800.0	1.21	40.50	1.06	-17.05	-8.12	83.43	1.08	15.1	7.0	17800.0	1.25	41.61	-04	-163.46	-17.23	84.06	1.13			
12900.0	1.21	40.65	91	-77.72	-7.22	84.47	1.08			17900.0	1.23	41.65	-08	131.06	-21.13	74.04	1.09	14.6	8.4	
13000.0	1.21	40.57	99	-136.96	-4.88	94.70	1.09			18000.0	1.26	41.18	38	63.72	-26.89	82.89	1.09			
13100.0	1.20	40.62	94	161.43	-4.91	88.94	1.08			LINEAR- IZATION RANGE	10700.0 TO 18000.0									
13200.0	1.20	40.81	75	100.60	-4.16	80.73	1.07													
13300.0	1.18	40.85	71	40.50	-2.68	82.54	1.07													
13400.0	1.16	40.99	57	-20.33	-1.92	83.60	1.04													
13500.0	1.19	41.16	40	-80.86	-1.87	98.51	1.06													
13600.0	1.16	41.09	47	-141.16	39	83.89	1.05													
13700.0	1.15	41.22	34	157.33	45	83.18	1.05													
13800.0	1.14	41.42	14	96.52	1.23	94.30	1.05													
13900.0	1.12	41.40	16	35.99	2.25	87.48	1.04	15.1	6.9											
14000.0	1.11	41.46	10	-25.74	2.12	89.23	1.04													
14100.0	1.10	41.45	11	-85.21	4.22	94.07	1.03													
14200.0	1.09	41.51	05	-148.31	2.70	93.24	1.03													
14300.0	1.07	41.67	-10	149.77	2.36	89.38	1.03													
14400.0	1.08	41.68	-11	90.49	4.65	82.98	1.04													
14500.0	1.08	41.71	-14	28.49	4.23	82.19	1.06													
14600.0	1.08	41.70	-13	-32.54	4.77	87.44	1.06													
14700.0	1.09	41.55	01	-92.88	6.02	92.50	1.07													
14800.0	1.10	41.73	-16	-154.73	5.74	82.81	1.07													
14900.0	1.12	41.80	-23	144.45	6.50	85.73	1.08													
15000.0	1.12	41.69	-12	83.53	7.16	81.54	1.09													
15100.0	1.13	41.72	-19	22.13	7.33	85.89	1.08													
15200.0	1.13	41.69	-12	-39.14	7.64	77.99	1.08													
15300.0	1.15	41.67	-17	-100.85	7.51	79.79	1.08													
15400.0	1.19	41.83	-26	-162.72	7.22	86.62	1.10													
15500.0	1.19	41.83	-26	-162.72	7.22	86.62	1.10													
15600.0	1.20	41.77	-20	136.98	8.50	83.44	1.10													

* Bad Data

TABLE XXXI

SH
SEPT 29, 197710.7 TO 18 GHZ AMPLIFIER
NO CABLES

S21 IN DB

FREQ	S/N 1		DG12	DP12	S/N 2	
	GAIN	PHASE			GAIN	PHASE
10600.	41.91	.2	-.23	4.1	42.14	-3.9
10800.	42.15	-133.3	-.10	4.7	42.25	-138.0
11000.	42.18	95.8	.06	4.7	42.12	91.1
11200.	42.23	-35.8	.18	4.7	42.05	-40.5
11400.	42.05	-163.8	.29	4.4	41.76	-168.2
11600.	41.87	67.5	.31	3.8	41.57	63.7
11800.	41.70	-58.9	.30	3.6	41.40	-62.5
12000.	41.55	176.6	.28	3.6	41.27	173.0
12200.	40.60	56.0	.44	3.8	40.16	52.2
12400.	40.79	-69.1	.13	4.3	40.66	-73.4
12600.	40.63	168.5	.17	3.0	40.47	165.5
12800.	40.68	47.1	.12	3.6	40.55	43.5
13000.	40.74	-74.7	.05	3.4	40.69	-78.1
13200.	40.66	164.4	-.06	3.2	40.73	161.1
13400.	40.74	43.9	-.20	3.6	40.94	40.3
13600.	40.98	-77.2	-.31	4.2	41.29	-81.4
13800.	40.98	161.6	-.37	5.1	41.35	156.5
14000.	41.16	40.9	-.38	6.2	41.54	34.8
14200.	41.23	-79.5	-.35	7.0	41.58	-86.5
14400.	41.49	156.4	-.32	7.9	41.81	148.5
14600.	41.52	35.8	-.28	9.2	41.80	26.6
14800.	41.61	-85.2	-.15	10.4	41.76	-95.6
15000.	41.85	152.1	-.02	10.1	41.87	141.9
15200.	41.89	30.4	.06	10.2	41.83	20.3
15400.	41.93	-92.5	.11	9.5	41.82	-101.9
15600.	42.06	145.5	.21	9.1	41.85	136.4
15800.	42.21	22.1	.31	9.0	41.91	13.1
16000.	42.32	-99.8	.37	9.1	41.95	-108.9
16200.	42.56	135.7	.46	8.4	42.10	127.3
16400.	42.53	10.9	.38	7.0	42.15	3.9
16600.	42.69	-114.5	.35	6.4	42.33	-120.9
16800.	42.46	122.8	.19	6.6	42.27	116.2
17000.	42.34	-5.0	.08	6.5	42.25	-11.5
17200.	42.33	-131.7	-.01	6.3	42.33	-138.0
17400.	42.51	101.3	-.02	5.5	42.52	95.7
17600.	41.96	-27.1	-.15	7.5	42.11	-34.6
17800.	41.65	-155.2	-.06	8.5	41.71	-163.7
18000.	41.62	75.4	-.01	9.1	41.63	66.3

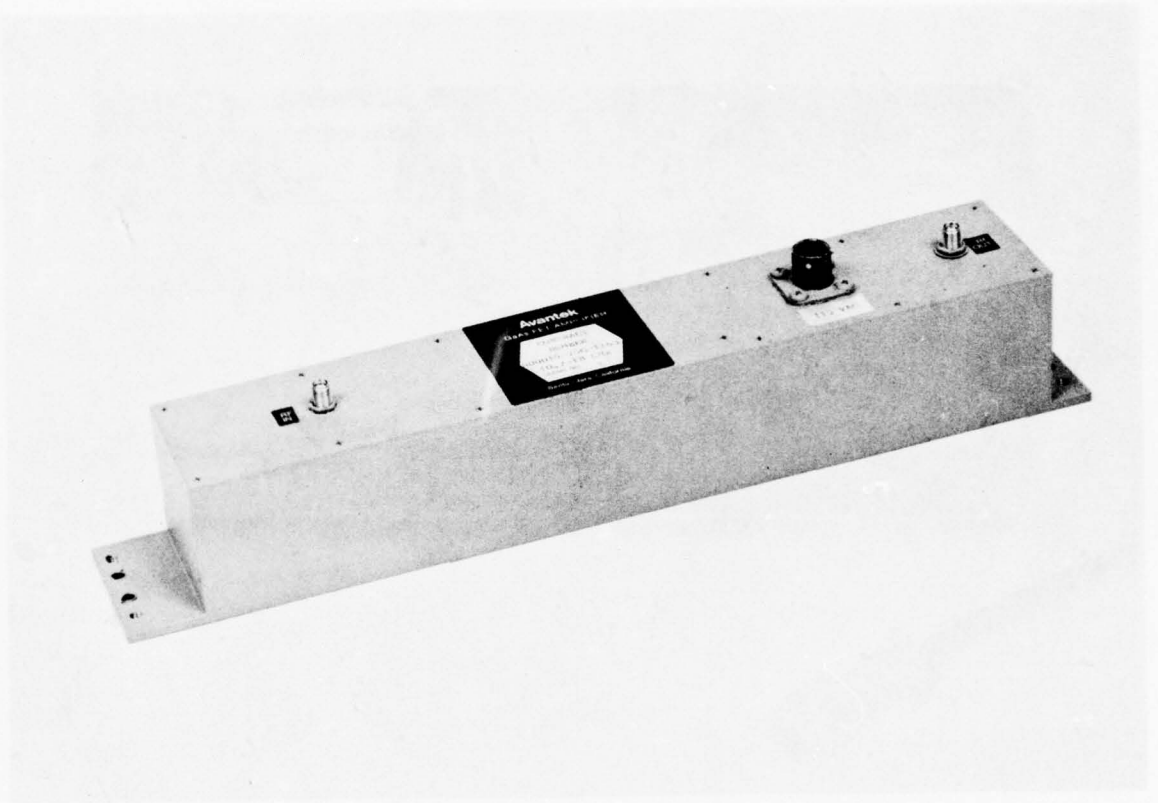


Figure 62
Complete 10.7 to 18 GHz Amplifier and Power Supply

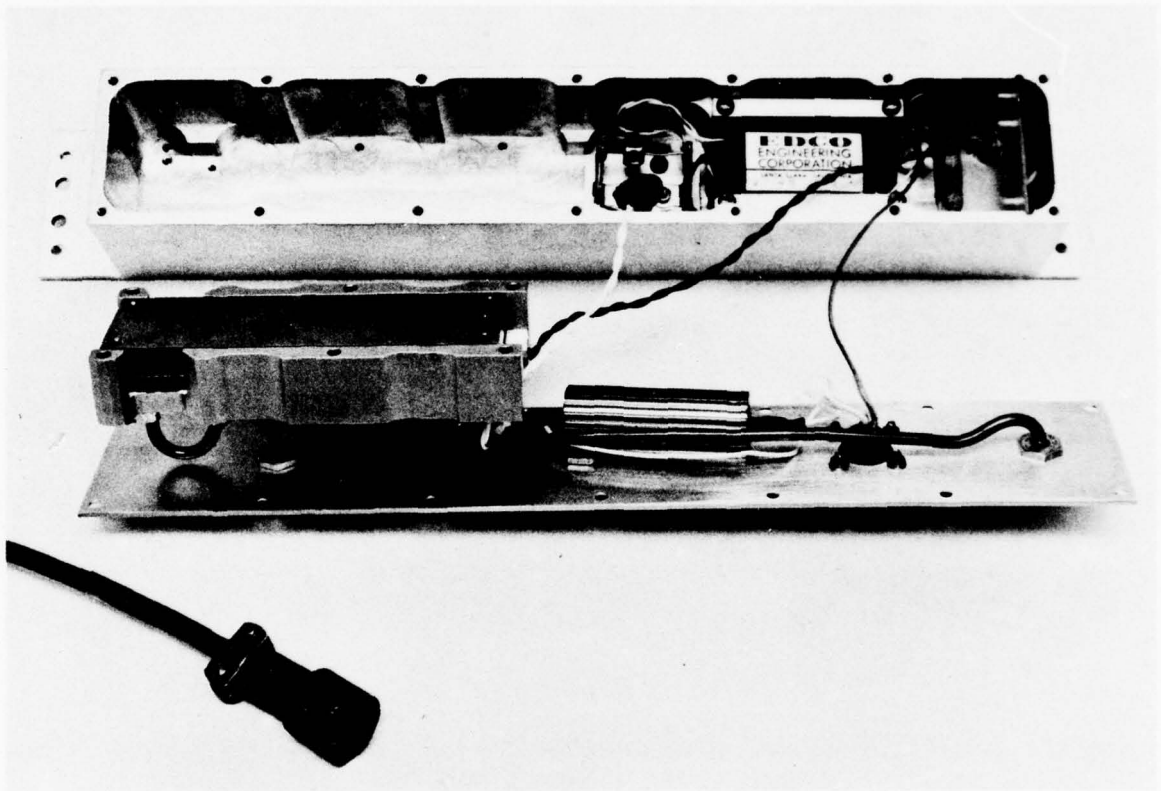


Figure 63
Exploded View of 10.7 to 18 GHz Amplifier and Power Supply

Final ANA data, noise figure, power output at 1 dB gain compression are shown in Tables XXXII and XXXIII and in the Temperature Test data in Appendix C. Tables XXXII and XXXIII show an ANA listing for every 100 MHz from 10.7 to 18 GHz, and is primarily presented to show the phase deviation from linear for the two amplifiers. Measured data compared to specification requirements are summarized in Table XXXIV. Most specification items are met such as gain, gain variation, and VSWR. The VSWR is higher with the cables as would be expected. The specifications which are not met are noise figure, gain variation over any 0.5 GHz band, phase variation from linear, phase matching between amplifier pairs, and safe input power. At operating temperatures from 0°C to 65°C the following comparison could be made of the out-of-specification items.

	<u>Specification</u>	<u>S/N 1</u>	<u>S/N 2</u>
Noise Figure	10 dB	10.4 dB	10.2 dB
Gain Variation over any .5 GHz band below 16.8 GHz	.5 dB	.84 dB	.72 dB
Phase Variation from Linear	±10°	±14°	±13°
Phase Matching	≤5°		≤8.2°

The out-of-specification items are seen to be close to the specification limits over the restricted temperature range. (In our proposal we said we expected the phase variation from linear to be less than 20° and phase matching less than 10°.)

TABLE XXXII

OCT 24, 1977
 10.7 TO 18 GHz AMPLIFIER
 FINAL DATA
 S/N 1

FREQ MHZ	VSWR IN	GAIN DB	FLAT DB	PHASE DEV	GPDEL NSEC	ISOL DB	VSWR OUT	NOISE FIG	1DBPWR DBM	FREQ MHZ	VSWR IN	GAIN DB	FLAT DB	PHASE DEV	GPDEL NSEC	ISOL DB	VSWR OUT	NOISE FIG	1DBPWR DBM
10700.0	1.26	41.15	-38	22.88	.00	99.10	1.12	7.2	14.6	15600.0	1.51	40.71	.05	12.97	2.88	79.19	1.62		
10800.0	1.36	41.23	-46	18.32	3.05	78.99	1.23			15700.0	1.45	41.37	-60	13.94	2.92	82.86	1.28		
10900.0	1.46	41.23	-46	14.20	3.03	74.94	1.24			15800.0	1.31	41.48	-71	13.73	2.95	77.61	1.22		
11000.0	1.45	41.38	-61	11.05	3.03	78.70	1.09			15900.0	1.18	41.42	-65	12.71	2.95	84.02	1.47		
11100.0	1.44	41.18	-41	6.95	3.05	84.16	1.08			16000.0	1.12	41.47	-70	12.06	2.95	81.35	1.53	8.1	14.9
11200.0	1.36	41.29	-52	2.72	3.02	78.31	1.14			16100.0	1.09	41.48	-71	11.43	2.94	78.75	1.51		
11300.0	1.23	41.22	-45	.32	3.01	88.75	1.20			16200.0	1.13	41.74	-97	11.59	2.95	102.14	1.28		
11400.0	1.10	41.17	-40	-2.77	3.00	82.89	1.26			16300.0	1.22	41.86	-1.09	10.02	2.97	82.18	1.03		
11500.0	1.05	41.20	-43	-4.86	3.00	85.44	1.16			16400.0	1.28	41.73	-96	8.73	2.96	80.10	1.10		
11600.0	1.19	41.04	-27	-7.84	2.99	85.30	1.02			16500.0	1.37	41.74	-97	7.82	2.97	84.83	1.17		
11700.0	1.32	40.92	-15	-9.45	2.99	80.24	1.11			16600.0	1.40	41.63	-86	6.10	2.97	87.77	1.12		
11800.0	1.41	40.75	.01	-11.76	2.95	79.33	1.17			16700.0	1.42	41.70	-93	4.89	2.98	81.73	1.10		
11900.0	1.42	40.60	.16	-10.99	2.94	83.41	1.29			16800.0	1.47	41.40	-63	2.77	2.94	82.90	1.30		
12000.0	1.39	40.44	.32	-12.70	2.93	80.14	1.29	7.7	15.0	16900.0	1.47	41.49	-72	4.00	2.93	78.17	1.54		
12100.0	1.30	40.43	.33	-11.14	2.83	81.24	1.12			17000.0	1.43	41.35	-58	2.91	2.97	80.03	1.50	8.2	14.8
12200.0	1.16	40.15	.61	-5.68	2.96	69.56	1.03			17100.0	1.45	41.80	-1.03	1.00	3.01	79.18	1.32		
12300.0	1.05	40.17	.59	-13.27	3.03	77.95	1.10			17200.0	1.37	41.57	-80	-2.66	3.02	82.93	1.27		
12400.0	1.07	40.01	.75	-13.10	2.91	88.79	1.26			17300.0	1.30	41.38	-61	-5.63	3.00	75.93	1.49		
12500.0	1.17	39.93	.83	-11.58	2.90	101.59	1.39			17400.0	1.19	40.89	-12	-7.91	2.97	83.44	1.71		
12600.0	1.24	39.87	.89	-10.90	2.91	91.40	1.29			17500.0	1.18	41.04	-27	-8.59	2.97	80.46	1.79		
12700.0	1.28	39.87	.89	-10.19	2.92	87.76	1.12			17600.0	1.20	40.92	-15	-10.52	3.03	69.84	1.61		
12800.0	1.23	39.83	.93	-10.09	2.91	101.54	1.02			17700.0	1.28	41.11	-34	-15.48	3.08	77.33	1.46		
12900.0	1.19	39.89	.87	-8.94	2.91	83.08	1.12			17800.0	1.32	40.58	.18	-21.01	3.05	77.29	1.40		
13000.0	1.18	39.78	.98	-8.68	2.91	88.95	1.30	7.3	14.8	17900.0	1.37	40.17	.59	-23.86	3.01	72.71	1.68	8.9	13.6
13100.0	1.19	39.89	.87	-7.68	2.90	78.80	1.33			18000.0	1.49	39.22	1.54	-26.52	.00	71.39	1.84		
13200.0	1.28	39.79	.97	-6.74	2.91	92.93	1.19			LINEAR- IZATION RANGE									
13300.0	1.35	39.95	.81	-5.88	2.91	86.59	1.15			10700.010700.0 TO TO 18000.018000.0									
13400.0	1.42	39.96	.60	-5.02	2.89	82.45	1.07												
13500.0	1.44	40.01	.75	-3.11	2.89	84.57	1.11												
13600.0	1.31	40.22	.84	-2.07	2.91	83.21	1.27												
13700.0	1.17	40.16	.60	.54	2.91	85.35	1.33												
13800.0	1.07	40.35	.41	.10	2.92	87.99	1.29												
13900.0	1.11	40.43	.33	1.49	2.92	94.22	1.13												
14000.0	1.24	40.48	.28	1.03	2.91	84.67	1.15												
14100.0	1.36	40.49	.27	3.08	2.92	85.88	1.28												
14200.0	1.46	40.29	.47	2.06	2.91	97.47	1.45												
14300.0	1.53	40.38	.38	4.53	2.89	85.62	1.55												
14400.0	1.53	40.40	.36	4.74	2.88	88.08	1.44												
14500.0	1.47	40.54	.22	7.85	2.90	88.15	1.23												
14600.0	1.37	40.78	-.01	7.20	2.93	85.17	1.27												
14700.0	1.24	40.74	.02	8.03	2.93	89.24	1.50												
14800.0	1.11	40.73	.03	7.25	2.93	91.06	1.77												
14900.0	1.04	40.81	-.04	8.39	2.90	93.51	1.78												
15000.0	1.19	40.87	-.10	9.64	2.91	88.00	1.51												
15100.0	1.44	40.95	-.18	9.36	2.93	92.60	1.33												
15200.0	1.53	40.78	-.01	9.11	2.92	84.25	1.71												
15300.0	1.55	40.67	.09	10.36	2.88	82.35	1.78												

Table XXXIV
Comparison of Specified and Measured Data

Frequency Range of Operation:	10.7 - 18 GHz
Input and Output Impedance	50 ohms
AC Coupling at Input and Output:	
Stability:	Amplifier did not oscillate with input and/or output open or short circuited

	<u>Specification</u>	<u>S/N 1</u>	<u>Measurement</u> <u>S/N 2</u>
Gain:	37 dB (min)	38.9 (min)	38.9 (min)
	43 dB (max)	41.6 (max) (0°C to 65°C)	41.4 (max)
Gain Variation	5 dB (max)	2.7 (max) (0°C to 65°C)	2.5 (max)
Noise Figure	10 dB (max)	10.4 (max)	10.2 (max)
Input VSWR	2.5:1 (max)	1.63:1 (max)	2.11:1 (max)
Output VSWR	2.5:1 (max)	1.88:1 (max)	1.47:1 (max)
Spurious Output at 1 dB Gain Com- pression Point:	40 dB below	≥40 dB	≥40 dB
Gain Variation Over any .5 GHz Band:	.5 dB	.84 dB (max)	.72 dB (max) These are maximum values for all frequencies below 16.8 GHz (0°C to 65°C)
Reverse Isolation:	50 dB (min)	>68 dB (min)	>66 dB (min)
Phase Variation from Linear:	±10° (max)	+13.9° -13.3° (max)	+11.1 -12.5 (max)
Phase Matching between Amplifier Pairs:	≤5°		≤8.2° (0° to 65°C)
Safe Input Power, CW RF:	+30 dBm (min)	+30 dBm	+30 dBm
10% Duty - Peak Pulse:	+50 dBm (min)	+50 dBm 1% Duty	+50 dBm 1% Duty

As was mentioned in Section III-C, the gain of M-107 gain modules fell off too rapidly above 17 GHz to meet the 0.5 dB/0.5 GHz specification. This gain variation can be seen in the data in Tables XXIX and XXX, which is much smoother than the Temperature Test data of Appendix C. This measurement is approaching the accuracy of our ANA.

Plots of gain vs. frequency of the amplifiers for various temperatures before and after welding the amplifier cases are shown in Figs. 64 and 65. Figure 64 shows the measured gain of the amplifiers before welding, plus the measured loss of the cables. Figure 63 is for the complete amplifiers after welding. The corresponding plots in Figs. 64 and 65 should be the same. However, welding caused both amplifiers, particularly serial No. 2, to show a reduction in gain between 11 and 14 GHz at -28°C . Although the reduction in gain is not sufficient to go below the 37 dB minimum gain requirement, the gain variation over any 0.5 GHz band and phase matching were adversely affected. In Fig. 65, it is seen that the gain of each amplifier tracks within about 1 dB from 0°C to $+65^{\circ}\text{C}$, so that gain variation over any 0.5 GHz band and phase matching remain nearly constant over this restricted temperature range. (A 6°C difference in temperature has been measured between the amplifier case and the 2 x 2 x 11 chassis. The curves in Fig. 65, therefore, represent chassis temperatures of -26°C , 24°C and 64°C .)

To facilitate delivery of the amplifiers, the gain dip at -28°C was not adjusted for since this would mean cutting open the amplifier welds.

Figure 66 shows plots of power output at 1 dB gain compression, saturated power output, and third order intercept point vs. frequency for each of the two amplifiers. For both amplifiers the 1 dB compression power is between +13.5 and +15.5 dBm; the saturated power is between +16 and +17 dBm; and the third order intercept point is between +23 and +27 dBm.

An outline drawing of the 2 x 2 x 11 chassis is shown in Fig. 67.

Many additional tests were performed on these 10.7 to 18 GHz amplifiers toward meeting the requirements of the "Statement of Work" of the contract. In

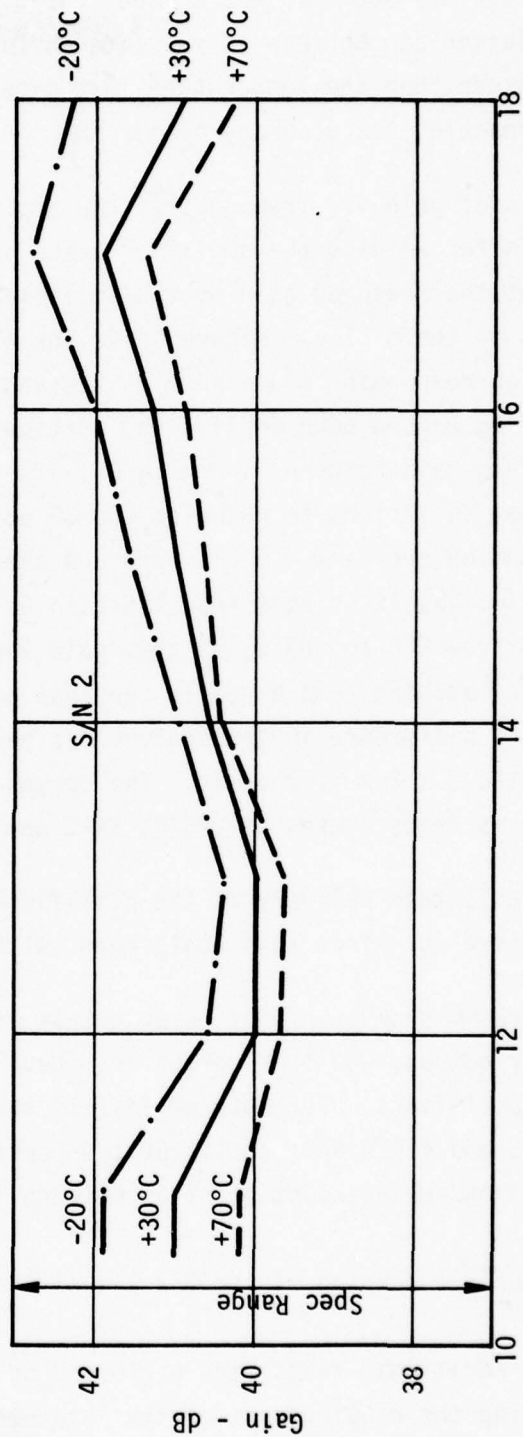
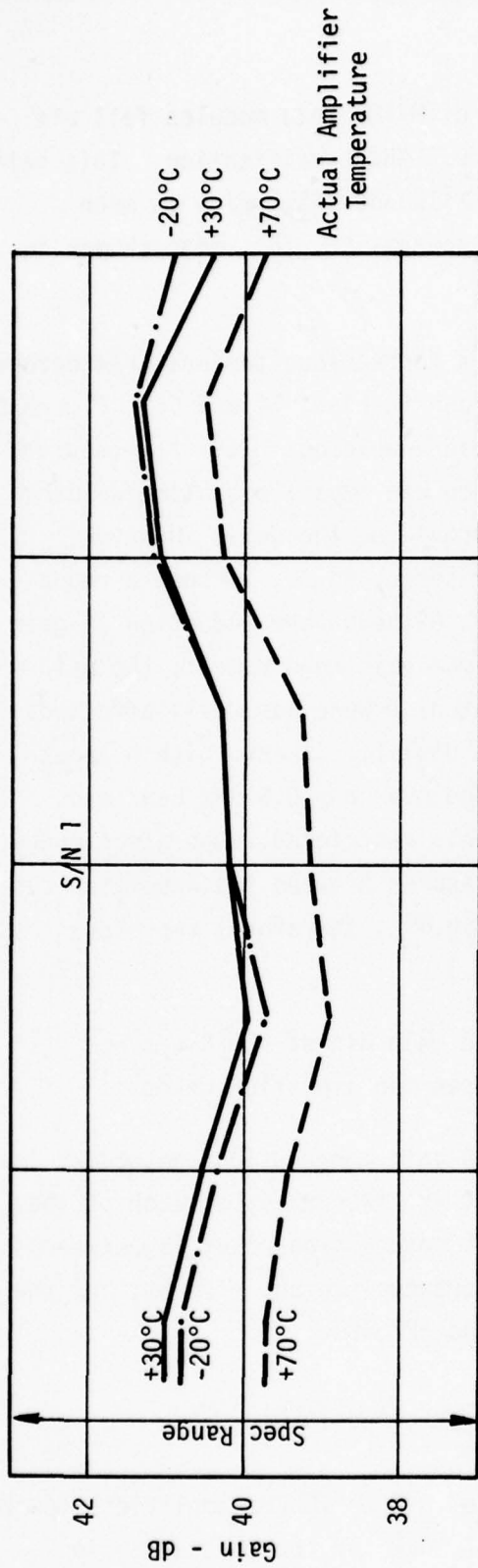


Figure 64
Gain vs. Temperature 10.7 to 18 Amplifiers Before Welding

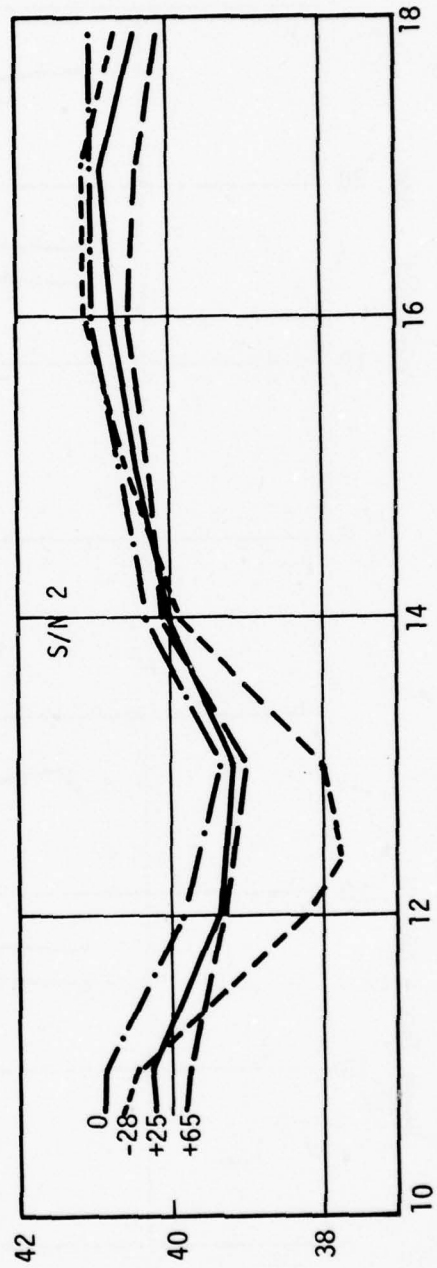
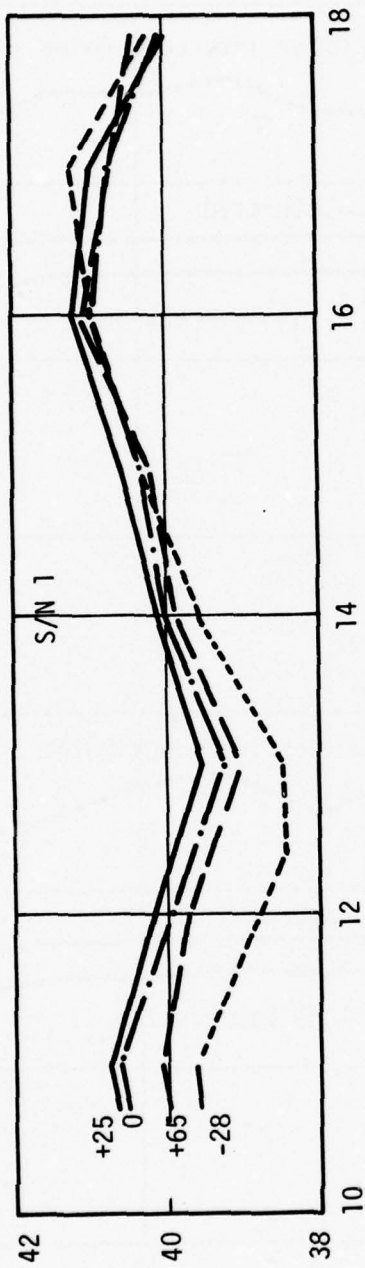


Figure 65
Gain vs. Temperature of Completed 10.7 to 18 GHz Amplifiers

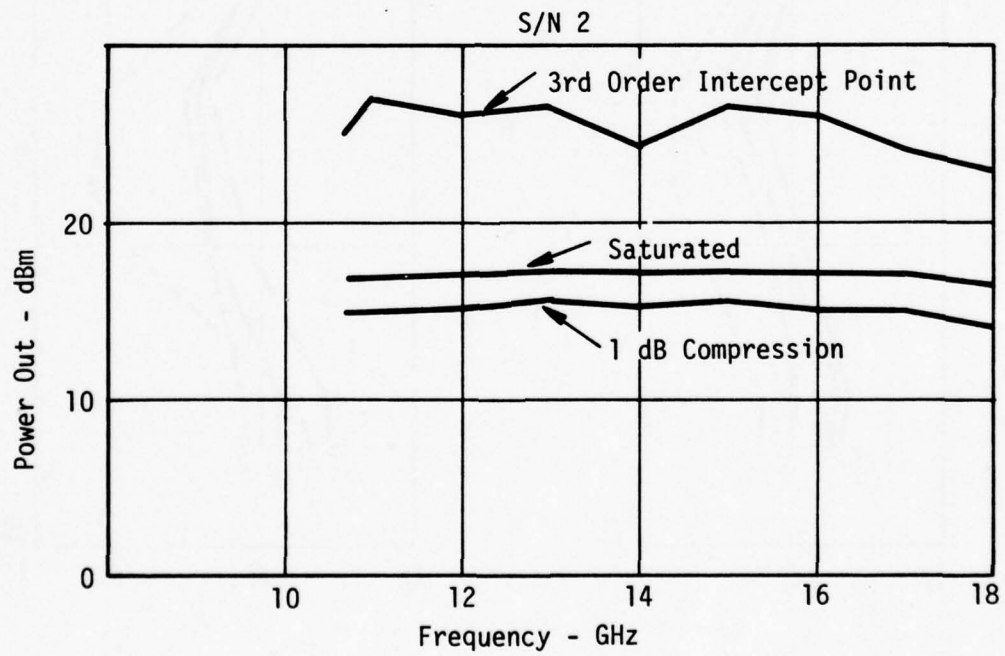
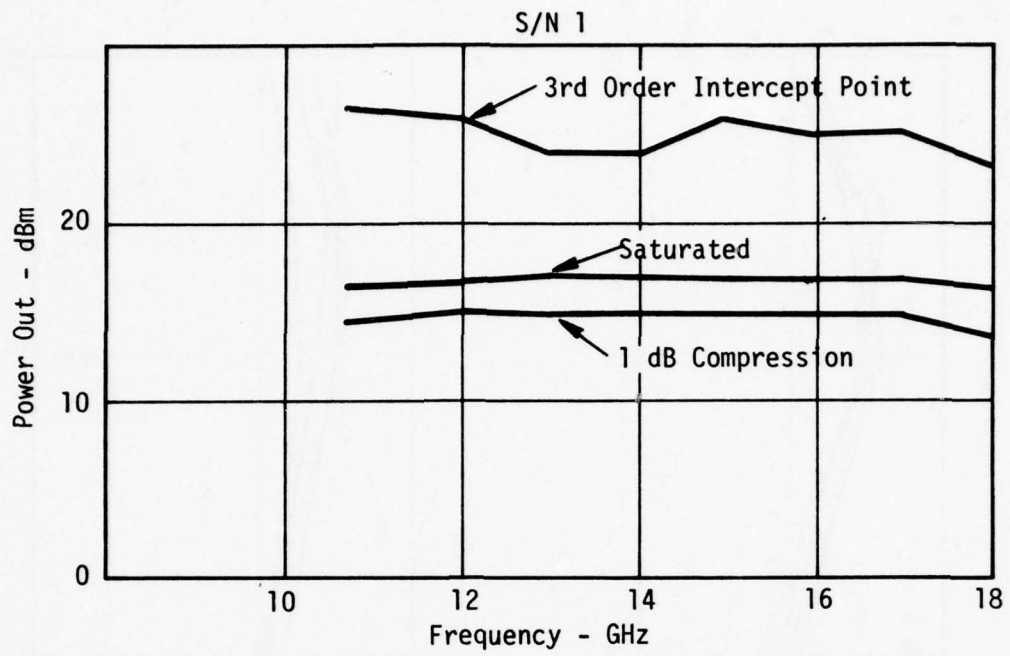
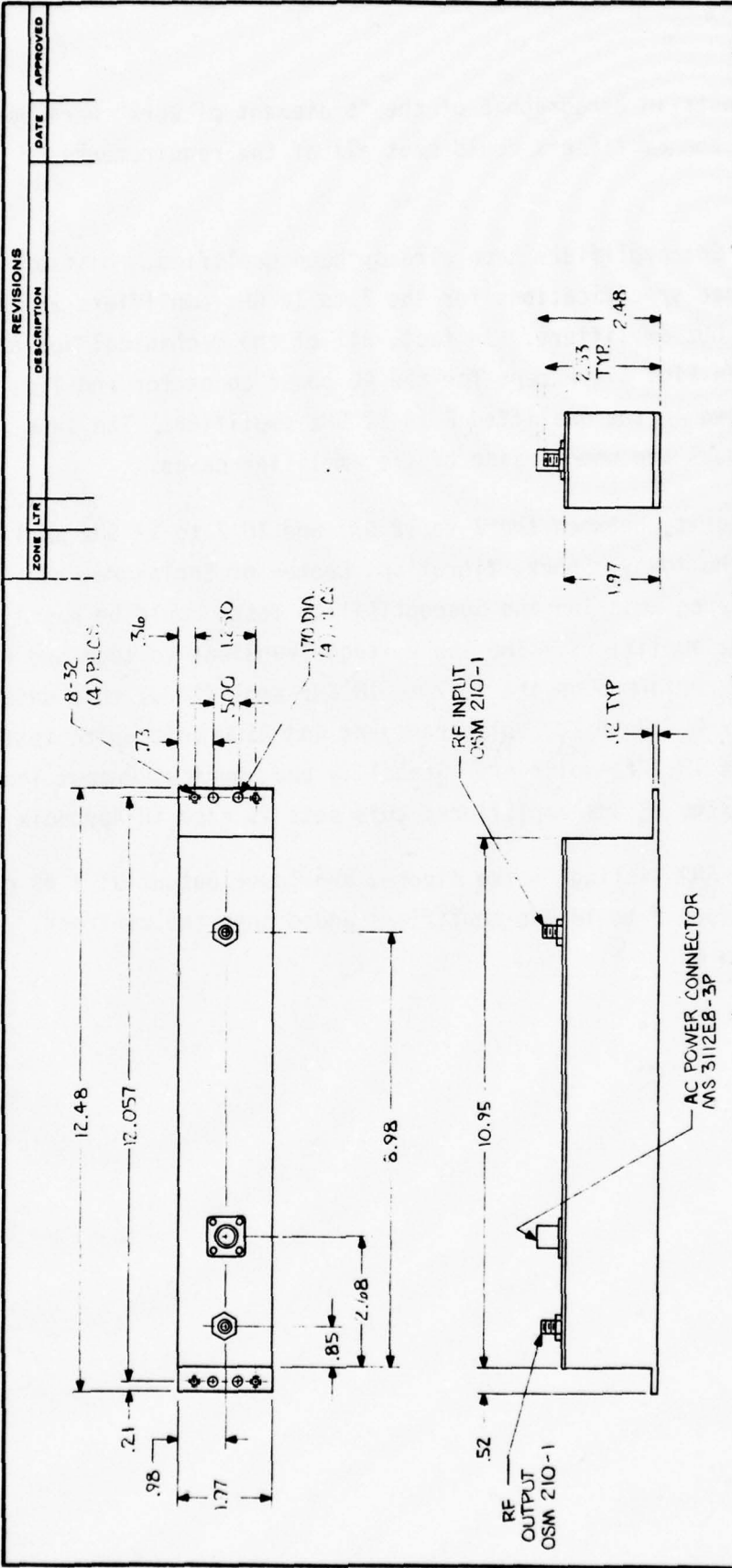


Figure 66
Power Output - 10.7 to 18 GHz Amplifiers



REVISIONS	ZONE	DATE	APPROVED

QTY REQD	NOMENCLATURE OR DESCRIPTION	CODE IDENT	IDENTIFYING NUMBER	SPECIFICATION	MATERIAL OR NOTE	ITEM NO.

LIST OF MATERIALS			APPROVALS	SIGNATURE AND DATE
DESIGNER				7-13-72
CHECKED				
REWORK ENG				
BY				

UNLESS OTHERWISE SPECIFIED	UNLESS OTHERWISE SPECIFIED
DIMENSIONS ARE IN INCHES	DIMENSIONS ARE IN INCHES
FRACTIONS ARE 1/32 INCHES	FRACTIONS ARE 1/32 INCHES
DECIMALS ARE TO .010	DECIMALS ARE TO .010
ALL SURFACES UNLESS NOTED	ALL SURFACES UNLESS NOTED
MATERIAL	MATERIAL

CODE IDENT	DESCRIPTION	SCALE

Avantek	Santa Clara, California
OUTLINE DRAWING, MICROWAVE AMPLIFIER WITH INTEGRAL POWER SUPPLY	
CODE IDENT NO.	
SIZE	
B	24539
SCALE	1/2
WEIGHT	
SHEET	
REV	

Figure 67 -149-

particular, those tests in Paragraph 6 of the "Statement of Work" were performed to show that the amplifiers could meet all of the requirements of MIL-E-16400.

The Avantek 7 to 12 GHz amplifiers have already been qualified. Most of the electrical performance specifications for the 7 to 12 GHz amplifiers are met by these 10.7 to 18 GHz amplifiers. In fact, all of the mechanical and electrical parts shown in Fig. 61, except for the AC power connector and lid, are common with those used in the qualified 7 to 12 GHz amplifier. The same construction techniques are used inside of the amplifier cases.

Because of the similarity between the 7 to 12 GHz and 10.7 to 18 GHz amplifiers, it is felt that the Humidity, Shock, Vibration, Degree of Enclosure, and Electromagnetic Interference Emission and Susceptibility Tests could be easily met by the 10.7 to 18 GHz amplifiers. The low voltage Transient Voltage and Power Interrupt Tests were performed on the 10.7 to 18 GHz amplifiers; this data is contained in Appendix D. Both 700 Volt Transient and 2500 Volt Spike Tests were made on the 7 to 12 GHz amplifier. Stability and Spurious Output Tests were made on the 10.7 to 18 GHz amplifiers; this data is also in Appendix D.

Appendix B gives the PVA listing, noise figure, and power output at 1 dB gain compression for the four 7 to 18 GHz amplifiers added onto the contract. These are serial Nos. 37 to 40.

V. CONTRACT CHANGE

Near the end of the contract it became apparent that it would be of mutual advantage to the Navy and Avantek if the due date for the final amplifier could be extended. At that time Avantek efforts to build implanted FETs with very low noise figure were beginning to show definite signs of success. If the delivery were delayed, it would mean that the amplifier performance would be substantially improved. For example, the noise figure would be about 2 dB lower. A request for a no-cost extension was, therefore, forwarded to the appropriate Navy Office. A Contract Modification (#P00004) was granted on August 26, which allowed extended delays on the amplifiers and final report. Avantek continued to deliver additional monthly progress letters at no cost until the amplifiers were delivered.

VI. MEETINGS

A. July 27, 1976, at Avantek

Attended by Eliot Cohen, NRL, and other Navy personnel. Presentation by Avantek device and amplifier personnel.

B. October 19, 1976, at NRL

Attended by NRL, Navelex, and other personnel. Presentation by Hejmanowski, Hooper, and Policky of Avantek.

C. April 19, 1977, NRL

Attended by:

NRL - 13 people

Navy Electronics System Command - 1 person

Navair - 1 person

Avantek - 4 people

ECOM - 1 person

This was the final review.

Several informal reviews were held with Mr. Eliot Cohen at Avantek while he was present in the Bay Area.

VIII. REFERENCES

- [1] B.S. Hewitt, et al, "Low Noise GaAs MESFETs," Electronics Letters, Vol. 12, No. 12, June 10, 1976, pps. 309-310.
- [2] AvanteK, Reports Prepared for U.S. Army, ECOM, Ft. Monmouth, N.J., Nos. ECOM-76-C-1340-I and ECOM-76-C-1340-F.
- [3] R. Pucel, C. Krum, "Simple Method for Measuring Drift Mobility Profiles in Thin Semiconducting Films," Electr. Ltrts., Vol. 12, No. 10, May 1976.
- [4] H.F. Cooke and J.F. Gibbons, "Gate Design for Microwave FETs," WOCSEMMAD, Feb. 25, 1977, New Orleans, La.
- [5] A.R. Reinberg, "Radial Flow Reactor," U.S. Pat. No. 3,757,733, Sept. 11, 1973.
- [6] A. Lidow, J. Gibbons, T. Magee, and J. Peng, "Multilayer Encapsulant of GaAs and Compound Semiconductors," J.A.P. (to be published).
- [7] A. Lidow and J. Gibbons, "A Double-Layered Encapsulant for Annealing Ion-Implanted GaAs up to 1100°C," App. Physics Letter 31, No. 3, 1 Aug 1977.
- [8] K. Ohata, et al, "Improved Noise Performance of GaAs MESFETs with Selectively Ion-Implanted Source Regions," IEEE Trans. Elec. Dev., ED-24, 8 Aug 1977.
- [9] B.L. Mattes, et al, "Growth and Properties of Semi-insulating Epitaxial GaAs," J. Vac. Sci Technol., 12, 4 July/Aug 1975.
- [10] J. Lange, "Interdigitated Stripline Quadrature Hybrid," IEEE Trans. on MTT, Vol. MTT17, pp. 1150-1151, Dec. 1969.
- [11] R.M. Fano, "Theoretical Limitations on Broadband Matching of Arbitrary Impedances," Journal Franklin Institute, Jan & Feb 1950.
- [12] S. Plotkin and N.E. Nahi, "On Limitations of Broadband Impedance Matching without Transformers," IRE Transactions on Circuit Theory, pp. 125-132, June 1962.
- [13] Matthaei, Young, and Jones, "Microwave Filters, Impedance-Matching Networks and Coupling Structures," McGraw-Hill 1964.
- [14] D.J. Mellor, "Computer-aided Synthesis of Matching Networks for Microwave Amplifiers," PhD Thesis, Stanford University, 1975.
- [15] K. Kurokawa, "Design Theory of Balanced Transistor Amplifiers," B.S.T.J. Oct 1965.

APPENDIX A

Temperature Measurements on 7 to 18 GHz Amplifiers

MEASUREMENTS AT 30°C

NOV 22, 1977

7 TO 18 GHZ AMPLIFIER
TEMPERATURE TEST
S/N 01

NOV 22, 1977

7 TO 18 GHZ AMPLIFIER
TEMPERATURE TEST
S/N 02

FREQ MHZ	VSWR IN	GAIN DB	FLAT DB	PHASE DEG	ISOL DB	VSWR OUT	10BPMR DBM	NOISE FIG	FREQ MHZ	VSWR IN	GAIN DB	FLAT DB	PHASE DEG	ISOL DB	VSWR OUT	10BPMR DBM	NOISE FIG	FREQ MHZ	VSWR OUT	ISOL DB	PHASE DEG	FLAT DB	GAIN DB	NOISE FIG	10BPMR DBM	VSWR OUT	MATCH DG12 DP12
7000.0	1.52	28.13	1.79	-66.78	81.61	1.06	13.0	6.9	7000.0	1.47	28.66	1.19	-63.08	85.11	1.04	12.5	6.6	7000.0									
7333.3	1.53	28.79	1.13	136.63	86.25	1.03			7333.3	1.40	29.10	.76	139.39	102.20	1.19			7333.3									
7666.7	1.45	29.18	.75	-14.54	78.00	1.00			7666.7	1.30	29.09	.41	-159.03	93.28	1.55			7666.7									
8000.0	1.36	29.56	.37	-162.62	79.02	1.03	14.2	6.4	8000.0	1.23	29.45	.33	58.51	98.92	1.65	13.0	6.1	8000.0									
8333.3	1.27	29.72	.20	55.29	88.16	1.04			8333.3	1.19	29.52	.02	-81.41	90.86	1.71			8333.3									
8666.7	1.24	30.17	-.24	-87.11	86.25	1.02			8666.7	1.17	29.83	.02	138.30	89.24	1.67			8666.7									
9000.0	1.25	30.46	-.53	134.29	100.29	1.02			9000.0	1.21	30.25	-.39	138.30	89.24	1.67			9000.0									
9333.3	1.29	30.67	-.74	-4.98	84.82	1.04			9333.3	1.22	30.49	-.63	1.55	85.62	1.55			9333.3									
9666.7	1.34	30.80	-.87	-140.95	84.43	1.09			9666.7	1.23	30.82	-.96	-134.22	85.29	1.40			9666.7									
10000.0	1.36	30.85	-.92	82.79	85.96	1.14	15.0	6.8	10000.0	1.21	30.81	-.95	88.94	91.94	1.26			10000.0									
10333.3	1.32	30.82	-.89	-52.04	84.87	1.20			10333.3	1.15	30.85	-.99	-44.59	85.12	1.17			10333.3									
10666.7	1.22	30.58	-.64	174.96	81.19	1.26			10666.7	1.06	30.85	-.99	-177.64	83.06	1.12			10666.7									
11000.0	1.15	30.55	-.61	42.59	84.86	1.36			11000.0	1.11	30.62	-.76	50.03	97.88	1.09			11000.0									
11333.3	1.26	30.05	-.12	-87.89	91.76	1.46			11333.3	1.27	30.34	-.48	-80.84	97.80	1.06			11333.3									
11666.7	1.36	29.64	-.29	143.34	76.94	1.58			11666.7	1.38	30.02	-.16	150.73	80.61	1.02			11666.7									
12000.0	1.39	29.36	-.56	15.98	88.82	1.66			12000.0	1.42	29.91	-.05	22.47	80.30	1.04			12000.0									
12666.7	1.20	29.60	-.32	124.50	100.83	1.55			12666.7	1.26	29.87	-.01	124.82	85.25	1.10			12666.7									
13000.0	1.10	29.93	.00	-4.03	84.85	1.49	15.2	7.3	13000.0	1.15	29.99	-.12	-3.83	86.07	1.13			13000.0									
13333.3	1.10	30.19	-.26	-135.15	87.89	1.40			13333.3	1.07	29.71	-.14	-133.74	87.55	1.15			13333.3									
13666.7	1.18	30.69	-.76	96.53	85.48	1.32			13666.7	1.07	29.76	.09	97.63	84.61	1.21			13666.7									
14000.0	1.24	30.41	-.48	-33.31	84.49	1.21			14000.0	1.11	29.44	.41	-27.98	85.12	1.27			14000.0									
14333.3	1.24	30.19	-.25	-166.49	92.83	1.10			14333.3	1.13	29.03	.82	-155.36	85.42	1.36			14333.3									
14666.7	1.21	30.19	-.26	66.95	94.55	1.03			14666.7	1.13	29.61	.24	75.25	87.06	1.51			14666.7									
15000.0	1.15	29.93	.00	-65.18	84.58	1.13			15000.0	1.10	30.10	-.24	-51.66	87.59	1.67			15000.0									
15333.3	1.07	29.99	-.06	164.68	89.24	1.21			15333.3	1.09	30.03	-.17	-179.34	84.95	1.76			15333.3									
15666.7	1.02	29.94	.00	36.14	87.54	1.22			15666.7	1.12	29.62	.24	45.04	81.11	1.67			15666.7									
16000.0	1.03	29.75	.17	-95.88	81.05	1.26			16000.0	1.17	30.17	-.31	-86.31	76.95	1.35			16000.0									
16333.3	1.03	29.59	.23	130.49	86.81	1.27			16333.3	1.21	30.06	-.19	141.19	89.52	1.26			16333.3									
16666.7	1.06	29.74	.19	-5.03	84.14	1.26			16666.7	1.18	29.52	.33	7.07	70.56	1.54			16666.7									
17000.0	1.09	29.69	.23	-137.60	81.34	1.22			17000.0	1.15	29.67	.18	-127.92	80.54	1.88			17000.0									
17333.3	1.12	29.87	.05	86.10	76.56	1.19			17333.3	1.11	30.35	-.49	94.08	73.94	2.03			17333.3									
17666.7	1.12	29.64	.28	-55.14	85.83	1.14			17666.7	1.12	29.08	.77	-45.22	75.37	2.49			17666.7									
18000.0	1.13	28.87	1.05	160.97	75.39	1.07	15.7	8.4	18000.0	1.21	28.65	1.21	-178.38	71.43	3.55			18000.0									
LINEAR-IZATION RANGE																											
7000.0 TO 18000.0																											

* Bad Data

MEASUREMENTS AT -28°C

NOV 22, 1977

7 TO 18 GHZ AMPLIFIER
TEMPERATURE TEST
S/N 01

FREQ MHZ	VSMR IN	GAIN DB	FLAT DB	PHASE DEG	ISOL DB	VSMR OUT	1DBPWR DBM	NOISE FIG	FREQ MHZ	VSMR IN	GAIN DB	FLAT DB	PHASE DEG	ISOL DB	VSMR OUT	1DBPWR DBM	NOISE FIG	FREQ MHZ	VSMR OUT	ISOL DB	PHASE DEG	FLAT DB	GAIN DB	S/N	TEMPERATURE TEST	MATCH GAIN DG12	PHASE DP12
7000.0	1.54	33.28	.92	-50.07	84.42	1.03	13.6	5.4	7000.0	1.53	34.03	.25	-46.71	96.05	1.08	13.2	5.7	7000.0	1.08	96.05	25	34.03	75	-3.4			
7333.3	1.55	33.92	.28	153.50	83.87	1.03			7333.3	1.46	34.44	-.15	155.71	98.15	1.21			7333.3	1.21	98.15	-.15	155.71	15	-2.2			
7666.7	1.46	34.23	-.02	2.38	79.92	1.01			7666.7	1.33	34.37	-.09	4.73	80.47	1.36			7666.7	1.36	80.47	-.09	4.73	15	-2.3			
8000.0	1.36	34.49	-.28	-145.20	80.44	1.01	14.4	5.1	8000.0	1.22	34.64	-.36	-142.14	85.23	1.50	12.6	4.8	8000.0	1.50	85.23	-.36	-142.14	15	-3.1			
8333.3	1.27	34.57	-.36	73.45	88.27	1.02			8333.3	1.16	34.61	-.32	75.89	86.60	1.56			8333.3	1.56	86.60	-.32	75.89	15	-2.2			
8666.7	1.24	34.91	-.70	-68.71	86.69	1.01			8666.7	1.14	34.83	-.54	-64.25	94.03	1.60			8666.7	1.60	94.03	-.54	-64.25	15	-2.2			
9000.0	1.25	35.11	-.90	153.77	91.25	1.02			9000.0	1.15	35.18	-.89	156.35	91.53	1.57			9000.0	1.57	91.53	-.89	156.35	15	-2.6			
9333.3	1.28	35.29	-1.08	14.92	82.16	1.05			9333.3	1.16	35.37	-1.09	19.82	85.20	1.48			9333.3	1.48	85.20	-1.09	19.82	15	-4.9			
9666.7	1.33	35.35	-1.14	-120.74	85.92	1.09			9666.7	1.16	35.63	-1.35	-115.86	87.49	1.37			9666.7	1.37	87.49	-1.35	-115.86	15	-4.1			
10000.0	1.36	35.32	-1.11	103.40	82.77	1.14	15.0	5.6	10000.0	1.15	35.53	-1.24	107.50	96.41	1.26	13.7	5.1	10000.0	1.26	96.41	-1.24	107.50	15	-4.1			
10333.3	1.32	35.11	-.90	-30.05	86.78	1.20			10333.3	1.10	35.42	-1.13	-24.66	86.26	1.19			10333.3	1.19	86.26	-1.13	-24.66	15	-5.4			
10666.7	1.22	34.96	-.75	-162.00	81.37	1.26			10666.7	1.03	35.50	-1.21	-156.85	86.83	1.14			10666.7	1.14	86.83	-1.21	-156.85	15	-5.2			
11000.0	1.15	34.85	-.64	66.24	91.37	1.34			11000.0	1.11	35.24	-.95	72.06	85.28	1.12			11000.0	1.12	85.28	-.95	72.06	15	-5.8			
11333.3	1.27	34.40	-.19	-63.37	103.70	1.44			11333.3	1.25	34.97	-.68	-58.41	85.74	1.11			11333.3	1.11	85.74	-.68	-58.41	15	-5.0			
11666.7	1.41	33.94	-.26	168.23	80.44	1.55			11666.7	1.37	34.64	-.35	173.83	82.77	1.10			11666.7	1.10	82.77	-.35	173.83	15	-5.6			
12000.0	1.45	33.53	-.67	41.64	82.20	1.64			12000.0	1.42	34.45	-.16	46.65	85.24	1.09			12000.0	1.09	85.24	-.16	46.65	15	-5.0			
12666.7	1.28	33.79	-.41	152.58	99.12	1.55			12666.7	1.35	34.39	-.10	147.13	86.30	1.05	14.0	5.6	12666.7	1.05	86.30	-.10	147.13	15	-5.5			
13000.0	1.16	34.08	-.13	24.84	84.28	1.50	14.6	6.0	13000.0	1.27	34.64	-.35	19.71	79.79	1.01			13000.0	1.01	79.79	-.35	19.71	15	-5.1			
13333.3	1.12	34.33	-.12	-104.57	80.13	1.41			13333.3	1.18	34.34	-.09	-107.70	82.23	1.13			13333.3	1.13	82.23	-.09	-107.70	15	-5.0			
13666.7	1.17	34.91	-.70	126.46	80.30	1.35			13666.7	1.10	34.29	-.01	122.08	87.76	1.24			13666.7	1.24	87.76	-.01	122.08	15	-4.4			
14000.0	1.22	34.56	-.35	-2.77	85.16	1.26			14000.0	1.03	33.97	-.34	-3.83	85.38	1.33			14000.0	1.33	85.38	-.34	-3.83	15	-4.4			
14333.3	1.23	34.23	-.02	-134.13	81.66	1.15			14333.3	1.03	33.37	-.90	-129.25	96.17	1.42			14333.3	1.42	96.17	-.90	-129.25	15	-4.1			
14666.7	1.21	34.29	-.08	99.72	97.26	1.05			14666.7	1.07	33.60	-.68	99.22	95.12	1.54			14666.7	1.54	95.12	-.68	99.22	15	-4.9			
15000.0	1.15	33.99	-.21	-31.25	84.01	1.09			15000.0	1.14	34.06	-.22	-27.20	85.31	1.70			15000.0	1.70	85.31	-.22	-27.20	15	-4.0			
15333.3	1.07	33.95	-.23	-160.93	95.83	1.16			15333.3	1.20	33.92	-.36	-152.64	89.12	1.79			15333.3	1.79	89.12	-.36	-152.64	15	-8.3			
15666.7	1.03	33.89	-.31	71.49	85.55	1.17			15666.7	1.26	33.40	-.87	74.51	90.52	1.69			15666.7	1.69	90.52	-.87	74.51	15	-3.0			
16000.0	1.04	33.60	-.60	-59.60	85.84	1.24			16000.0	1.31	33.95	-.33	-54.55	79.09	1.38			16000.0	1.38	79.09	-.33	-54.55	15	-5.1			
16333.3	1.03	33.46	-.74	169.06	85.84	1.24			16333.3	1.33	33.84	-.43	175.81	81.22	1.31			16333.3	1.31	81.22	-.43	175.81	15	-6.8			
16666.7	1.04	33.32	-.89	34.97	79.31	1.23			16666.7	1.28	33.04	1.24	43.80	78.12	1.59			16666.7	1.59	78.12	1.24	43.80	15	-8.8			
17000.0	1.08	33.30	-.90	-94.83	71.96	1.24			17000.0	1.21	33.04	1.24	-89.08	82.60	1.99			17000.0	1.99	82.60	1.24	-89.08	15	-5.7			
17333.3	1.11	33.57	-.63	131.10	74.70	1.21			17333.3	1.09	33.93	-.35	133.57	81.90	2.24			17333.3	2.24	81.90	-.35	133.57	15	-2.5			
17666.7	1.12	33.41	-.79	-8.17	75.97	1.15			17666.7	1.07	32.59	1.68	-5.41	73.94	2.05			17666.7	2.05	73.94	1.68	-5.41	15	-2.8			
18000.0	1.12	32.84	1.36	-148.77	71.87	1.08	15.8	6.8	18000.0	1.17	32.09	2.19	-137.16	64.17	3.02			18000.0	3.02	64.17	2.19	-137.16	15	-12.0			

LINEARIZATION RANGE 7000.0 TO 18000.0

* Bad Data

MEASUREMENTS AT +50°C

NOV 22, 1977 7 TO 18 GHZ AMPLIFIER
TEMPERATURE TEST
S/N 01

NOV 22, 1977 7 TO 18 GHZ AMPLIFIER
TEMPERATURE TEST
S/N 02

7 TO 18 GHZ AMPLIFIER TEMPERATURE TEST S/N 01		7 TO 18 GHZ AMPLIFIER TEMPERATURE TEST S/N 02																					
FREQ MHZ	VSMR IN	GAIN DB	FLAT DB	PHASE DEG	ISOL DB	VSMR OUT	IDBPMR DBM	NOISE FIG	FREQ MHZ	VSMR IN	GAIN DB	FLAT DB	PHASE DEG	ISOL DB	VSMR OUT	IDBPMR DBM	NOISE FIG	FREQ MHZ	VSMR OUT	IDBPMR DBM	NOISE FIG	MATCH GAIN DG12 DP12	PHASE
7000.0	1.52	26.22	2.10	-71.78	94.96	1.07	12.8	9.1	7000.0	1.52	26.56	1.73	-67.41	93.52	1.07	12.1	7.1	7000.0				-34	-4.4
7333.3	1.54	26.89	1.43	131.66	82.05	1.04			7333.3	1.47	27.04	1.25	135.26	86.42	1.21			7333.3				-15	-3.6
8000.0	1.38	27.28	1.04	-19.55	80.35	1.01			8000.0	1.35	27.09	1.20	-15.84	84.04	1.36			8000.0				-20	-3.7
8333.3	1.30	27.70		62-167.63	83.35	1.02	13.8	6.7	8333.3	1.25	27.52		77-163.30	79.47	1.52	12.7	6.6	8333.3				-18	-4.3
8666.7	1.26	28.37		42 49.98	88.62	1.03			8666.7	1.18	27.65		64 54.13	85.87	1.58			8666.7				-38	-6.4
9000.0	1.26	28.67		-04 -92.58	99.32	1.02			9000.0	1.15	27.99		-30 -86.20	90.79	1.63			9000.0				-26	-4.8
9333.3	1.30	28.97		-34 129.15	86.82	1.00			9333.3	1.17	28.73		-12 133.94	88.71	1.59			9333.3				-24	-7.0
9666.7	1.34	29.14		-64 -10.73	88.70	1.04			9666.7	1.18	29.10		-43 -3.74	84.80	1.50			9666.7				-04	-7.3
10000.0	1.36	29.18		-80-146.92	88.43	1.08	10.0	7.3	10000.0	1.19	29.09		-80-139.66	86.44	1.38	13.5	7.0	10000.0				-08	-7.1
10333.3	1.31	29.14		-84 76.28	90.49	1.13			10333.3	1.15	29.16		-79 83.34	94.84	1.26			10333.3				-02	-8.3
10666.7	1.21	28.92		-81 -58.86	85.49	1.18			10666.7	1.07	29.21		-86 -50.60	110.88	1.18			10666.7				-30	-8.1
11000.0	1.14	28.91		-58 168.13	80.50	1.25			11000.0	1.04	29.04		-91 176.25	85.04	1.14			11000.0				-13	-8.4
11333.3	1.22	28.42		-09 -95.37	91.59	1.44			11333.3	1.17	28.79		-74 43.92	87.03	1.12			11333.3				-38	-7.8
11666.7	1.33	28.03		29 135.73	80.04	1.55			11666.7	1.29	28.55		-26 143.90	82.42	1.13			11666.7				-52	-8.2
12000.0	1.35	27.60		72 7.88	77.24	1.63			12000.0	1.34	28.29		00 14.91	93.47	1.12			12000.0				-69	-7.0
12666.7	1.18	28.03		29 115.88	90.03	1.54			12666.7	1.26	28.72		-42 116.74	97.05	1.08			12666.7				-50	-2
13000.0	1.08	28.36		-03 -12.96	82.62	1.49	15.0	7.9	13000.0	1.19	28.86		-56 -13.17	80.50	1.01	14.0	7.7	13000.0				-50	-2
13333.3	1.11	28.64		-31-144.40	84.58	1.41			13333.3	1.13	28.51		-21-143.80	81.17	1.10			13333.3				-13	-6
13666.7	1.19	29.17		-84 86.87	90.96	1.33			13666.7	1.10	28.46		-16 86.16	81.00	1.22			13666.7				-71	-7
14000.0	1.25	28.89		-55 -43.07	82.42	1.23			14000.0	1.08	28.19		-09 -40.02	81.71	1.33			14000.0				-69	-3.0
14333.3	1.26	28.70		-36-176.49	84.56	1.11			14333.3	1.08	27.77		-52-167.31	92.98	1.46			14333.3				-93	-9.2
14666.7	1.23	28.71		-38 56.60	85.98	1.04			14666.7	1.07	28.23		05 62.02	83.08	1.63			14666.7				-47	-5.4
15000.0	1.16	28.45		-12 -76.03	89.19	1.13			15000.0	1.09	28.80		-50 -65.78	88.59	1.80			15000.0				-35	-10
15333.3	1.08	28.46		-13 153.31	87.57	1.22			15333.3	1.15	28.62		-32 167.38	94.24	1.86			15333.3				-16	-14
15666.7	1.03	28.50		-17 25.00	88.26	1.25			15666.7	1.21	28.06		23 31.69	79.41	1.73			15666.7				-44	-6.7
16000.0	1.03	28.33		00-107.30	79.69	1.29			16000.0	1.27	28.67		-37-100.16	75.37	1.38			16000.0				-34	-7.1
16333.3	1.05	28.34		00 118.45	88.97	1.29			16333.3	1.30	28.58		-29 126.99	83.81	1.32			16333.3				-25	-8.5
16666.7	1.08	28.33		00 -17.69	80.90	1.27			16666.7	1.24	27.99		30 -7.03	78.35	1.61			16666.7				-34	-11
17000.0	1.10	28.34		-01-151.30	73.77	1.21			17000.0	1.16	28.25		04-142.43	79.87	1.98			17000.0				-10	-8.9
17333.3	1.12	28.56		-23 71.35	85.18	1.17			17333.3	1.04	28.92		-62 77.74	88.77	2.13			17333.3				-36	-8.4
17666.7	1.13	28.27		05 -70.55	75.72	1.13			17666.7	1.13	27.61		68 -60.99	69.39	2.58			17666.7				-66	-9.6
18000.0 *	1.11	27.40		-92 145.11	86.05	1.08	15.7	9.3	18000.0 *	1.25	27.16		1.12 165.30	75.58	3.47	12.5	8.7	18000.0 *				-24	-20

LINEAR-IZATION RANGE 7000.0 TO 18000.0

* Bad Data

MEASUREMENTS AT +70°C

NOV 22, 1977

7 TO 18 GHZ AMPLIFIER
TEMPERATURE TEST
S/N 1

FREQ MHZ	VSMR IN	GAIN DB	FLAT DB	PHASE DEG	ISOL DB	VSMR OUT	10BPMR DBM	NOISE FIG	FREQ MHZ	VSMR IN	GAIN DB	FLAT DB	PHASE DEG	ISOL DB	VSMR OUT	10BPMR DBM	NOISE FIG	FREQ MHZ	VSMR OUT	MATCH GAIN DG12 DP12
7000.0	1.53	24.18	2.44	-76.81	102.62	1.07	13.0	8.1	7000.0	1.55	24.39	2.07	-74.44	91.65	1.06	12.1	7.8	7000.0	1.06	-21 -2.4
7333.3	1.54	24.88	1.74	126.59	81.78	1.04			7333.3	1.50	24.89	1.57	128.14	83.02	1.20			7333.3	1.20	-00 -1.6
7666.7	1.47	25.32	1.30	-24.72	79.44	1.01			7666.7	1.37	25.00	1.46	-22.96	78.49	1.36			7666.7	1.36	-32 -1.8
8000.0	1.38	25.78	.84	-173.19	88.62	1.02	14.1	7.6	8000.0	1.26	25.49	.96	-170.95	79.15	1.51	12.7	7.3	8000.0	1.51	-29 -2.2
8333.3	1.30	26.00	.62	44.14	84.51	1.03			8333.3	1.19	25.62	.84	46.26	87.90	1.59			8333.3	1.59	-38 -2.1
8666.7	1.27	26.50	.12	-98.44	84.86	1.01			8666.7	1.16	26.00	.46	-94.04	82.87	1.63			8666.7	1.63	.50 -4.4
9000.0	1.28	26.80	-.17	123.23	90.43	1.01			9000.0	1.16	26.45	.01	125.94	84.82	1.60			9000.0	1.60	.36 -2.7
9333.3	1.32	27.12	-.49	-16.90	88.86	1.03			9333.3	1.19	26.79	-.32	-11.99	83.50	1.51			9333.3	1.51	.33 -4.9
9666.7	1.37	27.31	-.68	-153.34	85.74	1.08			9666.7	1.20	27.20	-.73	-148.20	92.58	1.39			9666.7	1.39	.11 -5.1
10000.0	1.39	27.37	-.74	69.75	85.80	1.14	14.7	8.0	10000.0	1.21	27.21	-.75	74.48	85.52	1.27	14.0	7.8	10000.0	1.27	.15 -4.7
10333.3	1.34	27.34	-.71	-65.44	83.67	1.19			10333.3	1.17	27.32	-.86	-59.75	81.67	1.18			10333.3	1.18	.02 -5.7
10666.7	1.23	27.13	-.50	161.19	83.50	1.26			10666.7	1.09	27.35	-.89	166.79	86.99	1.15			10666.7	1.15	-.02 -5.6
11000.0	1.14	27.15	-.52	28.50	83.37	1.36			11000.0	1.02	27.20	-.73	34.37	87.95	1.13			11000.0	1.13	-.05 -5.9
11333.3	1.22	26.69	-.06	-102.67	83.49	1.46			11333.3	1.15	27.00	-.53	-97.60	84.32	1.13			11333.3	1.13	-.05 -5.1
11666.7	1.31	26.33	-.29	128.14	76.25	1.57			11666.7	1.25	26.78	-.31	133.45	82.34	1.13			11666.7	1.13	-.30 -5.1
12000.0	1.31	25.79	.83	.07	81.77	1.64			12000.0	1.28	26.48	-.01	3.61	81.05	1.12			12000.0	1.12	-.45 -5.3
12666.7	1.14	26.33	.29	107.09	91.53	1.55	15.0	8.6	12666.7	1.23	26.94	-.47	104.45	93.24	1.08			12666.7	1.08	-.69 -3.5
13000.0	1.05	26.71	-.07	-21.45	81.65	1.48			13000.0	1.18	27.04	-.58	-25.44	82.03	1.01	14.0	8.6	13000.0	1.01	-.34 4.0
13333.3	1.12	27.01	-.38	-153.39	87.90	1.40			13333.3	1.15	26.69	-.23	-156.16	79.17	1.11			13333.3	1.11	.32 2.8
13666.7	1.20	27.55	-.92	77.99	85.19	1.31			13666.7	1.13	26.67	-.20	73.67	96.41	1.24			13666.7	1.24	.88 3.9
14000.0	1.25	27.26	-.53	-52.61	82.17	1.20			14000.0	1.10	26.41	.05	-52.91	83.61	1.35			14000.0	1.35	.85 3.3
14333.3	1.20	27.12	-.49	173.50	85.34	1.09			14333.3	1.07	26.08	.38	179.62	88.97	1.49			14333.3	1.49	1.04 -6.1
14666.7	1.22	27.09	-.45	46.06	91.84	1.04			14666.7	1.05	26.47	.00	48.26	101.98	1.67			14666.7	1.67	.62 -2.2
15000.0	1.15	26.87	-.24	-86.91	81.88	1.14			15000.0	1.10	27.10	-.63	-80.25	103.23	1.83			15000.0	1.83	-.23 -6.7
15333.3	1.08	26.92	-.28	142.16	88.32	1.23			15333.3	1.17	26.95	-.48	152.47	92.17	1.88			15333.3	1.88	-.03 -10.1
15666.7	1.03	27.00	-.37	13.47	91.33	1.25			15666.7	1.23	26.39	.07	16.58	86.96	1.68			15666.7	1.68	.62 -3.1
16000.0	1.02	26.85	-.22	-119.15	82.04	1.29			16000.0	1.28	26.97	-.50	-115.93	77.96	1.35			16000.0	1.35	-.12 -3.2
16333.3	1.04	26.90	-.27	105.98	80.81	1.29			16333.3	1.30	26.94	-.47	110.44	80.56	1.35			16333.3	1.35	-.04 -4.5
16666.7	1.07	26.80	-.17	-30.84	76.04	1.27			16666.7	1.24	26.19	.27	-24.18	77.94	1.67			16666.7	1.67	.61 -6.7
17000.0	1.11	26.87	-.24	-165.20	77.05	1.20			17000.0	1.15	26.55	-.08	-159.91	80.83	2.02			17000.0	2.02	.32 -5.3
17333.3	1.14	27.04	-.41	56.82	92.58	1.15			17333.3	1.07	27.16	-.69	59.36	87.96	2.16			17333.3	2.16	-.12 -2.5
17666.7	1.13	26.73	-.10	-86.03	94.29	1.11			17666.7	1.17	25.86	.60	-79.24	75.43	2.72			17666.7	2.72	.87 -6.8
18000.0*	1.15	25.91	-.71	129.68	81.68	1.07	15.5	10.1	18000.0*	1.29	25.69	.77	146.57	68.34	3.66	12.6	9.9	18000.0*	3.66	.22 -17.1

LINEAR- IZATION RANGE 7000.0 TO 18000.0

* Bad Data

MEASUREMENTS AT 30°C

NOV 22, 1977
7 TO 18 GHZ AMPLIFIER
TEMPERATURE TEST
S/N
01

NOV 22, 1977
7 TO 18 GHZ AMPLIFIER
TEMPERATURE TEST
S/N
02

7 TO 18 GHZ AMPLIFIER TEMPERATURE TEST S/N 01				7 TO 18 GHZ AMPLIFIER TEMPERATURE TEST S/N 02				MATCH															
FREQ MHZ	VSWR IN	GAIN DB	FLAT DB	PHASE DEG	ISOL DB	VSMR OUT	VSMR IN	FREQ MHZ	VSWR IN	GAIN DB	FLAT DB	PHASE DEG	ISOL DB	VSMR OUT	1DBPWR DBM	NOISE FIG	FREQ MHZ	VSWR OUT	1DBPWR DBM	NOISE FIG	GAIN DB	DP12 DP12	
7000.0	1.53	27.78	1.96	-63.60	99.46	1.06	1.55	7000.0	1.55	28.08	1.51	-59.69	82.35	1.06			7000.0					-30	-3.9
7333.3	1.53	28.47	1.27	139.95	83.09	1.03	1.48	7333.3	1.48	28.56	1.03	143.00	85.12	1.20			7333.3					-09	-3.1
7666.7	1.45	28.87	87	-11.26	78.53	1.01	1.35	7666.7	1.35	28.60	99	-7.86	79.59	1.35			7666.7					-27	-3.4
8000.0	1.36	29.25	49	-159.28	83.22	1.02	1.24	8000.0	1.24	28.99	61	-155.28	79.76	1.51			8000.0					26	-4.0
8333.3	1.27	29.35	39	58.93	86.95	1.03	1.16	8333.3	1.16	29.12	47	62.65	92.51	1.57			8333.3					22	-3.7
8666.7	1.23	29.78	-03	-83.50	92.22	1.02	1.13	8666.7	1.13	29.43	16	-77.61	87.52	1.52			8666.7					35	-5.9
9000.0	1.25	30.08	-33	138.86	90.70	1.01	1.13	9000.0	1.13	29.84	-24	142.99	86.04	1.59			9000.0					23	-4.1
9333.3	1.29	30.38	-62	-92	84.80	1.04	1.15	9333.3	1.15	30.14	-53	5.48	90.01	1.50			9333.3					24	-6.4
9666.7	1.34	30.54	-79	-136.96	90.49	1.09	1.17	9666.7	1.17	30.49	-88	-130.31	93.20	1.39			9666.7					05	-6.6
10000.0	1.37	30.60	-85	86.43	87.73	1.14	1.17	10000.0	1.17	30.49	-88	92.81	90.94	1.27			10000.0					01	-7.7
10333.3	1.32	30.49	-74	-48.53	83.48	1.20	1.13	10333.3	1.13	30.48	-87	-40.79	82.92	1.19			10333.3					01	-7.7
10666.7	1.22	30.30	-55	179.10	77.98	1.26	1.06	10666.7	1.06	30.56	-95	-173.35	85.58	1.15			10666.7					-26	-8
11000.0	1.15	30.25	-50	46.56	81.74	1.35	1.06	11000.0	1.06	30.34	-74	54.67	90.78	1.13			11000.0					-09	-8.1
11333.3	1.24	29.79	-04	-83.71	83.15	1.45	1.19	11333.3	1.19	30.14	-53	-76.42	84.69	1.13			11333.3					-35	-7.3
11666.7	1.35	29.38	36	147.58	81.14	1.56	1.31	11666.7	1.31	29.90	-30	155.16	78.34	1.13			11666.7					-52	-7.6
12000.0	1.37	28.89	86	20.18	79.07	1.64	1.36	12000.0	1.36	29.58	02	26.58	85.12	1.11			12000.0					-59	-6.4
12666.7	1.20	29.44	30	128.90	97.44	1.55	1.28	12666.7	1.28	30.00	-40	129.34	84.60	1.06			12666.7					-56	-4
13000.0	1.10	29.76	-01	-58	87.77	1.49	1.22	13000.0	1.22	30.15	-54	-42	83.63	1.02			13000.0					-38	1.0
13333.3	1.10	30.05	-30	-130.61	88.24	1.40	1.16	13333.3	1.16	29.80	-20	-130.79	91.51	1.13			13333.3					25	2
13666.7	1.17	30.57	-82	101.20	88.59	1.33	1.11	13666.7	1.11	29.74	-13	99.26	80.28	1.26			13666.7					84	1.9
14000.0	1.23	30.30	-55	-28.73	83.76	1.22	1.07	14000.0	1.07	29.46	14	-26.69	78.53	1.36			14000.0					84	-2.0
14333.3	1.24	30.08	-33	-161.60	84.50	1.11	1.03	14333.3	1.03	29.02	-58	-152.77	86.19	1.47			14333.3					1.06	-8.8
14666.7	1.21	30.11	-36	71.86	96.52	1.05	1.04	14666.7	1.04	29.46	13	76.52	89.53	1.63			14666.7					65	-4.7
15000.0	1.15	29.84	-09	-60.33	88.70	1.14	1.10	15000.0	1.10	30.01	-41	-50.90	91.54	1.79			15000.0					-17	-9.4
15333.3	1.07	29.89	-14	169.42	86.31	1.22	1.18	15333.3	1.18	29.81	-21	-177.50	84.45	1.85			15333.3					08	-13
15666.7	1.01	29.90	-15	41.34	87.36	1.24	1.25	15666.7	1.25	29.28	32	46.97	85.36	1.71			15666.7					62	-5.6
16000.0	1.02	29.74	01	-90.85	79.32	1.27	1.31	16000.0	1.31	29.87	-27	-84.42	90.78	1.39			16000.0					-13	-6.4
16333.3	1.03	29.69	05	135.61	87.38	1.25	1.34	16333.3	1.34	29.71	-11	143.37	85.97	1.38			16333.3					-02	-7.8
16666.7	1.05	29.66	08	-03	87.35	1.25	1.28	16666.7	1.28	28.94	66	9.69	73.05	1.72			16666.7					73	-9.7
17000.0	1.08	29.71	03	-132.10	77.04	1.21	1.20	17000.0	1.20	29.32	28	-123.87	79.11	2.12			17000.0					40	-8.2
17333.3	1.12	29.93	-18	91.77	83.23	1.18	1.08	17333.3	1.08	30.10	-90	97.53	83.16	2.26			17333.3					-17	-5.8
17666.7	1.12	29.72	02	-49.52	71.51	1.13	1.14	17666.7	1.14	28.86	73	-41.24	75.65	2.67			17666.7					86	-8.3
18000.0*	1.12	29.04	71	167.48	70.42	1.07	1.23	18000.0*	1.23	28.53	1.07	-173.88	70.86	3.70			18000.0*					51	-19

LINEAR-
IZATION
RANGE

7000.0
TO
18000.0

LINEAR-
IZATION
RANGE

7000.0
TO
18000.0

* Bad Data

APPENDIX B

Data on the Four 7 to 18 GHz Amplifiers
which were added onto the contract. Phase
Matching was not required.

18 8111
 NOV 23 1977

SF6 0552H
 SN 37
 SN 37

FREQ MHZ	USMR IN	GAIN DB	FLAT DB	PHASE DEG	PHASE DEG	ISOL DB	USMR OUT	TOTPKR DBM	NOISE FIG
7000.0	1.23	29.62	1.09	-89.39	67.99	88.67	1.18	15.6	6.8
7250.0	1.51	30.21	.51	152.25	48.44	83.19	1.11		
7500.0	1.68	30.49	.22	39.56	34.54	80.99	1.07		
7750.0	1.72	30.55	.16	-71.28	22.50	84.89	1.08		
8000.0	1.65	30.65	.07	179.32	11.90	91.19	1.10	15.8	6.3
8250.0	1.57	30.75	-.03	74.28	5.67	95.55	1.13		
8500.0	1.51	31.02	-.29	-30.61	-.40	111.73	1.14		
8750.0	1.46	31.32	-.60	-136.20	-7.19	86.05	1.14		
9000.0	1.39	31.49	-.76	120.89	-11.31	91.10	1.13		
9250.0	1.30	31.83	-1.10	16.21	-17.19	86.33	1.15		
9500.0	1.21	31.85	-1.12	-86.84	-21.43	92.30	1.21		
9750.0	1.15	32.10	-1.38	173.38	-22.42	91.05	1.30		
10000.0	1.13	31.83	-1.10	70.47	-26.53	84.82	1.41	15.4	6.3
10250.0	1.11	31.93	-1.20	-29.43	-27.62	82.23	1.52		
10500.0	1.08	31.43	-.70	-128.32	-27.71	87.46	1.61		
10750.0	1.22	31.79	-1.07	129.43	-31.17	89.40	1.69		
11000.0	1.47	31.49	-.76	31.84	-29.96	82.45	1.67		
11250.0	1.78	31.23	-.50	-64.00	-26.99	76.59	1.64		
11500.0	2.09	30.77	-.04	-162.55	-26.73	80.45	1.61		
11750.0	2.30	30.57	.15	102.02	-23.36	83.33	1.62		
12000.0	2.31	30.37	.34	6.85	-19.73	83.54	1.72	15.8	7.5
12250.0	2.29	29.96	.75	-81.98	-9.76	74.41	1.81		
12500.0	1.67	29.53	1.19	-178.45	-7.43	92.72	1.74		
12750.0	1.33	29.67	1.04	86.35	-3.83	83.53	1.73		
13000.0	1.04	30.30	.42	-7.13	1.48	82.32	1.69		
13250.0	1.24	30.58	.13	-101.97	5.43	86.68	1.64		
13500.0	1.54	30.70	.02	158.22	4.43	89.58	1.60		
13750.0	1.73	30.82	-.10	59.64	4.63	84.82	1.50		
14000.0	1.80	30.98	-.26	-35.99	7.80	95.44	1.40	16.4	8.0
14250.0	1.74	30.54	.17	-133.58	9.02	90.64	1.27		
14500.0	1.61	30.53	.18	130.56	11.96	93.78	1.13		
14750.0	1.42	30.64	.07	32.69	12.87	102.98	1.04		
15000.0	1.31	30.94	-.22	-66.46	12.51	93.15	1.27		
15250.0	1.37	30.77	-.04	-165.89	11.88	104.07	1.74		
15500.0	1.49	29.94	.78	97.65	14.22	84.26	2.37		
15750.0	1.58	30.01	.70	1.07	16.44	100.58	2.60		
16000.0	1.55	30.60	.11	-97.73	16.44	84.99	2.37	16.9	8.8
16250.0	1.46	31.06	-.34	162.44	15.40	74.43	2.15		
16500.0	1.36	31.67	-.94	62.64	14.40	77.88	2.10		
16750.0	1.23	30.94	-.22	-40.99	9.57	76.14	1.99		
17000.0	1.25	30.34	.38	-142.96	6.40	68.54	1.75		
17250.0	1.48	29.94	.78	110.82	-1.01	74.58	1.68		
17500.0	1.52	29.88	.83	11.19	-1.84	72.95	1.39		
17750.0	1.59	29.83	.89	-92.56	-6.78	64.27	1.20		
18000.0	1.47	28.90	1.81	159.86	-15.57	66.42	1.17	15.2	8.7
LINEAR- IZATION RANGE			7000.0 70 18000.0		7000.0 70 18000.0				

DBY 18 20758
12/2/77

SF 6-0362
FINAL TEST
S/n 38

FREQ MHZ	USMR IN	GAIN DB	FLAT DB	PHASE DEG	PHASE DEV	ISOL DB	USMR OUT	TDBPWR DBM	NOISE FIG
7000.0	1.30	30.35	-.17	74.23	69.89	119.73	1.06	11.0	6.3
7200.0	1.39	30.35	-.18	-26.27	54.56	87.85	1.05		
7400.0	1.46	30.28	-.11	-123.86	42.15	83.40	1.04		
7600.0	1.48	30.54	-.37	139.12	30.31	86.90	1.04		
7800.0	1.46	30.57	-.39	45.10	21.44	88.19	1.06		
8000.0	1.44	30.70	-.52	-48.60	12.90	100.51	1.08	11.8	6.2
8200.0	1.38	30.88	-.70	-142.02	4.66	88.38	1.12		
8400.0	1.31	30.87	-.69	127.24	-8.89	86.87	1.15		
8600.0	1.25	30.86	-.69	35.38	-7.58	98.92	1.19		
8800.0	1.21	30.77	-.60	-54.80	-12.58	83.07	1.22		
9000.0	1.17	30.74	-.57	-142.95	-15.54	85.66	1.25	12.2	6.2
9200.0	1.15	30.91	-.74	128.17	-19.24	88.42	1.27		
9400.0	1.13	30.81	-.64	40.50	-21.73	79.84	1.30		
9600.0	1.12	30.73	-.56	-46.58	-23.63	97.09	1.29		
9800.0	1.10	30.79	-.62	-134.34	-26.19	82.54	1.30		
10000.0	1.09	30.63	-.45	140.74	-25.92	88.69	1.29	12.0	6.5
10200.0	1.05	30.61	-.44	53.72	-27.76	81.44	1.26		
10400.0	1.06	30.43	-.26	-31.67	-27.95	79.02	1.23		
10600.0	1.07	30.27	-.09	-116.39	-27.49	78.35	1.20		
10800.0	1.14	30.24	-.06	157.76	-28.16	83.14	1.17		
11000.0	1.22	29.98	.19	74.69	-26.06	79.67	1.15	12.4	7.5
11200.0	1.32	29.77	.39	-8.68	-24.25	86.26	1.14		
11400.0	1.41	29.61	.56	-91.72	-22.10	81.03	1.14		
11600.0	1.48	29.52	.64	-172.65	-17.85	88.03	1.13		
11800.0	1.51	29.68	.49	103.19	-16.84	83.32	1.11		
12000.0	1.52	29.76	.40	21.66	-12.98	93.92	1.11	13.2	7.6
12200.0	1.47	30.49	-.32	-60.45	-16.11	80.08	1.10		
12600.0	1.42	30.14	.02	133.52	-5.78	90.78	1.17		
12800.0	1.40	30.18	-.01	49.30	-4.82	95.89	1.20		
13000.0	1.44	30.10	.06	-34.52	-3.45	84.38	1.25	12.3	7.3
13200.0	1.49	30.07	.09	-117.61	-1.36	82.16	1.29		
13400.0	1.54	29.97	.19	157.07	-1.50	90.42	1.32		
13600.0	1.55	29.83	.33	75.32	1.93	89.30	1.32		
13800.0	1.55	29.85	.32	-7.89	3.90	89.95	1.31		
14000.0	1.57	29.80	.36	-90.72	6.25	89.83	1.28	13.4	7.3
14200.0	1.57	29.73	.43	-171.87	16.29	92.91	1.23		
14400.0	1.56	29.75	.41	103.20	16.54	90.64	1.17		
14600.0	1.56	29.95	.21	21.42	13.96	87.99	1.11		
14800.0	1.47	29.94	.22	-61.54	16.18	84.69	1.10		
15000.0	1.43	30.01	.16	-146.71	16.20	80.87	1.17	13.7	7.4
15200.0	1.35	30.14	.02	129.67	17.76	93.32	1.24		
15400.0	1.29	30.16	.00	44.17	17.43	85.84	1.33		
15600.0	1.26	30.18	-.01	-39.92	18.53	94.88	1.38		
15800.0	1.24	30.37	-.20	-124.62	19.01	84.51	1.40		
16000.0	1.26	30.41	-.24	149.15	17.95	85.24	1.44	14.0	7.8
16200.0	1.30	30.54	-.36	62.95	16.94	78.76	1.43		
16400.0	1.39	30.74	-.56	-24.76	14.42	79.13	1.38		
16600.0	1.42	30.44	-.27	-112.75	11.62	82.98	1.29		
16800.0	1.45	30.34	-.17	159.28	8.82	76.83	1.24		
17000.0	1.49	30.16	.01	71.44	6.17	75.25	1.14	13.1	7.9
17200.0	1.57	29.84	.32	-19.18	.72	75.74	1.16		
17400.0	1.69	29.50	.67	-109.66	-4.56	74.36	1.23		
17600.0	1.69	29.15	1.02	161.12	-8.59	74.59	1.34		
17800.0	1.72	28.78	1.39	69.66	-14.88	78.27	1.39		
18000.0	1.74	27.99	2.17	-25.20	-24.58	67.31	1.40	12.0	8.3
LINEAR- IZATION RANGE			7000.0 10 18000.0		7000.0 10 18000.0				

THIS PAGE IS BEST QUALITY PRACTICABLE
FROM COPY FURNISHED TO DDG

DBY 18 2075B
 DECEMBER 14, 1977

SF6-0882
 FINAL TEST
 S/N 39

FREQ MHZ	VSWR IN	GAIN DB	FLAT DB	PHASE DEG	PHASE DEV	ISOL DB	VSWR OUT	1DBPWR DBM	NOISE FIG
7000.0	1.71	28.84	-.70	51.85	67.31	78.28	1.30	12.6	7.2
7250.0	1.75	28.82	-.68	-73.56	49.37	78.08	1.30		
7500.0	1.68	28.91	-.77	161.87	32.26	86.19	1.30		
7750.0	1.57	28.83	-.69	43.91	21.77	81.84	1.30		
8000.0	1.44	28.92	-.78	-75.17	10.14	85.26	1.31	10.1	7.2
8250.0	1.31	29.06	-.92	170.28	3.05	81.69	1.30		
8500.0	1.22	29.09	-.95	54.88	-4.88	85.76	1.24		
8750.0	1.20	29.19	-1.05	-58.19	-10.47	81.32	1.17		
9000.0	1.19	29.36	-1.22	-169.63	-14.46	91.45	1.10	12.0	7.2
9250.0	1.17	29.36	-1.22	78.00	-19.38	82.80	1.07		
9500.0	1.11	29.38	-1.24	-32.62	-22.55	92.01	1.09		
9750.0	1.03	29.43	-1.29	-143.27	-25.74	80.86	1.12		
10000.0	1.07	29.26	-1.12	105.44	-29.57	90.90	1.16	11.8	7.2
10250.0	1.19	29.05	-.91	-3.06	-30.61	77.65	1.18		
10500.0	1.34	28.64	-.50	-111.36	-31.44	89.44	1.19		
10750.0	1.49	28.28	-.14	142.11	-30.52	84.19	1.19		
11000.0	1.61	27.84	.29	35.43	-29.74	78.53	1.21	10.8	8.6
11250.0	1.70	27.46	.67	-68.17	-25.88	81.22	1.24		
11500.0	1.73	27.15	.98	-171.93	-22.18	89.90	1.23		
11750.0	1.71	27.11	1.02	84.92	-17.87	86.28	1.21		
12000.0	1.64	27.02	1.11	-18.66	-14.00	89.64	1.18	13.4	8.6
12250.0	1.53	26.98	1.15	-122.50	-10.37	78.37	1.16		
12500.0	1.39	26.92	1.21	134.83	-5.59	88.74	1.15		
12750.0	1.26	27.03	1.10	30.42	-2.55	84.99	1.18		
13000.0	1.15	27.10	1.03	-72.32	2.15	84.47	1.21	11.7	7.3
13250.0	1.11	27.25	.88	-178.46	3.48	96.76	1.23		
13500.0	1.20	27.37	.76	78.76	8.16	84.73	1.22		
13750.0	1.32	27.46	.67	-26.95	9.90	90.68	1.21		
14000.0	1.43	27.58	.55	-131.94	12.36	99.03	1.25	12.4	7.3
14250.0	1.51	27.44	.69	120.57	12.33	85.12	1.29		
14500.0	1.55	27.46	.67	17.16	16.37	92.96	1.32		
14750.0	1.54	27.40	.73	-88.51	18.16	86.75	1.32		
15000.0	1.50	27.50	.63	166.66	20.80	115.37	1.28	11.0	7.6
15250.0	1.40	27.71	.42	59.19	20.78	90.98	1.21		
15500.0	1.31	27.81	.32	-47.08	21.97	91.50	1.15		
15750.0	1.24	27.99	.14	-155.76	20.73	78.31	1.26		
16000.0	1.18	28.08	.05	96.27	20.23	78.75	1.39	13.6	8.0
16250.0	1.21	28.14	.00	-13.33	18.09	94.14	1.50		
16500.0	1.19	28.14	.00	-125.01	13.86	77.69	1.58		
16750.0	1.15	28.33	-.19	125.53	11.87	76.25	1.60		
17000.0	1.10	28.58	-.44	12.47	6.26	75.42	1.48	14.4	7.9
17250.0	1.13	28.57	-.43	-103.02	-1.76	90.18	1.41		
17500.0	1.20	28.39	-.25	139.63	-11.65	69.38	1.18		
17750.0	1.27	28.27	-.13	21.36	-22.46	75.54	1.13		
18000.0	1.39	27.48	.65	-101.35	-37.72	69.29	1.29	13.6	8.3
LINEAR - IZATION RANGE			7000.0 TO 18000.0	7000.0 TO 18000.0					

DECEMBER 20, 1977

SF6-0882
 FINAL TEST
 S/N 40

FREQ MHZ	VSWR IN	GAIN DB	FLAT DB	PHASE DEG	PHASE DEV	ISOL DB	VSWR OUT	TDBPWR DBM	NOISE FIG
7000.0	1.71	28.73	-.25	56.07	60.51	85.92	1.02	10.6	6.1
7250.0	1.81	28.40	.07	-70.49	41.76	90.74	1.09		
7500.0	1.80	28.18	.29	166.33	26.39	86.02	1.16		
7750.0	1.70	28.09	.38	50.70	18.57	83.18	1.19		
8000.0	1.57	28.24	.23	-66.97	8.70	88.31	1.19	12.2	6.0
8250.0	1.45	28.60	-.12	178.69	2.16	88.63	1.17		
8500.0	1.35	28.81	-.33	62.75	-5.95	91.77	1.16		
8750.0	1.31	28.92	-.44	-51.17	-12.07	97.02	1.16		
9000.0	1.31	29.09	-.61	-162.29	-15.38	85.97	1.16	13.5	5.9
9250.0	1.33	29.03	-.55	85.10	-20.17	88.02	1.16		
9500.0	1.36	29.01	-.53	-25.07	-22.54	87.46	1.13		
9750.0	1.38	29.05	-.57	-135.47	-25.13	90.09	1.11		
10000.0	1.39	28.92	-.44	114.51	-27.34	79.19	1.11	13.8	6.0
10250.0	1.35	28.80	-.32	6.91	-27.14	85.52	1.14		
10500.0	1.28	28.60	-.12	-100.91	-27.14	98.38	1.19		
10750.0	1.18	28.43	.04	153.03	-25.39	80.62	1.23		
11000.0	1.13	28.20	.27	46.07	-24.55	81.45	1.24	15.0	6.3
11250.0	1.22	28.04	.43	-58.53	-21.35	81.44	1.22		
11500.0	1.34	27.80	.67	-163.16	-18.17	80.69	1.23		
11750.0	1.47	27.85	.62	93.28	-13.90	89.43	1.26		
12000.0	1.57	27.77	.70	-10.71	-10.09	90.05	1.31	14.6	7.3
12250.0	1.63	27.87	.60	-114.62	-6.19	81.88	1.35		
12500.0	1.67	27.93	.54	141.53	-2.24	85.45	1.38		
12750.0	1.65	28.17	.30	36.27	.30	89.40	1.41		
13000.0	1.58	28.30	.17	-68.30	3.54	82.17	1.45	14.0	7.2
13250.0	1.49	28.39	.08	-175.39	4.26	91.10	1.45		
13500.0	1.47	28.41	.06	80.98	8.44	93.07	1.40		
13750.0	1.47	28.46	.01	-24.55	10.70	90.40	1.30		
14000.0	1.48	28.61	-.13	-130.06	13.00	91.49	1.17	15.1	7.2
14250.0	1.52	28.59	-.11	122.60	13.47	92.02	1.06		
14500.0	1.59	28.63	-.15	17.41	16.08	93.30	1.11		
14750.0	1.62	28.42	.05	-89.80	16.69	87.64	1.24		
15000.0	1.68	28.45	.02	165.58	19.87	88.49	1.36	15.2	7.5
15250.0	1.68	28.55	-.07	58.37	20.46	82.37	1.45		
15500.0	1.62	28.65	-.17	-48.57	21.33	77.42	1.51		
15750.0	1.46	28.86	-.38	-156.46	21.25	82.60	1.61		
16000.0	1.30	29.07	-.59	94.66	20.18	82.97	1.66	15.6	8.0
16250.0	1.19	29.02	-.54	-15.98	17.34	79.78	1.65		
16500.0	1.14	28.98	-.50	-128.40	12.73	76.76	1.52		
16750.0	1.07	29.03	-.55	120.16	9.09	91.36	1.35		
17000.0	1.08	29.04	-.56	5.80	2.53	81.64	1.17	14.4	7.9
17250.0	1.23	28.86	-.38	-110.35	-5.80	78.32	1.12		
17500.0	1.40	28.33	.14	132.04	-15.59	78.63	1.21		
17750.0	1.53	27.69	.78	13.87	-25.96	69.51	1.25		
18000.0	1.54	26.69	1.78	-105.26	-37.29	69.79	1.29	14.6	8.2

LINEAR-
 IZATION
 RANCE

7000.0 TO 18000.0 7000.0 TO 18000.0

APPENDIX C
Temperature Measurements on 10.7 to 18 GHz Amplifiers

MEASUREMENTS AT +25°C

OCT 21, 1977

10.7 TO 18 GHz AMPLIFIER
TEMPERATURE TEST
S/N 1

Table with columns: FREQ MHZ, VSMR IN, GAIN DB, FLAT DB, PHASE DEG, ISOL DB, VSMR OUT, NOISE FIG, 10BPMR DBM, FREQ MHZ, VSMR IN, GAIN DB, FLAT DB, PHASE DEG, ISOL DB, VSMR OUT, NOISE FIG, 10BPMR DBM, FREQ MHZ, VSMR IN, GAIN DB, FLAT DB, PHASE DEG, ISOL DB, VSMR OUT, NOISE FIG, 10BPMR DBM, MATCH GAIN DB, PHASE DP12.

OCT 21, 1977

10.7 TO 18 GHz AMPLIFIER
TEMPERATURE TEST
S/N 2

Table with columns: FREQ MHZ, VSMR IN, GAIN DB, FLAT DB, PHASE DEG, ISOL DB, VSMR OUT, NOISE FIG, 10BPMR DBM, FREQ MHZ, VSMR IN, GAIN DB, FLAT DB, PHASE DEG, ISOL DB, VSMR OUT, NOISE FIG, 10BPMR DBM, MATCH GAIN DB, PHASE DP12.

LINEARIZATION RANGE 10700.0 TO 18000.0

LINEARIZATION RANGE 10700.0 TO 18000.0

* Bad Data

APPENDIX D

Portions of the Qualification Test Procedure and Functional Test Procedure for the qualified 7 to 12 GHz amplifier have been copied. Using these test procedures, Power Line Transient and Power Interrupt, and Stability Tests were made on the 10.7 to 18 GHz amplifiers.

EXCERPTS FROM QUALIFICATION TEST PROCEDURE
QTP-760510

5.19 Steady-State Voltage and Frequency Test

- a) Connect the equipment necessary to measure Small-Signal Gain in accordance with FTP-760510. Energize the amplifier by supplying 115 Volt, 60 Hz power to the AC input. Maintain this condition for a minimum duration of 15 minutes. Measure and record Small-Signal Gain.
- b) Change the input power to 103.5 Volts at 57 Hz. Maintain this condition for a minimum of 15 minutes. Measure and record Small-Signal Gain.
- c) Change the input power to 126.5 Volts at 57 Hz. Maintain this condition for a minimum of 15 minutes. Measure and record Small-Signal Gain.
- d) Change the input power to 126.5 Volts at 420 Hz. Maintain this condition for a minimum duration of 15 minutes. Measure and record Small-Signal Gain.
- e) Change the input power to 103.5 Volts at 420 Hz. Maintain this condition for a minimum duration of 15 minutes. Measure and record Small-Signal Gain.

5.21 Transient Voltage Test

5.21.1 Upper and Lower Limit Test

- a) Connect the test equipment necessary to measure Small-Signal Gain in accordance with FTP-760510. Energize the amplifier by connecting 115 Volts, 60 Hz power to the AC input.
- b) Manually adjust the AC power to 135 Volts, 60 Hz. Maintain this condition for a minimum duration of 2 seconds. Manually adjust the AC power to 115 Volts, 60 Hz. Measure and record Small-Signal Gain.
- c) Manually adjust the AC power to 94 Volts, 60 Hz. Maintain this condition for a minimum duration of 2 seconds. Manually adjust the AC power to 115 Volts, 60 Hz. Measure and record Small-Signal Gain.

- d) Manually adjust the AC power to 115 Volts, 400 Hz. Manually adjust the AC power to 135 Volts, 400 HZ. Maintain this condition for a minimum duration of 2 seconds. Manually adjust the AC power to 115 Volts, 400 Hz. Measure and record Small-Signal Gain.
- e) Manually adjust the AC power to 94 Volts, 400 Hz. Maintain this condition for a minimum duration of 2 seconds. Manually adjust the AC power to 115 Volts, 400 Hz. Measure and record Small-Signal Gain.

5.23 Transient Frequency Test

- a) Connect the test equipment necessary to measure Small-Signal Gain in accordance with FTP-760510. Energize the amplifier by connecting 115 Volt, 420 Hz power to the AC input.
- b) Manually adjust the frequency of the AC power to 433 Hz. Maintain this frequency for a minimum duration of 2 seconds. Manually adjust the frequency of the AC power to 420 Hz. Measure and record Small-Signal Gain.
- c) Manually adjust the frequency of the AC power to 57 Hz. Maintain this frequency for a minimum duration of 2 seconds. Manually adjust the frequency of the AC power to 55 Hz. Maintain this condition for a minimum duration of 2 seconds. Manually adjust the frequency of the AC power to 57 Hz.

5.27 Power Interruption Test

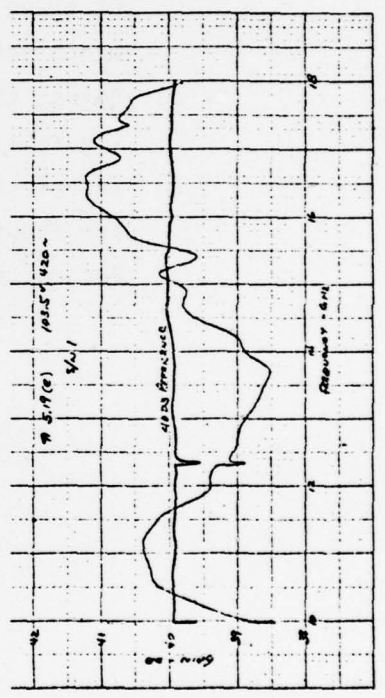
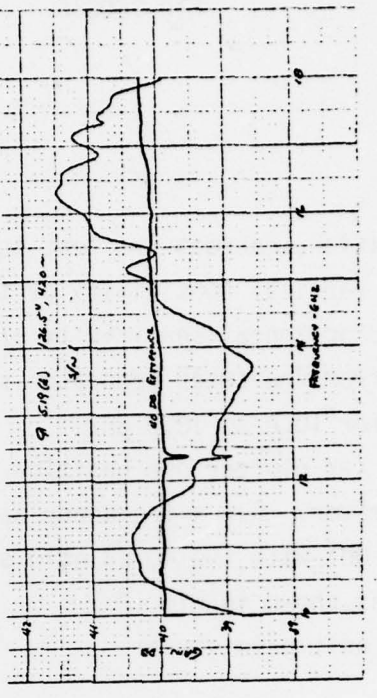
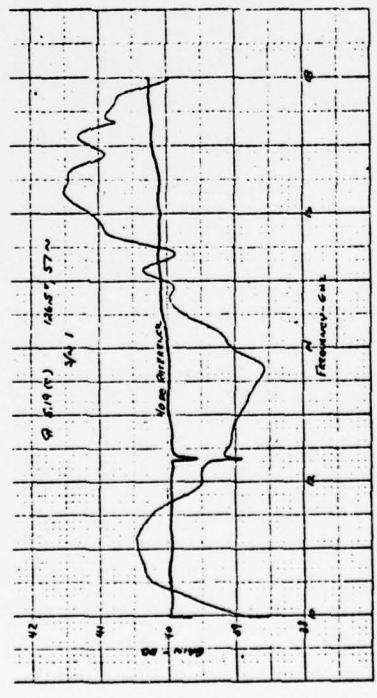
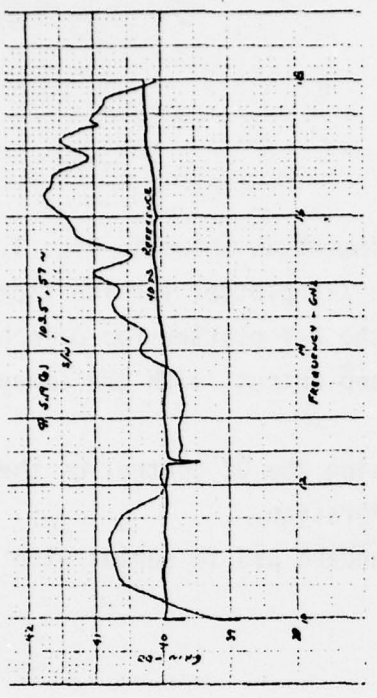
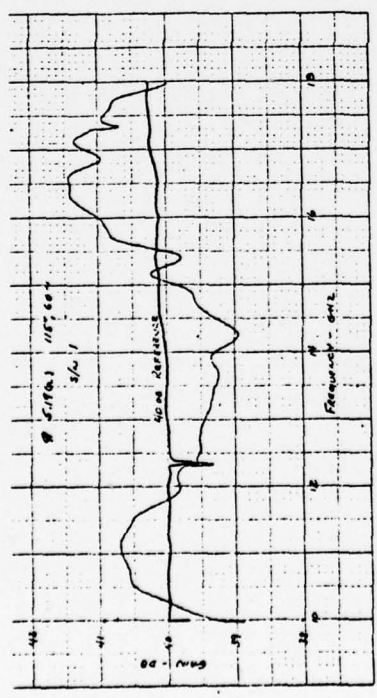
- a) Connect the test equipment necessary to measure Small-Signal Gain in accordance with FTP-760510. Energize the amplifier by connecting 115 Volt, 60 Hz power to the AC input.
- b) Disconnect the AC power for 3 to 4 seconds and then reconnect it. Measure and record Small-Signal Gain.
- c) Disconnect the AC power for 29 to 30 seconds and then reconnect it.
- d) Repeat step c three times. Measure and record Small Signal Gain.

EXCERPTS FROM FUNCTIONAL TEST PROCEDURE
FTP-760510

5.1.2 Procedure

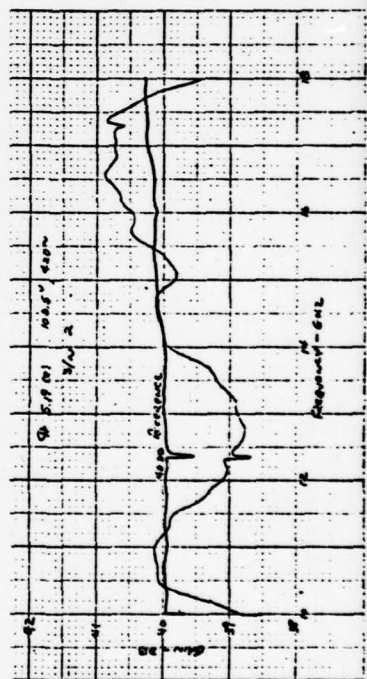
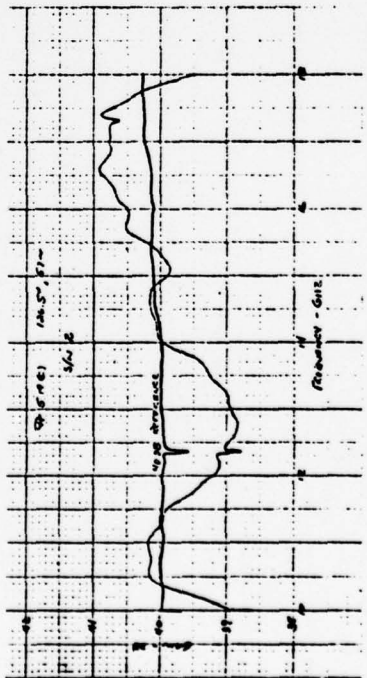
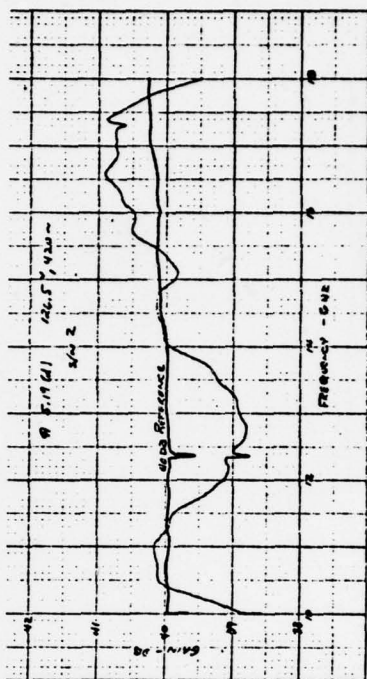
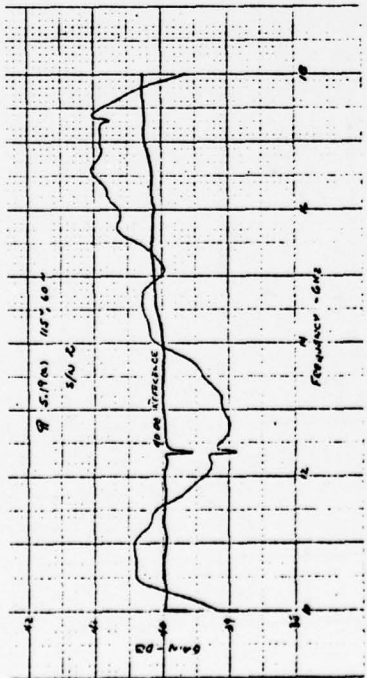
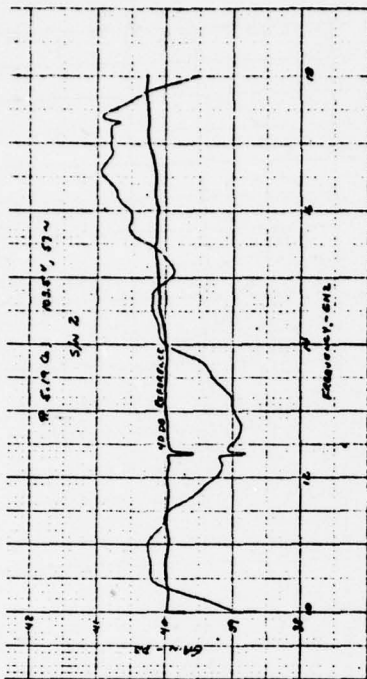
- a) For calibration, connect the test equipment as shown in Fig. 1.
- b) Adjust the vertical sensitivity of the X-Y plotter for 1dB/inch. Adjust the horizontal sensitivity of the X-Y plotter for 8 inches of travel from the sweep generator sweep output, with the sweep width set for 10.0 to 18.0 GHz.
- c) Adjust the X-Y plotter pen position using the DC control on the log level meter. Run a frequency calibration.
- e) Insert the UUT with the 40 dB gain standard pad in series with the input as shown in Fig. 2.
- f) Record the unit gain curve.

PAR. 5.19 STEADY-STATE VOLTAGE AND FREQUENCY TEST



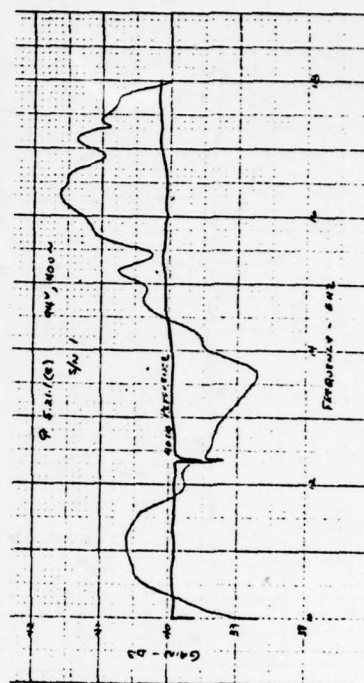
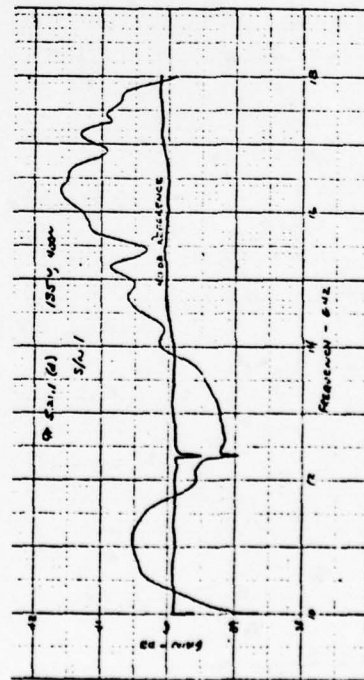
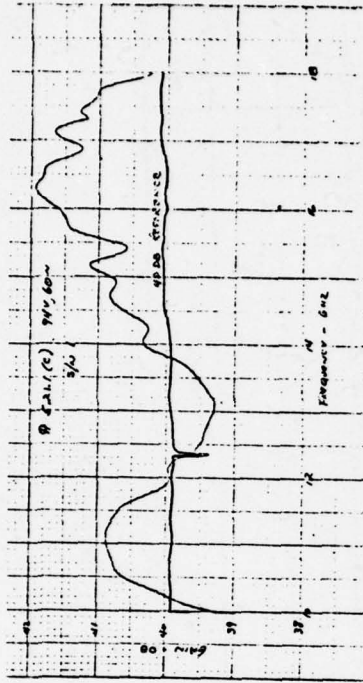
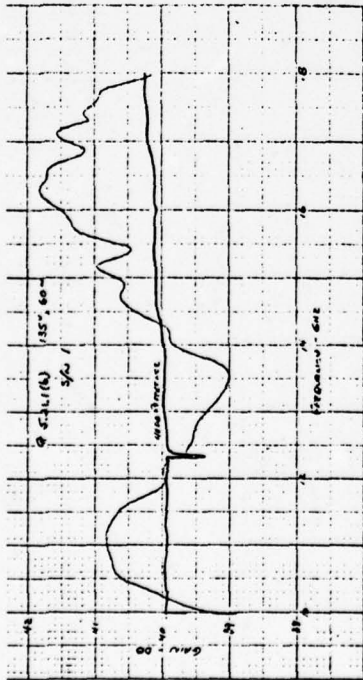
Kenneth C. Stoffy
10/25/77

PAR. 5.19 STEADY-STATE VOLTAGE AND FREQUENCY TEST



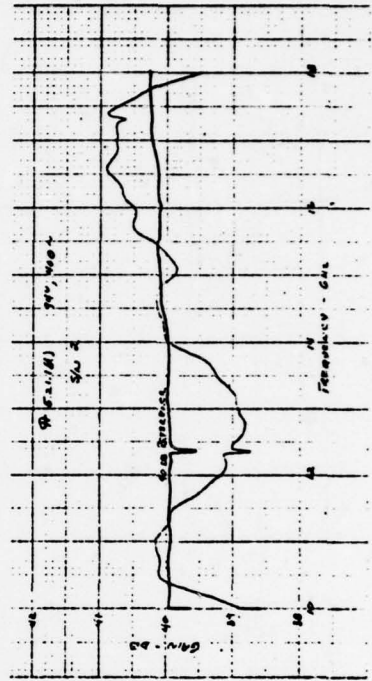
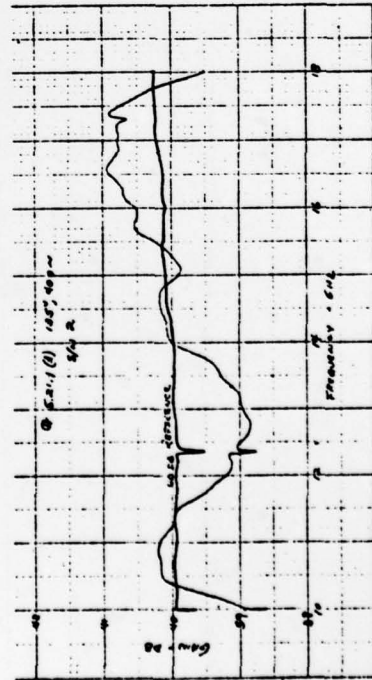
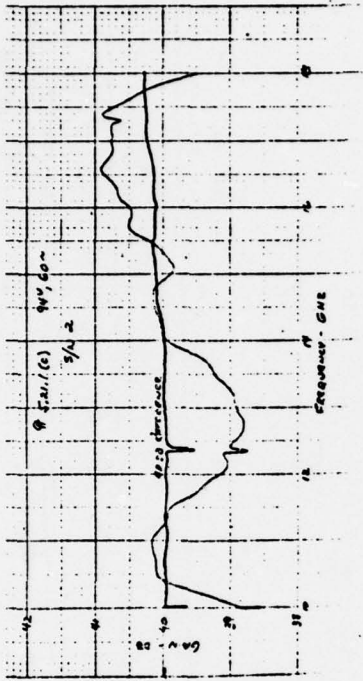
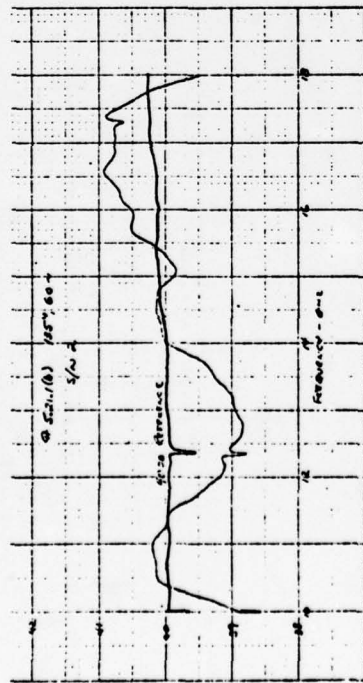
Kenneth C. Stiffley
10/25/77

PAR. 5.21.1 TRANSIENT VOLTAGE TEST - UPPER AND LOWER LIMIT TEST



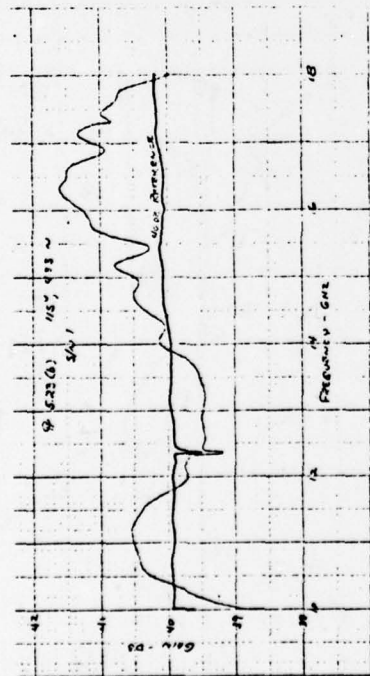
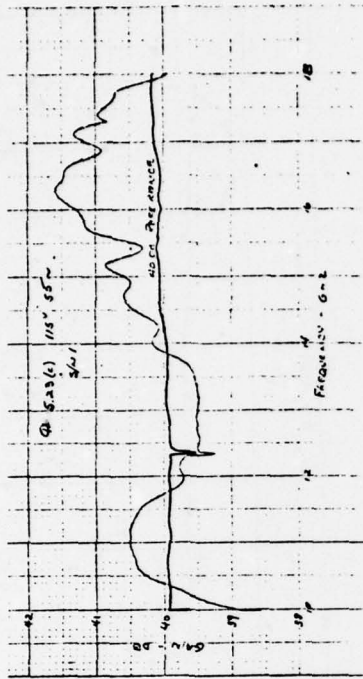
Kenneth C. Stoffey
10/25/77

PAR. 5.21.1 TRANSIENT VOLTAGE TEST - UPPER AND LOWER LIMIT TEST

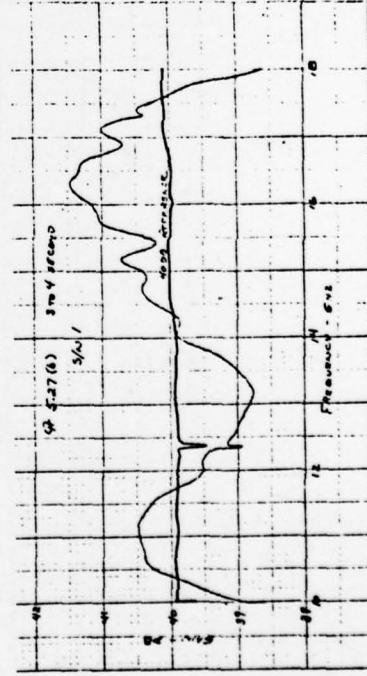
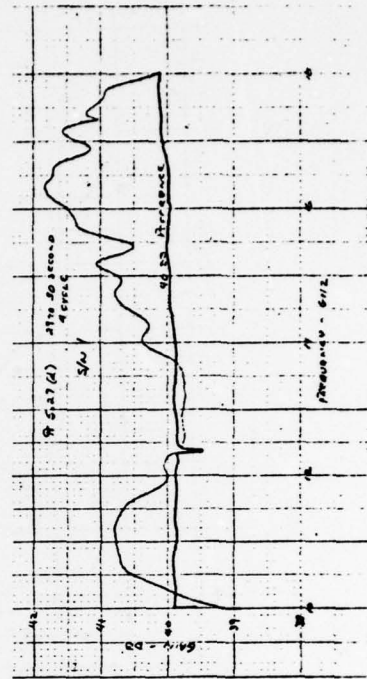


Kenneth C. Saffery
10/25/77

PAR. 5.23 TRANSIENT FREQUENCY TEST

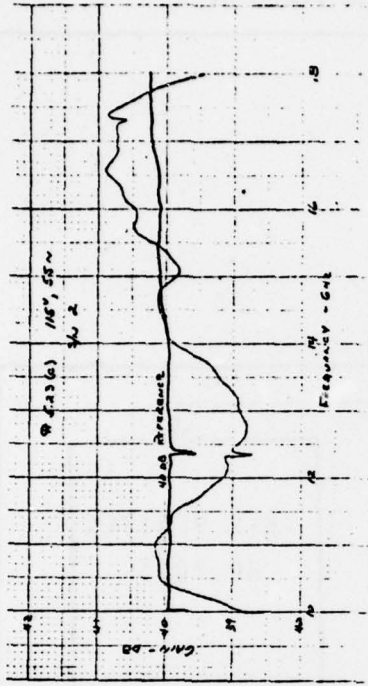
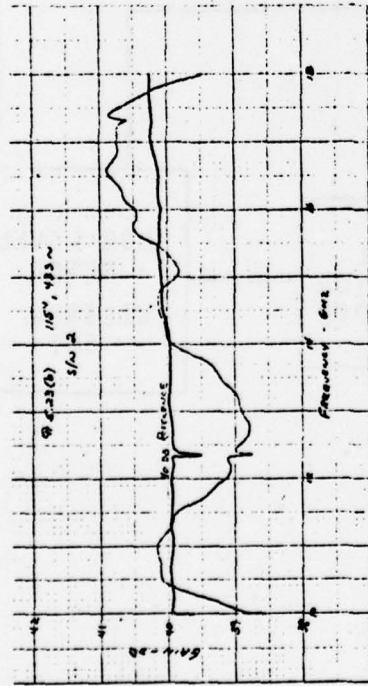


PAR. 5.27 POWER INTERRUPTION TEST

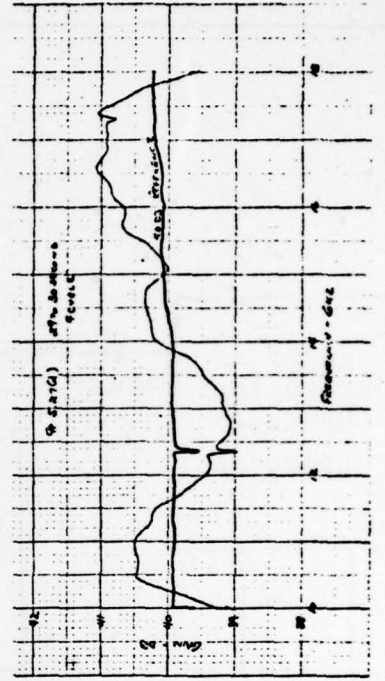
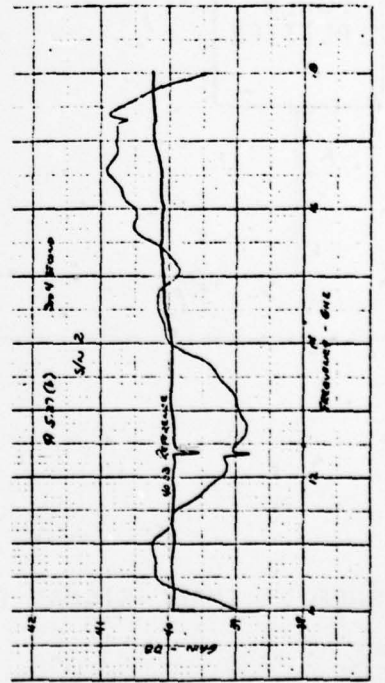


Kenneth C. Steffey
10/25/77

PAR. 5.23 TRANSIENT FREQUENCY TEST



PAR. 5.27 POWER INTERRUPTION TEST



Kenneth C. Coffey
10/25/77

TITLE:

EFFECTIVE DATE

APPROVED BY

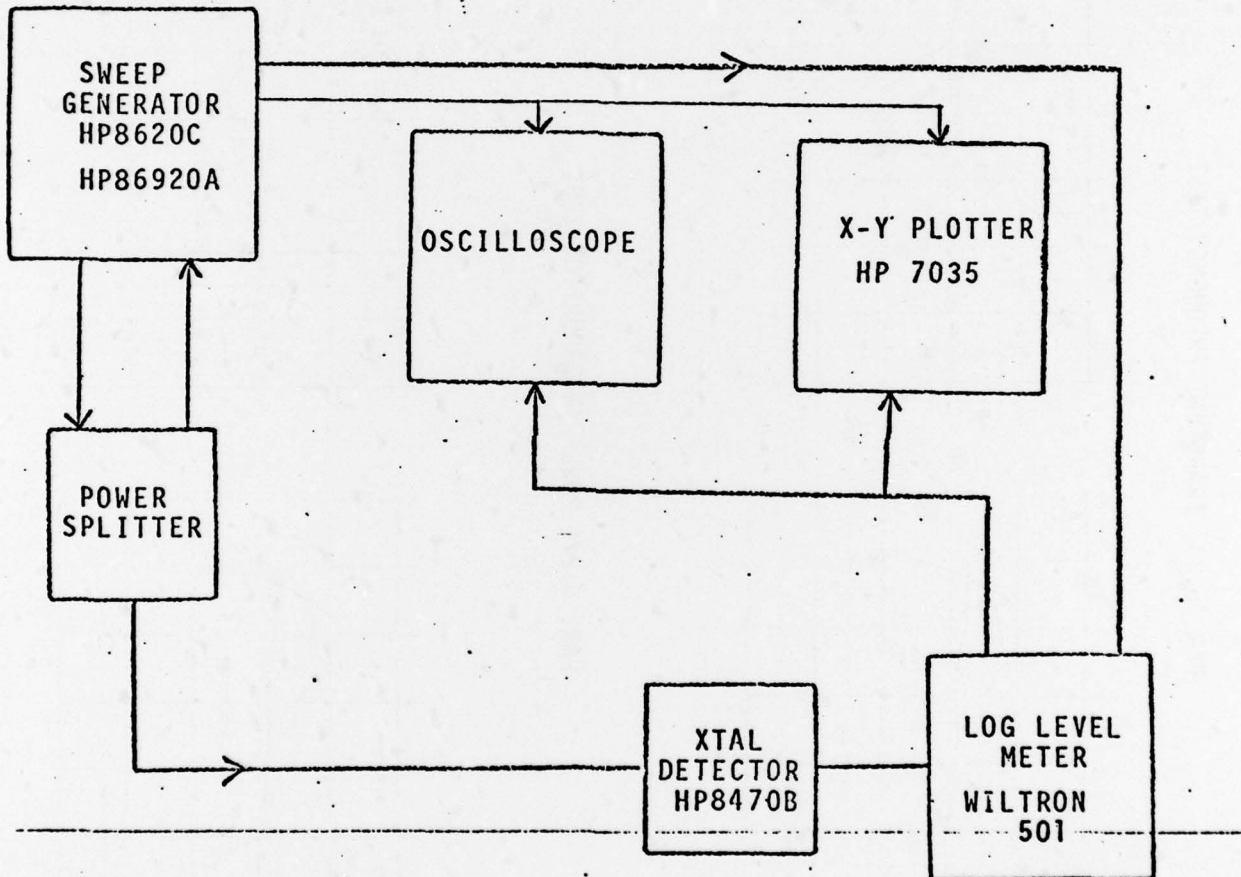


FIGURE 1: SMALL-SIGNAL GAIN CALIBRATION

TITLE:

EFFECTIVE DATE

APPROVED BY

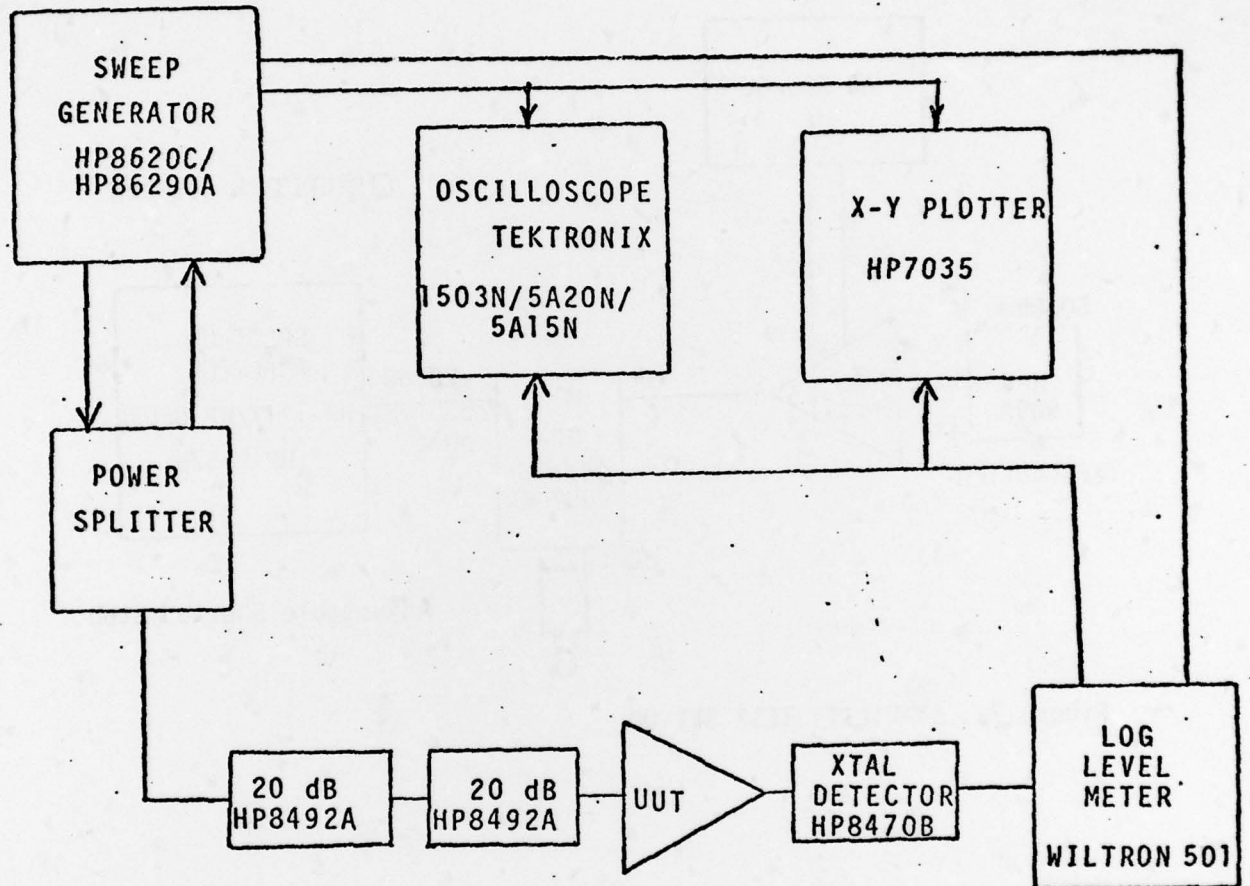


FIGURE 2: SMALL-SIGNAL GAIN TEST SET-UP

TITLE:

EFFECTIVE DATE

APPROVED BY

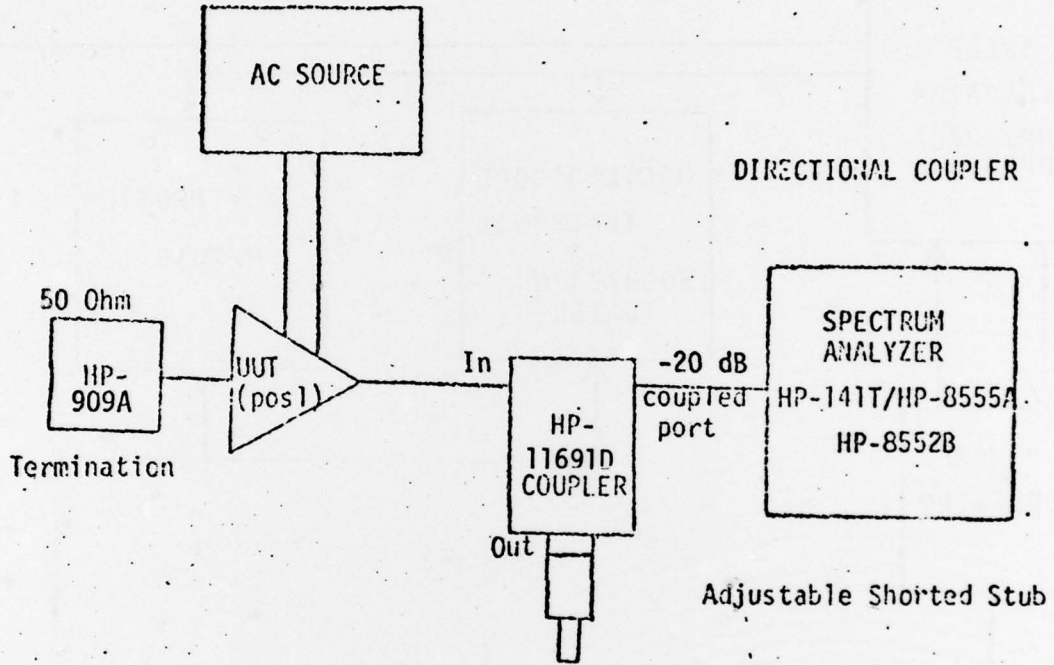


Figure 7a: STABILITY TEST SET-UP

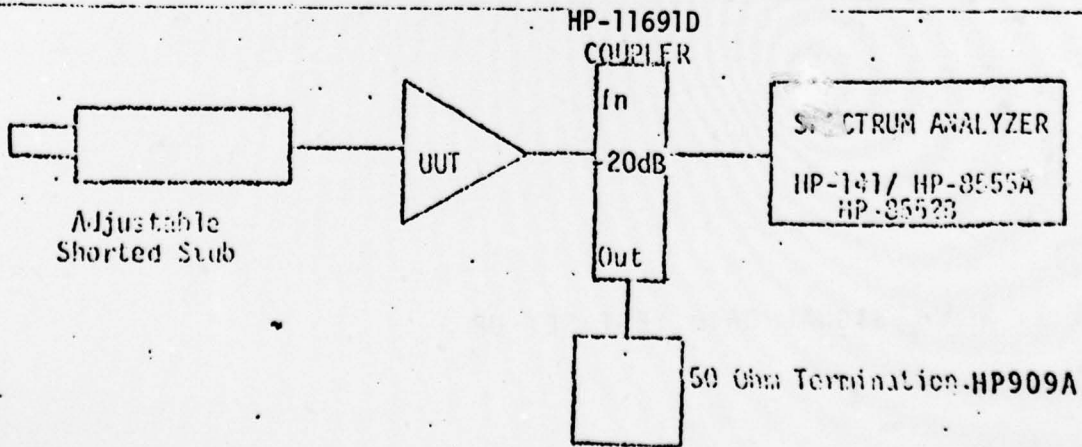


Figure 7b: STABILITY TEST SET-UP

EXCERPTS FROM FUNCTIONAL TEST PROCEDURE
FTP-760510

5.5 Stability Test

5.5.2 Test Procedure

- a) Connect the test equipment and UUT as shown in Fig. 7a. Adjust the spectrum analyzer scan width to 200 MHz/div; connect the input of the UUT test to the 50 ohm termination.
- b) Move the shorted stub in and out at least 5 cm repeatedly while slowly scanning the spectrum from 100 MHz to 18 GHz. Note any signals greater than 10 dB above the noise floor 100 MHz to 18 GHz.
- c) Disconnect the 50 termination from the input. Repeat Step b.
- d) Connect the test equipment and UUT test as shown in Fig. 7b. Connect the output of the UUT to the 50 ohm termination.
- e) Move the shorted stub in and out at least 5 cm repeatedly while slowly scanning the spectrum from 100 MHz to 18 GHz. Note any signals greater than 10 dB above the noise floor.
- f) Disconnect the 50 ohm termination from the output of the coupler. Repeat step e.
- g) The amplifier is stable if no signal was identified at a power level greater than 10 dB above the noise floor as viewed on the display of the spectrum analyzer.

DISTRIBUTION LIST FOR FINAL REPORT ON CONTRACT NO. N00014-75-C-1163

MICROWAVE GALLIUM ARSENIDE FET AMPLIFIERS PROGRAM

	<u># OF COPIES</u>
Defense Documentation Center Building 5, Cameron Station Alexandria, Virginia 22314	12
Advisory Group on Electron Devices 201 Varick Street, 9th Floor New York, New York 10014	3
Commanding Officer Naval Research Laboratory Attn: Library, Code 2627 Washington, DC 20375	6
Commanding Officer Naval Research Laboratory Attn: Mr. Eliot D. Cohen, Code 5211 Washington, DC 20375	53
Commanding Officer Naval Research Laboratory Attn: Dr. John E. Davey, Code 5210 Washington, DC 20375	1
Commanding Officer Naval Research Laboratory Attn: Mr. Albert Brodzinsky, Code 5200 Washington, DC 20375	1
Commanding Officer Naval Research Laboratory Attn: Dr. Kenneth J. Sleger, Code 5211S Washington, DC 20375	1
Commanding Officer Naval Research Laboratory Attn: Mr. William A. Douglas, Code 5334 Washington, DC 20375	1
Commanding Officer Naval Research Laboratory Attn: Mr. Ronald Chilluffo, Code 5733B Washington, DC 20375	1

	<u># OF COPIES</u>
Commanding Officer Naval Research Laboratory Attn: Mr. John M. Eardley, Code 5733 Washington, DC 20375	1
Commanding Officer Naval Research Laboratory Attn: Mr. K. Reed Gleason, Code 5211G Washington, DC 20375	1
Commanding Officer Naval Research Laboratory Attn: Mr. A. C. Macpherson, Code 5210.2 Washington, DC 20375	1
Commanding Officer Naval Research Laboratory Attn: Mr. R. Neidert, Code 5251 Washington, DC 20375	1
Commanding Officer Naval Research Laboratory Attn: Mr. H. Willing, Code 5258 Washington, DC 20375	1
Commanding Officer Naval Research Laboratory Attn: Dr. L. Young, Code 5203 Washington, DC 20375	1
Commanding Officer Naval Research Laboratory Attn: Dr. B. Spielman, Code 5251 Washington, DC 20375	1
Commanding Officer Naval Research Laboratory Attn: Mr. J. T. McCullough, Code 5709 Washington, DC 20375	1
Commander Naval Electronic Systems Command Attn: Mr. L. W. Sumney, Code 3042 Washington, DC 20360	10
Commander Naval Air Systems Command Attn: Mr. Andrew Glista, Jr., AIR 52022 Washington, DC 20361	10

	<u># OF COPIES</u>
Dr. John K. Smith Naval Air Development Center Code 2042 Warminster, PA 18974	1
Office of Naval Research Attn: Dr. J. O. Dimmock, Code 427 800 N. Quincy Street Arlington, VA 22217	1
Office of Naval Research Attn: Mr. M. N. Yoder, Code 427 800 North Quincy Street Arlington, VA 22217	1
Commander Naval Electronic Systems Command Attn: Mr. R. A. Wade, Code 3042-1 Washington, DC 20360	1
Director Naval Weapons Center Attn: Mr. Joseph A. Mosko, Code 35023 China Lake CA 93555	1
Officer of Naval Research Code 102CP 800 North Quincy Street Arlington, VA 22217	1
Office of Naval Research Attn: Mr. C. R. Paoletti, Code 613CRP 800 North Quincy Street Arlington, VA 22217	1
Commander Naval Electronic Systems Command ATTN: PMR-107 (Project REWSON), JP #1, Rm 554 Washington, D.C. 20360	1
Commander Naval Air Systems Command Attn: Mr. Dennis Distler, AIR-5333 Washington, D.C. 20361	1
Commander Naval Ocean Systems Center Attn: Mr. John Griffin 297 Catalina Blvd San Diego, CA 92152	1

	<u># OF COPIES</u>
Commander Naval Ocean Systems Center Attn: Dr. Harry Wieder 297 Catalina Boulevard San Diego, CA 92152	1
Commander Naval Ocean Systems Center Attn: Library 297 Catalina Boulevard San Diego, California 92152	1
Commander Naval Ships Engineering Center Attn: Code 6157D Prince Georges Center Hyattsville, Maryland 20782	1
Commander Naval Electronic Systems Command Engineering Office U. S. Naval Station Norfolk, Virginia 23511	1
Commander U. S. Army ERADCOM Attn: DLET-MK, Mr. V. G. Gelnovatch Fort Monmouth, New Jersey 07703	1
Commander U. S. Army ERADCOM Attn: DELET-MK, Mr. R. Weck Fort Monmouth, N.J. 07703	1
Commanding Officer Harry Diamond Laboratories Advanced Research Laboratory Attn: AMXDO-RAA, Mr. H. W. A. Gerlach Washington, DC 20438	1
Commander Air Force Avionics Laboratory Attn: Mr. R. L. Remski Wright Patterson Air Force Base, Ohio 45433	1
Commander Air Force Avionics Laboratory Attn: Mr. T. Kemerley Wright Patterson Air Force Base, Ohio 45433	1

	<u># OF COPIES</u>
Commander Air Force Avionics Laboratory Attn: Mr. C. Huang Wright Patterson Air Force Base, Ohio 45433	1
Commander Rome Air Development Center Attn: Mr. R. H. Chilton Griffiss Air Force Base, New York 13441	1
Director of Defense Research and Engineering Attn: Tech Library Room 3E1039, The Pentagon Washington, DC 20301	1
Defense Advanced Research Projects Agency Attn: Dr. Richard Reynolds 1400 Wilson Boulevard Arlington, Virginia 22309	1
Director U. S. Army Ballistic Missile Defense Advanced Technology Center Attn: ATC-R, Mr. G. Jones P. O. Box 1500 Huntsville, Alabama 35807	1
Dr. N. Walter Cox Georgia Institute of Technology Engineering Experiment Station Atlanta, Georgia 30332	1
Dr. Walter Ku Cornell University Electrical Engineering Department Phillips Hall Ithaca, New York 14850	1
Dr. Jeffrey Frey Cornell University Electrical Engineering Department Phillips Hall Ithaca, New York 14850	1
Aertech Industries 825 Stewart Drive Sunnyvale, California 94088	1

	<u># OF COPIES</u>
Communication Transistor Corporation Attn: Dr. W. H. Weisenberger 301 Industrial Way San Carlos, California 95051	1
Hewlett-Packard Company, Inc. Attn: Dr. B. Berson HPA Division 640 Page Mill Road Palo Alto, California 94304	1
Hewlett-Packard Company, Inc. Attn: Dr. C. Liechti 1501 Page Mill Road Palo Alto, California 94304	1
Hughes Aircraft Company Hughes Research Laboratories Attn: Dr. G. Ladd 3100 W. Lomita Blvd Torrance, CA 90509	1
Raytheon Company Research Division Attn: Dr. Robert Pucel 28 Seyon Street Waltham, Massachusetts 02154	1
Varian Associates Attn: Dr. B. Fank 611 Hansen Way Palo Alto, California 94304	1
Watkins-Johnson Company Attn: Mr. Martin G. Walker 3333 Hillview Avenue Palo Alto, California 94304	1
Westinghouse Research Laboratories Attn: Dr. H. C. Nathanson Beulah Road Pittsburgh, Pennsylvania 15235	1
Alpha Industries, Inc. Attn: Mr. Martin Reid 20 Sylvan Road Woburn, MASS 01801	1

OF COPIES

Hughes Aircraft Company Attn: Dr. T. Midford Torrance Research Center 3100 West Lomita Blvd Torrance, California 90509	1
Teledyne/MEC Attn: Dr. Martin Grace 3165 Porter Drive Palo Alto, California 94304	1
Bell Telephone Laboratories Attn: Dr. J. V. DiLorenzo 600 Mountain Avenue Murray Hill, New Jersey 07974	1
Rockwell International Attn: Dr. Cheng P. Wen MS 406-246 Richardson, Texas 75081	1
Microwave Associates Attn: Dr. Joseph A. Saloom Northwest Industrial Park Burlington, Massachusetts 01803	1
Microwave Semiconductor Corp. Attn: Dr. Ira Drukier 100 Schoolhouse Road Somerset, New Jersey 08873	1
Rockwell International Science Center Attn: Dr. Dan Ch'en 1049 Camino Dos Rios (P. O. Box 1085) Thousand Oaks, California 91360	1
RCA Laboratories David Sarnoff Research Center Attn: Dr. Y. Narayan Princeton, New Jersey 08540	1
The Narda Microwave Corporation Attn: Dr. John Eisenberg 2900 Coronado Drive Santa Clara, California 95051	1

	<u># OF COPIES</u>
General Electric Company Space Division Attn: Dr. Deen D. Khandelwal P.O. Box 8555 Philadelphia, PA 19101	1
Airborne Instruments Laboratory Attn. Dr. J. Caviello Melville, L.I. N.Y. 11746	1
Dexcel, Inc. Attn: Dr. George Vendelin 2285 C Martin Ave Santa Clara, CA 95050	1
Motorola, Inc. Attn: Dr. Robert Adams 5005 East McDowell Road Phoenix, Arizona 85036	1
Texas Instruments, Inc. Attn: Dr. D. N. McQuiddy P. O. Box 5936, MS 118 Dallas, Texas 75222	1
Texas Instruments, Inc. Central Research Labs Attn: Dr. W. R. Wisseman Dallas, Texas 75222	1
Hydrotronics, Inc. Attn: Mr. Don Burns 803 West Broad Street Falls Church, Virginia 22046	1
General Electric Company Heavy Military Equipment Dept. Attn: Mr. William H. Perkins Court St. Plant, Bldg 5, Room H-1 Syracuse, New York 13201	1
Sperry Marine Systems Attn: Mr. Dale Jessen Route 29 North and Hydraulic Road Charlottesville, Virginia 22901	1
Dexcel, Inc. Attn: Dr. S. Kahihana 2285C Martin Avenue Santa Clara, CA 95050	1